## *Crustal structure of the eastern Caribbean in the region of the lesser Antilles and Aves Ridge*

Kearey, Philip

# CRUSTAL STRUCTURE OF THE EASTERN CARIBBEAN IN THE REGION OF THE LESSER ANTILLES AND AVES RIDGE

by

PHILIP KEAREY



**A thesis submitted for the degree of**

**Doctor of Philosophy**

**in the**

**University of Durham**

**Graduate Society** **September, 1973**

## ABSTRACT

The results of two marine gravity, magnetic and seismic reflection surveys in the eastern Caribbean are presented, the principal structures surveyed being the Venezuela Basin, Aves Ridge, Grenada Trough and Lesser Antilles island arc. The data are presented in the form of charts of bathymetry, free air anomalies, Bouguer anomalies and total field magnetic anomalies.

The Venezuela Basin is a broad, extensive basin with a sediment thickness in excess of 1.5 km. At its eastern margin it exhibits small negative free air anomalies and is in approximate isostatic equilibrium.

The Aves Ridge is an elevated linear volcanic prominence parallel to the Lesser Antilles characterised by positive free air anomalies. Its typical form is of two basement ridges marking its western and eastern flanks enclosing a sediment filled trough. The western ridges are shown to be more dense and less magnetic than the main body of the Aves Ridge and may represent a series of intrusive bodies. The Aves Ridge exhibits strong magnetic-gravity correlations. It is underlain by a root attributed to depression of the Moho and lowest crustal layer and exhibits negative isostatic anomalies.

The Grenada Trough is a basin of subdued topography in the south and more rugged topography in the north. It contains a sediment thickness in excess of 2 km. and is characterised by predominantly negative free air anomalies. It is underlain by an elevated Moho and exhibits predominantly negative isostatic anomalies.

The Lesser Antilles lie on a narrow elevated ridge rising

abruptly out of the Grenada Trough. The island arc exhibits extreme free air gravity gradients. It is underlain by a root attributed to depression of the Moho and is the site of a linear belt of positive isostatic anomalies.

Possible modes of origin of the Aves Ridge are discussed.

ACKNOWLEDGEMENTS

I wish to thank Professor M.H.P. Bott for his supervision and for allowing use of the facilities of the Department of Geological Sciences.

I am very grateful for the assistance and enthusiastic support provided by the officers and crew of H.M.S. 'Hecla', and for their generous hospitality, during my stay on board.

Discussions with many of my colleagues in the Department of Geological Sciences proved very helpful in the writing of this thesis.

INDEX

# CHAPTER 1

# GENERAL CARIBBEAN GEOLOGY AND GEOPHYSICS

## 1.1 Introduction

During the summers of 1971 and 1972, Durham University, in co-operation with the Hydrographic Department, R.N., mounted two geophysical surveys in the eastern Caribbean. These two surveys formed part of the United Kingdom contribution to CICAR (Co-operative Investigation into the Caribbean and Adjacent Regions), a project organised under the auspices of UNESCO and FAO for international investigations into the resources of the Caribbean area. The surveys were performed from H.M.S. 'Hecla', an ocean class survey vessel of the Royal Navy, and in addition to the bathymetric, magnetic, gravity and seismic reflection surveys which this thesis describes, other oceanographic, geological and geophysical investigations were made in the fields of geochemistry, seismic refraction, coring, dredging and plankton sampling. Fig. 1-1 shows the locations of the surveys which Durham University, in conjunction with the Royal Navy, performed as part of the U.K. contribution to CICAR.

## 1.2 Tectonic and Geological Setting

The Caribbean and Scotia arcs provide the only representatives of circum-Pacific type island arcs to be found in the Atlantic Ocean. The Caribbean in particular is proving a critical testing and proving ground for the new global tectonics (Isacks et al., 1968).

The Caribbean is a small oceanic plate of approximately rectangular shape and three million square kilometres in area (fig. 1-2).

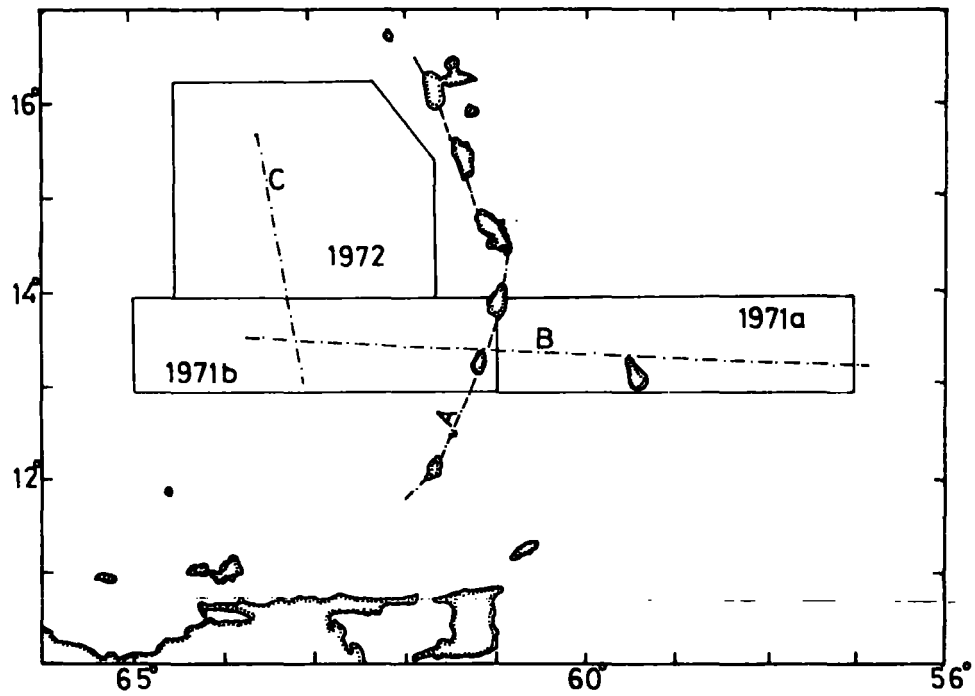


Figure 1-1: Durham surveys in the Caribbean.
Solid lines - boundaries of gravity, magnetic & air-gun surveys.
Broken lines - seismic refraction lines (1972).

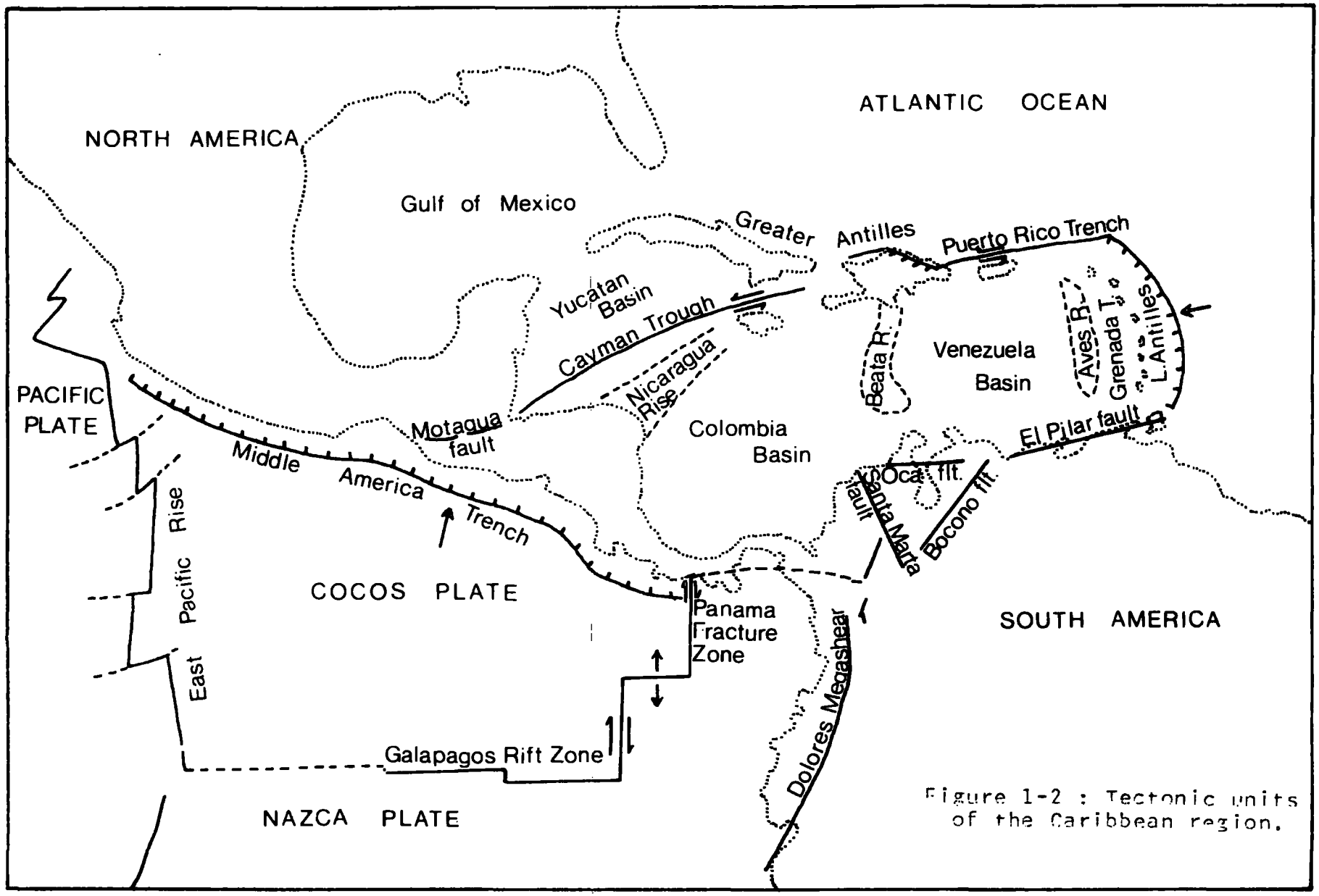


Figure 1-2 : Tectonic units of the Caribbean region.

Its small size has usually precluded its inclusion in a global plate system (Le Pichon, 1968). The Caribbean plate is bounded to the west by the Cocos plate, a relatively small oceanic plate defined in the west by the east Pacific rise and in the south by the Galapagos rift and Panama fracture zones. The Cocos plate underthrusts the Caribbean plate in a north-easterly direction at the Middle America Trench, and is responsible for the volcanic and seismic activity in Central America (Sykes & Ewing, 1965), of which the Managuan earthquake of December 1972 provides a recent example. The Middle America Trench divides the oceanic area of the Pacific Ocean from the pre-Mesozoic orogenic and serpentinite belt of Central Guatemala in northern Central America and to the south Mesozoic red beds and evaporites are overlain by extensive younger volcanics. (MacGillavry, 1970).

The northern boundary with the North American plate is a composite of two sinistral transform faults. The Cayman Trough, and its western extension into Central America, the Motagua fault, is the most westerly of these, and stretches from the Gulf of Honduras to the Gulf of Gonave in western Hispaniola. The Trough is marked by bathymetry in excess of 3000 fathoms. Although primarily strike-slip, Bowin (1968) has shown that there is also a component of movement perpendicular to the Trough such that the North American and Caribbean plates are undergoing slight separation. The connection of the Cayman Trough to the eastern fault system, the Puerto Rico Trench, is not yet known in detail and requires further definitive work. The Puerto Rico Trench is usually considered as a typical ocean trench. However, it trends WNW at 15° to the island of Puerto Rico (Monroe, 1968) and present movement is predominantly strike-slip (Molnar & Sykes, 1969). This eastern fault system is not continuous and shows a step to the

south in the area of eastern Hispaniola. Bracey & Vogt (1970), from a study of fault plane solutions of earthquakes in this area, have identified this step as a Benioff zone, with the North American plate underthrusting the Caribbean in a westerly direction along the north-eastern coast of Santo Domingo.

The northern margin divides the carbonate evaporite region stretching from the Bahamas to Yucatan, an area of subsidence in which a Mesozoic succession is underlain, at least in Central America, by a Palaeozoic basement, from the Greater Antilles. The Greater Antilles are taken to include Cuba, for although at the present day it lies to the north of the fault system its geological affinities are with the islands of the North Caribbean. MacGillavry (1970) has identified four phases in Greater Antillean history:

(i) submarine volcanism in lower Cretaceous

(ii) compression and tectogenesis in upper Cretaceous and lower Palaeogene

(iii) subsidence and carbonate deposition in the Tertiary

(iv) formation of present day morphology from Tertiary to Recent

No proximity to a sialic source is implied, and major volcanic activity ceased at the end of the Eocene.

The Puerto Rico Trench, in which depths greater than 4000 fathoms have been recorded, extends to the north of the Virgin Islands. Talwani (1965) considers that the negative free air anomaly belt of the northern margin is continuous with the belt to the east of the Lesser Antilles passing through Barbados and thence into Trinidad and Venezuela. Although possibly genetically true, it is preferred to consider the predominantly strike-slip northern boundary and dip-slip eastern boundary as separate regions.

The southern boundary of the Caribbean plate with the South American plate is open to more ambiguity. Classical plate tectonic theory interprets this boundary as a dextral transcurrent fault (Rod, 1956). This simple picture is confused by other geophysical data. The strike-slip system would involve movement along four major faults (fig. 1-2), from west to east the Santa Marta, Oca, Boconó and El Pilar faults. Although strike-slip movement is indicated along the Santa Marta, Oca and particularly the Boconó faults (Dewey, 1972), their very angular configuration would seem to preclude any major movements of the required order of hundreds of kilometres unless their positions have greatly changed over geological time. The El Pilar fault of northern Venezuela and Trinidad has a much more linear outcrop. However, Metz (1968) has mapped the area surrounding its outcrop in northern Trinidad and from the occurrences of the distinctive Cutacual formation, a euxinic facies of Albian age, on either side of the fault, he has concluded that the maximum lateral displacement is 15 kms. The chart of earthquake epicentres of northern Venezuela (Sykes & Ewing, 1965) reveals a gap in seismicity along the fault's outcrop, which may indicate lack of movement, although it may be a function of the time interval of observation. The preferred interpretation is that the Caribbean and South American plates are locked at the present day (Freeland & Dietz, 1971) and that differential lateral movements between North and South America are taken up on east-west striking fracture systems to the east of the Lesser Antilles (G. Peter, pers. comm., Ball et al., 1969), as well as along the northern boundary.

This southern boundary divides, at least in its eastern part, the Venezuelan Coast Range of the Caribbean plate from the rest of

northern Venezuela. The Venezuelan Coast Range stretches from the Araya Peninsula, Venezuela through Trinidad to Tobago and consists of a metasedimentary sequence in the north and a metavolcanic sequence in the south, the metamorphism being Cretaceous to early Tertiary. A pre-Mesozoic basement is inferred but has not been proved (Nagle, 1970). In Trinidad the sequence is metasedimentary, while in Tobago the sequence is predominantly metavolcanic. The El Pilar fault represents the southern boundary of the Venezuela Coast Range, and to the south of the fault thick Mesozoic and Tertiary sediments overlie pre-Mesozoic rocks throughout most of northern Venezuela.

The Dutch Lesser Antilles lie on a ridge-trough system north of the South American continental margin and have a history similar to the Greater Antilles, but with greater proximity to a sialic source (MacGillavry, 1970).

The central areas of the Caribbean plate appear but little disturbed, are aseismic and appear to have remained stable during tectonic events around the margins (MacGillavry, 1970, Edgar et al., 1971a). Within this central area, intraplate structures define regions of ridges and basins.

The Nicaragua Rise is a broad uplifted feature of less than 1000 fathoms stretching from the Honduran coast to Jamaica. It separates the Cayman Trough and Yucatan Basin from the Colombian Basin, an area of bathymetry of the order of 3000 fathoms containing a thick fill of turbidites derived from the Magdalena River of northern Colombia. It is bounded to the east by the Beata Ridge which trends SSW from Central Hispaniola almost to the continental edge of South America. Fox et al. (1970) consider the Ridge was formed by normal faulting in early Tertiary times, and had subsided to deep water by

late Eocene. The Beata Ridge forms the western boundary of the Venezuela Basin, an area of fairly uniform bathymetry between 2000 and 3000 fathoms.

The areas surveyed by Durham University in 1971 and 1972 are shown in fig. 1-3. The Aves Ridge or Swell forms the eastern margin of the Venezuela Basin. This is a linear feature aligned north-south centred on approximately 63°30'W extending from approximately 16°10'N to the Venezuelan continental borderland. Although its topographic expression is not apparent beyond this northern limit, its geophysical expression may extend as far north as 18°N (Bunce et al., 1971). In the south the Ridge rarely reaches an elevation of less than 1 km. below sea level, but in the north culminates in Aves Island. This small island has exposures of sedimentary rock only, but Gallovich & Aguilera (1970), from the results of a small seismic refraction experiment, have proposed igneous or metamorphic rocks about 70m. below the surface. Several seamounts occur along the Ridge and have been described by Rona (1961), Marlowe (1971) and Nagle (1971).

The Aves Ridge and Lesser Antilles form the western and eastern limits of the Grenada Trough. In its southern part, the Trough is extremely flat across its entire width and varies in depth by no more than a few metres from 2997m. Such subdued topography is indicative of a thick sediment cover, probably derived from the Orinoco River of Venezuela. North of about 14°N, the topography becomes gradually more rugged and in places the distinction between Aves Ridge and Grenada Trough is difficult from bathymetric data alone.

The eastern boundary of the Grenada Trough is marked by the volcanic arc of the Lesser Antilles, which also defines the eastern margin of the Caribbean plate. The island chain has an arcuate

outcrop, convex eastwards, extending from Sombrero in the north to Los Testigos in the south (Edgar et al., 1971a) and may even extend as far south as Margarita (Ewing et al., 1957). Bowin (1967) has indicated that the radius of curvature of the arc is one of the smallest found, along with the Scotia arc and the eastern portion of the Indonesian arc. In the north the island chain is divided into a western volcanic arc and an eastern limestone arc. The limestone arc is underlain by Eocene lava flows and coarse volcanic debris which are overlain by Oligocene and Miocene limestones with some volcanic debris. The arcs converge at Dominica, whence the islands exhibit characteristics of both limestone and volcanic parts (Weyl, 1966, Bowin, 1967). No volcanic rocks older than Oligocene have been found in the volcanic arc north of Dominica, whereas Eocene volcanics have been described from Carriacou and Grenada. Thus, although volcanism has occurred in the Lesser Antilles since the Eocene, it appears that the limestone arc north of Dominica is underlain by a volcanic ridge which may represent a previous zone of underthrusting before an anticlockwise rotation caused a readjustment and movement of the Benioff zone to the east. The description of a suite of Jurassic igneous rocks from Désirade (Fink et al., 1971) confuses this simple picture and will be discussed later. The calc-alkaline volcanism of the Lesser Antilles has occurred since the Eocene and its initiation coincided with cessation of volcanic activity in the Greater Antilles. The volcanism continues to the present day with the recent eruptions of Souffrière, St. Vincent, and Kick-'em-Jenny off Grenada. Evidence for an older substructure underlying the Lesser Antilles is lacking (MacGillavry, 1970), although some interpretations of Caribbean history require an eastern margin to have been present

at least since Cretaceous time (Edgar et al., 1971a). Whether this boundary was formed by a pre-Lesser Antilles or the Aves Ridge is uncertain and will be discussed later.

The Caribbean plate is being underthrust in a westerly direction by the Atlantic, which is descending at an angle of 40-60° (Molnar & Sykes, 1969). Hatherton & Dickinson (1969) estimate, from the potash content of Lesser Antillean volcanics, that the depth to the Benioff zone below the island arc is between 120 and 130 kms. No classical deep sea trench is developed east of the Lesser Antilles, since the topographic expression of the trench is masked by the thick, deformed sedimentary sequences comprising the Tobago Trough and Barbados Ridge (Chase & Bunce, 1969). A strong belt of negative free air anomalies marks the axis of the "trench" along the eastern side of the Lesser Antilles. To the east of the island arc lie the Tobago Trough, the Barbados Ridge, which culminates in the island of Barbados, and finally the Atlantic Ocean.

Structural relations of the eastern Caribbean have been discussed by Weeks et al. (1971).

## 1.3 Adjacent Survey Areas

The 1971 survey area is continuous with another area surveyed by Durham University in 1971, bounded by the same latitude limits and extending east to 57°W (fig. 1-1).

The U.S. Geological Survey (1972a, 1972c) have compiled composite charts of free air and Bouguer anomalies for the Venezuelan Continental Borderland, including surveys by Peter (1972), Lattimore et al. (1971) and Bassinger et al. (1971), who have also made magnetic traverses. These charts form an area to the south and southwest of the Durham survey areas.

The National Oceanographic and Atmospheric Administration have performed seismic reflection, magnetic and gravity surveys in the Atlantic to the east of the Lesser Antilles (G. Peter, pers. comm.).

The U.S. Geological Survey have performed seismic reflection profiling in the region of the eastern Greater Antilles and northern Lesser Antilles. (U.S.G.S., 1972b).

Non-systematic magnetic, gravity and reflection profiles have been made in the eastern Caribbean by Bunce et al. (1971), seismic reflection and refraction profiles by Edgar et al. (1971a), seismic refraction profiles by Officer et al. (1959), and seismic reflection profiles to the east of the Lesser Antilles by Chase & Bunce (1969).

## 1.4 Geological and Geophysical Investigations in the Eastern Caribbean

A summary chart of sites investigated in the eastern Caribbean is given in fig. 1-3.

### 1.4.1 Geological Sampling on the Aves Ridge and Grenada Trough

A number of geological samples have been collected in the eastern Caribbean, and have mostly taken the form of dredge hauls and cores. Recently, JOIDES have drilled several sites in the Caribbean during legs 4 and 15 of the Deep Sea Drilling Project.

Hurley (1965) has reported the dredging of basaltic rocks from the crest of the Aves Ridge and inferred that the Ridge is, at least in part, volcanic.

Fox et al. (1971) have described the results of 13 dredge hauls on the southern Aves Ridge. Limestones, marls and cherts were sampled ranging in age from middle Eocene to Recent. The mid-Miocene samples were interpreted to have been formed in an open-ocean planktonic

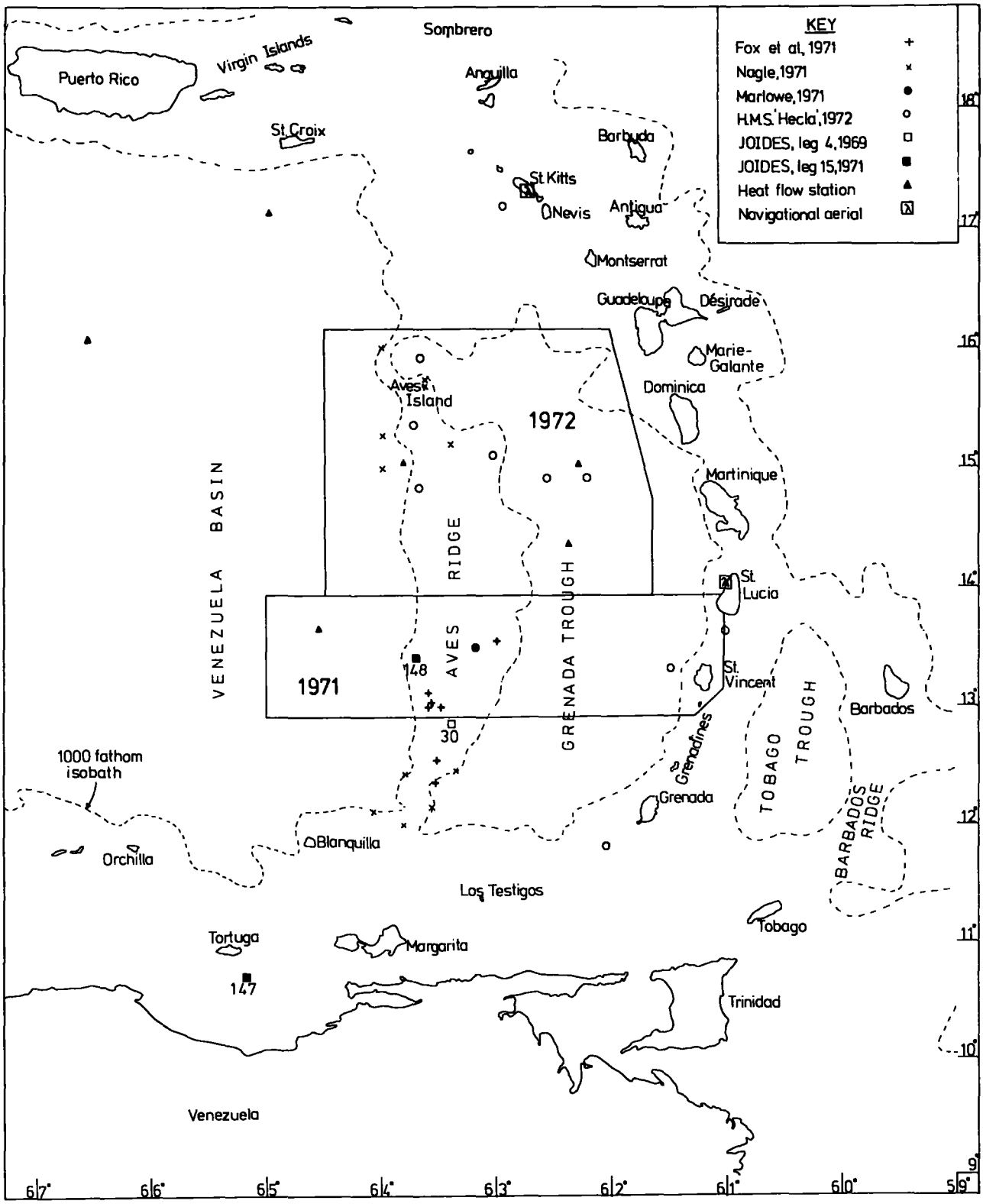
KEY
Fox et al, 1971
Nagle, 1971
Marlowe, 1971
H.M.S. 'Hecla', 1972
JOIDES, leg 4, 1969
JOIDES, leg 15, 1971
Heat flow station
Navigational aerial
Sombrero
Virgin Islands
Puerto Rico
Anguilla
St. Croix
Barbuda
St. Kitts
Nevis
Antigua
Montserrat
Guadeloupe
Désirade
Marie-Galante
Dominica
Martinique
St. Lucia
St. Vincent
Grenadines
Grenada
Barbados
Aves Island
1972
1971
148
30
147
VENEZUELA BASIN
AVES RIDGE
GRENADA TROUGH
TOBAGO TROUGH
BARBADOS RIDGE
1000 fathom isobath
Orchilla
Blanquilla
Los Testigos
Tortuga
Margarita
Tobago
Trinidad
Venezuela
18°
17°
16°
15°
14°
13°
12°
11°
10°
9°
61.7°
61.6°
61.5°
61.4°
61.3°
61.2°
61.1°
61.0°
59°

Figure 1-3

environment while the mid-Eocene to lower Miocene samples were deposited in a shallow, carbonate shelf environment. Two dredge hauls at the very southern tip of the Ridge recovered 3,500 kg. of granodiorite and subsidiary adamellite. A third haul contained dolerite, porphyritic basalt and metamorphosed basalt. Potassium-argon dates of granitic and dolerite samples have produced ages between middle Cretaceous and Palaeocene. Determinations of compressional wave velocities indicated values for the granitic rocks from 6.0 to 6.4 km/sec. which were correlated with the 6.0 to 6.4 km/sec. crustal layer recorded under the Aves Ridge by seismic refraction (Edgar et al., 1971a, Officer et al., 1959). It was suggested that the Ridge is underlain by granitic rocks of late Mesozoic age, and that the basalts represent extinct volcanoes and subsided microatolls penetrating this layer.

This occurrence of granitic rocks in an oceanic environment is unique. Walker et al. (1972) have proposed a model whereby the granitic rocks were derived from the mantle. Christman (1953) has described granodioritic rocks from the Lesser Antillean Islands of St. Bartholemew and St. Martin whose chemical analyses show many similarities with the samples from the Aves Ridge analysed by Fox et al. (ibid). It is probable that the samples from the Lesser Antilles represent an acidic plutonic differentiate of the magma whose calc-alkaline differentiates are represented by surface volcanism (K. Wills, pers. comm.), and a similar mode of origin may be proposed for the granitic rocks from the Aves Ridge. However, since the samples are from the southern tip of the Ridge, it is possible that they are related to the granitic rocks of the Dutch Lesser Antilles rather than to the Ridge itself, as rocks of a similar type have been

described from the islands of Blanquilla and Orchilla (Weyl, 1966).

Nagle (1971) has repeated dredging operations in the same locality as Fox et al. and has found no occurrences of granitic rocks. Instead, he found unfoliated metavolcanic greenschist facies rocks, basalts, volcanic conglomerates and tuffaceous limestones and concludes that granitic rocks do not represent a major constituent of the Ridge. It was not certain whether the metamorphic rocks were due to burial metamorphism, deuteric alteration or hydrothermal alteration, but similar rocks have been described from the Lesser Antilles (Johnston et al., 1971). Also investigated were a submarine ridge north and east of Aves Island and two seamounts southwest and southeast of the island. Volcanic conglomerates, breccias, andesites, basalts, dacites, tuffs and limestones were recovered. The conglomerates contained rounded pebbles and suggest subaerial or near surface processes implying later sinking of the site. The rocks are very similar to Lesser Antillean samples. Also reported were andesitic and basaltic cobbles from the beaches of Aves Island and many rounded pumice pebbles and cobbles. The andesites were found to be far more fresh than dredge samples and it was suggested that they represent discarded ships' ballast.

This conclusion is in accord with my own observations made during a brief visit to Aves Island on 17th April, 1972. The island was found to be covered with a calcarenite sand, fining to the centre of the island where it supports a thin cover of vegetation. Guano probably forms a reasonable portion of the sedimentary cover, since the island supports a large bird population. Large cobbles of coral rock are common and probably owe their origin to fierce surf action during the hurricane season. Igneous fragments were observed in the

coarse beach sand, and on the north shore large cobbles and pebbles of grey andesitic rock were found. However, the presence of a wreck 50 metres to the west made the conclusion that these rocks are indigenous to the island somewhat unlikely, and the finding of a squared-off cobble of granitic rock in shallow water seemed to support this. This isolated island and its fringing coral reefs represent a considerable navigational hazard, and the area was subjected to a small, large scale bathymetric survey by H.M.S. 'Hecla' during the summer of 1972.

Marlowe (1968) has reported the recovery of glassy flows, brecciated rocks and bombs with impact structures from several seamounts on the Aves Ridge. In a later work (Marlowe, 1971) he describes the dredging of carbonate rocks from a seamount at 13°30'N, 63°10'W (Durham 1971 survey area), consisting of micritic phosphite, reefoid conglomerate and calcarenite. From a geochemical study he concluded that the coarsely clastic texture of the conglomerate and an abundant shallow water fauna suggest that the seamount may have been partly emergent during Pleistocene-early Holocene time after which increasing water depths caused cessation of reef growth and life.

Coring was performed from H.M.S. 'Hecla' by University College, London during the 1972 field season. The location of the cores is shown in fig. 1-3. The principal sediment recovered in the Grenada Trough was a brown limy mud with subsidiary ash bands in cores near the Lesser Antilles (B. D'Ollier, pers. comm.). One small sample of a light brown, indurated limestone with macrofossils was obtained on the Aves Ridge.

### 1.4.2 JOIDES Investigations

Three boreholes were sunk in the Caribbean during 1969 on leg 4 of the Deep Sea Drilling Project (JOIDES). The sites 29, 30 & 31, were situated in the Venezuela Basin, Aves Ridge and Beata Ridge respectively (JOIDES, 1970). None of the boreholes reached basement, but have provided much information on the sediment cover of the area.

Site 29, in the Venezuelan Basin, was chosen since the two principal reflectors of the basin (see section 5.1.3) were anomalously close to the sea floor. Pleistocene and Pliocene calcareous nanoplankton and planktonic forams were abundant in the top 30 m., but from 30 to 61 m. barren clays were encountered. From 61 m. to 79 m. some calcareous nanoplankton were observed, but at 108 m. numerous lower Miocene calcareous plankton were found in a chalky matrix. The section from 122 m. to 229 m. was a uniform pure radiolarian ooze of lower upper Eocene and middle Miocene age with pumice and ash at several levels. A major hiatus was found between lower Miocene and the lower part of the upper Eocene. The hole terminated at 450 m., when an impenetrable chert layer of middle Eocene Age was encountered.

Site 30 was on the Aves Ridge. The upper 305 m. were soft clays rich in calcareous plankton, the top 244 m. being Pleistocene, and overlying Miocene. From 305 to 490 m., more indurated Miocene siltstones were encountered, and the middle Miocene from 397 to 490 m. was globigerina ooze or sand with hard basal strata. Ash beds were penetrated in the lower part of the section and were considered important contributors to the thickness of the Pleistocene, during which sedimentation rates were about twenty times greater than the Miocene and Pliocene.

Site 31, on the Beata Ridge, penetrated 325 m., the upper section

from 0 to 183m. being Pleistocene, Pliocene and upper and middle Miocene, all showing normal depositional rates for globigerina ooze. The lower part was in indurated chalks of lower Miocene age and is considered indicative of higher sedimentation rates.

Benson et al., in the summary of the report, propose that the 40 cm/sec. North Equatorial Current flowing west from the Lesser Antilles would accumulate thick sediments of fine sand size and turbidites in the Grenada Trough and that the Aves Ridge would trap most of the silt so that only very fine silts and clays would pass into the Venezuela Basin. However, comparison of sediment thicknesses from west to east from site 29 to 31 show a marked increase in thickness of the Plio/Pleistocene deposits towards the western flank of the Aves Ridge, although the Miocene deposits are far more uniform. This increase has been attributed to accumulation of volcanic debris. If, however, only silt sized particles cross the Grenada Trough, the thickening would seem to be caused by volcanics produced at the Aves Ridge and not, as suggested in the JOIDES report, from the Lesser Antilles. It is possible, however, that wind blown volcanic ash from the Lesser Antilles is also a contributer to this thickened sequence.

The reports of leg 15 of the JOIDES project of 1970/71 have not as yet been published in their entirety, and the following descriptions are based on preliminary reports. Edgar et al. (1971b) have published a summary of cores taken during this leg, the purpose of which was to produce a standard biostratigraphic section for the region. The perfection of hole re-entry techniques made this leg particularly successful.

Sites 146, 149 and 150 were in the Venezuela Basin. Holes 146 and 149 produced a complete section down to solid rock, and penetrated

Pleistocene, Pliocene, Miocene, Oligocene and upper Eocene chalk, oozes, marls and clays with ash bands in the lower part before reaching chalk interbedded with chert (reflector A"). Next penetrated were volcanic clays, Maestrichtian marls and chalks and Campanian/Coniacian radiolarian limestone and chert before passing through a dolerite sill 140 cm. thick overlying 35 cm. of metamorphosed limestone of Coniacian age. In hole 150 the Oligocene, part of the Eocene and Palaeocene and possibly the Maestrichtian and Campanian were missing. The absence of continental debris except in the Miocene was taken to indicate an efficient sediment trap on the continental margin of South America, although the reason for the absence of sediment representing such large time intervals is as yet unknown.

Site 148 was on the western crest of the Aves Ridge in the 1971 Durham survey area. 272m. were cored, and the sequence was divided into two parts. The upper sequence of Plio/Pleistocene marls and clays continued to 200m. and contained abundant ash beds, possibly derived from the Lesser Antilles. Six volcanic episodes could be identified, with the most severe in the middle Pleistocene, which correlates well with the inferred ages of the major volcanic centres on the Lesser Antilles. The high sedimentation rate, however, suggests derivation from nearby islands, possibly on the Aves Ridge itself. The Pliocene rests unconformably on a reworked sequence of volcanic sands and clays containing Miocene, Palaeocene and Cretaceous fossils. The unconformity corresponds to the only acoustic reflector recorded in the area. The lower sequence was capped by a possibly subaerially weathered surface which may have been, from the mineralogy of the sands, an emergent volcanic prominence. Extensive vertical movements are thus suggested over a very brief time

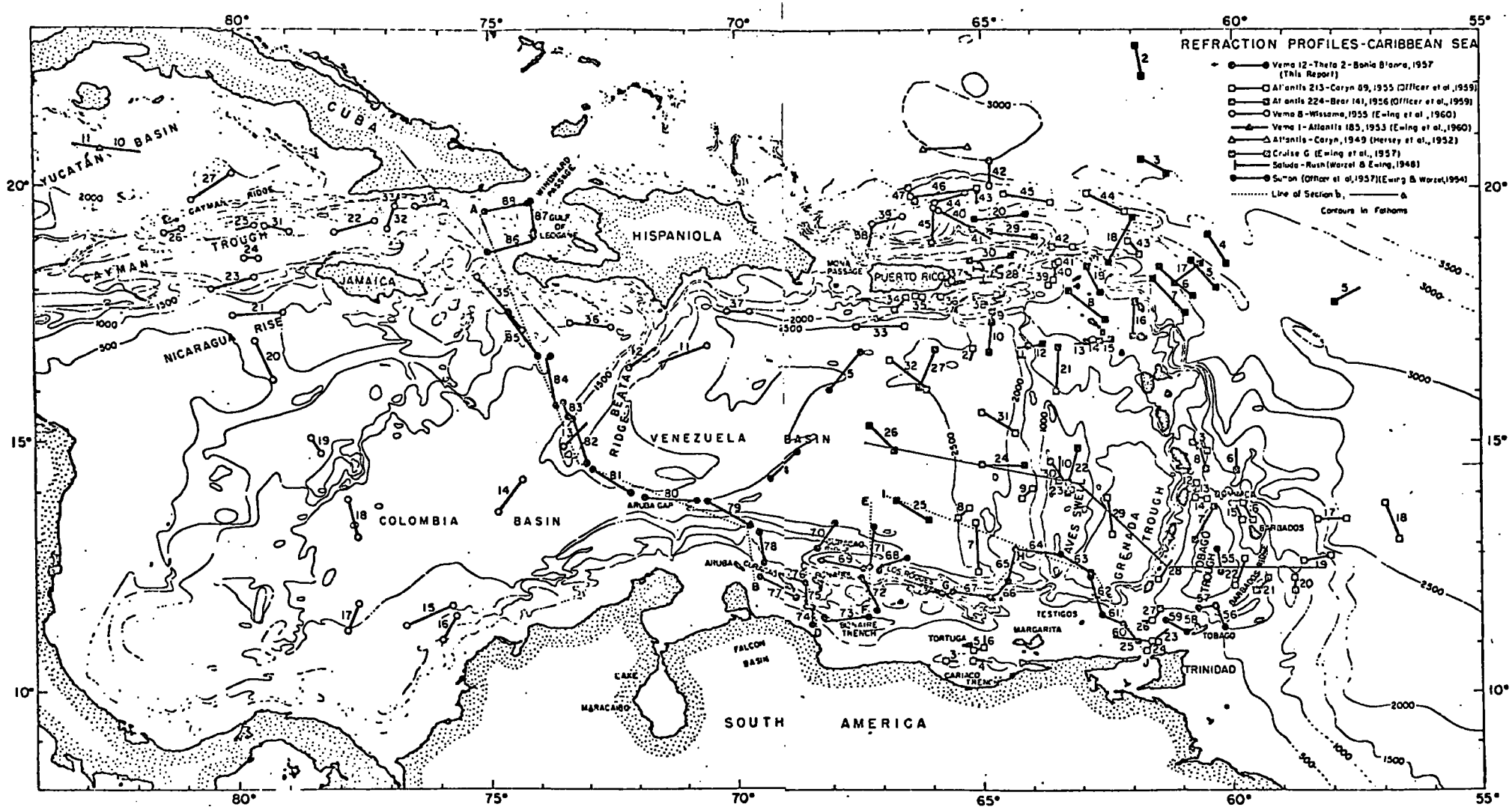


Figure 1-1 : Caribbean refraction profiles in the Caribbean Sea.
(from Ewing et al., 1971a)

span. The unconformity was not encountered at site 30, leg 4, and such differences make generalisations on the history of the Ridge difficult.

Purrett (1971) has reported on the oldest ages encountered in several of the sites of leg 15. The oldest sediments have given ages between 75 and 80 m.y., which contrast surprisingly with the 180 m.y. ages from the north Atlantic. This has severe implications as to the origin of the Caribbean. Confirmation of these ages by potassium-argon dating of the basalts would be highly desirable.

The other sites investigated during this leg, namely 147 (Cariaco Trench), 151 & 153 (Beata Ridge), 152 (Nicaragua Rise) and 154 & 154A (Panama) are not directly relevant to the eastern Caribbean, although the identification of the reflector B" as basalt at site 153 is discussed in a later section.

1.4.3 Seismic Refraction and Crustal Structure

The technique of seismic refraction gives a broad view of crustal layering and is insensitive to small scale variations of structure. It is essentially complimentary to the seismic reflection technique which gives good definition of small scale structures with far less penetration.

A summary of seismic refraction surveys in the Caribbean is given in Edgar et al. (1971a), and their composite chart is reproduced here as fig. 1-4. The refraction results of Edgar et al. (1971a) and Officer et al. (1959) were used in the present work for controls on magnetic and gravity interpretations.

The crust of the Caribbean is anomalous in that it conforms neither to classical concepts of true oceanic nor true continental types of crust and seems to be transitional between the two. Although the

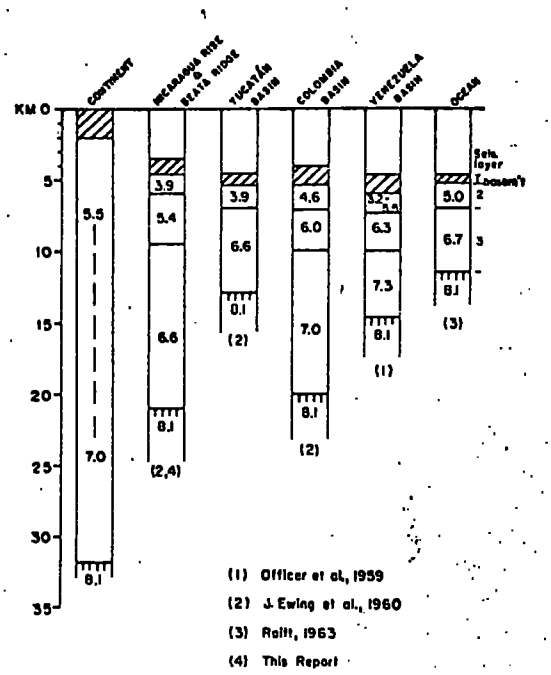


Figure 1-5 : Comparison of velocity structures of Caribbean basins and ridges with those of continents and ocean basins.(from Edgar et al.,1971a)

crust under the Yucatan Basin is similar to typical oceanic, both the Colombia and Venezuela Basins are markedly different. Fig. 1-5, reproduced from Edgar et al. (1971a), illustrates this well. Both show a greater sediment thickness than oceanic crust, although this is to be expected for a small, enclosed basin. Although a typical crustal thickness in the Colombia Basin is 20 km. and in the Venezuela Basin 15 km. both show similarity in velocity structure. The Venezuela Basin typically has 1 km. of sediments overlying a layer of similar thickness with velocities from 3.2 to 5.5 km/sec. This layer may be sedimentary in part. Below this a 6.3 km/sec. layer extends down to approximately 10 km. and overlies the lowest crustal layer with a velocity of 7.3 km/sec. Below the Moho, normal mantle velocities of 8.1 km/sec. have been recorded.

The correlation of Caribbean with typical oceanic crust is uncertain. Ocean basins typically exhibit two hard rock crustal layers of 4-6 km/sec (layer 2) and 6.3-7.3 km/sec (layer 3) overlain by approximately 500m. of sediment, whereas the Caribbean exhibits three. Ewing et al. (1970) discuss possible correlations and conclude that the upper Caribbean layer may be equivalent to layer two and the lower two equivalent to layer three, or the middle layer is the layer two equivalent and is covered by a thick high impedance layer not found in the oceans. Other major differences are lack of linear magnetic anomalies and the presence of a <u>smooth</u> basal seismic reflector.

The Aves Ridge is underlain by crust of similar structure to the Venezuela Basin, with the 6.2 km/sec layer thickening to cause the major topography (Edgar et al., 1971a). This is also the case for the Lesser Antilles arc. This crustal layering is markedly different from that found under the Nicaragua Rise and Beata Ridge (Edgar et al., 1971a). The Grenada Trough is also similar to the Venezuela Basin.

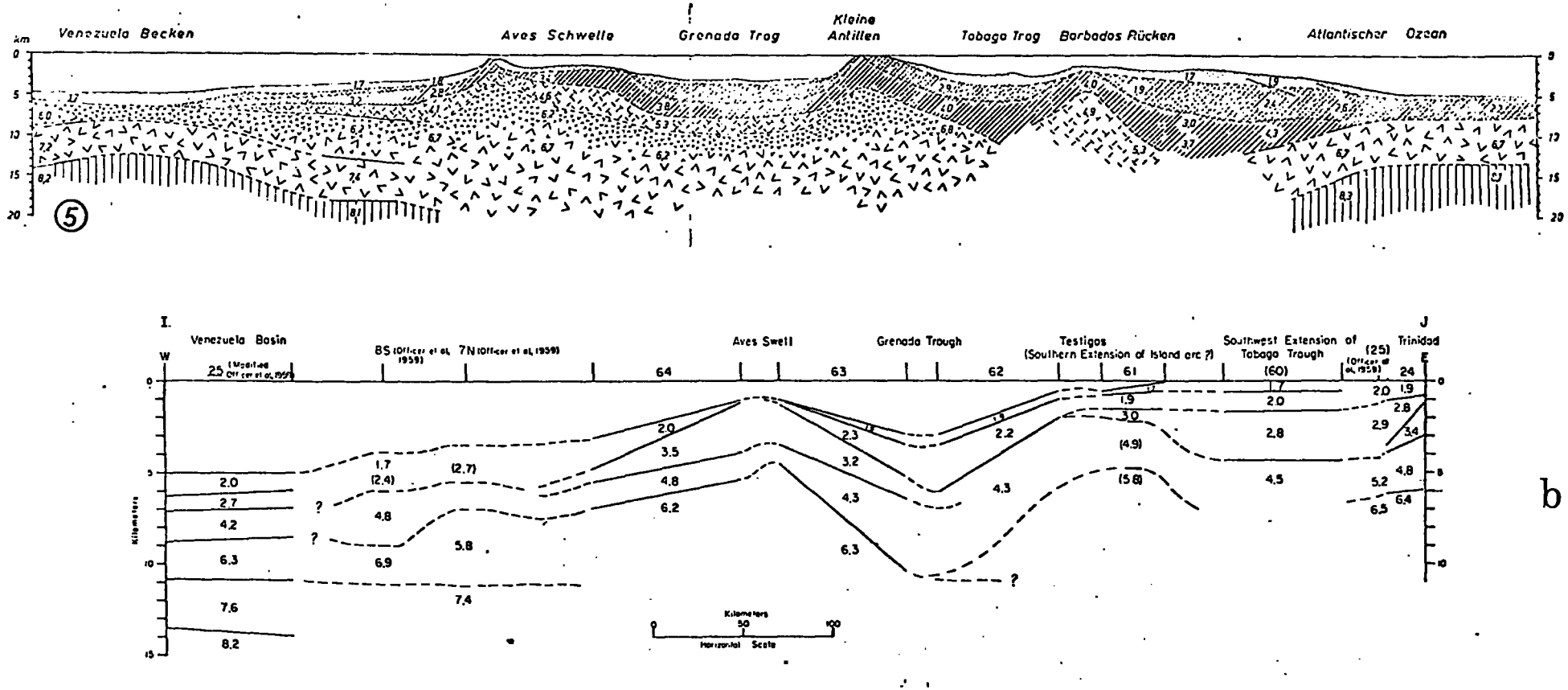


Figure 1-6 : Crustal sections across the eastern Caribbean. For the location of the sections see figure 1-4.
(a - from Officer et al., 1959, b - from Edgar et al., 1971a)

The Moho has not been recorded under the Aves Ridge, Grenada Trough or Lesser Antilles. This is probably due to inadequate ship to shot distances. However, Aggarwal et al. (1972) have recorded anomalously low mantle velocities behind the Tonga Arc and it is possible, but not probable, that this situation could apply under the Grenada Trough.

Two composite crustal sections compiled from seismic refraction data by Officer et al. (1959) and Edgar et al. (1971a) are presented here as fig. 1-6 and summarise well the crustal structure of the eastern Caribbean.

Menard (1967) has attributed the crustal thickness of the Caribbean to addition of rising mantle differentiates to normal oceanic crust, while Hess (1960) considered partial serpentinisation of mantle material to be a contributing factor. Ewing et al. (1957) also conclude the Caribbean is derived from oceanic crust. Škvor (1969), however, considers that the Caribbean was originally continental crust which was intruded by melted ultrabasic and basic material derived from the upper mantle causing the sialic crust to partially dissolve to give a crust of basaltic and andesitic composition. The resulting disequilibrium caused movements and finally andesitic volcanism. This last hypothesis seems unlikely. Certainly Wilson's (1966) idea of 'ice-rafting', whereby the Caribbean was formed by one oceanic plate's sliding over another does not deserve serious consideration for such a large area.

1.4.4 Heat flow

Of nine heat flow measurements documented for the eastern Caribbean (Nason & Lee, 1964, Vacquier & Von Herzen, 1964, Simmons & Horai, 1968), all values but one lie between 1.1 and 1.4 microcal/cm.$^2$sec. The anomalous value is 2.0 microcal./cm.$^2$sec. Thus no strong heat flow

anomalies are present in this area and Epp et al. (1970) have noted that the average heat flow in the Venezuela Basin is nearly the same as the average for all ocean basins.

### 1.4.5 Seismicity

The eastern Caribbean margins are highly active seismically, with events recorded since 1536 (Robson, 1964). More recent studies of epicentres and fault plane solutions have proved instructive in the definition of the boundaries of the plate (Sykes & Ewing, 1965, Molnar & Sykes, 1969). Sykes & Ewing (1965) have produced a chart of earthquake epicentres for 1950 to 1964.

The boundaries of the Caribbean plate are marked by an almost continuous zone of seismic activity with the central areas nearly aseismic. The implication is that the plate itself is relatively stable and that activity is caused by interaction of plate boundaries. The gap in seismicity in northern Venezuela has already been discussed, although absence of events may be due to the time interval of observation since Fielder (1961) has described several events in this area prior to 1950 when Sykes & Ewing's (1965) observations commenced. However, Sykes & Ewing (1965) discuss the possibility of this area's being a separate earthquake province.

Analyses of focal mechanisms for the circum-Caribbean seismic zone show that the movements on the Cayman Trough and Puerto Rico Trench are predominantly left-lateral strike-slip, while motions on the Middle America Trench are predominantly dip-slip. The events in northern Venezuela are usually associated with the major fault zones discussed previously and although several fault plane solutions for events in this area give right-lateral strike-slip movements, the configuration of the known outcrops of the faults, especially in northwest South America, does not seem to conform to a consistent

pattern. A recent study by Dewey (1972) on the seismicity of western Venezuela argues strongly for right-lateral movement on the Boconò fault and that the Caribbean and South American plates are not welded. His data suggest that this southern boundary has changed in position during the last five million years and this change may have commenced dextral motion on the Boconò fault.

The area around northern Trinidad has been interpreted as a region of hinge faulting by Isacks et al. (1969). The Atlantic plate is underthrusting the Caribbean plate in a westerly direction along a zone parallel to the Lesser Antilles. Focal mechanisms indicate dip-slip motions on a plane dipping from 40° to 60° west with events confined to a zone about 50 km. wide and extending in places to depths in excess of 200 km. Gravity studies (present worker) and preliminary results of the Durham seismic project of 1972 (G.K. Westbrook, pers. comm.) suggest that the dip of the underthrust Atlantic plate beneath Barbados is as little as 1°, necessitating a rapid increase in dip under the Lesser Antilles. This simple concept of underthrusting is confused at the northern end of the arc since intermediate depth earthquakes beneath Puerto Rico suggest an island arc structure extending east-west parallel to the trench. Cessation of volcanic activity in the Greater Antilles from Eocene onwards (Monroe, 1968, MacGillavry, 1970) suggests that this area is not now related to the volcanic arc, although the possibility of a genetic relationship (Malfait & Dinkelman, 1972) must not be discounted.

Using several different techniques, Molnar & Sykes (1969) have estimated the rate of underthrusting under the Lesser Antilles to be between 0.5 and 2.2 cm/year, with rates for the Middle America region rather higher, between 2.0 and 9.1 cm/year.

The area of the eastern Caribbean covered by this thesis is thus shown to be virtually seismically inactive, although the location of two events on the Aves Ridge (Molard, 1952, Sykes & Ewing, 1965) will be discussed later. This absence of earthquakes implies a now stable structural configuration of Venezuela Basin, Aves Ridge, Grenada Trough and Lesser Antilles.

# CHAPTER 2

# THE SURVEYS

## 2.1 Introduction

The track charts and limits of the 1971 and 1972 survey areas are shown in fig. 2-1. The 1971 area was defined by 12°54'N, 13°54'N, 65°00'W and 61°00'W and abuts at its eastern end onto another area surveyed by Durham University in 1971 between the same latitude limits east to 57°00'W (Westbrook, 1973). The 1972 area is continuous northwards with the 1971 area and is defined by longitudes 64°30'W and 61°40'W north to 16°10'N. The width of the survey area decreases slightly in the north where the Aves Ridge narrows, and these narrower limits were considered sufficient to define the anomalies of the Ridge.

## 2.2 Navigation

Navigation for both surveys was by Lambda, a Decca phase comparison system. Slave transducers were erected on the islands of St. Lucia and St. Kitts by the Royal Navy allowing adequate triangulation from the master transmitter on the ship. The accuracy of the system is dependent on its accuracy of calibration and for these surveys fix positions were considered to be accurate to 200m. (B. Earle, pers. comm.). The system was found to suffer from sky-wave effects during 1972 and so the track lines for this survey do not represent time-sequential lines as it was necessary to arrange the ship's schedule so as to survey the area farthest from the slave transducers during daylight. Other navigational aids used during the survey were satellite navigation, which is not particularly accurate

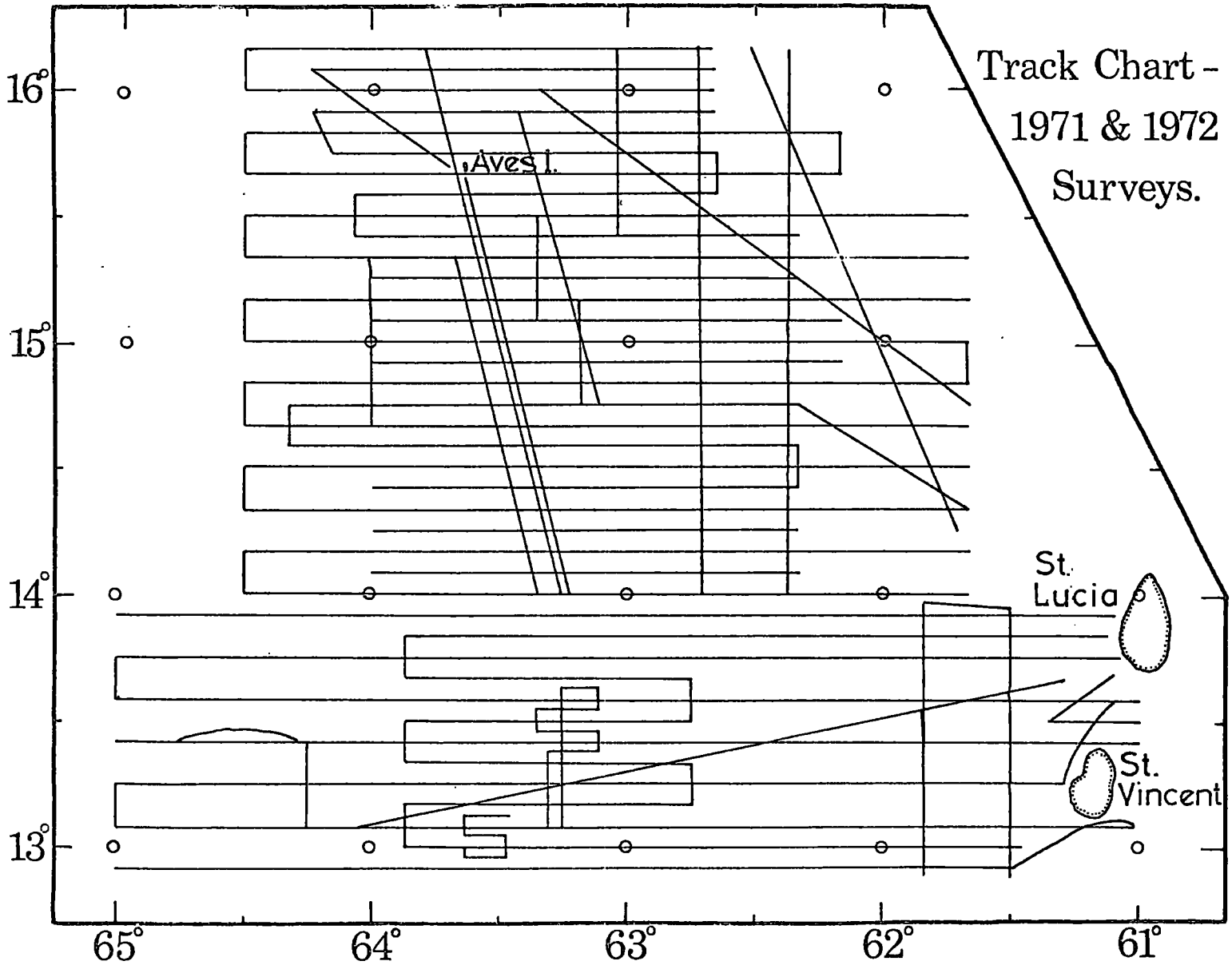
Track Chart -
1971 & 1972
Surveys.
Aves I.
St.
Lucia
St.
Vincent
16°
15°
14°
13°
65°
64°
63°
62°
61°

Figure 2-1

in this region, and radar when in sight of land.

The accurate navigation by Lambda enabled 10 n. mile spacing of east-west lines across the survey areas. Interlines giving 5 n. mile spacing were controlled by the 1000 fathom isobath for the 1971 survey, but were extended in 1972 to obtain better definition of the magnetic anomalies produced by the Aves Ridge. In addition, several north-south lines were run, the line through Aves Island coinciding with one of the seismic refraction lines run by Durham University earlier in the field season.

## 2.3 Instruments

Depths were recorded continuously while on survey using a precision depth recorder, with receiver either hull mounted or towed beside the ship, and were considered accurate to 3 m.

Total field magnetic variations were monitored with a Bassinger proton precession magnetometer, belonging to the Royal Navy, towed behind the ship. Some lines lack magnetic data on the 1972 survey due to the cable and fish suffering severe damage from sharks. The instrument is considered accurate to one gamma, although it spiked occasionally when other equipment was switched on.

Gravity was measured with an Askania gravity meter, belonging to the Royal Navy, mounted on a stabilised table near the ship's centre of gravity. A summary of techniques of gravity measurement at sea is given by Lacoste (1967). On the 1971 survey, the meter was run in manual mode whereby the upper spring is turned manually to keep the analogue trace within limits. This mode was used since it was considered that the extreme gravity gradients expected over the island arc would cause severe off-levelling errors in automatic mode, whereby a servo-motor adjusts the upper spring. The 1972

survey was run in automatic mode. Tests were performed on survey by repeating lines at different speeds to check repeatability of results over high gravity gradients on the Aves Ridge. This was possible due to the accuracy of navigation and the direct reduction to free air anomaly on line by one of the ship's computers.

The results of five such tests are given in fig. 2-2. It was observed that repeatability of lines run at 12kts. with those run at slower speeds is not good, the effect being to truncate gravity peaks and cause a lag in response to the anomaly. For lower gradients 12 kts. was accepted as a reasonable survey speed. Lines run at 8 kts. show good repeatability with those run at slower speeds, although some detail is lost. The 200 m. accuracy of navigation may have caused some distortion of results, especially over such localised anomalies, but results are considered good. Thus it was decided to run the ends of east-west lines at 12 kts. and to slow down to 8 kts. over a ten minute period when approaching the steeper gravity gradients of the Aves Ridge. This ten minute period was found to be adequate to keep off-levelling errors, due to deceleration or acceleration of the ship, to a minimum.

On the 1971 survey, an air gun seismic reflection profiling system was used on three lines at 12°54'N, 13°24'N and 13°54'N. Whereas gravity and magnetic lines in 1971 were run at 12 kts., the profiling lines were run at 6 kts. The system used was developed at Durham University by Mr. J.H. Peacock. Equipment breakdown caused all three lines to be incomplete. The acoustic source was developed from air guns, mounted either singly or doubly on a frame towed just aft of the ship, which discharged compressed air from an engine room compressor when triggered electronically. The seismic signals were received at an array of hydrophones 200 m. long consisting of two, hundred instrument, sets towed 200 m. astern. The signals from each

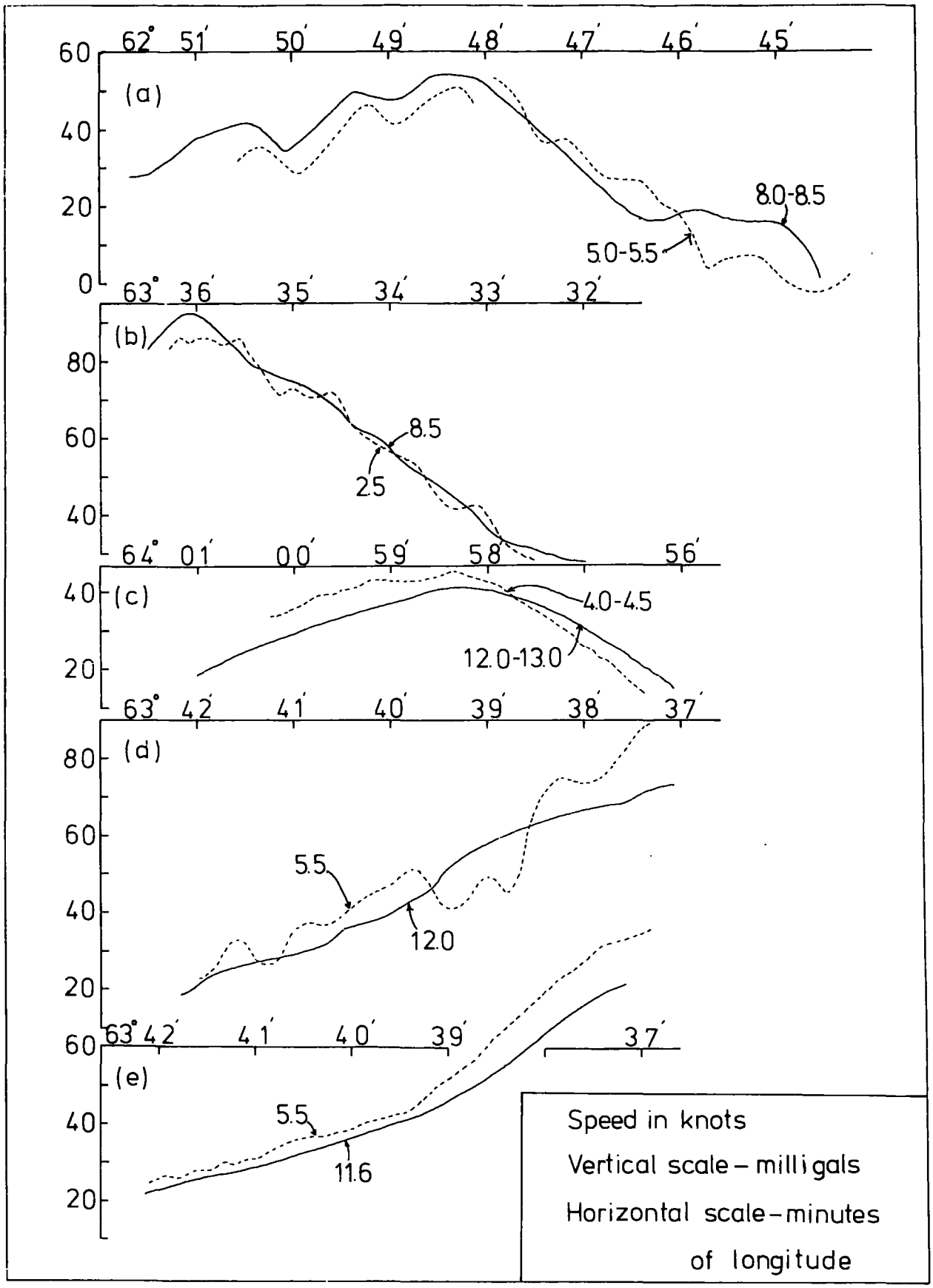


Figure 2-2 : Tests on gravimeter in automatic mode.

hydrophone set and timing marks were recorded both on magnetic tape at 1 7/8 i.p.s. and on photographic paper using a geospace recorder. The triggering interval was 17 seconds for the major part of the lines.

## 2.4 Data Processing

### 2.4.1 Gravity

During the 1971 survey, three base stations were used in the calculation of gravimeter drift:

| Station | Gravity (mgal) |
|---|---|
| 1. Castries, St. Lucia | 978528.9 |
| 2. Admiral Brion Wharf, Willemstaad, Curaçao | 978441 |
| 3. Kingstown Harbour, St. Vincent | 978491.5 |

The value at Curaçao is approximate, as it was impossible to locate the previously documented base station.

The drift rates were:

| Period | Stations | Drift | Drift/day |
|---|---|---|---|
| S.D. 180 - 204 | 1 → 2 | 6.0 mgal. | 0.25 mgal. |
| S.D. 210 - 214 | 2 → 3 | -1.1 mgal. | -0.25 mgal. |

It was hoped to tie in the gravimeter at Castries during the period S.D.180 to 204, but a water shortage in northern St. Lucia necessitated the ship's docking at Vieux Fort in the south. In fact the ship docked twice in Vieux Fort during this period on S.D.'s 193 and 197. The drift during this period was -0.07 mgals/day, but

this could not be incorporated in the above drift rates since the berth had not been calibrated and logistical problems prevented the present investigator from doing this himself.

Where the ship's berth was sufficiently far from the base station, a Worden gravimeter, owned by the Royal Navy, was used in tying in the ship's instrument. A height correction was applied to correct for elevation of the ship's meter above the station level.

During the 1972 survey, as well as stations 1 and 3, two other stations were used in calculation of gravimeter drift.

| Station | Gravity (mgal) |
|---|---|
| 4. No.34 bollard, Deep Water Harbour, Bridgetown, Barbados | 978295.6 |
| 5. 5th bollard from end of new railway wharf, Kingston, Jamaica | 978598.4 |

Station 4 was established using a station at Ocean View Hotel, Bridgetown. The new site alongside the ship's berth was not perfect due to much microseismic noise but is considered correct to 1 mgal. Station 5 was established from a station at the now demolished Hanover Wharf, Kingston, Jamaica.

The drift rates were:

| Period | Stations | Drift(mgal) | Drift/day |
|---|---|---|---|
| S.D. 117 - 126 | 1 → 1 | +0.1 | +0.01 |
| 129 - 140 | 1 → 1 | -3.1 | -0.28 |
| 140 - 141 | 1 → 4 | -0.4 | -0.6 |
| 141 - 148 | Period moored in Barbados | +2.3 | +0.32 |
| 148 - 162 | 4 → 3 | -5.9 | -0.42 |
| 165 - 179 | 3 → 5 | -2.8 | -0.20 |

Throughout both surveys drift rates were thus low.

During both surveys shipboard computers were used for processing of data. For the 1971 survey, the automatic data logging computer (ADL) was used on line to convert navigational co-ordinates to latitude and longitude and to digitise magnetic observations at one minute intervals. The analogue gravimeter trace was digitised manually and the satellite navigator computer used off-line for reduction to free air anomaly. During the 1972 survey the ADL was used on line for gravity reduction, this being possible only in automatic mode. A punched paper tape record was produced on line, copies of which were obtained for analysis in Durham.

The reduction from free air anomalies, drift corrected, to Bouguer anomalies was performed in Durham using the N.U.M.A.C. I.B.M.360/67 digital computer. Since the Aves Ridge and Grenada Trough approximate well to a two-dimensional system striking north-south, it was decided to apply a two-dimensional type of Bouguer correction. Peter (1972) has shown the necessity of such a correction in areas of rough topography since the difference between two-dimensional and simple slab-type Bouguer corrections (Nettleton, 1940) can be as great as 40 mgal. The reduction is essentially the calculation of the gravitational effect of sea water corrected to the desired density at each datum point and its addition to the free air anomaly. This computation was performed approximating the body of sea water to a polygon with corners defined by digitised bathymetry and using the summation of attractions of semi-infinite prisms defined by edges for computation of the gravity attraction at each datum point after the fashion of GRAVN (Bott, 1969a). The basic routine, subroutine GRAV, is listed in Appendix 1. Data not on east-west lines were either incorporated into the nearest line or reduced with a simple slab-type correction.

The density chosen for the Bouguer reduction was 2.00 gm/cc. This value corresponds to the upper layer of sediments covering the area and the Bouguer anomaly so obtained is for a structure of increasing density with depth. This correction is also most convenient for interpretation, since the upper sedimentary layer is effectively incorporated into the correcting body of sea water.

The Bouguer correction was applied to the free air anomaly digitised at ten minute intervals, which was considered adequate for contouring purposes.

Cross-over errors in the free air anomalies were as follows:

| Survey | No. cross-overs | Mean cross-over error | Standard Deviation |
|---|---|---|---|
| 1971 | 38 | 4.1 mgals. | 3.0 mgals. |
| 1972 | 137 | 2.8 mgals. | 2.2 mgals. |

In spite of possible navigational errors, cross-over errors are considered good. Since the ship was large and stable, sea conditions calm, and navigational control good, cross-coupling, off-levelling and navigational errors are considered small for east-west lines. For north-south lines, however, Eotvos corrections are critical since heading direction errors induce a greater percentage error than for east-west lines. However, it is considered that the majority of calculated anomalies are correct to within a conservatively estimated four milligals.

2.4.2 Magnetic Observations

Total field magnetic observations were extracted at 10 minute intervals from the ADL tapes and are considered accurate to one gamma. For both the 1971 and 1972 surveys, secular variation of the earth's

magnetic field was removed by the subtraction of a regional background calculated for each datum point from the International Geomagnetic Reference Field (I.G.R.F.). A computer program REGMAG (Durham University computer program) was used to perform this calculation, which expresses the earth's main magnetic field as a spherical harmonic equation of the eighth order, and calculates the regional value for coefficients for the epoch 1955-1972. The I.G.R.F. increases to the NNW in the survey area with a mean value of 40,000 gamma and a gradient of 6 gamma/km. Anomalies with respect to this field are normally negative, and Peter (1972) has found them to be 160 gamma below a mean value for the eastern Caribbean.

For the 1971 survey, an attempt was made to remove the short period magnetic variations due to diurnal variation. Riddihough (1971) has made an assessment of the errors involved in such corrections. In the absence of a magnetic observatory in close proximity to the survey area, it was necessary to use results from two observatories flanking the area to north and south. The available observatories were at San Juan, Puerto Rico (18°09'N, 67°07'W) and Paramaribo, Surinam (05°49'N, 55°13'W) (Annals of Int. Geophys. Year, 1969).

In order to apply the results from these distant observatories to the survey area, corrections for both latitude and longitude are necessary.

The latitude correction was applied by scaling the magnetograms by a factor representing the ratio between maximum observed diurnal variation at observatory and survey area. These values were obtained from curves published by Matsushita (1967).

Roden & Mason (1965) have experimented on shipboard magnetic diurnal corrections for two observatories at approximately the same latitude as the survey area in the Indian Ocean, and have concluded

that a longitude correction based on a weighted mean is the most satisfactory. Although this method may lower amplitude, phase prediction, which is of critical importance, is accurate. For observatories X & Y, whose magnetic variations are represented by the equal interval time series $x_0, x_1 \ldots x_n$ and $y_0, y_1 \ldots y_n$, and an intermediate station P defined by a time series $p_0, p_1 \ldots p_n$,

$$p_k = wx_k + (1-w)y_k$$

where $$w = (g_p - g_y)/(g_x - g_y)$$

w is the weighting function and $g_p$, $g_x$, $g_y$ the longitudes of P, X & Y respectively. The method of diurnal and secular variation corrections was as follows:

i) Digitisation of magnetograms at hourly intervals and conversion into gamma values from a base line
ii) Conversion to total field values
iii) Subtraction of I.G.R.F. from total field values to correct for temporal secular variations at the observatories using REGMAG
iv) Cubic interpolation to give 10 minute values
v) Scale values for latitude
vi) For each datum point, application of longitude scaling factor
vii) Subtraction of calculated diurnal variation and I.G.R.F.

The process was lengthy and had to be performed in several steps. Since I.G.R.F. values were subtracted from the magnetograms of the observatories, the anomalies finally produced are no longer with respect to the I.G.R.F. but are shifted by a constant factor dependent on the local anomalies at the observatories. Consequently a factor of 200 gamma was subtracted from all observed values to correct for this.

Cross-over errors for the 1971 survey were as follows. Of 32 cross-over points, the average value of error of uncorrected data was 14 gamma, with standard deviation 16 gamma, while for corrected data the average value was 13 gamma, with standard deviation 16 gamma. The method thus caused only a slight decrease in cross-over errors and it was decided not to apply the correction to 1972 data for both this reason and the time factor.

During the 1972 survey, the mean cross-over error for 93 points was 20 gamma with standard deviation 16 gamma. This low value is taken to vindicate the non-application of a diurnal correction.

2.4.3 Seismic Profiling

During the 1971 survey a reflection profiler was used on three lines. Original records were very poor in quality due to the ship's cathodic protection imparting two harmonics of noise of 50 and 100 Hz to the system.

Magnetic tapes produced on survey were processed in Durham, and it was found that optimum results were obtained by stacking the channels of the two hydrophone sets and using a band pass filter of 20 to 60 Hz. The original record was also compressed.

For display purposes the processed records were digitised with a D-Mac pen follower to produce paper tape containing coordinates representing all principal reflecting horizons. The tapes were used as input data to a plotting routine written by Mr. G.K. Westbrook which produced scaled line drawings on the peripheral cal-comp plotter of the N.U.M.A.C. I.B.M. 360/67 computer.

## 2.5 Data Handling

The large amount of data amassed during two seasons of surveying required an economical method of data storage. A final card copy of all data was produced, one card per datum point, containing the following information:

i) Day and Time of observation
ii) Latitude and longitude degrees and minutes
iii) X and Y co-ordinates from a selected origin
iv) Depth in kilometres
v) Free air anomaly
vi) Bouguer anomaly
vii) Total field magnetic reading
viii) Magnetic diurnal correction, where applied
ix) Magnetic anomaly

A convenient format for the data card was found to be:

(I3, I5, 2X, 2(F3.0,F6.2,1X), F7.3, F8.3, F6.3, 2F6.1,F7.0, 2F5.0)

The X & Y co-ordinates were calculated from an origin of 12°45'N, 65°00'W with X & Y increasing east and north respectively. Distances were calculated from a spherical earth approximation and a flat earth approximation used in all interpretations.

Each east-west line is identified by a name consisting of a letter and number. The letter refers to a long line (L) or interline (S) and the number to its approximate latitude. Thus L1530 refers to a long line at 15°30'N.

## 2.6 Presentation and Description of the Survey Charts

Charts of bathymetry, free air anomalies, Bouguer anomalies and total field magnetic anomalies with respect to the I.G.R.F. are

contained in the pocket at the back of this volume.

All charts were originally drawn to a scale of 1:200,000 and the charts presented are photographic reductions of original charts, drawn to a scale of 1:1,000,000.

Contours are based on data from the ship's tracks presented in fig. 2-1.

2.6.1 Bathymetry

The Venezuela Basin slopes gently up to the Aves Ridge from a mean depth of 3600 m., although the slope increases markedly onto the western flank of the Ridge. Extremely rough topography was encountered on this western slope between 15°N and 16° N, which could not be contoured at 200 m. intervals. This feature was unexpected and has not been recorded on previously published bathymetric charts.

The western flank of the Aves Ridge is marked by a series of north-south trending ridges which include the aforementioned region of rough topography. In the south, a large, flat topped seamount occurs centrally on the Ridge, and has been described by Marlowe (1971). Several small circular to subcircular features are apparent on the central and eastern parts of the Ridge. Aves Island lies on a broad, north-south ridge exhibiting steep gradients especially in its northern part around the island. Two seamounts southwest and southeast of Aves Island have been investigated by Nagle (1971).

The eastern flank of the Aves Ridge is marked by very steep gradients in the south, but north of 15°N the boundary between Aves Ridge and Grenada Trough is difficult to define on bathymetric data alone.

The southern Grenada Trough exhibits extremely subdued topography, with depths deviating by no more than a few metres from its mean value.

North of 14°30'N the topography is far more rugged and depths are similar to those over the Aves Ridge. The extreme flatness of the southern Trough is indicative of a substantial sediment cover, while the probable thinning of this cover in the north is indicative of a sediment source south of the survey area, probably the Orinoco river of Venezuela.

The Lesser Antilles lie on a narrow ridge rising abruptly from the Grenada Trough.

2.6.2 Free Air Anomalies

In the southern Venezuela Basin mean free air anomalies are zero. This is not in accord with the regional value of approximately -25 mgal. suggested by Talwani (1970) from satellite data, although it is possible that the Aves Ridge is still contributing a finite gravitational attraction at the western part of the 1971 survey area where the values of zero milligals were monitored. The free air anomalies decrease as the Aves Ridge is approached, which is probably due to the presence of a mass deficiency underlying the Aves Ridge.

The Aves Ridge is characterised by positive free air anomalies, negative anomalies being recorded only rarely. Steep gradients were monitored over positive bathymetric features, and anomalies in excess of 80 mgal. were recorded over several of these prominences. No regional north-south anomaly trend is apparent.

The eastern flank of the Aves Ridge in the south is represented by a steep free air gradient, while in the north the boundary with the Grenada Trough is far less clearly defined.

The Grenada Trough is characterised by low free air anomaly gradients. There is a regional trend from south to north, with anomalies increasing from values less than -70 mgal. in the south

to small positive values in the north. This gradient is greater in the south than in the north. The negative free air anomalies are probably due in part to the presence of mass deficiencies under both the Aves Ridge and Lesser Antilles. Implications of this to isostasy will be discussed in a later chapter.

The Lesser Antilles are marked by extreme free air anomaly gradients and maximum values between the islands in excess of 150 mgal. The abrupt change in gradients observed when passing from the Aves Ridge into the Grenada Trough and from the Grenada Trough onto the Lesser Antilles may be attributed to rapid changes in sediment thicknesses.

2.6.3 Bouguer Anomalies

The Bouguer anomalies were calculated for a density of 2.00 gm/cc for the reasons given in section 2.4.1.

In the Venezuela Basin a regional decrease in anomalies from west to east is apparent, with a regional value in the west of 140 mgal.

Bouguer anomalies over the Aves Ridge still reflect topographic features although this is to be expected from the density employed in the reduction. However, the steep free air gradients observed on the flanks of the Ridge are no longer apparent.

Bouguer anomalies increase northwards in the Grenada Trough, from 50 mgal. in the south to a maximum at c.14°20'N whence there is a gentle decrease northwards. The anomalies in the Grenada Trough are of the same order of magnitude as those over the Aves Ridge.

The steep free air gradient over the island arc is decreased in slope after Bouguer correction.

2.6.4 Total Field Magnetic Anomalies

The magnetic anomalies of the region under study are complex.

There is no evidence of magnetic lineations of the type found in the major ocean basins (Vine & Matthews, 1963).

Gradients are low in the Venezuela Basin, and the sub-circular features observed in the south are probably related to either changes in magnetisation contrast in the basement or basement domes such as those described by Ewing et al. (1965).

Gradients are higher over the Aves Ridge since basement features are at a relatively shallow depth. Little direct correlation is apparent between bathymetric features and magnetic anomalies, in particular the line of north-south ridges defining the western edge of the Aves Ridge do not register on the magnetic anomaly chart. Magnetic anomalies in the eastern Caribbean are usually negative with respect to the I.G.R.F., but one feature on the southern part of the Aves Ridge has anomalies in excess of +150 gamma.

Gradients are low in the Grenada Trough, which exhibits quite a smooth magnetic field. The mean anomaly of approximately -200 gamma is usually greater than the anomalies of the Aves Ridge.

# CHAPTER 3

# INTERPRETATION TECHNIQUES

## 3.1 Introduction

The ability to calculate the magnetic or gravity anomaly caused by a given body is fundamental to most interpretation procedures and the majority of techniques used in interpretation of data in this thesis are based on these simple calculations.

All computations were performed on the Northumbrian Universities Multiple Access Computer (NUMAC), an I.B.M. 360/67. The principal language employed was FORTRAN IV, although use was made of programs written by other workers in PL1.

## 3.2 Indirect Method of Interpretation

The methods of calculating the magnetic or gravity anomalies over two-dimensional bodies have been adequately described elsewhere (Al Chalabi, 1970, Laving, 1971) and are based on the method of approximating the body to a polygon and summing the effects of semi-infinite slabs with an edge bounded by each side of the polygon for each field point (Talwani et al., 1959). In their simplest form these computations have been programmed in PL1 and named GRAVN and MAGN (Bott, 1969a & 1969b). These basic programs were usually used on a starting model before the use of a more sophisticated interpretation procedure and, in the case of bodies of simple shape, were found sufficient in themselves to produce adequate interpretations by manual adjustment of parameters. For simple magnetic anomalies a comparison of shape and amplitude of observed anomalies with anomalies calculated for bodies with

different magnetisation angles was sometimes found sufficient to constrain the angle and intensity of magnetisation. The curves produced by Reford (1964) for magnetic anomalies over thin sheets were useful in this respect.

## 3.3 Non-Linear Optimisation

Non-linear optimisation is a process whereby a function value is minimised by the automatic adjustment of variable parameters defining the function. The principle use in geophysics is the minimisation of the difference between an observed anomaly and the anomaly calculated from a body defined by variable parameters. Al Chalabi (1970) has presented several applications of non-linear optimisation to geophysics.

Although a relatively inefficient technique, non-linear optimisation provides the only method of interpretation of bodies of complex configuration without recourse to several steps. Where, however, causative bodies could be considered as having only one density contrast or one intensity and angle of magnetisation, the matrix methods described in section 3.4 are several orders more efficient.

The optimisation procedures used were contained in a computer program MINUIT (CERN, 1970), a main program for which the user provides a subroutine calculating the function to be minimised. Subroutines for magnetic and gravity optimisations are given in Appendix 1. Three optimisation procedures are available, Monte Carlo, Rosenbrock and Davidon. The Monte Carlo method (James, 1968) involves the calculation of the function to be minimised a given number of times during which all variable parameters are chosen randomly according to Gaussian distributions centred at the starting value with widths equal to a specified parameter error. The Rosenbrock method

(Rosenbrock, 1960) is an extension of co-ordinate variation whereby minimisation proceeds by mapping the function value minima in multi-dimensional space. The Davidon method (Davidon, 1968) is based on a variable metric method and proceeds towards a minimum by making successive approximations to the covariance matrix. It has been found that the Monte Carlo method is most suitable when no reasonable starting point is known, the Rosenbrock method reasonably fast when far from a minimum and converges well, and the Davidon method of use when close to the minimum. It was found that the Rosenbrock method was entirely satisfactory for most magnetic and gravity optimisations where an approximate starting model had been tested with GRAVN or MAGN, although the Monte Carlo method may be useful when many variables are employed. The fine definition of the Davidon method was never required.

The function to be minimised was defined as the sum of the squares of the differences between observed and calculated anomalies. Thus for n values of the observed anomaly, $O_1$ ..... $O_n$, and calculated anomaly, $C_1$ ..... $C_n$, the function to be minimised, f, is defined by:

$$f = \sum_{i=1}^{n} (O_i - C_i)^2$$

f was calculated using either a GRAVN or MAGN type computation (subroutines GRAV and MAG, see appendix 1), written in FORTRAN IV to be compatible with MINUIT, which calculate the effect of a body defined in terms of both variable and constant parameters. Al Chalabi has shown the necessity of adequate definition of the anomaly curve for unambiguous interpretation.

It was found that a weighting factor applied to each observation

point aided minimisation when some data points were more reliable than others or when a peak was only defined by one or two data points in the digitisation of the anomaly, as the ill-defined peak will be 'ignored' in the optimisation procedure. The maximum value of the weighting function, $w_1 \ldots\ldots w_n$, was taken as the approximate maximum expected residual, and f defined as:

$$f = \sum_{i=1}^{n} ((O_i - C_i)w_i)^2$$

Problems of ambiguity will be evident in all but very well defined cases, and although optimisation procedures will produce a minimum, it will only be unique in very well-behaved cases and different starting values of the parameters may well produce a different minimum (Al Chalabi, 1970). In gravity optimisations it is prudent to specify both a regional value and density contrasts if body points are to vary, and regional background, intensity and angle of magnetisation in magnetic optimisations. These conditions may be relaxed if the configuration of body points is reasonably well constrained by other data such as seismic reflection, refraction or spectral analysis of magnetic data. The definition of bodies in terms of both fixed and variable parameters allows incorporation of these other data into the optimising body. The number of variables should be kept to a minimum as it was found that optimisations involving more than about 25 variables were prohibitively costly in computer time. Parameters should be fixed for part of the optimisation process where possible. For example, if both x and z-co-ordinates of body points are both variable, the x-co-ordinates should be fixed

for the first optimisation step and restored to variable status only after the z-co-ordinates have been allowed to vary. Such a procedure was found to greatly enhance optimisation time.

A plotting routine, subroutine OPLOT (see Appendix 1), was incorporated into the user subroutine, displaying observed and calculated anomalies on the line printer. Success of optimisation was found to be far more easily judged from a graphical plot than from a simple study of residuals.

Example execution times are 280 seconds for decreasing f from $0.1482639 \times 10^5$ to $0.9187897 \times 10^2$ for a gravity model with 21 variables, fixing x-co-ordinates for 100 iterations and restoring for a further 100, and 88 seconds for decreasing f from $0.3394827 \times 10^2$ to $0.1789148 \times 10^2$ for a magnetic model with 9 variables, fixing 7 for 70 iterations and fixing 2 only for a further 50 iterations.

In spite of large execution times, both gravity and magnetic optimisations were found to produce good results. All relevant programs are listed in Appendix 1.

## 3.4 Matrix optimisations

Programs using matrix optimisation written by Laving (1971) were used for both magnetic and gravity interpretations of bodies that could be considered as having either one density contrast or a specified intensity and angle of magnetisation. The method involves the division of the source body into a thin layer of blocks defining either the top of the body (for a body with inward sloping contacts) or the base of the body (for outward sloping contacts). The density or intensity of magnetisation of each block is then solved by a least squares procedure to obtain the best least squares fit between

observed and calculated anomalies providing the number of blocks is less than the number of observation points. The blocks are then expanded upwards or downwards until they reach the desired density or intensity of magnetisation, the effect of this new body computed, and the same technique applied to the residual anomalies, fitting blocks of ever decreasing height to top or bottom of each principal block. After about 10 such iterations residuals are usually of the required order. Either the top of the body (for inward sloping contacts) or a point on the top surface (outward sloping contacts) must be specified. The programs, written in PL1, make use of the IBM Scientific Subroutine LLSQ for solution of the least squares problem. The programs actually used were GRAVIT1, GRAVIT2 and MAGGIT4, (Laving).

Very good results were obtained with MAGGIT4, using models of up to 59 blocks and 76 data points, and models were produced giving far more definition than a non-linear optimisation technique, since the number of body points is limited only by the number of data points and not the number of variables. The gravity optimisations proved of more limited use, as it was found that the optimised body caused by only a mildly complicated anomaly was made up of z-co-ordinates which tended to oscillate quite violently. Consequently gravity interpretation was performed using non-linear optimisation except for very simple anomalies.

## 3.5 Magnetic to Gravity transforms

Extensive use was made of the two-dimensional magnetic to gravity transform program TRMG written in PL1 by Ingles (1971). The method entails the solution of the magnetic anomaly in terms of an equivalent layer of blocks of different intensities of magnetisation

by a least squares process using LLSQ by a method similar to Laving's (1971). Each block is then assigned a density proportional to its magnetisation and the pseudogravity anomaly calculated by means of the Poisson equation relating magnetic and gravity potentials. The method is only valid for two-dimensional anomalies for bodies in which the ratio of intensity of magnetisation to density is constant (the Poisson condition).

This program was principally employed to determine angle of magnetisation and estimate intensity of magnetisation by transforming magnetic anomalies to pseudogravity anomalies for varying angles of magnetisation. The pseudogravity anomaly was compared with the observed Bouguer anomaly and correlations with principal troughs and peaks examined. This process was hampered by the strong regional gradients due to the Moho and lowest crustal layer, discussed in a later chapter, but strong correlations were usually easily apparent. An estimate of the intensity of magnetisation was obtained by comparing the amplitudes of pseudogravity and Bouguer anomalies, since estimation of densities was possible from graphs of P-wave velocity and density, the seismic velocities being obtained from refraction data.

The strong regional gradients, which were due to deep, probably non-magnetic, crustal or upper mantle features, precluded the use of Ingles' program SBETA for direct calculation of angle of magnetisation except in very simple cases. Also, the presence of both positive and negative correlations in the same profile would have been masked by this procedure.

Bott and Ingles (1972) give a summary of the technique and its application to the Iceland-Faeroe Rise.

For the area of the eastern Caribbean surveyed, the azimuth and

inclination of the earth's field are 349° and 43° respectively. All magnetic profiles considered were east-west and resolution of the earth's field vector in this direction gives an inclination to the west of 78°. This almost vertical component causes the close correlation between observed gravity and magnetic anomalies for profiles with induced magnetisation, which is a useful guide in interpretation. However, it also causes ambiguities in the estimation of true angle of magnetisation, since it is difficult to differentiate between angles within about 20° to the vertical (see Chapter 6).

## 3.6 Spectral Analysis of Magnetic Anomalies

Spectral analysis provides an independent check on magnetic interpretations since it makes possible an estimation of depths to magnetic structures which are independent of body shape, intensity and angle of magnetisation. Lee (1972) has made a study of the technique and written a computer program performing spectral analysis of digitised magnetic data.

It can be shown that, for a flat magnetic basement containing infinite line sources of random intensities and angles of magnetisation, a graph of the log normalised power spectrum of the magnetic anomaly against wave number will give a straight line plot with slope equal to minus twice the depth to the basement. The method gives spurious results if the anomaly does not contain all representative frequencies and if the record contains noise induced by external sources such as solar activity. The method will give an estimate of depth even for non-flat basements, although this departure from the initial assumptions of the technique must be treated with caution. Total field magnetic observations uncorrected for secular variation could

be used as long as a regression line was subtracted from the data, since this variation is of low frequency. Prewhitening of the anomaly was used in all cases and a Hanning window taper applied to the data. It was considered that some of the spurious results obtained were due, in part, to the slight inefficiencies of this taper although Lee considered it the most effective.

Data for spectral analysis was prepared in the following manner:

i) Translation of ADL tapes from Elliott5 code and extraction of magnetic readings at one minute intervals with their calculated x-co-ordinate from 65°00'W. This one minute sampling produced an interval no greater than 500 m. and in many cases less than 200 m. Since the Aves Ridge is only rarely less than 1000 m. below sea level, this 500 m. maximum was adequate to define all component frequencies

ii) The magnetic data were converted to equally spaced data at an interval compatible with their original sampling by use of a cubic interpolation procedure. During this process readings were examined and spurious fix positions and magnetic spikes removed

iii) The resulting data were input to the spectral analysis routine

Results were satisfactory although had to be critically examined as external noise could lead to spurious results. In cases where the power spectrum did not conform to a straight line, two lines were drawn with maximum and minimum possible gradient to give upper and lower bounds to the depth. It was important to disregard points below the noise level.

## 3.7 Correlation Coefficients

The term correlation coefficient in this thesis refers to the Pearson product moment correlation coefficient (Runyon & Haber, 1967).

For two sets of n data points, $x_1 \ldots x_n$ and $y_1 \ldots y_n$, the correlation coefficient, r, is defined by:

$$r = \frac{\sum_{n} x_i y_i - \frac{\sum_{n} x_i \sum_{n} y_i}{n}}{\sqrt{\left[\sum_{n} x_i^2 - \frac{(\sum_{n} x_i)^2}{n}\right]\left[\sum_{n} y_i^2 - \frac{(\sum_{n} y_i)^2}{n}\right]}}$$

r can take values from +1.00 to -1.00. Positive values refer to positive correlations and v.v. A value of zero indicates no correlation.

The significance of correlations was tested by reference to tables of random correlations expected for a two-tailed test from Runyon & Haber.

## 3.8 Estimation densities from P-wave velocity

For the purposes of gravity interpretation, densities were estimated using curves relating P-wave velocity to density, the velocities being obtained from a seismic refraction line on or near the relevant profile. The curves were obtained from Pálmason (1970), and are a compilation of the results of several workers. The curves

imply ambiguity in density estimation, and usually the best mean value was taken. Errors of the order of 0.1 gm/cc are to be expected. In several cases interpretations were made on models incorporating both upper, lower and mean densities giving end members of possible causative bodies.

# CHAPTER 4

# SEISMIC REFLECTION PROFILING

## 4.1 Introduction

The technique of seismic reflection allows fine definition of shallow structures but with far less depth of penetration than seismic refraction. The use of this technique in the Caribbean has provided much information on the structure and distribution of sediments, which has contributed greatly to knowledge of Caribbean history.

## 4.2 Previous work and general description of sediments

Several reflection profiling lines have been run in the eastern Caribbean, including studies by Ewing et al. (1965, 1967, 1971), Edgar (1968), Bunce et al.(1971), Edgar et al. (1971a) and the U.S. Geological Survey (1972b).

Sediments of the Caribbean show remarkable uniformity in that two principal reflectors are almost always present. These reflectors, named A" & B" for upper and lower respectively, define the bases of two beds of total thickness 1 km. for which the name Carib Beds has been proposed (Ewing et al., 1965). The Carib Beds are internally rather transparent and are overlain by a sequence of acoustically transparent sediments named the younger turbidites, the boundary between them being marked by a much weaker reflector. A diagrammatic illustration of a typical Caribbean sediment section is presented in fig. 4-1. Reflector B" is usually very smooth and has not been considered to represent true basement as it overlies strata with seismic velocities between 3 and 4 km/sec. which are low for igneous rock. The presence of weak sub-B" reflectors (Eaton & Driver, 1967)

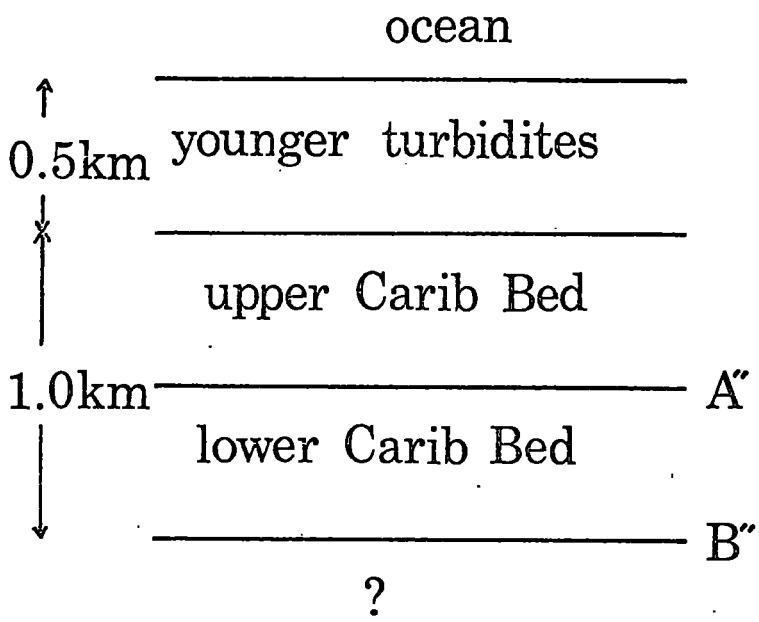


Figure 4-1: A diagrammatic Caribbean sedimentary section.

supports this conclusion. However, basement domes, considered to represent volcanic features, have been described in the Venezuela Basin by Ewing et al. (1967).

Ewing et al. (1965) have described the coring of horizon A" from a fault scarp on the Beata Ridge and its identification as a chert bed of lower Eocene age. By extrapolation of sedimentation rates, the age of B" was placed between upper Jurassic and lower Cretaceous, although this was later disproved by JOIDES investigations. The internal acoustic transparency of the Carib Beds was taken to suggest either high stratification, so that individual reflectors cannot be identified, or partial lithification of the sediments. The former postulate is considered more likely. The impersistent reflectors observed within the Carib Beds have been interpreted as local accumulations of coarser turbidites by Ewing et al. (1965).

JOIDES legs 4 & 15 (JOIDES, 1970, Edgar et al., 1971b) have provided information on the ages and compositions of the sediments and reflectors. Site 29, leg 4 identified the top of the Carib Beds as the boundary between a red zeolitic clay and a radiolarian ooze at 130m. The ooze, which extended to 230m., was of lower upper Eocene to middle Eocene age and was taken to represent the upper part of the Carib Beds. Reflector A" was identified as a lower Eocene chert at 230m. A major hiatus between lower Miocene and lower upper Eocene was taken to refer to the Phase II/Phase III interval (see later). B" was not penetrated, but was assumed to be a chert horizon at about 450m. The Carib Beds were thus identified as a period of pelagic siliceous sedimentation. At site 146/149, leg 15, although the top of the Carib Beds was not distinguished, A" was found to represent the contact of middle and upper Eocene chalks with a chert bed overlying a sequence of lower to upper Palaeocene

chalks at 440m., while B" was probably represented by chert beds dividing Campanian marls and chalks from Campanian-Coniacian radiolarian limestones. At site 150, leg 15, the reflectors were not encountered. Site 153, leg 15, on the Beata Ridge was of interest in that B" was represented by basalt, and so, in this area at least, B" corresponds to true basement.

Reflectors A" & B" have been correlated with both the A & B reflectors of the Atlantic and the A' & B' reflectors of the Pacific. However, dating of these layers in the major ocean basins is less simple than in the Caribbean, for while the A reflector is the top of a middle Eocene chert, A' appears to be a diachronous zone of different lithologies. Edgar et al. (1971a) have indicated the possible diachronaity of A", and, if it everywhere represents a thin chert bed, conclude that it would be a remarkable example of deep sea lithification. Such a chert bed would indicate the availability of free silica concentrated in an extensive,relatively thin layer before diagenetic alteration to the chert.

The central Caribbean Sea exhibits a uniform thickness of the Carib Beds although Edgar's (1968) isopachyte map of sediments shows gentle doming of the sediments in the central Venezuela Basin. The southern margin of the Caribbean is marked by the Carib Beds' dipping under a vast volume of unstratified sediments, almost certainly derived from South America, while at the northern margin the Carib Beds dip under the Greater Antilles to form a marginal trench (Ewing et al., 1965). The presence of reflectors similar to A" & B" on top of intra-Caribbean ridges has been taken to imply the action of vertical movements in their formation. Other possibilities, however, would seem to be deposition on the top of pre-existing structures, which would imply sediment transport in the upper water layers, or the

uplift of the ridges by horizontal compression after deposition of the sediments. The latter possibility is discounted as no evidence of horizontal compression is apparent in the sediment cover of either the basins or the ridges.

Ewing et al. (1965) have identified three phases in the history of Caribbean sedimentation. Phases I, II & III refer to events before, during and after deposition of the Carib Beds. The Caribbean was considered free of deformation during latter Phase I, Phase II initiated a change in sediment type without tectonic deformation with homogenous, transparent sedimentation and Phase III represents the time after the warping of the Carib Beds and their gradual burial by younger turbidites. Both the Aves and Beata Ridges were considered to be elevated near the end of Phase II. JOIDES results indicate the Phase I/Phase II boundary to be Campanian-Coniacian and Phase II/Phase III upper Eocene-Oligocene.

The essential tranquility of sedimentation during Phase II implies shelter from open-ocean circulation since late Jurassic or Cretaceous times (Edgar, 1968). This implies that the Isthmus of Panama and either the Aves Ridge or Lesser Antilles were emergent barriers at this time to restrict Caribbean circulation.

## 4.3 General description of all seismic profiling lines

A total of 15 seismic reflection profiles have been recorded over the eastern Caribbean. These were performed by Bunce et al. (1971), Edgar et al. (1971a), the U.S. Geological Survey (1972b) and Durham University (present work). The approximately east-west profiles extend from a possible extension of the Aves Ridge at 18°N to 12°54'N and provide a reasonably complete picture of the whole region.

All profiles show the western flank of the Aves Ridge to be mantled by the relatively gently rising sedimentary layers of the Venezuela Basin. Identification of A" & B" is not always clear, but reflectors in the Venezuela Basin are usually horizontal with only mild undulations as the Aves Ridge is approached. Identification of basement is never clearly possible.

Basement is always identifiable over the Aves Ridge and in places crops out or has little sedimentary cover. The typical form of the Aves Ridge is of two outer ridges enclosing a central trough. All three units are elevated with respect to the flanking basins. The western ridge is apparent on every profile, while the eastern ridge is sometimes only poorly developed although it may be better developed than the western ridge. Inter-ridge troughs are developed on every profile and seismic layering is usually apparent which may correspond to layering in the basins. Sediment layering in the troughs is observed to have been controlled by undulations in the basement.

The transition from Aves Ridge to Grenada Trough is far more abrupt than the transition from Venezuela Basin to Aves Ridge. The horizontal layering in the Grenada Trough terminates relatively abruptly against the eastern flank of the Aves Ridge, with only minor 'upwarping' of sediment layers. This may imply relative movements between Ridge and Trough after deposition of the sediments, although this effect is not apparent on the more northerly profiles. Other workers have found difficulty in identifying the Carib Beds in the Grenada Trough since the younger turbidites are believed to attain a thickness of approximately 1 km. in this area. The profiling line at c.15°20'N (Bunce et al., 1971) is particularly interesting in that

the sedimentary layers show clear undulations. If these reflect structures in the underlying basement,it is possible that the basement of the Grenada Trough has quite rugged topography. However, as with other parts of the Caribbean, basement has not been identified, and when traced eastwards from the Aves Ridge is soon lost in noise below the deepest sedimentary reflector. The transition from Grenada Trough to Lesser Antilles is observed on few profiles. The abrupt change in gravity gradient as the island arc is approached is probably due to a rapid decrease in sediment thickness.

## 4.4 Velocities

Although wide angle reflection experiments were attempted during the 1971 survey using disposable sono-buoys, none were successful since signals were lost from the buoys after only a few minutes.

Edgar (1968), from a combination of wide angle reflection and refraction data, has determined that the younger turbidites are characterised by a velocity of c.1.9 km/sec., the horizons below A" between 2.2 and 3.0 km/sec. and the horizons below B" between 3.2 and 4.2 km/sec.

## 4.5 Detailed descriptions of Durham Profiling lines

Three air gun profiles were performed by Durham University during the 1971 survey. Equipment breakdown was responsible for the incompleteness of the profiles, and although original records were of poor quality, due to noise induced by the ship's cathodic protection, identification of the principal reflectors was possible on the processed records.

4.5.1 Line L1254

Line L1254 was the most southerly profile made of the Aves Ridge at 12°54'N and is the most complete of the three Durham lines. A line drawing of the processed record is presented in fig. 4-2.

In the Venezuela basin a sometimes weak, but quite persistent, reflector occurs between 0.25 to 0.3 seconds below sea bed, and was interpreted as the base of the younger turbidites. The turbidites are typically acoustically transparent, although occasionally reasonably strong reflectors occur within them which are locally persistent. Such reflectors have been interpreted by Ewing et al. (1965) as local accumulations of coarser turbidites. The principal reflector below this occurs typically between 0.6 and 0.8 seconds below sea bed, and was interpreted as reflector A". It is rather poorly defined and occasionally impersistent, and although subhorizontal it occasionally exhibits undulations. Strong, confused subhorizontal reflectors sometimes occur beneath it in the top 2/3rds of the upper Carib Bed, the rest being relatively transparent. Reflector B" is poorly defined and occurs between 1.1 & 1.4 seconds below sea bed. It is subhorizontal with minor undulations. The most westerly part of the profile in the Venezuela Basin shows several strong reflectors, but a gap in the profile makes correlation with other reflectors uncertain and their identification unsure. Occasionally a weak reflector was observed beneath B" whose shape seemed to preclude the possibility of its being a multiple. This may represent true hard rock basement, but its poor definition does not allow rigorous interpretation.

The sedimentary cover mantles the western flank of the Aves Ridge, which dips at approximately 4°. Only the reflector probably

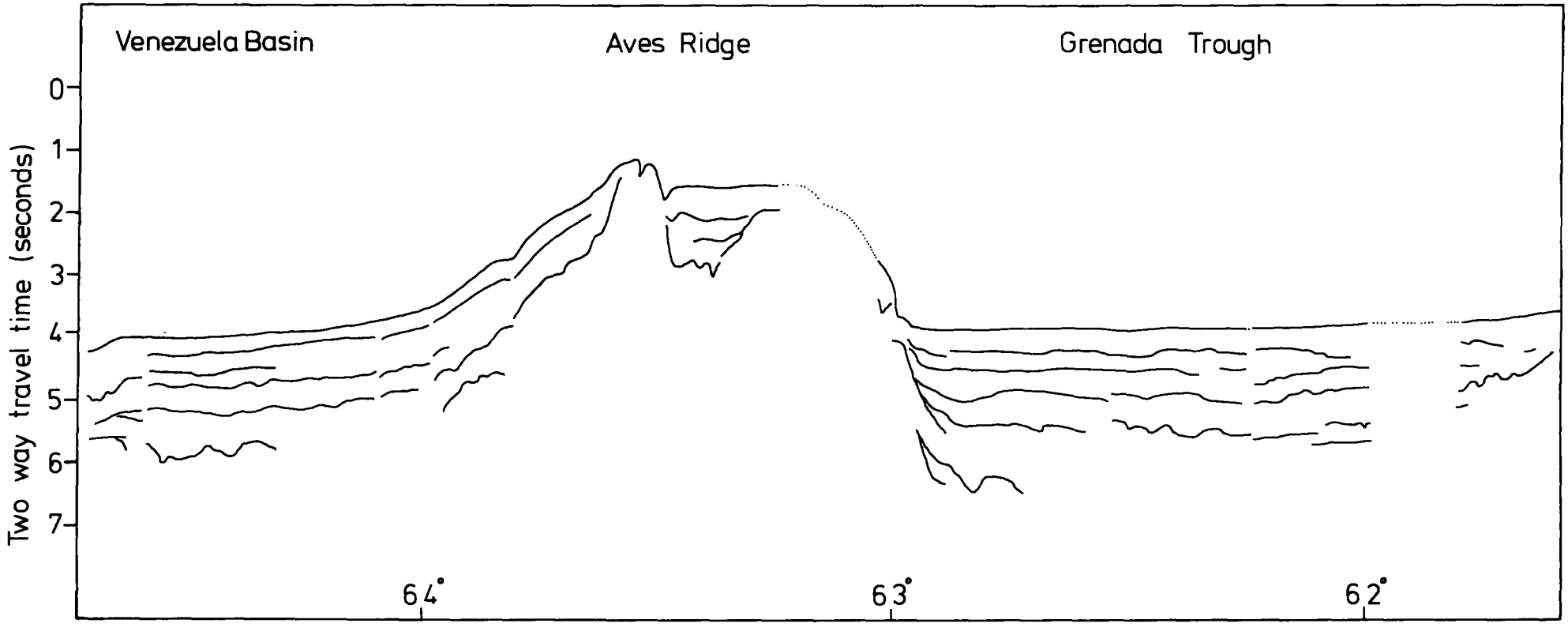


Figure 4-2 : Seismic reflection profile at 12° 54′ N.

representing the base of the younger turbidites is apparent between sea bed and basement although other workers have identified A" and B" in this area. The Aves Ridge is seen to be composed of a steep western peak and a less well developed, broader eastern peak over which data are incomplete. The western peak shows little, if any, sediment cover, although the reverberation pulse effect may mask the presence of a thin sedimentary sequence. A trough is developed between the peaks, and within this trough two reflectors were noted above the basement at 1.2 and 1.4 seconds below sea bed. The top 0.4 seconds are acoustically transparent and are underlain by an impersistent reflector. This unit may be the equivalent of the younger turbidites. A strong reflector occurs at 0.8 seconds with further, less persistent reflectors above and below it. It is possible that this horizon corresponds to reflector A". The slight downdip of both the sea bed and upper reflector on the eastern flank of the western ridge may be indicative of slumping caused by subsidence of this feature.

The sediments of the Grenada Trough terminate far more abruptly against the eastern flank of the Aves Ridge than the western flank. The actual dip of this eastern flank is 10°, and data are not considered good enough to determine whether this feature is a low angle normal fault truncating the sedimentary sequence to the east, or whether the feature simply represents a thinning of the sequence towards a pre-existing upstanding feature. Comparison with the situation attaining on the western flank of the Aves Ridge, however, suggests that the former proposal is worthy of consideration.

Within the Grenada Trough, a usually continuous, weak reflector occurs at 0.3-0.4 seconds, underlying a transparent sequence con-

taining a few impersistent reflecting horizons. This reflector was tentatively interpreted as the base of the younger turbidites, although other workers' data suggest the younger turbidite sequence to be somewhat thicker in the Grenada Trough. This reflector is underlain by two strong reflectors at 0.85 - 1.0 and 1.5 - 1.75 seconds which were identified as reflectors A" & B". They are locally impersistent with the upper stronger than the lower. Both are sub-horizontal and the beds defined by them are usually transparent with occasional internal reflectors. A further reflector was impersistently observed below these reflectors, and may represent basement, although near the Aves Ridge a further reflector was apparent below it. Identification of reflecting horizons in the Grenada Trough was thus somewhat more complicated than in the Venezuela Basin. Data over the Lesser Antilles are lacking, but the eastern part of the profile shows basement rising as the island arc is approached.

4.5.2 Line L1324

The profiling line at 13°24'N is incomplete due to instrument malfunction. A line drawing of the processed record is presented in fig. 4-3.

The Venezuela Basin is characterised by an upper acoustically transparent sequence 0.4 seconds thick underlain by a weak, sometimes impersistent reflector. A strong, undulating reflector occurs at 0.65 seconds below sea bed and is underlain by a strong, locally impersistent reflector at 1.05 - 1.1 seconds. These three reflectors probably correspond to the base of the younger turbidites, A" & B" respectively. In places, definition of the upper two reflectors was confused and occasionally up to two weak, impersistent reflectors were noted below B".

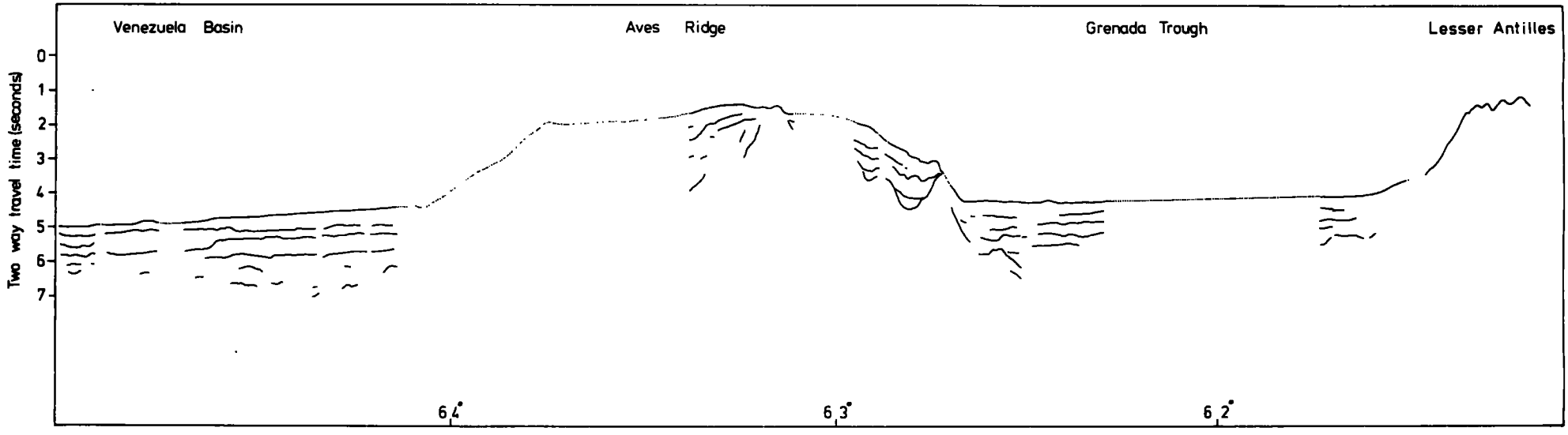


Figure 4-3 : Seismic reflection profile at 13° 24′ N.

The transition from Venezuela Basin to Aves Ridge was not recorded, neither was the western flank of the Ridge due to instrument malfunction. However, two parallel reflectors, 0.3 seconds apart, were observed gently rising onto a basement peak on the centre of the Ridge, although basement was soon lost in noise beneath them. These reflectors may correspond to A" & B". On the eastern part of the Aves Ridge a sediment pocket is apparent in which three well defined reflectors were noted above the basement reflector. The upper, at c. 0.45 seconds, is overlain by a transparent sequence. This is underlain by a strong undulating reflector at c. 0.8 seconds. The lowest sedimentary reflector is smooth, and followed, although is less concave than, the basement reflector and is underlain by a transparent sequence. The whole sequence is similar to sections found in both the Grenada Trough and Venezuela Basin and implies possible uplift of this part of the Aves Ridge after deposition, if correlation of reflectors is correct, although other possible causative mechanisms were discussed in a previous section. The undulations of the middle reflector (A") may indicate that it was still in an unconsolidated state during uplift and was deformed by slumping. However, A" also exhibits such undulations in the Venezuela Basin so this conclusion must be treated with caution.

Reflectors of the Grenada Trough terminate gently against the Aves Ridge. The Ridge was observed to extend eastwards of its topographic expression into the Grenada Trough, although only one reflector was apparent above this extension. This reflector to some extent follows the undulations of the basement, a situation interpreted to be indicative of possible post depositional vertical movements. In the Grenada Trough, a weak reflector at 0.45 - 0.5 seconds underlies an acoustically transparent sequence. A relatively strong horizontal

reflector underlies this at 0.8 - 0.95 seconds and a further horizontal reflector occurs at 1.2 - 1.45 seconds. These reflectors were interpreted as the base of the younger turbidites, A" & B" respectively. Weak, impersistent reflectors were occasionally observed below B". Near the Lesser Antilles, definition of the three principal reflectors is lost, and many impersistent, horizontal reflectors are apparent. The upper, transparent sequence is not developed. This whole sequence was interpreted as impersistent beds of coarse and fine clastic sediments locally derived from the Lesser Antilles.

The Lesser Antilles show no sediment cover, and the basement develops a strong multiple reflection. The transition from Grenada Trough to island arc was lost in noise.

4.5.3 Line L1354

The profile at 13°54'N was the most northerly of the lines surveyed by Durham in 1971. Severe equipment malfunction caused data over both Aves Ridge and Venezuela Basin to be lacking, but the profile is complete over the width of the Grenada Trough. A line drawing of the processed record is presented in fig. 4-4.

Correlation of reflectors in the Grenada Trough was difficult since several horizons occur at different positions along the profile. However, a weak, impersistent reflector at 0.3 - 0.4 seconds, which is occasionally masked by the reverberation pulse, was tentatively interpreted as the base of the younger turbidites. The reflectors identified as A" & B" are both usually strongly developed, although A" is in some places locally impersistent. A" occurs between 0.5 - 0.65 seconds and B" between 1.2 - 1.3 seconds. However, locally, strong internal reflectors are apparent and confused identification of A" & B". Weak reflections were occasionally noted below the lowest strong reflector and in the western part,

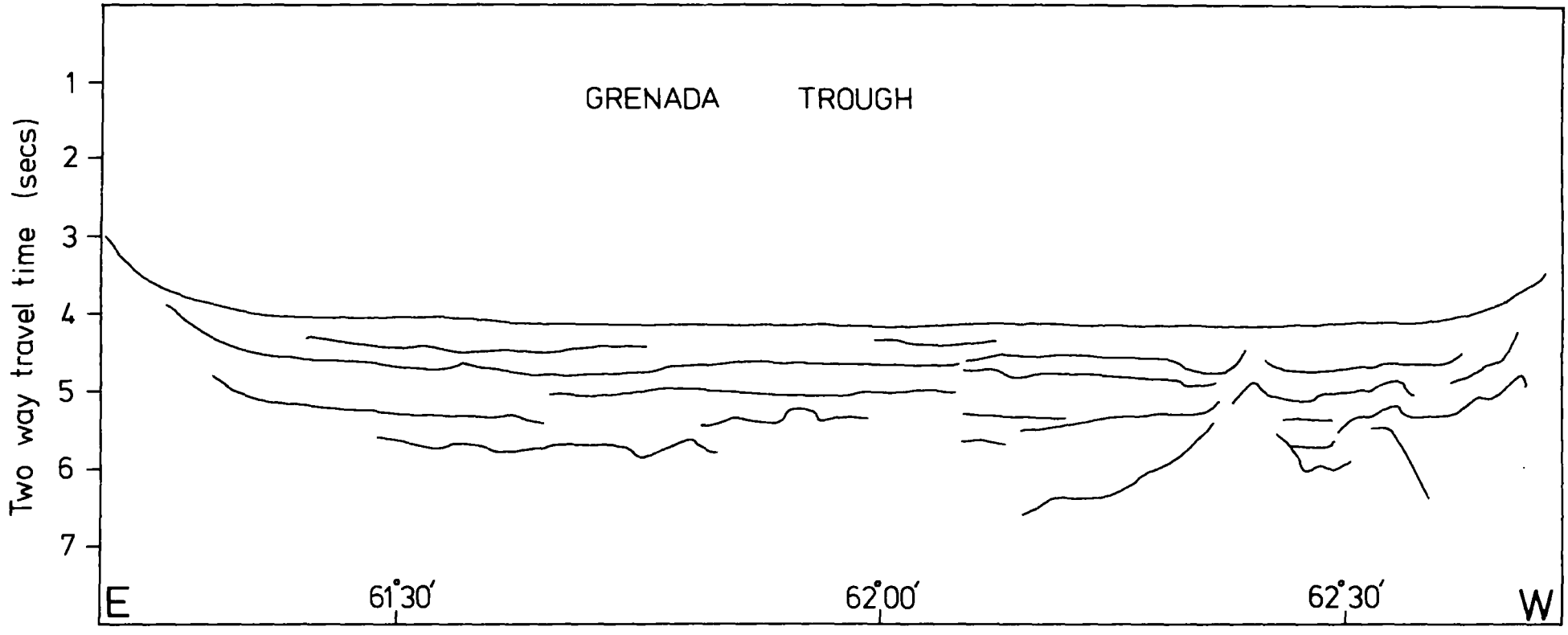


Figure 4-4 : Seismic reflection profile at 13° 54′ N.

where true basement was recognized, it was seen to pass under the reflector identified as B" before being lost in noise. The eastern end of the profile commenced on the Lesser Antilles, which were shown to have little, if any, sediment cover and developed strong multiple reflections.

The western part of this profile is especially interesting in that identification of the basement was possible. The basement takes the form of two broad peaks overlain by approximately one second of sediments in which two reflecting horizons occur. These reflectors, 0.4 seconds apart, seem to correlate with A" & B". The undulations on these horizons reflect undulations in the underlying basement, the lower more than the upper. This basement rise is interpreted as an intrusion associated with the Aves Ridge, on whose eastern flank it lies, and shows that the Ridge extends in places beyond its topographic expression. Since the layering of overlying strata are affected by this structure, it is suggested that it is either of a younger age than the sediments or that it is older and the whole succession has undergone later tectonic uplift. In either case vertical movements are suggested.

## 4.6 Conclusions on Seismic Reflection Results

i) The presence of two principal reflectors noted elsewhere in the Caribbean is confirmed in the survey area.

ii) The typical form of the Aves Ridge is of two flanking ridges enclosing a central sediment filled trough.

iii) The presence of reflectors in the central trough which are similar to those of the Venezuela Basin and Grenada Trough may indicate post-depositional uplift of the Aves Ridge.

iv) The Aves Ridge extends beyond its topographic expression in places into the Grenada Trough.

v) True basement was recorded under neither the Venezuela Basin nor the Grenada Trough.

vi) The possible truncation of sediments of the Grenada Trough by the southern Aves Ridge may be indicative of post-depositional uplift of the Aves Ridge.

vii) The younger turbidite sequence in the Grenada Trough seems to be rather less thick than observed by other workers if identification of reflectors was correct.

viii) The increase in ruggedness of topography northwards in the Grenada Trough implies a southerly direction of sediment transport for the major part of the younger sediments. The source is probably the Orinoco river, from which sediments would reach the Grenada Trough via the Gulf of Paria and Bocas del Dragon. A further contributor would be volcanic ashes from the Lesser Antilles, transported both by sea and air.

# CHAPTER 5

# GRAVITY ANOMALIES OF THE EASTERN CARIBBEAN

## 5.1 Introduction

The presence of large positive and negative gravity anomaly belts in and around the Caribbean Sea has long been recognised. These belts are of major importance in defining both the extents and history of the region. Both the Aves Ridge and Lesser Antilles are representatives of these positive anomaly belts.

## 5.2 Regional Gravity Field

Talwani (1970) has presented maps of long wavelength variations of the earth's gravity field based on coefficients of the spherical harmonics given in Kalua (1966). These show a gravity gradient in the eastern Caribbean decreasing from west to east with a mean value of approximately -25 mgal. (Bunce et al., 1971). Edgar (1968) has observed an average value of -20 mgal. in the Venezuela Basin, but the present survey does not extend far enough into the Venezuela Basin for a true undisturbed value to be registered.

## 5.3 Previous studies

The first studies of the gravity field of the Caribbean were performed by Vening Meinesz (1948).

Edgar (1968) has observed that the Caribbean basins are characterised by slightly negative, and the ridges by positive, free air anomalies. He has computed the mass per unit area for several localities based on seismic refraction data and found values negative with respect to the mean for ocean basins. This Edgar considers to be due to a slightly less dense mantle underlying the region.

Talwani (1965) has described the major gravity anomaly belts of the Caribbean. The most northerly is a negative belt associated with the Cayman Trough and Puerto Rico Trench which he considers to be continuous with the belt to the east of the Lesser Antilles passing through Barbados into Trinidad and Venezuela. This belt is flanked to the west by the positive axis of the Lesser Antilles which terminates at the Isla de Margarita. Andrew et al. (1970) consider that the steep gravity gradients of the negative belt preclude an origin of the anomalies in either the lower crust or mantle and conclude that the negative anomalies are in part due to the thickness of recent sediments filling the 'trench'. Talwani describes a further belt of positive and negative anomalies off northern South America stretching from the Guajira Peninsula through the Dutch Lesser Antilles, the positive part of which he considers to curve northwards into the Aves Ridge while the negative part terminates at the Aves Ridge. Laagay (1969) has described the southern part of this belt, and Edgar (1968) considers a great thickness of sediment is responsible for the negative anomalies. A survey by Peter (1972), however, would seem to indicate that the positive part of the belt is not continuous to the east and may terminate between the islands of Blanquilla and Orchilla. Consequently connection between the causative structures of the Dutch Lesser Antilles and Aves Ridge is considered unlikely.

Bunce et al. (1971), from the results of seven traverses across the eastern Caribbean, have proposed that the curvature of the axes of the anomaly belts of the Lesser Antilles and its 'trench' is far more concave to the west than the positive free air axis of the Aves Ridge, which exhibits but little deviation from linearity. The present survey shows, however, that the Aves Ridge is a somewhat

broader feature than the Lesser Antilles, and the location of its free air anomaly maxima dependent on local topographic features making the regional trend difficult to delineate.

## 5.4 Regional gradients and the problems of interpretation

The interpretation of gravity anomalies was hampered by the presence of long wavelength regional effects which obscure the nature of the anomalies due to shallow structures. A further complication is that the Moho has never been recorded by seismic refraction under the Aves Ridge, Grenada Trough or Lesser Antilles . Consequently control on the Moho is limited to refraction surveys performed in the Venezuela Basin. It is considered that the long wavelength regional effects are due to variation in depth to the Moho and also possibly the 7.4 km/sec. seismic layer (hereafter referred to as the lowest crustal layer). Two methods were used to attempt to isolate the effects of deep structures from the observed gravity anomalies, and are described in the following sections.

## 5.5 Isolation of the anomalies of deep structures using seismic reflection, refraction and spectral analysis data

In order to isolate the anomalies due to deep structures, i.e. the effects of variation in depth to the Moho, it is necessary to correct all crustal and supracrustal units to a density representative of a mean crustal value. The application of a simple two-dimensional Bouguer correction is not completely adequate for this purpose as only the overlying body of sea-water is corrected to the crustal density. If, however, sufficient data are available to accurately define the sediment/basement interface as well as the bathymetry, correction of both water and sediments to a crustal density should prove effective in isolating the gravitational effects of deep structures.

Seismic reflection data provide good control on basement over the Aves Ridge. In the Venezuela Basin and Grenada Trough, however, it is considered that the basal reflector does not everywhere represent true basement (Chapter 4). Consequently in these areas control on the basement is limited to seismic refraction and magnetic anomaly spectral analysis data.

A density of 2.85 gm/cc was taken to represent a mean crustal value. This is considered more realistic than the value of 2.67 gm/cc usually assumed by other workers.

The isolation of the effects of the crust/mantle boundary permits the computation of isostatic anomalies. The procedure involved is presented in the following sections.

## 5.6 Isostatic Anomalies

### 5.6.1 Introduction

Isostasy is a direct application of Archimedes principle to large scale structures whereby the weight of a surface mass is compensated by an underlying mass deficiency commonly regarded either as a root of constant density and varying depth (Airy hypothesis) or columns of varying densities reaching the same depth, D, at the level of compensation (Pratt hypothesis). A description of the historical development of these two hypotheses is given in Heiskanen & Vening Meinesz (1958). Seismic refraction has now indicated that isostatic equilibrium most commonly occurs according to the Airy assumption (e.g. Woolard, 1955), and so Airy's hypothesis was used as the basis for all computations presented in this chapter.

5.6.2 Two-dimensional isostatic anomalies

For marine structures, if $h_w$ is the depth of water and $\rho_w$, $\rho_c$ and $\rho_m$ the densities of sea water, crust and mantle, then the height of the antiroot, r, above a standard crustal thickness $T_c$ according to Airy's hypothesis for 100% isostatic compensation, is given by (figs. 5-1 A & B):

$$r_1 = h_w (\rho_c - \rho_w)/(\rho_m - \rho_c) \quad (1)$$

Similarly, for continental structures of height $h_c$, the depth, $r_3$, of the root below a standard crustal thickness $T_c$ for 100% isostatic compensation, is given by (fig. 5-1 D):

$$r_3 = h_c \rho_c/(\rho_m - \rho_c) \quad (2)$$

The isostatic anomalies over the structure are then defined as the Bouguer anomalies (for a crustal density) minus the computed effect of the root or antiroot at each datum point. It may be shown that over a feature of subdued topography which is at least ten times as wide as the depth of compensation, the free air anomaly is approximately the same as the isostatic anomaly (Bott, 1971).

Correcting the free air anomaly to a Bouguer anomaly for a crustal density should isolate the effects of the actual root from the combination of deep and shallow effects represented by the free air anomaly. Errors in the isostatic anomalies so calculated will result from the non-uniformity of density distribution with depth within the crust. In particular, the short wavelength anomalies due to the basement/sediment interface will not be removed from the Bouguer anomaly, and the assignment to the main portion of the crust of a single density is a questionable approximation. Also, the use of a two-dimensional assumption must be treated with caution in areas of rough topography, and this point will be amplified in a following

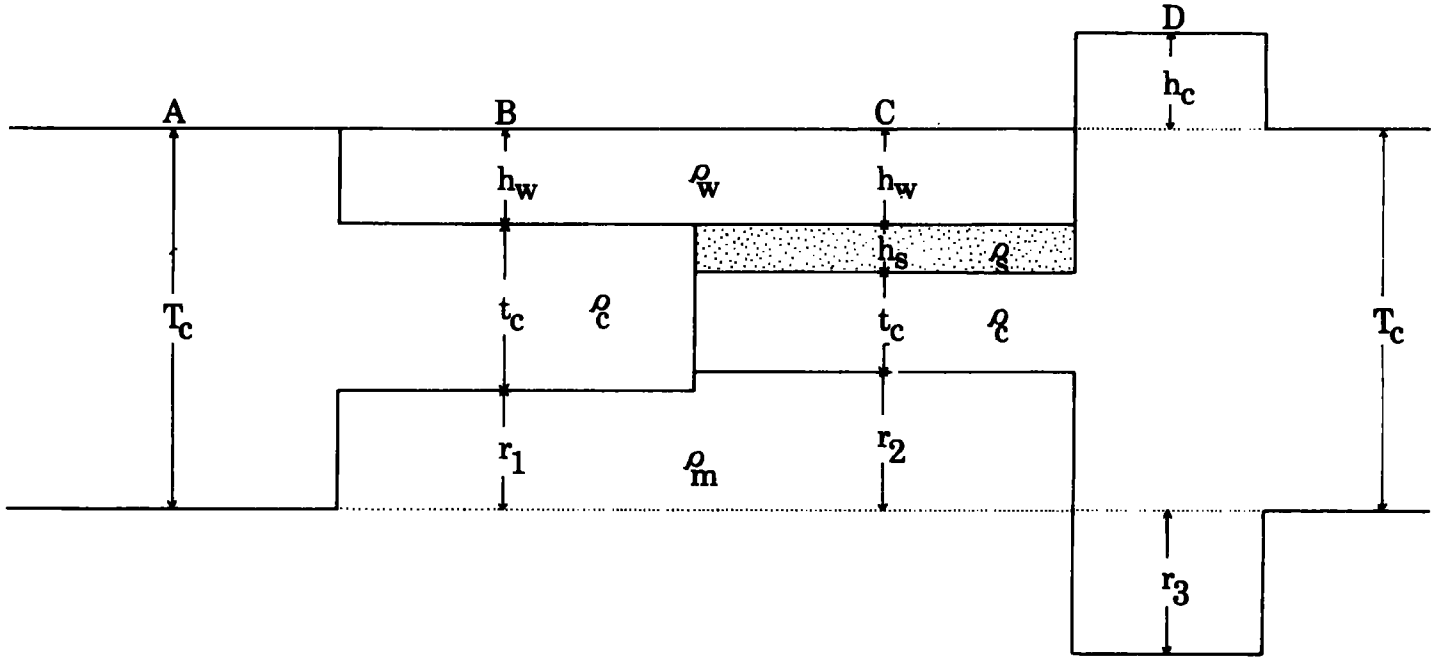
A
B
C
D
$h_c$
$h_w$
$\rho_w$
$h_w$
$h_s$
$\rho_s$
$T_c$
$t_c$
$\rho_c$
$t_c$
$\rho_c$
$T_c$
$r_1$
$\rho_m$
$r_2$
$r_3$
$r_1 = \frac{h_w(\rho_c - \rho_w)}{(\rho_m - \rho_c)}$
$r_2 = \frac{h_w(\rho_c - \rho_w) + h_s(\rho_c - \rho_s)}{(\rho_m - \rho_c)}$
$r_3 = \frac{h_c \rho_c}{(\rho_m - \rho_c)}$

Figure 5-1.

section.

In marine areas, seismic reflection profiling permits a refinement of the computation of two-dimensional isostatic anomalies since the sediment/basement interface may be defined.

If $h_s$, $\rho_s$ refer to the thickness and density respectively of the sediment cover (fig. 5-1 C), then equation (1) above becomes:

$$r_2 = (h_w(\rho_c - \rho_w) + h_s(\rho_c - \rho_s))/(\rho_m - \rho_c) \qquad (3)$$

where $r_2$ represents the height of the antiroot above a standard crustal thickness, $T_c$.

Division of the structure into a number of columns allows the delineation of the isostatically compensating Moho over a complex structure. Equations (2) and (3) were used for this purpose in the computation of two-dimensional isostatic anomalies.

When using this modified approach it is necessary to correct for both sea water and sediments in order that the Bouguer anomalies represent a structure of constant crustal density from sea-level to Moho. This computation was performed using a procedure similar to the Bouguer reduction described in Chapter 2, including an additional body of sediment corrected to a crustal density. Seismic reflection, refraction and spectral analysis of magnetic data were used to define the sediment/basement interface.

The densities of sea water, sediments, crust and mantle were taken as 1.03, 2.00, 2.85 and 3.30 gm/cc respectively. The value for sediments is low for the deeper layers, while the crustal value is high for the upper crust. However, errors in these assumptions are not expected to affect the significance of the isostatic anomalies so computed, a critical test being the effectiveness of the Bouguer reduction in removing the short wavelength, positive anomalies from the free air anomalies of the Aves Ridge and Lesser Antilles.

5.6.3 Procedure

The computation of two-dimensional isostatic anomalies was performed in three steps:

(i) Computation of the space form of the 100% isostatically compensating Moho using equations (2) and (3).

(ii) Input of digitised bathymetry, basement and free air anomalies to a Bouguer reduction routine.

(iii) Input of the Bouguer anomalies from (ii) and root from (i) to a routine which computed the effect of the roots and antiroots at each datum point and subtracted it from the Bouguer anomaly to give the isostatic anomaly with respect to a standard crustal thickness.

The Bouguer anomalies computed during step (ii) were also used for computing the actual shape of the Moho for comparison with the shape computed for 100% isostatic compensation. Such computations were hampered in the eastern Caribbean by the Moho's never having been recorded in seismic refraction experiments under the Aves Ridge, Grenada Trough or Lesser Antilles. Consequently interpretations were performed using control depths to the Moho which were taken to represent reasonable upper and lower limits.

Three seismic refraction profiles only have been described from the Grenada Trough (line 7, Officer et al., 1959, lines 62 & 63, Edgar et al., 1971a), and seismic reflection profiles are not considered to have recorded true basement. Consequently, in the absence of contradictory data, the basement of the Grenada Trough was assumed to be flat.

5.6.4 Three-dimensional Isostatic Anomalies

In order to check the adequacy of the two-dimensional approximation, it was decided to perform a three dimensional isostatic reduction on

selected points in the survey area. Similar reductions have been performed in the eastern Caribbean by Bush & Bush (1969), who present a Pratt anomaly map of the area incorporating the results of several other workers, and Andrew et al. (1970), who present Airy anomaly maps of the islands of the Lesser Antilles and the results of some marine gravity profiles.

The Airy isostatic anomalies were calculated according to standard procedures (Heiskanen & Vening Meinesz, 1958) using graticules constructed for the standard Hayford zones (Hayford & Bowie, 1912) A to 11. The scale of the survey necessitated the combination of zones A to D into a single zone. For bathymetric data in zones A to M the original survey chart of scale 1:250,000 was used, for zones N to O, the reduced 1:1,000,000 survey chart, for zones 18 to 13 the Royal Navy chart 762, scale 1:2,190,000, and for zones 12 and 11 an unpublished chart of the U.S. Undersea Surveillance Oceanographic Center (USOC) of scale 1:4,667,00.

The contributions of the topography, roots and antiroots in zones A to O were computed using a computer program based on the method given in Heiskanen (1931) for a standard crustal thickness, $T_c$, of 40 km. and for densities of sea water, crust and mantle of 1,03, 2.67 and 3.27 gm/cc respectively. The contributions of zones 18 to 11 were computed using the tables given in Heiskanen (1931), and the contributions of zones 10 to 1 taken from the world charts presented by Niskanen & Kivioja (1951).

The very accurate bathymetric charts constructed from the present survey gave excellent control of depths for the zones A to O, although the difficulty in estimating the mean depth in zone compartments of rough topography must be stressed. Inaccuracies in depth estimation

are far greater in the outermost zones, where, for example, it was necessary to estimate the mean depth in a compartment containing both the island of Puerto Rico and the Puerto Rico Trench. These compartments are sufficiently distant from the observation point, however, that the error involved in depth estimation will not substantially affect the accuracy of the computed isostatic correction. The computed isostatic corrections have a probable error of $\pm$ 2 mgal.

5.6.5 The value of the standard crustal thickness, $T_c$

Isostatic anomalies are essentially anomalies of the second order in that they represent the free air anomaly to which a correction has been applied for the attractions of both topography and for its compensating underlying mass deficiency. Representation of this mass deficiency by either a root of the same density as the topography or a column of lesser density should not significantly affect the nature of the isostatic anomaly so calculated. Consequently anomalies calculated according to both the Airy and Pratt hypotheses are good tests of the state of isostatic equilibrium. Similarly the values selected for the standard crustal thickness, $T_c$, and densities of crust and mantle, when computing Airy isostatic anomalies should also not affect greatly the significance of the isostatic anomalies so obtained.

For compatibility with the results of Andrew et al. (1970), the two-dimensional isostatic anomalies were computed for $T_c$ = 35km. The three-dimensional anomalies, however, were computed for $T_c$ = 40 km., Heiskanen's tables not being available for $T_c$ = 35 km.

The data points reduced to isostatic anomalies are presented in table 5-1. They will be discussed in relation to the two-dimensional anomalies in the following four sections.

TABLE 5-1

Computed Airy Isostatic Anomalies for $T_c$ = 40 km.

| Latitude (N) deg. & min. | | Longitude (W) deg. & min. | | Station Depth (m) | Free Air Anomaly (mgal) | Isostatic Correction (mgal) | Isostatic Anomaly (mgal) | Location |
|---|---|---|---|---|---|---|---|---|
| 12 | 54.02 | 61 | 50.53 | 2966 | -75.8 | +41.9 | -33.9 | Grenada Trough |
| 13 | 24.07 | 61 | 56.28 | 2978 | -33.8 | +29.3 | - 4.5 | Grenada Trough |
| 14 | 10.06 | 62 | 16.40 | 2964 | -31.6 | +25.8 | - 5.8 | Grenada Trough |
| 15 | 29.89 | 62 | 30.44 | 2012 | -10.5 | - 5.1 | -15.6 | Grenada Trough |
| 13 | 24.02 | 63 | 10.22 | 1048 | +36.6 | -46.8 | -10.2 | Aves Ridge |
| 14 | 09.96 | 62 | 57.15 | 1542 | +12.4 | -24.1 | -11.7 | Aves Ridge |
| 15 | 30.00 | 63 | 35.79 | 33 | +75.3 | -110.0 | -34.7 | Aves Ridge |
| 13 | 23.91 | 64 | 28.98 | 3322 | - 9.4 | +16.2 | + 6.8 | Venezuela Basin |
| 14 | 09.98 | 64 | 07.85 | 3054 | -26.6 | +18.9 | - 7.7 | Venezuela Basin |
| 13 | 25.52 | 61 | 07.53 | 836 | +108.7 | -54.8 | +53.9 | Lesser Antilles |
| 13 | 34.41 | 61 | 06.41 | 605 | +134.0 | -51.5 | +82.5 | Lesser Antilles |

## 5.7 Interpretation of Profiles

### 5.7.1 Line L1254

The profile designated L1254 is a composite of data from the present survey at 12°54'N, present survey data at 13°04'N for data across the island arc, and data from another Durham survey at 13°04'N for data to the east of the arc. Relevant data are presented in fig. 5-2.

The free air anomalies have a mean value of approximately -15 mgal. in the Grenada Trough, which falls slightly as the Aves Ridge is approached. Over the Aves Ridge the anomalies are predominantly positive and exhibit the form of a double peak reaching maxima of 56 and 31 mgal. which correspond to bathymetric highs. The Grenada Trough is marked by negative free air anomalies with a mean value of approximately -75 mgal. The Lesser Antilles exhibit extreme free air anomaly gradients, and reach a maximum value of 147 mgal. To the east of the island arc, the free air anomalies reach a minimum value of -95 mgal. over the 'trench'.

Basement under the Aves Ridge was defined by Durham reflection data, with its position inferred where data were lacking due to instrument malfunction. A sediment velocity of 2 km/sec. was assumed. The depth to basement under the Venezuela Basin was taken as 6.5 km., a value controlled by refraction line 7 of Officer et al. (1959) to the west of the profile. The depth to basement under the Grenada Trough was taken as 6 km., implying a sediment thickness of 3 km. This value was controlled by refraction lines 62 and 63 of Edgar et al. (1971a) to the south of the profile. No refraction or reflection data were available over the Lesser Antilles, necessitating inference of basement position.

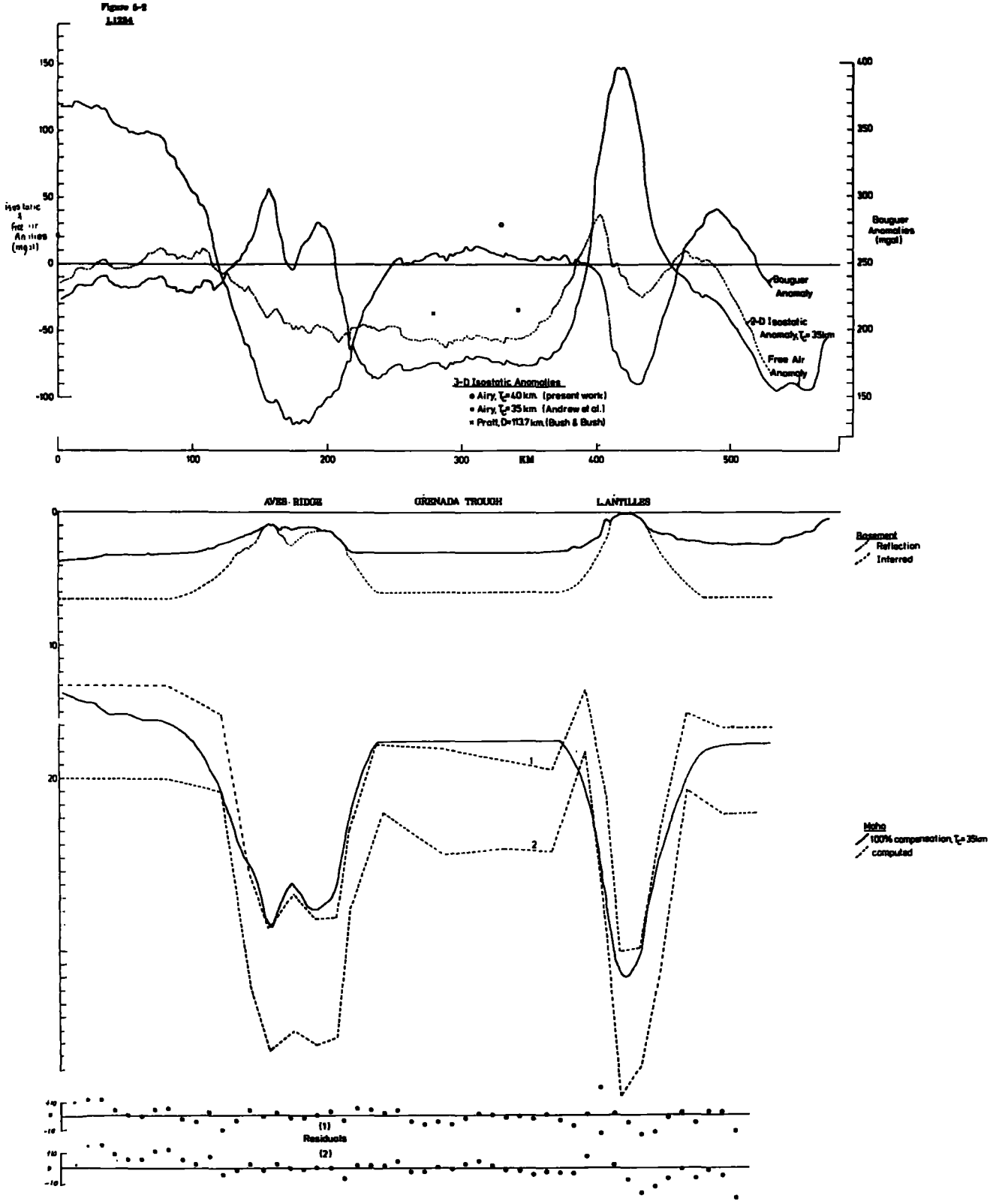
Bouguer Anomalies (mgal)
Bouguer Anomaly
3-D Isostatic Anomaly, Te= 35km
Free Air Anomaly
3-D Isostatic Anomalies
Airy, Te=40 km (present work)
Airy, Te=35 km (Andrew et al.)
Pratt, D=113.7 km (Bush & Bush)
KM
AVES RIDGE
GRENADA TROUGH
LANTILLES
Basement
Reflection
Inferred
Moho
100% compensation, Te=35km
computed
Residuals
(1)
(2)

The Moho computed for 100% isostatic compensation relative to a standard crustal thickness of 35 km. was found to reach a depth of 13.6 km. in the Venezuela Basin at the most westerly point on the profile. Refraction line 25 of Officer et al. in the Venezuela Basin c.150 km. west of the profile indicates a depth to Moho of 13 km., and so if it can be shown that the Venezuela Basin is in approximate isostatic equilibrium, the value chosen for $T_c$, namely 35 km., is an adequate value for the standard crustal thickness. The depth to Moho increases under the Aves Ridge to a maximum value of 31.2 km., and rises under the Grenada Trough to a depth of 17.2 km. The isostatically compensating Moho reaches greater depths under the Lesser Antilles than under the Aves Ridge, the maximum depth being 34.6 km.

On performing the Bouguer correction for water and sediments, the short wavelength, positive anomalies of the free air anomaly over the Aves Ridge were removed and a long wavelength low substituted. The Grenada Trough negative anomalies became a high relative to both the Aves Ridge and Lesser Antilles, although all three units form a regional low with respect to the Venezuela Basin. The extreme gradients and anomalies of the island arc were reduced to a regional low of lesser amplitude than the Aves Ridge anomaly. Low amplitude, short wavelength perturbations are present in both free air and Bouguer anomalies, and are considered to represent errors of observation. An interesting feature is that the minimum Bouguer anomaly over the island arc is displaced slightly to the east of the maximum free air anomaly.

The Bouguer anomaly was interpreted in terms of variation in depth of the Moho. In the absence of seismic refraction lines

recording the Moho in the close proximity of the line, two interpretations were performed assuming depths to Moho under the eastern Venezuela Basin of 13 km. and 20 km. Refraction line 25 of Officer et al., c.150 km. to the west of the profile, indicates a depth to the Moho of 13 km. Edgar (1968), however, has noted crustal doming towards the centre of the Venezuela Basin, and so this depth of 13 km. is most probably an underestimate of the depth to Moho at the eastern margin of the Venezuela Basin. A value of 20 km. is taken to represent a reasonable lower limit. The interpretations were performed using non-linear optimisation procedures. An attempt was made to use the matrix procedures of Laving (1971) for this purpose, but although an excellent least squares fit was obtained between observed and computed anomalies, the models produced were geologically unreasonable in that the z-coordinates of the computed body oscillated violently.

The computed models are presented in fig. 5-2 and are compared with the Moho computed for 100% isostatic compensation. The models indicate that the root beneath the Aves Ridge is slightly larger than required for isostatic equilibrium, while the root beneath the Aves Ridge is approximately the same as for equilibrium. Mean depths computed under the Aves Ridge, Grenada Trough and Lesser Antilles for a depth to Moho under the Venezuela Basin of 13 km. are 31, 18.5 and 33 km. respectively, and for 20 km. are 40, 25.5 and 43.km. respectively. The easterly offset of the Bouguer anomaly minimum from the free air maximum is seen to be in part due to a relatively sharp decrease in depth to the Moho. The relatively large residuals in this area, however, would seem to indicate that this simple model is not completely sufficient, and that the source of this feature is probably a high density body at a somewhat higher level in the crust.

The two-dimensional isostatic anomalies indicate that the Venezuela Basin is in approximate isostatic equilibrium, although a Pratt anomaly (Bush & Bush) in this region indicates a positive anomaly of 21 mgal. The anomalies decrease from west to east under the Aves Ridge to a mean value of -50 mgal. and maintain this value beneath the Grenada Trough. Three-dimensional isostatic anomalies computed according to both the Airy (present work) and Pratt (Bush & Bush) assumptions indicate that the two-dimensional anomalies are rather too low, with the true value under the Grenada Trough being -35 mgal. The Airy anomalies computed by Andrew et al. in this region give a positive value of 30 mgal., and it will be shown that all isostatic anomalies computed by Andrew et al. are consistently greater than these computed by Bush & Bush and the present worker. This will be discussed in a later section. The overestimate provided by the two-dimensional anomalies would seem to be due to an inadequacy of the two-dimensional approximation. The profile passes south of the island of St. Vincent, beneath which the compensating Moho reaches far greater depths than beneath the marine passage south of the island. Isostatic anomalies are defined as the Bouguer anomaly minus the effect of the underlying compensating mass, which in a marine area is represented by an antiroot. The effect of the island of St. Vincent is to decrease the size of the antiroot and so the isostatic anomaly will be smaller than the anomaly obtained if the root under the island is ignored. The root underlying northern South America and Trinidad will also produce a similar, though smaller, effect. The topographic effect of St. Vincent and northern South America have little effect on the isostatic anomalies in the central Grenada Trough, as topographic effects were found to be insignificant in the Hayford zones greater

than 100 km. from the observation point. The two-dimensional isostatic anomalies over the island arc indicate positive values up to 37 mgal. on its western flank and negative anomalies over its eastern flank. In the absence of computed three-dimensional isostatic anomalies in this region, the significance of these anomalies will be discussed in a later section.

5.7.2 Line L1324

The profile designated L1324 is a composite of the present survey data at 13°24'N to the west of the Lesser Antilles and data from another Durham survey line at 13°24'N to the east. The profile passes just south of the prominent seamount in the southern part of the survey area and between the islands of St. Lucia and St. Vincent. Relevant data are presented in fig. 5-3.

The free air anomalies in the Venezuela Basin decrease from approximately zero mgal. to -20 mgal. as the Aves Ridge is approached. Free air anomalies are positive over the Aves Ridge and decrease to approximately -65 mgal. east of its eastern flank. Free air anomalies are negative in the Grenada Trough with a mean value of approximately -40 mgal. The Lesser Antilles are again the site of extreme free air anomaly gradients, with a maximum of 109 mgal. Negative anomalies mark the 'trench' to the east of the island arc.

Seismic reflection data for this profile are far less complete than for L1254 due to instrument malfunction, and estimates of the depths to basement over the western part of the Aves Ridge had to be made from spectral analysis of magnetic data. Over the eastern part of the Aves Ridge a sediment velocity of 2 km/sec. was assumed. The depth to basement under the Venezuela Basin was taken as 6.5 km., a value controlled both by refraction Line 7 of Officer et al. (1959) and spectral analysis data. The depth to basement under the Grenada

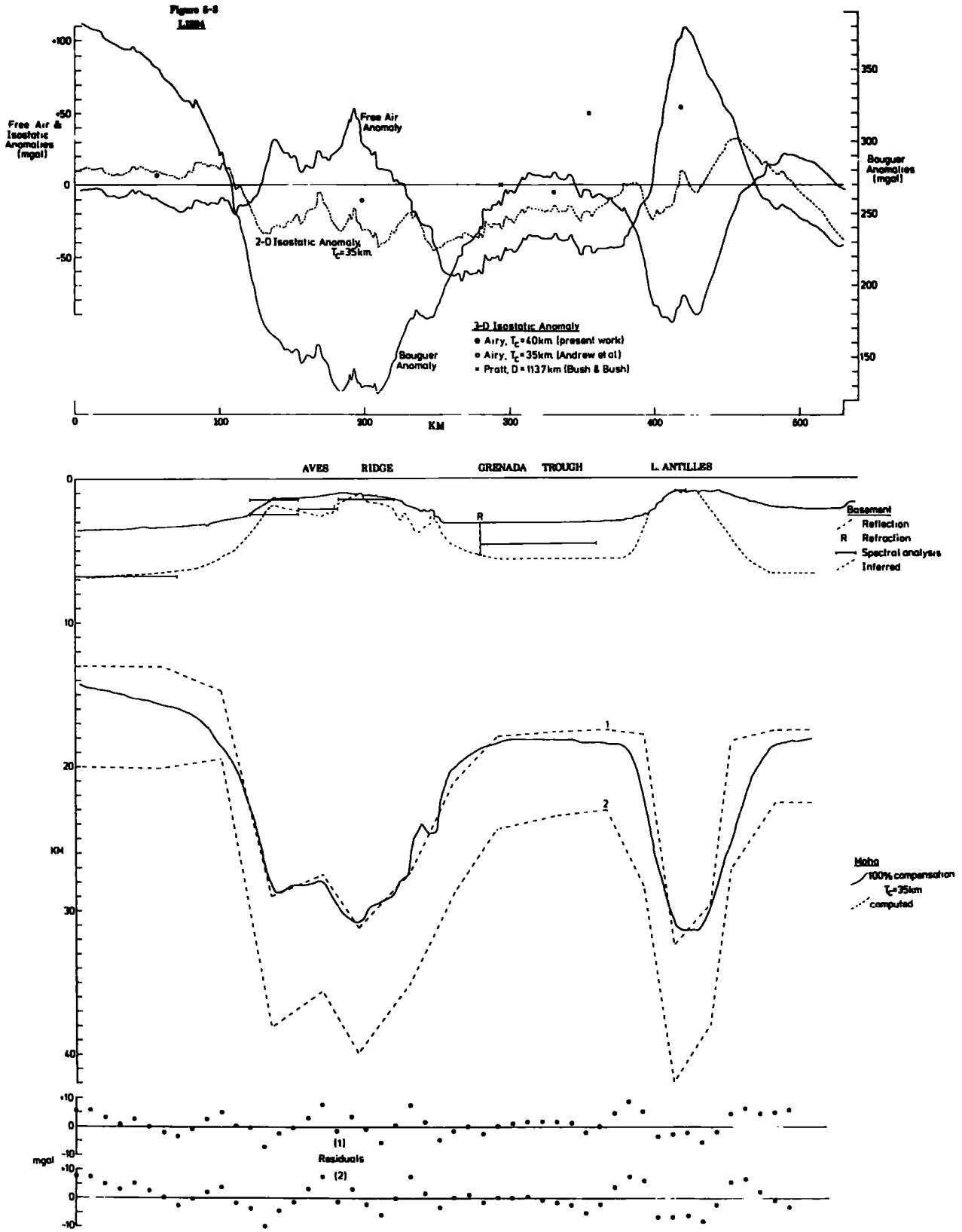
Free Air & Isostatic Anomalies (mgal)
+100
+50
0
-50
Free Air Anomaly
2-D Isostatic Anomaly, $T_c$=35km
Bouguer Anomaly
3-D Isostatic Anomaly
Airy, $T_c$=40km (present work)
Airy, $T_c$=35km (Andrew et al)
Pratt, D=113.7km (Bush & Bush)
Bouguer Anomalies (mgal)
350
300
250
200
150
0
100
200
300
400
500
KM
AVES RIDGE
GRENADA TROUGH
L. ANTILLES
R
Basement
Reflection
Refraction
Spectral analysis
Inferred
10
20
30
40
KM
1
2
Moho
100% compensation
$T_c$=35km
computed
+10
0
-10
mgal
(1)
Residuals
(2)

Trough was taken as 6.5 kms., a value controlled by refraction line 29 of Officer et al. on its western margin. In the absence of refraction and reflection data, basement position had to be inferred over the Lesser Antilles.

The Moho computed for 100% isostatic compensation relative to a standard crustal thickness of 35 km. reached a depth of 14 km. under the Venezuela Basin and increased to a maximum value of 30.8 km. under the Aves Ridge. The depth decreased to 18 km. under the Grenada Trough and descended rapidly to 31.4 km. under the Lesser Antilles. As for line L1254, the value of 14 km. under the Venezuela Basin is in good agreement with the 13 km. recorded on refraction line 25 of Officer et al. to the west of the profile.

The Bouguer correction was moderately successful in eliminating short wavelength anomalies from the free air anomalies. The elimination was least successful over the western part of the Aves Ridge where reflection data were lacking. However, the Bouguer anomalies over the Aves Ridge form a local low, over the Grenada Trough a local high, and the anomaly over the Lesser Antilles was reduced to a low of lesser amplitude than the Aves Ridge anomaly. The inferred basement position under the Lesser Antilles thus seems to have been quite accurate, for all that remains of the acute free air anomaly is a minor positive perturbation superimposed on the Bouguer anomaly low. Bouguer anomalies over the Aves Ridge, Grenada Trough and Lesser Antilles are all negative with respect to the Venezuela Basin anomaly.

The Bouguer anomaly was interpreted in terms of variation in depth of the Moho. For the reasons given in the previous section, models were computed for depths to Moho in the eastern Venezuela Basin of 13 km. and 20 km., using non-linear optimisation procedures.

The models are presented in fig. 5-3. The root beneath the Aves Ridge is somewhat larger than required for isostatic equilibrium, while the root beneath the island arc is approximately the same as that required for equilibrium. The mean depths beneath the Aves Ridge, Grenada Trough and Lesser Antilles for a depth to Moho under the Venezuela Basin of 13 km. are 29.5, 18 and 31 km. respectively, and for 20 km., 37.5, 24 and 40 km. respectively. The oscillation of the residuals is due to the short wavelength effects still apparent on the Bouguer anomaly.

The two-dimensional isostatic anomalies show small positive values in the Venezuela Basin with a mean value of 10 mgal. and agree well with a computed Airy anomaly (present worker). The anomalies decrease under the Aves Ridge. Although in reasonable agreement with the two-dimensional anomalies, a computed Airy anomaly (present worker) indicates that the two-dimensional anomalies are somewhat too large. This is probably due to the effects of the large seamount located slightly to the north of the profile on the Aves Ridge, whose effect will be to decrease the effect of the antiroot and so increase the isostatic anomaly relative to the two-dimensional anomaly in which no account is taken of this feature. The two-dimensional anomalies reach a minimum of -45 mgal. beneath the eastern part of the Aves Ridge, and thence increase eastwards over the Grenada Trough. A Pratt anomaly (Bush & Bush) computed in the Grenada Trough indicates a value of 0 mgal. while an Airy anomaly (present worker) indicates a value of -5 mgal. The two-dimensional anomalies indicate somewhat more negative anomalies, probably for the reasons discussed in the previous section, since the profile passes between islands of St. Lucia and St. Vincent. The roots beneath the

islands will have the effect of decreasing the isostatic correction with respect to the two-dimensional anomalies which do not take the islands into account. The Airy isostatic anomalies of Andrew et al. are some 50 mgal. more positive than the other three-dimensional isostatic anomalies computed for this area. The two-dimensional anomalies across the island arc show an increase from negative values in the east to a maximum value of 34 mgal. over the western flank. A computed Airy anomaly (present worker) over the centre of the arc has a value of 54 mgal., some 44 mgal. higher than the two-dimensional anomaly. A second Airy anomaly (present worker), located almost exactly between St. Lucia and St. Vincent, at latitude 13°34'N, has a value of 83 mgal. These large discrepancies are attributed to the inadequacy of the two-dimensional approximation where there is significant variation in topography along the strike of the body. The islands of St. Vincent and St. Lucia are underlain by roots reaching far greater depths than under the marine passage between the islands. Consequently the effect of the antiroot beneath the datum point is decreased. Also the topographic correction is increased by the attraction of the islands. Both these factors decrease the negative isostatic correction relative to that for a two-dimensional approximation, and so the isostatic anomaly is considerably larger. Andrew et al. have computed Airy isostatic anomalies for the islands of the Lesser Antilles, and their results will be critically examined in a later section.

5.7.3 Line L1412

The profile designated L1412 is a composite of the 1972 survey lines at 14°10'N in the west and at 14°15'N in the east, and was compiled to approximate the position of a Woods Hole Institute seismic reflection profile (Bunce et al., 1971). Bathymetry and gravity data

Figure 8-4
LH12

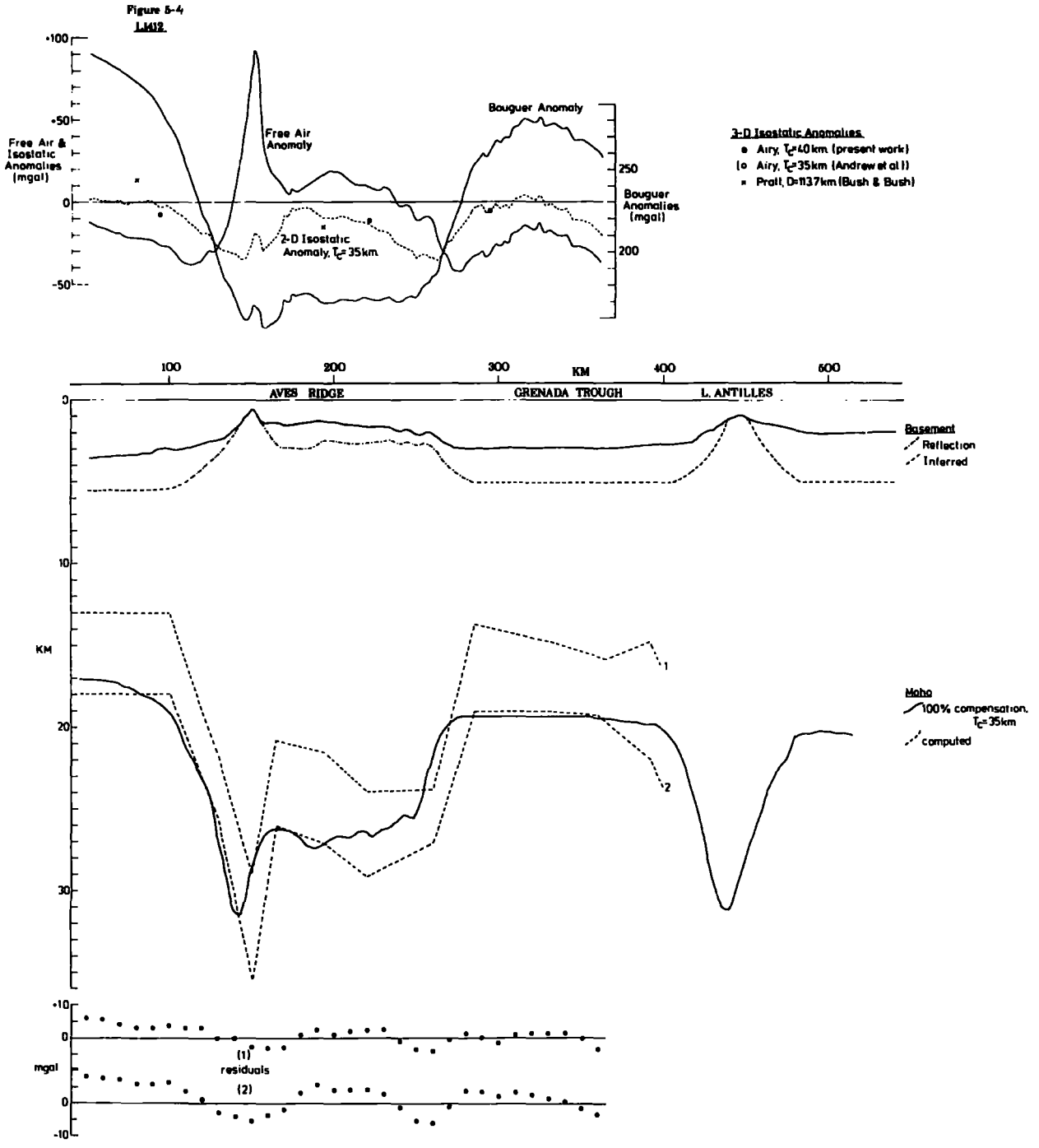

were only available for that part of the profile surveyed during 1972 and in order to complete the line over the Lesser Antilles, bathymetric data were taken from published naval charts. Errors in correlating the reflection data with other data were caused by a maximum latitude difference of 10 km. between these two data sets. Data relevant to the profile are presented in fig. 5-4.

Free air anomalies in the Venezuela Basin decrease towards the Aves Ridge from a value of -10 mgal. to a minimum of -38 mgal. The western part of the Aves Ridge exhibits a steep free air anomaly peak of maximum 93 mgal. centred over a bathymetric prominence. This prominence corresponds to one of the north-south trending ridges marking the western part of the Aves Ridge. The eastern part is characterised by smaller positive anomalies. Free air anomalies in the Grenada Trough decrease to a minimum of 42 mgal. near the eastern flank of the Aves Ridge, but increase gradually towards the centre of the Trough to a mean value of approximately -15 mgal. and thence decrease gradually as the island arc is approached.

The depth to basement in the Venezuela Basin was taken as 5.5 km., a value controlled by refraction line 9 of Officer et al. (1959) on the western flank of the Aves Ridge. Basement over the Aves Ridge was obtained from the aforementioned Woods Hole Institute reflection line assuming a sediment velocity of 2 km./sec. In the absence of refraction data in the Grenada Trough, it was necessary to assume a sediment thickness, a value of 2 km. being taken. Similarly, basement depths had to be assumed over the island arc, but were not critical as only an approximate depth to Moho was required as a control on the anomalies in the Grenada Trough.

The Moho computed for 100% isostatic compensation relative to a standard crustal thickness of 35 km. reached a depth of 17 km.

beneath the Venezuela Basin. This is in reasonable agreement with the depth of 18 km. recorded on refraction line 24 of Officer et al. 15 km. north of the profile. The Moho increased in depth to 31.4 km. to compensate for the prominent western ridge of the Aves Ridge, while the eastern part was compensated by a Moho at a mean depth of 26.5 km. The compensating Moho reaches a depth of 19.2 km. under the Grenada Trough, and increases in depth to 31 km. beneath the Lesser Antilles.

The Bouguer reduction was effective in removing short wavelength effects from the free air anomalies. The Aves Ridge became a broad low and the Grenada Trough a broad high, both units being negative with respect to the Venezuela Basin. The perturbations in the Bouguer anomaly beneath the western Aves Ridge are attributed to the errors involved in matching the reflection and gravity data, while other short wavelength, low amplitude perturbations are attributed to errors of observation.

The Bouguer anomaly was interpreted in terms of variation in depth of the Moho using non-linear optimisation procedures. Refraction line 24 of Officer et al. was shot c.30 km. north of the profile in the eastern Venezuela Basin, and shows a horizontal Moho at a depth of 18 km. This, then, would seem to be a reasonable depth to assume beneath the Venezuela Basin at the western end of the profile, although a model was also computed assuming this depth to be 13 km. for compatibility with the two profiles considered in the previous sections. The computed models indicate that the root underlying the Aves Ridge is somewhat larger than would be required for isostatic compensation.

In the absence of gravity data over the island arc, the Moho for 100% isostatic equilibrium under the Lesser Antilles was included as a constant in the optimising body during interpretation.

The two-dimensional isostatic anomalies indicate that the Venezuela Basin is in approximate isostatic equilibrium, although a Pratt anomaly (Bush & Bush) in this area is 14 mgal. and an Airy anomaly (present worker) -8 mgal. The two-dimensional anomalies decrease to -35 mgal. under the western flank of the Aves Ridge, increase to a mean of -10mgal. over the centre of the Ridge, and again decrease to -35 mgal. beneath the eastern part. The two-dimensional anomalies are in good agreement with both Pratt (Bush & Bush) and Airy (present worker) anomalies. The agreement is due to the two-dimensional nature of the Ridge at this latitude. The western Grenada Trough is in isostatic equilibrium, a fact illustrated by both two and three-dimensional anomalies. The two-dimensional anomalies decrease to negative values in the central Grenada Trough.

5.7.4 L1530

The profile designated L1530 was run at 15°30'N and coincides approximately with a Woods Hole Institute reflection profile (Bunce et al., 1971), although latitude differences between the two profiles are as great as 7 km. in places. Bathymetric data to complete the profile over the Lesser Antilles were taken from published naval charts. The profile passes over both the ridge marking the western flank of the Aves Ridge and the north-south trending ridge culminating in Aves Island 16 km. to the north of the profile. It also traverses the region of rugged topography in the northern Grenada Trough, and passes over the island of Dominica. Relevant data are presented in fig. 5-5.

Free air anomalies in the Venezuela Basin near the west flank of the Aves Ridge are -40 mgals. Both the ridges of the Aves Ridge are characterised by sharp peaks in the free air anomalies, reaching

Figure 5-5

L.1530

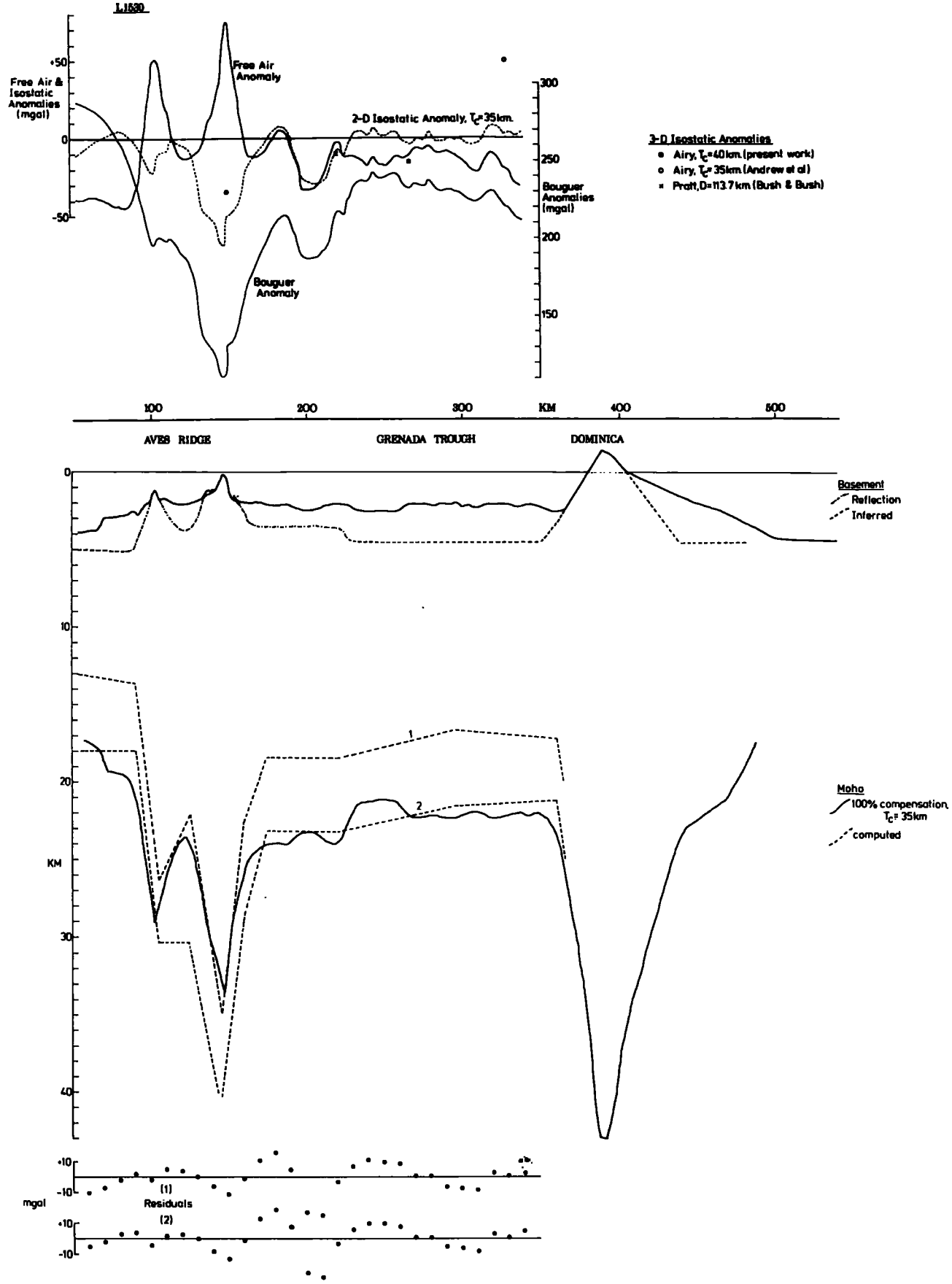

maxima of 51 and 75 mgal. The Grenada Trough exhibits free air anomalies varying little about a mean of approximately -10 mgal.

The depth to basement in the Venezuela Basin was taken as 5 km., and corresponds to a weak reflector traced westwards from the basement reflector of the Aves Ridge. Basement under the Aves Ridge was defined by the aforementioned Woods Hole Institute reflection profile. In these latitudes, the boundary between Aves Ridge and Grenada Trough is unclear on bathymetric data alone, and so this boundary was taken at 63°10'W, a position corresponding to a marked break in the basement reflector. Thereafter depth to basement under the Grenada Trough was assumed to be at a depth of 4.5 km. The island of Dominica was assumed to have no sediment cover.

The Bouguer reduction was not completely successful in eliminating short wavelength effects from the free air anomalies. Whether this was due to the inaccuracies of matching reflection and gravity data, or the assignment of a single density to the main part of the crust is uncertain. In spite of the presence of these short wavelength components, it is still possible to recognise the major trends in the Bouguer anomaly, which exhibits a relatively sharp low over the Aves Ridge and broad smooth high over the Grenada Trough. Short wavelength, low amplitude perturbations superimposed on both the free air and Bouguer anomalies are interpreted as errors of observation.

The Moho computed for 100% isostatic equilibrium relative to a standard crustal thickness of 35 km. was found to reach a depth of 17 km. under the Venezuela Basin. The two ridges of the Aves Ridge would be compensated by the Moho's reaching depths of 29.1 and 33.6 km. for the western and eastern ridges respectively, while the compensating depth under the Grenada Trough would be at a depth of c.22 km. The compensating Moho under the island arc would reach a depth of 42.9 km.

This depth is greater than that computed for the previous profiles, and is required to compensate for the surface load of the island of Dominica.

The Bouguer anomaly was interpreted in terms of variation in depth to the Moho using non-linear optimisation procedures. Refraction line 31 of Officer et al. (1959) was shot just to the south-west of the profile, and shows the Moho dipping gently from west to east with a gradient of 26m/km., reaching a depth of c.18 km. in the region of the western end of the profile. A depth to Moho of 18 km. was thus taken as the depth to the Moho under the Venezuela Basin at the western end of the profile, although a further model was computed for a depth to Moho in this area of 13 km. for compatibility with other profiles considered. The models computed both indicate that the root beneath the Aves Ridge is larger than that required for isostatic equilibrium. In the absence of gravity data over the island arc, the root under the arc was included as a constant in the optimising body during interpretation.

The two-dimensional isostatic anomalies indicate that the Venezuela Basin is in approximate isostatic equilibrium. Isostatic anomalies over the Aves Ridge are negative, with a minimum of -69 mgal. recorded over the prominent bathymetric peak on the centre of the Ridge. An Airy anomaly (present worker) computed on the eastern flank of this feature is 15 mgal. less negative than the two-dimensional anomaly at this point, a discrepancy probably explained by the rugged topography of this part of the Aves Ridge. The two-dimensional anomalies indicate that the Grenada Trough is in isostatic equilibrium, and agree almost exactly with a Pratt anomaly (Bush & Bush) computed in this area, although an Airy anomaly (present worker) has a value of -15 mgal. The Airy anomalies computed by Andrew et al. in this region are of the order of 50 mgals.

## 5.8 An Isostatic Anomaly Map of the Eastern Caribbean

It has been shown in the preceding sections that local two-dimensional isostatic anomalies are only sufficient to define general trends, and may be quite inaccurate quantitatively in areas of rough topography. Consequently it is preferred to discuss the state of isostatic equilibrium of the region in terms of the standard three-dimensional anomalies.

Fig.5-6 is a contour map of isostatic anomalies in the eastern Caribbean using data presented by Bush & Bush (1969) and data reduced by the present worker. The original contours of Bush & Bush have been modified in the light of the new reductions. It may be argued that incorporation of the Pratt anomalies of Bush & Bush and the Airy anomalies of the present worker into a single chart is not strictly valid. However, both reductions should give an adequate representation of the state of isostatic equilibrium, and the contour interval of 50 mgal. is considered insufficient to amplify the slight differences in the isostatic corrections between the two reductions.

The Airy isostatic anomalies produced by Andrew et al. (1971) were not used in the compilation of this contour map. All their marine reductions produce anomalies which are consistently greater than both the Pratt anomalies of Bush & Bush and the Airy anomalies of the present worker. Although bathymetric data at the time of reduction were sparse (Masson Smith, pers. comm.) the discrepancies would seem to be too great to be attributed to this. Neither are they due to differences in the measured free air anomaly, although these were up to 24 mgal. The anomalies were not computed using graticules, but by a computer routine using elevation estimates within 5-minute geographic squares. This program would seem to be

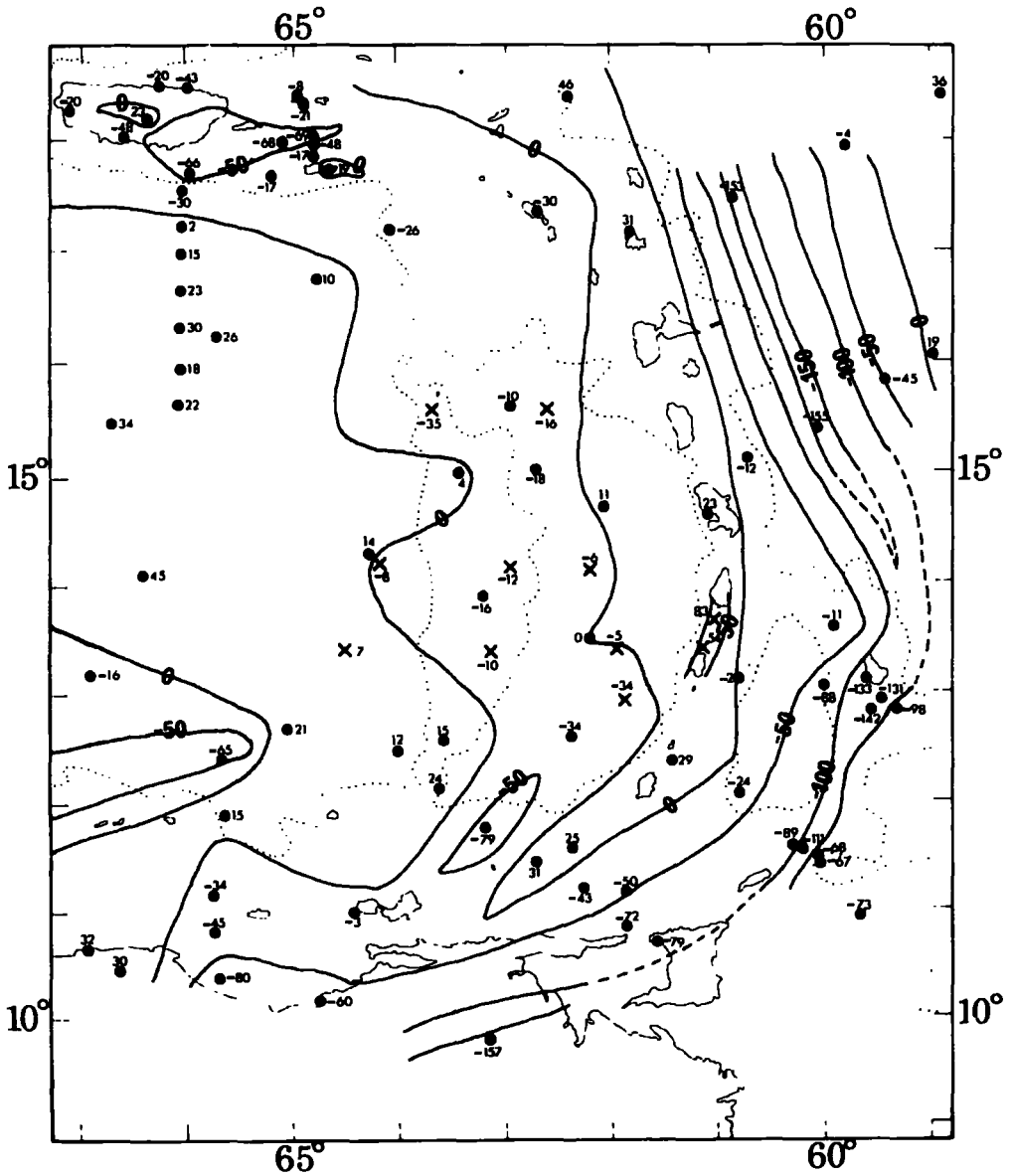


: [illegible]
[illegible]
● - [illegible]
(from Bunn & Bush, [illegible])
× - [illegible] $T_{e=1}$
(this work)

faulty. The method was also used in reducing the gravity data from the islands of the Lesser Antilles. However, the density used for the Bouguer reduction was 2.5 gm/cc., while the crustal density assumed for the isostatic correction was 2.67 gm/cc. Consequently their isostatic anomalies will be too low by an amount equal to $(h \times (2.67-2.5)\frac{2\pi G}{g})$ mgal., where h is the elevation of the station. This discrepancy, coupled with a possible fault in the computer program, did not lend sufficient confidence for their anomalies to be incorporated into the contour map.

The generalfeatures of the contour map are discussed below.

The central areas of the Venezuela Basin are characterised by positive isostatic anomalies. Edgar et al. (1971a) have shown that there is a gentle doming of the crust of the Venezuela Basin from its margins to its centre, and it is possible that this doming represents a response of the crust to compressive forces which are clearly expressed at the margins of the Caribbean. These positive anomalies, which decrease towards the margins of the Basin, would thus seem to support this proposed 'upwarping' of the crust.

The Aves Ridge and western Grenada Trough are characterised by negative isostatic anomalies with a mean value of -10 mgal., although positive anomalies have been recorded on the southern tip of the Aves Ridge. One negative anomaly of -35 mgal. recorded near Aves Island may be indicative of a somewhat late stage feature which has had insufficient time to reach the state of equilibrium of the rest of the Aves Ridge. Greater negative values occur in the southern Grenada Trough, and may in part represent the effects of a thickened sediment cover. Anomalies are positive in the north-eastern Grenada Trough.

The Lesser Antilles are characterised by a belt of positive isostatic anomalies stretching from the Venezuelan continental shelf to Guadeloupe. North of Guadeloupe the belt appears to follow the limestone Antilles rather than the volcanic arc, with a positive anomaly of 31 mgal. recorded on Antigua and a negative anomaly of -30 mgal. on St. Kitts. Fink (1972) has concluded that the limestone Antilles represent an ancient volcanic arc with a pre-Miocene history and that the late Miocene to Recent deposits of the present volcanic arc north of Dominica constitute a smaller volume than that of the limestone arc perched on the western flank of the pre-existing ridge. The isostatic anomalies would seem to support this conclusion.

The presence of positive isostatic anomalies over the Lesser Antilles indicates that the island arc would have to sink in order to attain isostatic equilibrium. There is no evidence of subsidence, and, indeed, the presence of raised beaches and elevated blocks of limestone around the volcanoes on some of the islands are indicative of past upwards movements. The mechanism by which the Lesser Antilles maintain their elevated positions is not known, but is probably due to some process related to the subduction zone beneath the island arc.

The isostatic anomalies decrease rapidly to the east of the Lesser Antilles to values of less than -150 mgal. in the region of the 'trench' and thence increase to small positive values in the Atlantic Ocean.

## 5.9 Interpretation of Deep and Shallow Structures by the removal of surface topography

Seismic reflection control was only available for the profiles described in the previous sections, and for the interpretation of other profiles it was necessary to adopt a different procedure.

The procedure, described below, arbitrarily separates the anomalies due to deep and shallow structures by a process akin to a Bouguer reduction and the separation, guided by this reduction, of the long and short wavelength anomalies attributed to deep and shallow crustal features. It should be stressed that this procedure was performed simply to obtain adequate crustal models and does not unambiguously separate the anomalies due to deep and shallow structures.

The method adopted was a process of subtraction from the free air anomaly of the gravitational effects of all surface topography above a level on the profile in the Venezuela Basin. This excess topography was assigned a density of 2.5 gm/cc., a value, taken from P-wave velocity-density curves, which was considered to represent an average value for both the sediments and volcanic rocks believed to be responsible for the topographic expression of the Aves Ridge. This value was also considered to be the most appropriate for terrain corrections on the Lesser Antilles by Andrew et al. (1970).

The effect of the topography was computed at each observation point using subroutine GRAV. This effect was subtracted from the free air anomaly and the resulting anomalies made relative to the Bouguer anomaly (for 2.00 gm/cc.) at the most westerly point on the profile in the Venezuela Basin. A typical plot of such anomalies is given in fig. 5-7b. It will be observed that the curve representing observed anomalies minus the effect of the topography (hereafter referred to as the anomaly due to deep structures) still contains the short wavelength effects of the free air anomalies although these may be reduced in amplitude. These effects are to be expected since they represent, in part, features in the sediment/basement interface, and since surface topography was considered uniform in density for

this first step, such short wavelength effects could not be eliminated. The next step was to draw, by eye, a smooth curve through the base of the deep gravity curve to remove these short wavelength effects. However, the Grenada Trough has been shown by seismic refraction and reflection to have a substantial sediment cover, and so negative anomalies are to be expected after the removal of deep gravity effects. It will be noted that the subtraction of the smooth curve through the computed points for deep gravity structures from the Bouguer anomalies would result in positive anomalies over the Grenada Trough. Bunce et al.(1971) have suggested that a possible cause of the gravity high is the presence of high density crustal rocks underlying the Grenada Trough, but the presence of similar seismic structures under the Venezuela Basin, Aves Ridge and Grenada Trough does not support this hypothesis. The preferred interpretation is that the source of this gravity high lies in a relatively shallow depth to the Moho and also possibly to the lowest crustal layer.

Consequently, when drawing a smooth line through the deep gravity curve, the line was drawn so as to give a maximum negative anomaly of approximately -10 mgal. over the Grenada Trough, a value compatible with the sedimentary thickness indicated from seismic refraction data. The limits of the negative anomaly were defined by the topographic expression of the Grenada Trough. It should be noted that the low amplitude, short wavelength anomalies registered over the Grenada Trough cannot have their origin in geological structures, and are attributed to errors of observation.

The smoothed deep gravity curve was then used in interpretation of deep structures. Where it was desired to perform an interpretation of shallow structures, the deep gravity curve was digitised at 10 km. intervals, a cubic interpolation performed to compute both Bouguer and

deep gravity anomalies at the same point, and the data subtracted to produce the gravity effects of shallow structures.

The method of separating the deep and shallow gravity effects described above must be considered as an approximation, since it assumes that the Moho and lowest crustal layer vary in depth only to compensate topographic features and that no compensation is necessary for variations in the bulk of the crust underlying these features. In fact, Edgar et al. (1971a) consider that a thickened 6.3 km/sec. seismic layer is responsible for the major topography of the Aves Ridge, in which case the estimate of 2.5 gm/cc. for the excess topography would be too low. Andrew et al. (1970), however, from a consideration of measurements both in situ and of hand specimens, have concluded that a density of 2.5 gm/cc. represents a reasonable value for terrain corrections on the Lesser Antilles. A test of the method is the production of reasonable models for the upper crustal structure after the subtraction of deep gravity effects from the Bouguer anomalies. Later sections will show that this is indeed possible, although the models produced must not be considered unambiguous.

Interpretations of shallow crustal structure were only performed where there was adequate seismic refraction control on the crustal layering. Consequently the profiles chosen for interpretation were selected taking regard of their approximation to two-dimensionality in an east-west sense and the number of refraction lines in close proximity to the profile. Occasionally it was necessary to sacrifice the former for the latter.

Lettered anomalies refer to the Bouguer anomaly chart.

5.9.1 Line L1500

The profile at 15°00'N crosses the southern part of the north-south striking ridge which culminates in Aves Island 16 km. to the north. Relevant data are presented in fig. 5-7. The most serious deviation from two-dimensionality occurs at 63°20'W, where the profile passes just south of a small subcircular feature rising relatively abruptly from the Aves Ridge. Consequently the profile passes through the southern part of the gravity field (gravity high C) associated with this feature. Elsewhere the two-dimensional approximation is good. Refraction lines 22 and 31 of Officer et al. (1959), in the Venezuela Basin and on the eastern flank of the Aves Ridge respectively, were used as controls on interpretation, although only the latter reached the Moho at a depth of 18.1 km., and is displaced slightly to the north of the profile.

The anomaly curve attributed to deep structures (fig.5-7c) exhibits a broad low under the Aves Ridge and slightly less broad high over the Grenada Trough.

The deep gravity curve was interpreted in terms of variation in depth to both the top and base of the lowest crustal layer. Refraction line 31 indicates that this layer has a vertical thickness of 6.9 km. beneath the Venezuela Basin, and it was assumed that it attained a constant thickness of 4 km. beneath both the Aves Ridge and Grenada Trough. Such an assumption was necessary to decrease the ambiguity of the interpretation. Models were computed, using a non-linear optimisation routine, for density contrasts across the top and bottom (i.e. the Moho) of the lowest crustal layer of 0.27 and 0.17 gm/cc., 0.3 and 0.2 gm/cc and 0.33 and 0.29 gm/cc., values computed from velocity-density curves which were considered representative of minimum, mean and maximum estimates. The model for the mean densities

Figure 5 -7 : Line L1500

a - observed Bouguer anomaly

b - Bouguer anomaly with effects of topography removed

c - smoothed anomaly of deep structures

d - anomaly of shallow structures

e - computed shallow structure, calculated anomalies shown as solid circles on curve d

f - computed deep structure, calculated anomalies shown as solid circles on curve c

Vertical lines refer to refraction profiles

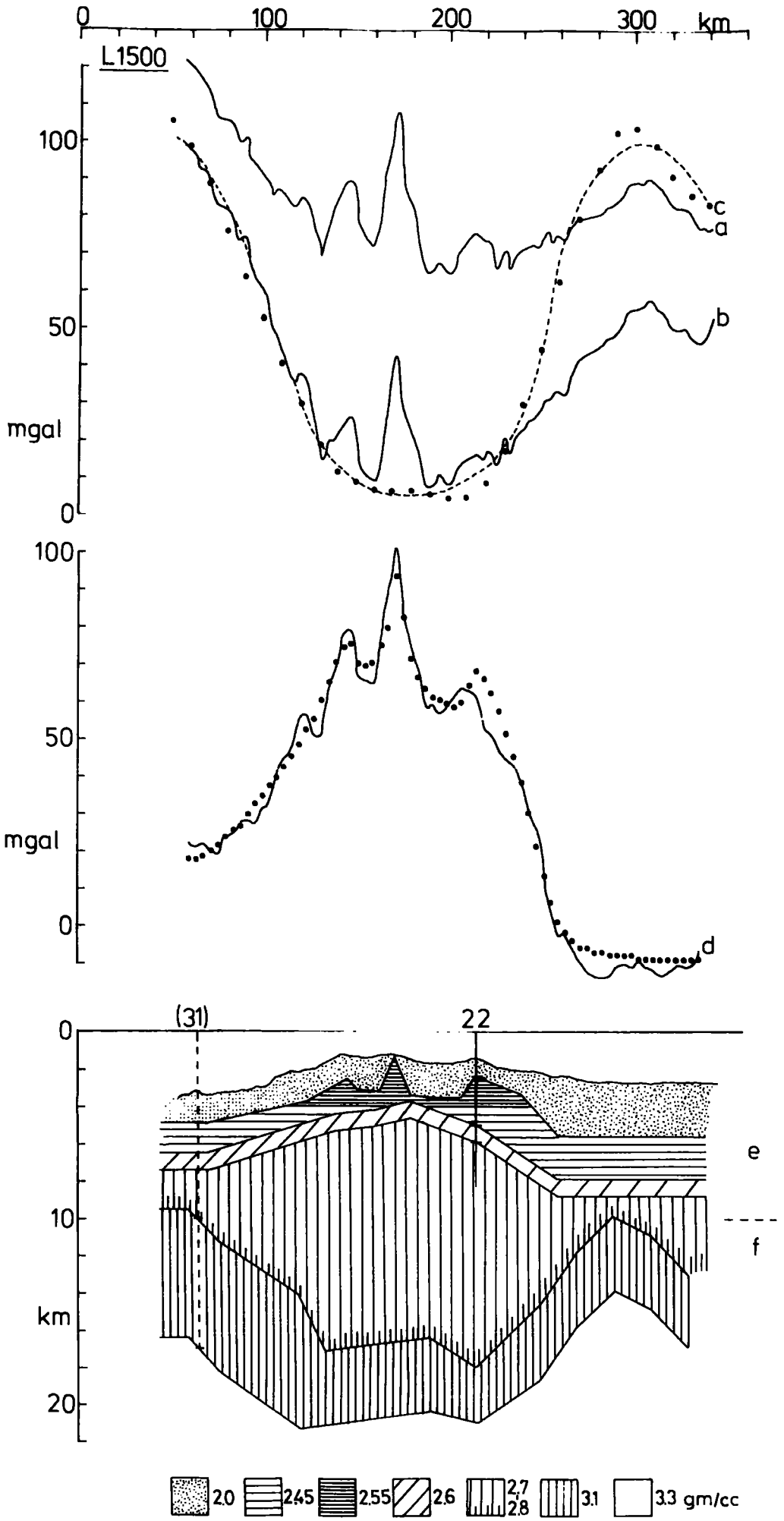
0
100
200
300
km
L1500
100
50
mgal
0
c
a
b
100
50
mgal
0
d
(31)
22
0
10
km
20
e
f
2.0
2.45
2.55
2.6
2.7
2.8
3.1
3.3 gm/cc

is presented in fig. 5-7f, and reached a maximum depth of 22.0 km. under the Aves Ridge and a minimum depth of 13.9 km. under the Grenada Trough. The maximum and minimum density contrasts gave limits of 22.0-23.1 km. and 13.6-14.4 km. to these values, but are not illustrated as the space-form of the body is not significantly changed. It should be stressed that these depths are dependent upon the original assumptions made in constructing the anomaly curve. In particular, the depths under the Grenada Trough are dependent on the anomaly assumed for the sediments of the Grenada Trough.

The shallow gravity curve is presented in fig. 5-7d. The three central gravity peaks are seen to correlate with bathymetric features, although, as previously stated, the central peak is in part due to more exaggerated bathymetry slightly to the north. The anomaly was interpreted using a non-linear optimisation routine in terms of variations in the four crustal layers indicated by seismic refraction using refraction line 22 of Officer et al. as a control. Correlations of velocity with density were taken as: 1.7 km/sec. = 2.0 gm/cc., 3.2 km/sec.= 2.5 gm/cc., 5.0 km/sec. = 2.6 gm/cc. and 6.2 km/sec. = 2.7 gm/cc.

The computed model is presented in fig. 5-7e. The peaks in the gravity anomaly were found to be due principally to structures developed by the 3.2 km/sec. seismic layer. It was found that a rather higher density was required for this layer under the Aves Ridge than under the flanking basins. In fact the density used, namely 2.55 gm/cc. is barely sufficient to fit the steep gradients of the peaks, and better fits would be obtained using higher densities, although these higher densities would not be compatible with values obtained from the velocity-density curves.

An increase in thickness of the 6.2 km/sec. seismic layer is seen to be responsible for the major part of the Aves Ridge, a result in

accordance with Edgar et al.'s (1971a) conclusions from seismic refraction results elsewhere on the Aves Ridge.

5.9.2 Line L1430

The profile at 14°30'N crosses the northern part of one of the prominent north-south trending ridges, centred on 63°40'W, which mark the western part of the Aves Ridge. It also passes over the centre of a small bathymetric prominence, centred on 63°10'W, and over a somewhat broader bathymetric high, elongate north-south, which marks the eastern flank of the Aves Ridge. These three topographic features are also marked by gravity highs (D, E and F respectively) which are elongate north-south. The two-dimensional approximation used in interpretation is thus considered valid. Relevant data are presented in fig. 5-8.

Refraction lines 10, 22, 24 and 30 of Officer et al. (1959) cross the profile, although line 24 was the only line to record the Moho. However, line 24 was shot in the direction of the profile and shows layers dipping gently eastwards. The observed gravity anomalies in the area of this line exhibit an easterly dipping gradient which is far too acute to be caused by the layering indicated by the refraction line. Consequently it is suggested that the navigation of Officer et al. was faulty, and this line was used only to control the depths of the Moho and lowest crustal layer at the western end of the profile.

The deep gravity curve shows the typical form of a broad low over the Aves Ridge and high over the Grenada Trough. The curve was interpreted in terms of variation in depth to the top and base of the lowest crustal layer using non-linear optimisation routines. Refraction line 24 of Officer et al. indicates that this layer is

Figure 5-8 : Line L1430

a - observed Bouguer anomaly

b - Bouguer anomaly with effects of topography removed

c - smoothed anomaly of deep structures

d - anomaly of shallow structures

e - computed deep structure, calculated anomalies shown as solid circles on curve c

f - computed shallow structure, calculated anomalies shown as solid circles on curve d

Vertical lines refer to refraction profiles

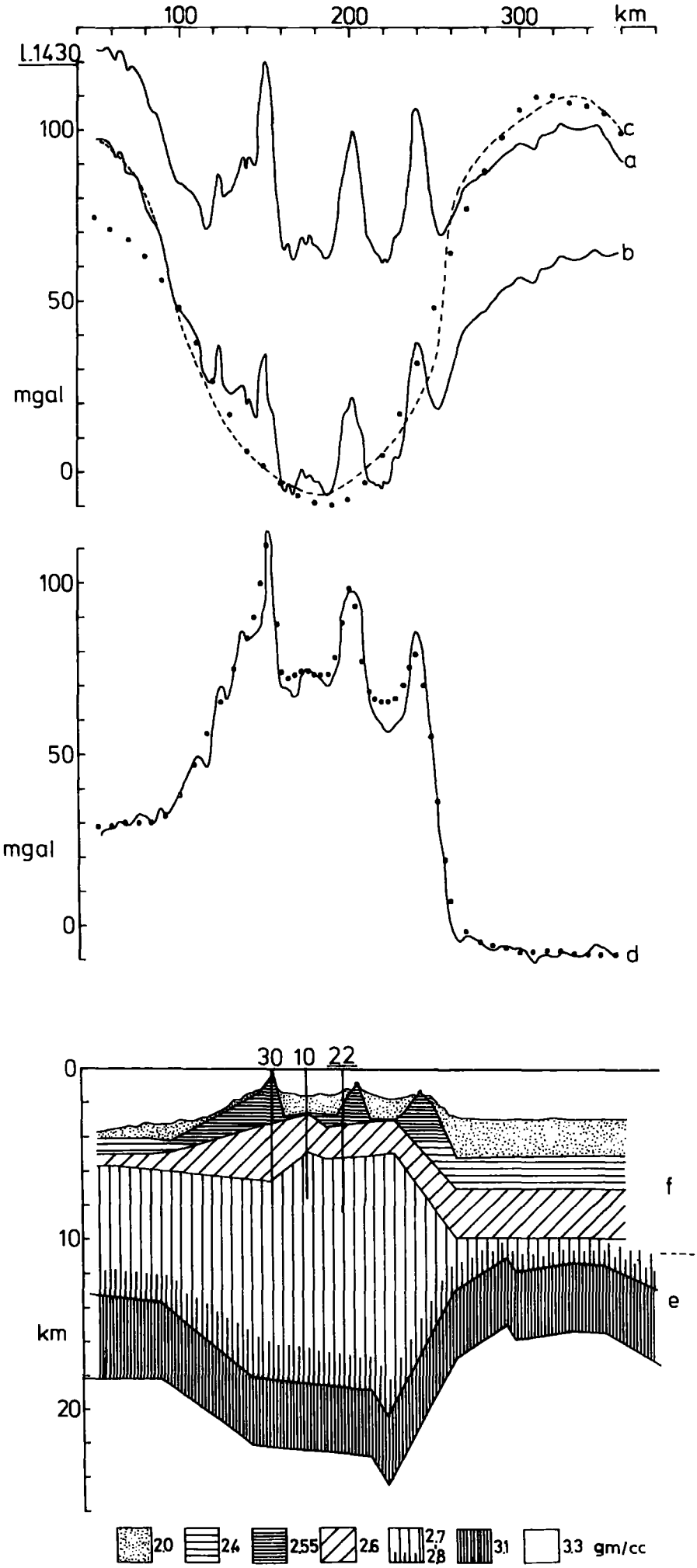
100
200
300
km
L.1430
100
50
mgal
0
c
a
b
100
50
mgal
0
d
30 10 22
0
10
km
20
f
e
2.0
2.4
2.55
2.6
2.7
2.8
3.1
3.3 gm/cc

4.5 km. thick under the Venezuela Basin and to decrease ambiguity in interpretation it was assumed that the layer attained a constant vertical thickness of 4 km. under both the Aves Ridge and Grenada Trough. Models were computed for density contrasts across the top and base of the lowest crustal layer of 0.27 and 0.17 gm/cc., 0.3 and 0.2 gm/cc. and 0.33 and 0.29 gm/cc. The model for 0.3 and 0.2 gm/cc. is presented in fig. 5-8e. The Moho was found to reach a maximum depth of c.23 km. beneath the Aves Ridge and a minimum depth of 15.1 km. beneath the Grenada Trough. The models for maximum and minimum density contrasts impart limits of 22.5-23.7 km. and 14.8-15.7 km. to these values, but are not illustrated as the space-form of the body is not significantly changed. The computed depths are dependent on the original assumptions made in constructing the anomaly curve.

The gravity anomaly attributed to shallow crustal features is presented in fig. 5-8d. The three principal gravity peaks correlate with bathymetric prominences. Four principal upper crustal seismic layers are revealed by the refraction lines with velocities of 1.8, 3.2-3.7, 4.4-5.0 and 6.2 (increasing with depth to 6.7) km/sec. Sediment velocities of 1.8 km/sec. were only recorded on the central line, implying the lack of sedimentary cover on the Aves Ridge in the region of the two flanking refraction lines. Refraction line 24 indicates the presence of all four layers in the Venezuela Basin.

The anomaly was interpreted using a non-linear optimisation routine with the refraction lines as controls. The densities of the layers were taken as 2.0, 2.4-2.55, 2.6 and 2.7-2.8 gm/cc. The computed body is presented in fig. 5-8f. It was found that the layer immediately underlying the sediments required a higher density under the Aves Ridge than under the flanking basins in order to

simulate the three short wavelength gravity peaks and produce reasonable depths to the interfaces in the basins. Again, a thickened 6.2 km/sec. layer is seen to be the major contributor to the topography of the Aves Ridge, a result in accordance with Edgar et al's (1971a) observations based on seismic refraction elsewhere on the Aves Ridge.

5.9.3 Line L1400

The profile at 14°00'N passes over the southern tip of the north-south trending ridge considered in the previous section, across the broad plateau to the north of the prominent sea-mount in the south of the survey area and across the minor ridge marking the eastern flank of the Aves Ridge. The gravity fields of the latter two features approximate well to two-dimensionality at the latitude of the profile, but the major deviation from the two-dimensional approximation occurs over the ridge on the western part of the Aves Ridge, as the profile passes over the southern end of its associated gravity field (gravity high D). However, it was decided to perform an interpretation of this profile since it is the most southerly for which there is adequate seismic refraction control. In the southern part of the survey area there is no seismic refraction coverage of the Aves Ridge. Data relevant to the profile are presented in fig. 5-9.

Seismic refraction control on this profile is good, with four lines of Officer et al. (1959) crossing the profile. Line 9 is in the Venezuela Basin, lines 23 and 30 on the Aves Ridge, and line 29 one of the only three lines run in the Grenada Trough. However none of these lines recorded the Moho and only line 29 recorded the top of the lowest crustal layer.

The gravity anomaly attributed to deep structures exhibits the typical low over the Aves Ridge and local high over the Grenada Trough,

Figure 5-9 : Line L1400

a - observed Bouguer anomaly

b - Bouguer anomaly with effects of topography removed

c - smoothed anomaly of deep structures

d - anomaly of shallow structures

e - computed shallow structure, calculated anomalies shown as solid circles on curve d

f - computed deep structure, calculated anomalies shown as solid circles on curve c

Vertical lines refer to refraction profiles

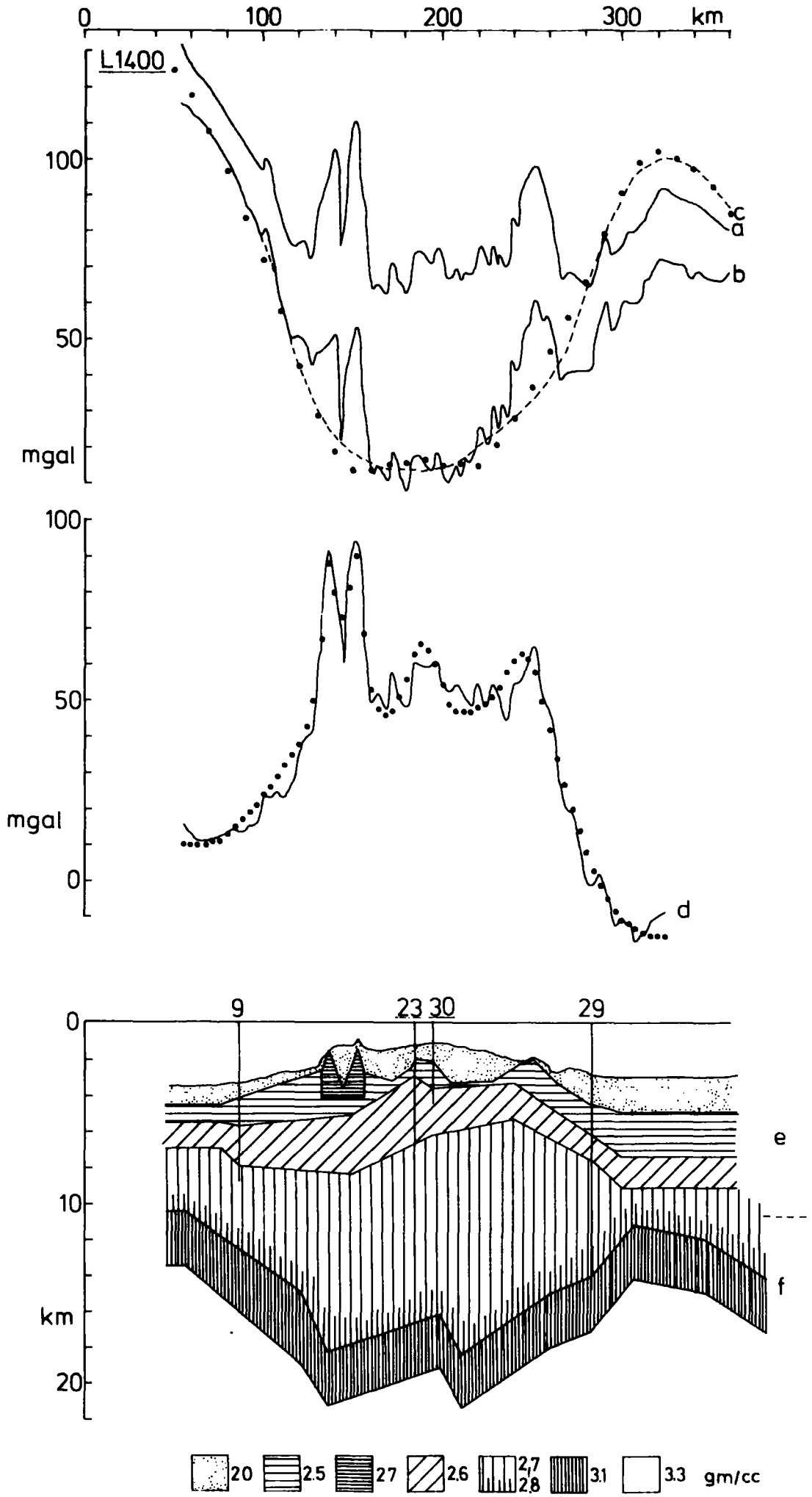
0
100
200
300
km
L1400
100
50
mgal
c
a
b
100
50
mgal
0
d
0
9
23 30
29
10
km
20
e
f
2.0
2.5
2.7
2.6
2.7
2.8
3.1
3.3
gm/cc

and was interpreted in terms of variation in depth to the top and base of the lowest crustal layer using a non-linear optimisation routine. In the absence of information on the depth to the Moho under the profile, it was necessary to assume its position at one point. Refraction line 25 of Officer et al., 130 km. to the west-south-west of the profile, indicates a vertical thickness of the lowest crustal layer of 3 km. The top of this layer was recorded on refraction line 29 at a depth of 14.1 km., and so the lowest crustal layer was assumed to attain a constant thickness of 3 km. under the profile, with the Moho reaching a depth of 17.1 km. under refraction line 29. Interpretations were performed for density contrasts across the top and base of the lowest crustal layer of 0.27 and 0.17, 0.3 and 0.2 and 0.33 and 0.29 gm/cc. The model for 0.3 and 0.2 gm/cc. is presented in fig. 5-9f. The Moho was found to reach a maximum depth of 21.4 km. beneath the Aves Ridge and a minimum depth of 14.2 km. beneath the Grenada Trough. The models for maximum and minimum density contrasts give limits of 20.8-21.9 km. and 13.7-14.8 km. to these values, and are not illustrated since the space-form of the bodies is not significantly affected. These computed depths are dependent upon the assumptions made in constructing the gravity curve.

The anomalies attributed to shallow crustal features are presented in fig. 5-9d. Four principal upper crustal seismic layers are apparent from the seismic refraction lines with velocities of 1.7-2.0, 2.8-3.8, 4.1-5.3 and 6.2-6.7 km/sec., and occur under the Venezuela Basin, Aves Ridge and Grenada Trough. The anomaly was interpreted using a non-linear optimisation routine with the refraction lines as control and using densities of 2.0, 2.5, 2.6 and 2.7-2.8 gm/cc. for the four seismic layers. The prominent double gravity peak over the

western ridge could only be explained by a body of somewhat higher density than its surroundings, and as such represents an anomalous feature of the Aves Ridge although the deviation from strict two-dimensionality may contribute to this higher density. The anomaly over the central and eastern parts of the Aves Ridge contains low amplitude, short wavelength effects, the majority of which are probably caused by observational errors. The model produced, however, fits the two peaks which are of somewhat longer wavelength. Again, a thickened 6.2 km/sec. seismic layer is seen to be responsible for the major part of the Aves Ridge, in accordance with the observations of Edgar et al. (1971a) elsewhere on the Aves Ridge.

5.9.4 Line L1304

Data relevant to the profile at 13°04'N are presented in fig.5-10. Only refraction line 29 of Officer et al. (1959) crosses the profile and did not record the Moho, although the top of the lowest crustal layer was recorded at 18.2 km. Refraction line 25 of Officer et al. was shot 110 km. to the west of the profile and indicated a horizontal configuration of the lowest crustal layer, which attained a vertical thickness of 3 km. It was assumed that the layer remained at this constant thickness under the Aves Ridge and Grenada Trough to decrease the ambiguity of interpretation. Consequently the Moho was inferred to reach a depth of 21.2 km. beneath refraction line 29. No interpretation of shallow structures was attempted due to the lack of adequate seismic refraction control.

The deep gravity curve was interpreted in terms of variation in depth to the top and base of the lowest crustal layer using a non-linear optimisation procedure. Interpretations were performed for density contrasts across the top and base of the lowest crustal

Figure 5-10 : Line L1304

a - observed Bouguer anomaly

b - Bouguer anomaly with effect of topography removed

Figure 5-11 : Line L1324

c - smoothed anomaly of deep structures

d - bathymetry

e - computed model, calculated anomalies shown as solid circles on curve c

Vertical lines refer to refraction profiles

Figure 5-12 : Line L1540

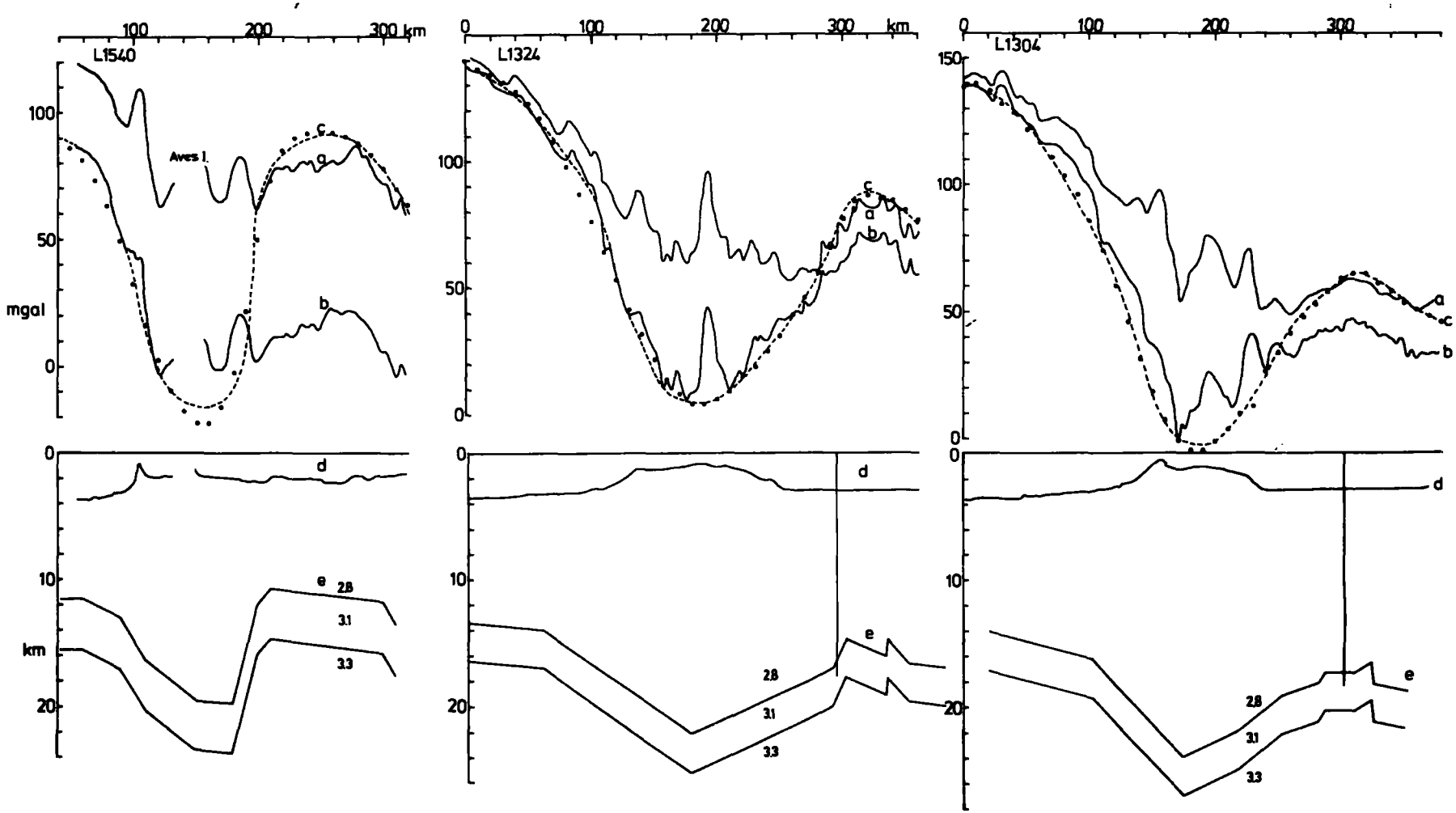
L1540
L1324
L1304
100
200
300 km
0
50
150
mgal
Aves I.
a
b
c
d
e
2.8
3.1
3.3
km
10
20

layer of 0.27 and 0.17, 0.3 and 0.2 and 0.33 and 0.29 gm/cc. The model for 0.3 and 0.2 gm/cc. is presented in fig. 5-10e, and indicates a maximum depth to the Moho beneath the Aves Ridge of 26.9 km., and a minimum depth of 19.5 km. beneath the Grenada Trough, these values being dependent upon the assumptions made in constructing the deep gravity curve. The maximum and minimum density contrasts impart limits of 22.1-24.2 km. and 19.5-19.9 km. to these depths without significantly affecting the space-form of the body.

5.9.5 Line L1324

Data relevant to the profile at 13°24'N are presented in fig. 5-11. Only refraction line 29 of Officer et al. (1959) crosses the profile and did not record the Moho, although the top of the lowest crustal layer was recorded at a depth of 17 km. For the reasons discussed in section 5.9.4, the lowest crustal layer was assumed to attain a thickness of 3 km. under the Aves Ridge and Grenada Trough, implying a depth to Moho of 20 km. beneath refraction line 29.

The deep gravity curve was interpreted in terms of variation in depth to the top and base of the lowest crustal layer using a non-linear optimisation procedure. Interpretations were performed for density contrasts across the top and base of the lowest crustal layer of 0.27 and 0.17, 0.3 and 0.2 and 0.33 and 0.29 gm/cc. The model for 0.3 and 0.2 gm/cc. is presented in fig. 5-11e, and indicates a maximum depth to Moho beneath the Aves Ridge of 25.2 km. and a minimum depth of 17.7 km. beneath the Grenada Trough, these values being dependent upon the original assumptions made in constructing the deep gravity curve. The maximum and minimum density contrasts

impart limits of 24.2-25.8 km. and 17.6-18.6 km. to these depths without significantly changing the space-form of the body.

This interpretation may be compared with that obtained by a different method discussed in section 5.7.2. It may be seen that the interpretation obtained here is in good agreement with that obtained previously assuming a depth to Moho beneath the eastern Venezuela Basin of 13 km.

5.9.6 Line L1540

The profile at 15°40'N is the most northerly considered and passes over the Aves Ridge at the approximate latitude of Aves Island. Relevant data are presented in fig. 5-12. No seismic refraction data are available for the section surveyed, but line 31 of Officer et al. (1959), 70 km. to the west of the profile, is available for control on depths to the top of the lowest crustal layer and Moho. Absence of refraction data precluded the unambiguous interpretation of upper crustal structure.

At these latitudes, although the western limit of the Aves Ridge is clearly defined, the boundary between the Aves Ridge and Grenada Trough is not certain on bathymetric data alone. On more southerly profiles the Grenada Trough appears as a broad high on the Bouguer anomalies, and so the Trough was assumed to commence at the start of a similar feature at x-coordinate 200 km. The deep gravity curve produced is of somewhat shorter wavelength than previously encountered, but it will be shown that it does not preclude the causative structure being due to variations in depth to the lowest crustal layer and Moho.

The anomaly was interpreted using a non-linear optimisation routine. Refraction line 31 indicates a vertical thickness of 4 km. for the lowest crustal layer in the Venezuela Basin, and it was assumed

that the layer attained this thickness under the Aves Ridge and Grenada Trough to decrease ambiguity in interpretation. The interpretation was performed for density contrasts across the top and base of the lowest crustal layer of 0.27 and 0.17, 0.3 and 0.2 and 0.33 and 0.29 gm/cc. The model for 0.3 and 0.2 gm/cc. is presented in fig. 5-12e and reached a maximum depth to Moho of 23.7 km. under the Aves Ridge and a minimum depth of 14.7 km. under the Grenada Trough, these values being dependent on the assumptions made in constructing the deep gravity curve. The maximum and minimum density contrasts impart limits of 22.1-24.2 and 14.5-14.9 km. to these depths without significantly changing the space-form of the body.

## 5.10 Interpretation of shallow crustal features

### 5.10.1 Investigation of a gravity low on the southern Aves Ridge

The elongate north-south gravity low H occurs in the southern part of the survey area centred on 63°25'W extending south from approximately 13°10'N and continuing outside the area surveyed. Two profiles across this feature were investigated.

The first profile is at 12°54'N. Relevant data are presented in fig. 5-13. The magnetic field (fig.5-13a) across the feature is smooth but disturbed on either side. Consequently the feature was interpreted as a low in the sediment/basement interface. The gravity anomaly was isolated by the subtraction of a linear'regional' (fig. 5-13b), and the resulting residual anomalies interpreted using a non-linear optimisation procedure. Models were computed for a series of density contrasts, and those for density contrasts of -0.5 and -0.9 gm/cc. between sediments and basement shown in fig. 5-13c.

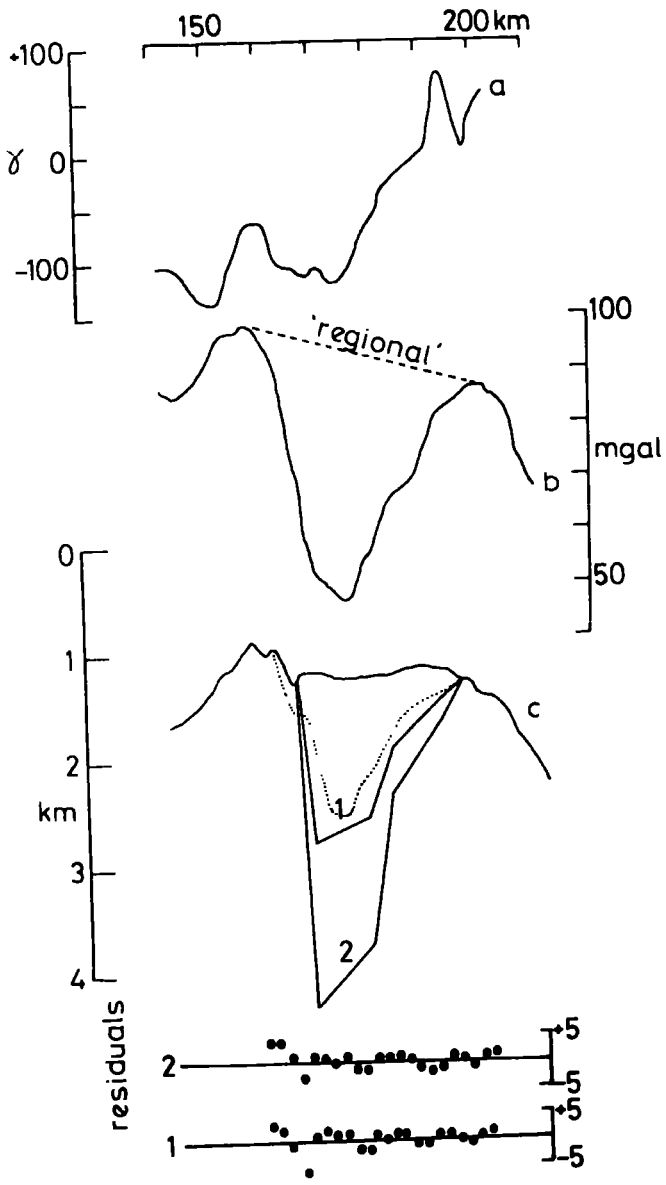


Figure 3-11 : Investigation of gravity low H at 17° 9'N
a- magnetic anomaly
b- observed anomaly and 'regional'
c- interpretations low density contrasts of
1)- .9 gm/cc and 2)-1.5 gm/cc. The basement
revealed by reflection is shown as a
broken line.

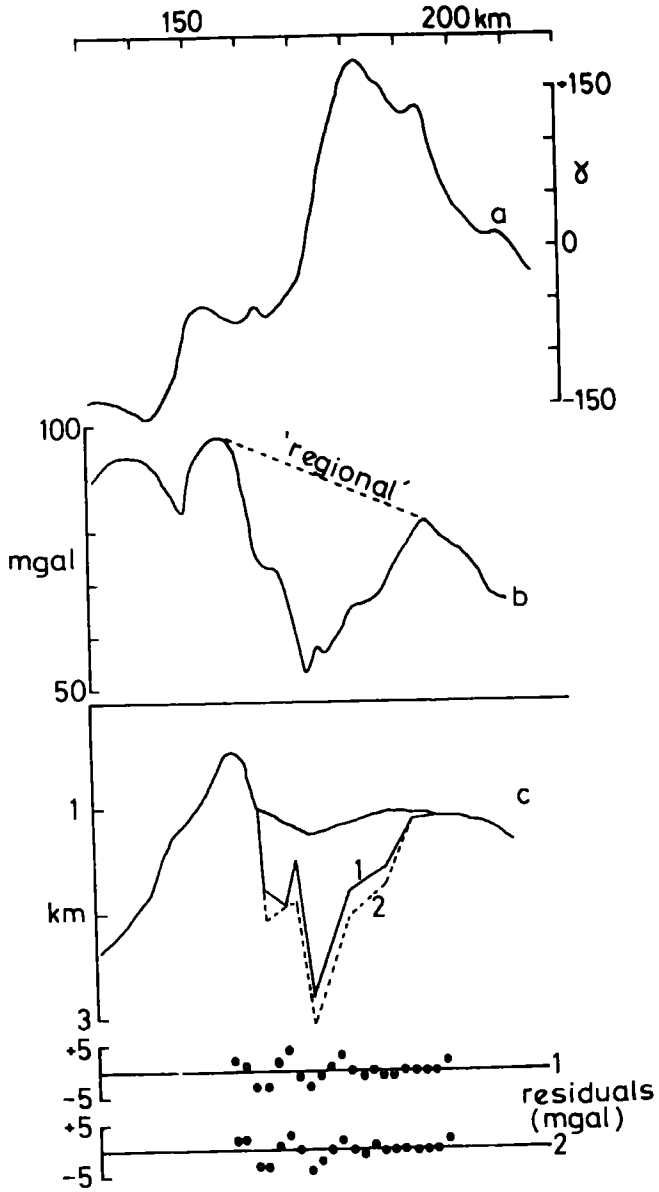


Figure 5-14 : Investigation of gravity low H at 15°04'
a-magnetic anomal.
b-Bouguer anomaly and 'regional'
c-interpretations for density contrasts of
1)-0.9gm/cc and 2)-0.7gm/cc

The dotted line shown in fig.5-13c represents the basement recorded by the air-gun profiler assuming a seismic velocity of 2.0 km/sec. for the sediments. It will be observed that the model for a density contrast of -0.9 gm/cc. more closely resembles the structure revealed by seismic reflection , the differences being due, in part, to the difficulty in isolating this small gravity anomaly from the regional gravity field. Consequently a density contrast of -0.9 gm/cc. was assumed.

The second profile is at 13°04'N. Relevant data are presented in fig. 5-14. The magnetic field (fig. 5-14a) is again relatively smooth over the gravity low. After isolating the anomaly by subtracting a linear 'regional' from the Bouguer anomaly (fig.5-14b), the feature was interpreted using a non-linear optimisation procedure for density contrasts of -0.9 and -0.7 gm/cc between sediments and basement. The resulting models are presented in fig. 5-14c.

The small gravity low is thus characterised by a sharp change in gradient across the minimum of the anomaly, and has been shown to be caused by a sediment filled depression with a V-shaped cross section. Bott et al. (1971) have described similar features from the Iceland-Faeroe Ridge, and have concluded that a likely origin is sub-aerial river erosion. However, it seems improbable that this feature on the Aves Ridge was formed in this way as it is not sufficiently continuous and it is difficult to envisage a river running the length of the Aves Ridge even were it elevated far above sea level. Other mechanisms of basin formation listed by Bott et al. are by contemporaneous subsidence and infill or by downfaulting after sediment deposition. As for the Iceland-Faeroe Ridge, the V-shaped cross section of the feature would seem to preclude either of these. A mode of origin that is considered likely in this case is the infill of a cleft in

the basement of the Aves Ridge caused by east-west extension. Such an origin would adequately explain the distinctive cross section of the feature, and the nature of the possible causative extensional forces will be discussed in a later chapter.

### 5.10.2 Investigation of two ridges on the western flank of the Aves Ridge

The western flank of the Aves Ridge is marked by a series of north-south striking ridges which are associated with gravity highs. Two profiles over these ridges were selected for study.

The first profile is at 14°15'N across the centre of the ridge centred on 63°30'W extending from 14°00 to 14°40'N and being the location of gravity high D.

Relevant data are presented in fig. 5-15. No distinctive magnetic anomaly is apparent over the feature (fig. 5-15b), and other magnetic profiles over the ridges indicate that their magnetic intensity is low. The anomaly was isolated from the Bouguer anomalies by the subtraction of a linear 'regional' (fig. 5-15a).

No information is available on the depth to the top of the causative body, although the bathymetry and gravity suggest that it is near surface. Consequently interpretations were performed assuming depths to the top of the body of 0.4, 0.7 and 1.0 km., and for density contrasts of 0.5 and 0.8 gm/cc., which were taken to represent reasonable upper and lower limits. This was one of the only occasions when a matrix procedure was found adequate for gravity interpretation.

Six possible interpretations are given in fig. 5-15. It will be observed that the minimum root mean square residual was obtained for the model of density contrast 0.8 gm/cc. and minimum depth. All interpretations show a steep sided causative body.

The second profile investigated was at 15°20'N across the ridge

Figure 5-15 : Interpretations of gravity high D at 14°15'N for density contrasts of 0.8 gm/cc. and 0.5 gm/cc. The figures in brackets refer to the root mean square residual anomaly.

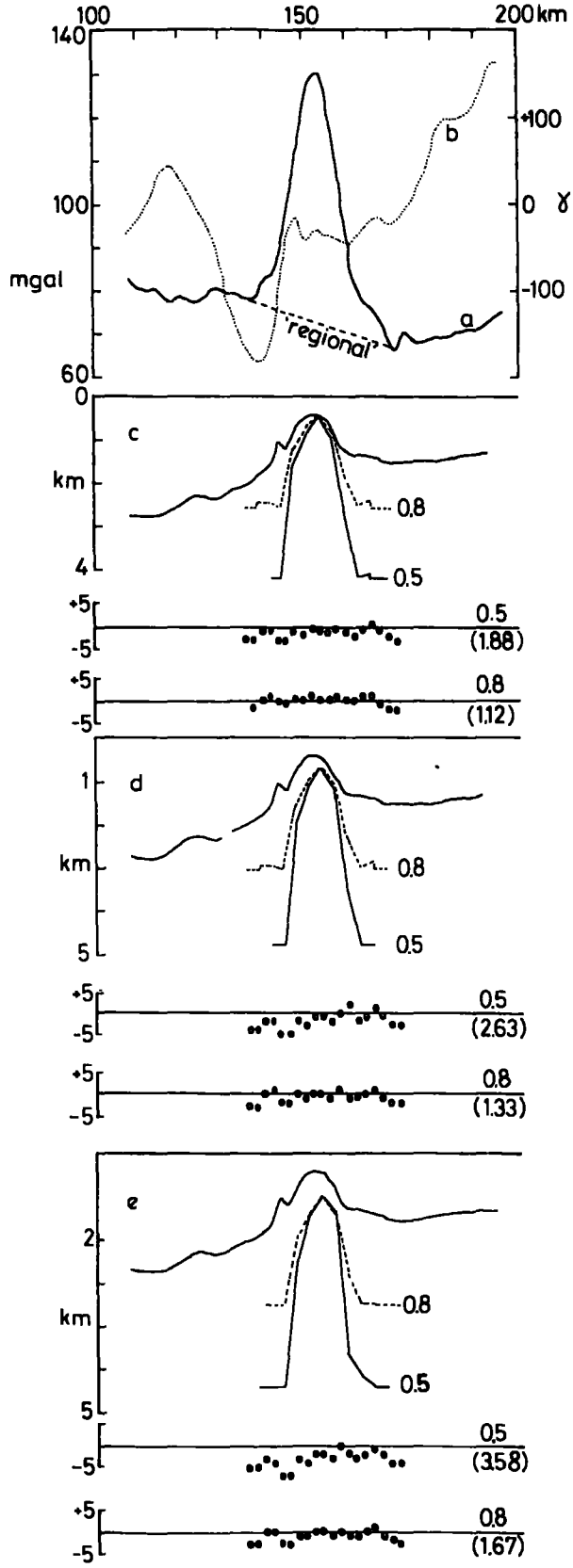
100
150
200 km
140
100
60
mgal
+100
0 γ
-100
b
a
'regional'
0
km
4
c
0.8
0.5
+5
-5
0.5
(1.88)
0.8
(1.12)
1
km
5
d
0.8
0.5
0.5
(2.63)
0.8
(1.33)
2
km
5
e
0.8
0.5
0.5
(3.58)
0.8
(1.67)

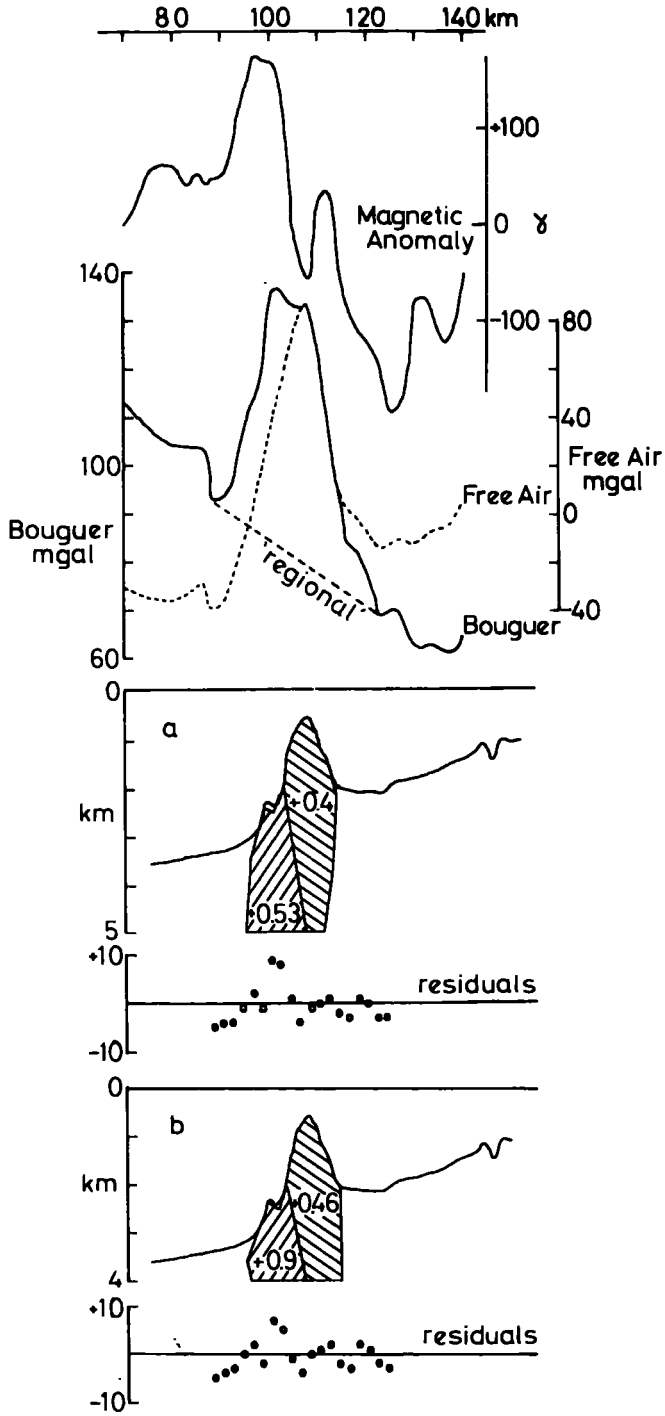


Figure 5-11 : Interpretations of gravity high B at 15° 20'N.

centred on 64°00'W extending from 15°10' to 15°40', and being the location of gravity high B. Relevant data are presented in fig. 5-16. In this case a distinctive magnetic anomaly was recorded over the ridge. The free air anomalies over the feature exhibit a single narrow peak centred on the ridge axis. Application of the Bouguer correction, however, broadens the peak to the west and indicates that the western part of the feature is rather more dense than the eastern. Both the bathymetry and gravity suggest that the causative body is at a shallow depth. The anomaly was isolated by the subtraction of a linear 'regional' and interpreted using a non-linear optimisation procedure assuming that the upper part of the causative body was defined by the sea bed. Two possible interpretations are presented in fig. 5-16a and b. The main bathymetric ridge was found to be composed of material significantly less dense than that forming the inferior western part.

The ridges marking the western flanks of the Aves Ridge were thus found to be rather more dense (2.8-2.9 gm/cc.) than the main part of the Aves Ridge (2.5-2.6 gm/cc.), and magnetic data (Chapter 6) also indicate that their intensity of magnetisation is somewhat lower. These ridges probably represent bodies intruding the main Aves Ridge and as such are probably of basaltic or dioritic composition with the major part of the Aves Ridge composed of lava flows and compacted volcaniclastic deposits. Andrew et al. (1970) have concluded that 2.5 gm/cc. is a representative density of the lava flows and volcaniclastic deposits of the Lesser Antilles. Fox et al. (1971) have proposed that the basalts encountered in their dredge hauls on the Aves Ridge represent intrusive bodies.

5.10.3 The Grenada Trough - Lesser Antilles boundary

Fig. 5-17 illustrates the very sharp change in gravity gradients

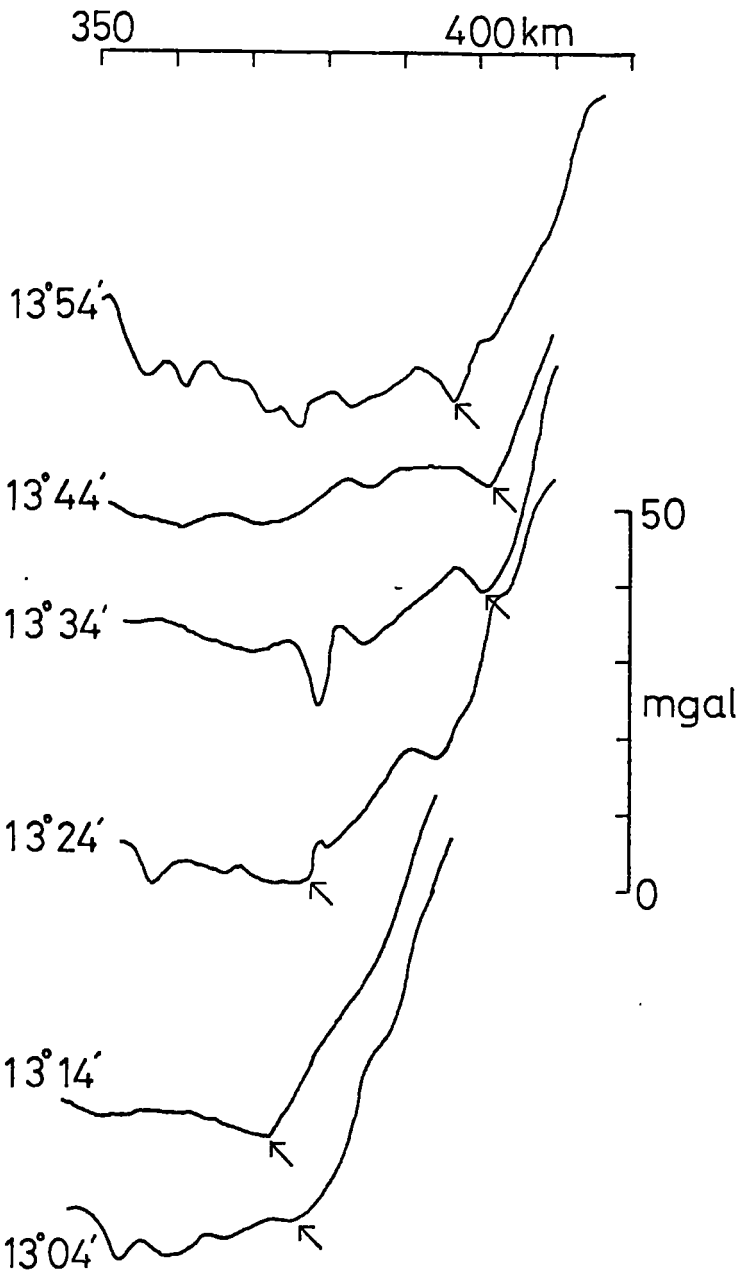


Figure 5-17 : The Grenada Trough - Lesser Antilles boundary. The sharp change in gravity gradients is indicated by arrows.

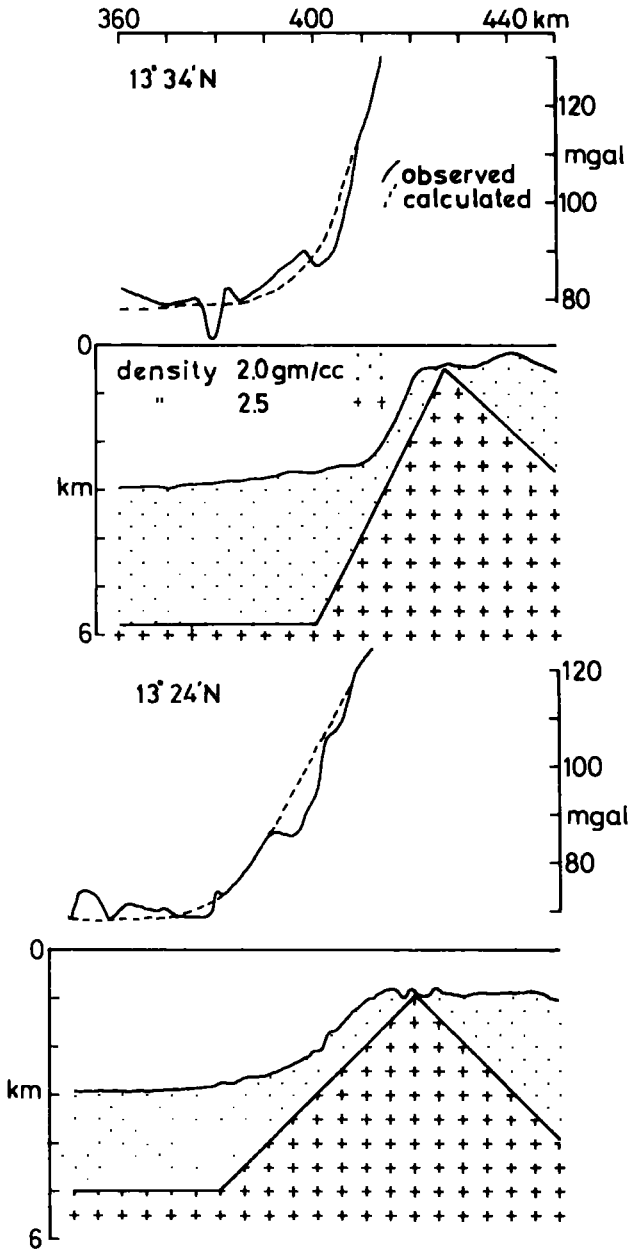
360
400
440 km
13°34'N
120
mgal
100
80
observed
calculated
0
density 2.0gm/cc
" 2.5
km
6
13°24'N
120
100
mgal
80
0
km
6

observed when passing from the Grenada Trough onto the Lesser Antilles during the 1971 survey. Such an abrupt feature is indicative of a shallow crustal source. Seismic refraction and reflection profiles indicate several kilometres of sediment overlying basement in the Grenada Trough, while the Lesser Antilles have little, if any, sediment cover. Consequently the abrupt change in gravity gradients is attributed to the rapid thinning of sediment cover from Grenada Trough to Lesser Antilles.

Simple models were produced using GRAVN (Bott, 1969a) for two profiles across the island arc at 13°34'N and 13°24'N between the islands of St. Lucia and St. Vincent. A density contrast of 0.5 gm/cc. was assumed between basement and sediment. The models are presented in fig. 5-18, and show that the break in gravity gradients can be adequately explained in terms of a thinning sediment cover.

## 5.11 Vertical Movements of the Aves Ridge

It has been shown that at the present day the Aves Ridge is characterised by negative isostatic anomalies, which indicate that the structure would have to rise to attain isostatic equilibrium. Several workers (JOIDES, 1970, Edgar et al., 1971b, Fox et al., 1971, Marlowe, 1971, Nagle, 1971) have proposed past vertical movements of the Aves Ridge.

The smooth, horizontal nature of the sediments in the Venezuela Basin and Grenada Trough and the similarity of crustal structure beneath them suggest that these basins were established by the upper Cretaceous (the age of the oldest dated reflector) and that no relative horizontal movements have affected them since this time.

The middle Eocene to lower Miocene sedimentary samples of Fox et al. (1971) suggest a shallow water, carbonate shelf facies,

although the globigerina oozes of similar ages encountered in JOIDES site 30 are indicative of a deep water depositional environment. The mid-Miocene to recent samples of Fox et al. indicate deep water deposition and a possible subsidence of 400-1400 m., while Nagle's (1971) estimate of subsidence is in excess of 1000 m. However, the two JOIDES sites on the Aves Ridge indicate a very high sedimentation rate during Pliocene/Pleistocene times, implying extreme proximity to sediment source, and the presence of a sub-aerial unconformity confirms that at least part of the Aves Ridge was emergent at this time. Marlowe (1971) has concluded that the prominent sea-mount in the south of the survey area was emergent during Pleistocene/Holocene times and has subsided since then.

Data thus indicate that the Aves Ridge must have had quite a complex history of emergence and subsidence, and that these movements were not necessarily contemporaneous for the whole Ridge.

To obtain quantitative estimates of possible movements, it is necessary to consider the contribution of eustatic changes in sea level, of which glacial events are the major cause. If one ignores the isostatic readjustments due to the loading or unloading of water, which will not exceed about 30 m. (Matthews, 1969), it is possible to obtain estimates of sea-level changes from tectonically stable areas at least for the last 40,000 years. Several workers (MacIntyre, 1967, Steinen et al., 1973) have described a low stand of the Pleistocene sea level around Barbados at a present day depth of c.70 m. However, the presence of elevated ancient reefs on Barbados indicate that it is not a tectonically stable unit. Curray (1965) proposes a relative depth of 120-125 m. for the late Wisconsin low stand of 18,000 years B.P. for the continental shelf of the eastern United States, with a possible 140-145 m. for the mid-Wisconsin low stand of 40,000 years B.P.

Consequently 145 m. is taken as the maximum possible eustatic contribution to apparent vertical movements.

A quantitative estimate of tectonic subsidence could be obtained for two features:

i) the seamount at 13°35'N, 63°15'W studied by Marlow (1971) and considered to have been emergent during Pleistocene/Holocene times. It has a planed top at a depth of 320 m., while the north-south ridge centred on 13°00'N, 63°15'W to the south-west of this feature also has a minimum depth of 318 m. Thus for the sea mount:

Present depth = 320 m.
Maximum eustatic contribution = 145 m.
∴ Minimum tectonic subsidence = 175 m.
∴ Minimum rate of subsidence = 87 m/M.Y.

ii) the subaerial unconformity encountered in JOIDES site 148, representing the Pliocene/Miocene boundary.

Present depth = 637 m.
Maximum eustatic contribution = 145 m.
∴ Minimum tectonic subsidence = 592 m.
∴ Minimum rate of subsidence = 85 m/M.Y.

The minimum rates of subsidence for these two features on the southern Aves Ridge are thus very similar.

The northern part of the Aves Ridge seems to have undergone rather less relative subsidence than the southern part. Aves Island is emergent, and four submarine benches have been noted around it (B. D'Olier, pers. comm.), the most prominent being at 283 m. and 439 m. Dating of these features is not possible without direct sampling, but if they represent erosional levels, both are greater than the proposed 145 m. eustatic contribution and may indicate tectonic

sinking. A submarine bench at 82-88 m. has been noted south of Aves Island and also on the southern and western flanks of Grenada. This may correspond to a low stand of the sea-level during the latter part of the Weichselian glaciation of 20,000 years B.P. (B.D'Olier, pers. comm.) in which case no tectonic subsidence is indicated since this time.

The only two seismic events recorded in the region behind the Lesser Antilles lie on the western and eastern flanks of the Aves Ridge (Molard, 1952, Sykes & Ewing, 1965). It is possible that these events represent readjustments on ancient fault planes along which vertical movements of the Aves Ridge took place.

## 5.12 Conclusions on gravity studies

i) The Aves Ridge is underlain by a mass deficiency which may be interpreted in terms of a thickened crust beneath it with a consequent depression of the Moho and lowest crustal layer. A thickened 6.2-6.7 km/sec. seismic layer is responsible for the major topography of the Aves Ridge. Lack of adequate seismic refraction control on the Moho inhibits accurate generalisations on the north-south variation in depth of the Moho beneath the Aves Ridge.

ii) The positive Bouguer anomalies of the Grenada Trough may be adequately explained by a relatively shallow depth to the Moho beneath it. The similarity of the velocity structures beneath the Venezuela Basin, Aves Ridge and Grenada Trough indicate these positive anomalies are probably not caused by high density crustal rocks beneath the Grenada Trough.

iii) The Lesser Antilles are also underlain by a mass deficiency which may be interpreted in terms of a thickened crust with the depressed Moho usually reaching greater depths than beneath the

Aves Ridge.

iv) The short wavelength, positive free air anomalies observed over both the Aves Ridge and Lesser Antilles may be adequately explained by features in the sediment/basement interface.

v) The presence of ridges marking the western and eastern flanks of the Aves Ridge revealed by seismic reflection is confirmed by the gravity data.

vi) The central Venezuela Basin exhibits positive isostatic anomalies, but is in approximate isostatic equilibrium at its eastern margin.

vii) Isostatic anomalies over the Aves Ridge are predominantly negative.

viii) Isostatic anomalies in the Grenada Trough are predominantly negative, with the largest negative anomalies occurring in the south. The anomalies become positive towards the Lesser Antilles.

ix) The Lesser Antilles define a belt of positive isostatic anomalies.

x) The ridges marking the western flank of the Aves Ridge are of higher density than other parts of the Ridge. They may represent dioritic or basaltic intrusions into the volcanic and volcaniclastic deposits believed to form the basement of the Aves Ridge.

xi) A depression in the sediment/basement interface on the southern Aves Ridge represented by a local gravity low may owe its origin to east-west extensional forces.

xii) The abrupt change in gravity gradient observed when passing from the Grenada Trough onto the Lesser Antilles can be adequately interpreted as being due to a rapid thinning of sediment cover.

xiii) The Aves Ridge has had a complex history of submergence and emergence.

# CHAPTER 6

# MAGNETIC ANOMALIES OF THE EASTERN CARIBBEAN

## 6.1 Previous work

Few detailed magnetic surveys have been performed in the Caribbean Sea and data have usually been limited to rather widely spaced random ships' tracks. Ewing et al. (1960) have summarised the general nature of magnetic anomalies in the eastern Caribbean and noted the smooth fields of the basins and high amplitude, short wavelength anomalies of the ridges, which, at least for the Aves Ridge, were correlated with near-surface volcanic activity. Bunce et al. (1971) have described the results of several magnetic traverses across the eastern Caribbean, and have recognised short wavelength anomalies over the Aves Ridge, volcanic island arc and limestone arc with more tranquil conditions over the Venezuela Basin and Grenada Trough. Amplitudes over the Aves Ridge were slightly lower than over both the volcanic and limestone arcs and the similarity of the anomalies over the two units of the island arc was considered good evidence for the latter's interpretation as an ancient volcanic arc. Good correlation of high frequency anomalies and bathymetry peaks was observed over the Aves Ridge, although the two-dimensional magnetic interpretations produced should be treated with caution for such widely spaced traverses.

Magnetic lineations of the type found in major ocean basins (Vine & Matthews, 1963) have not been recorded in the Caribbean Sea. This implies either loss of lineations due to a long history or crustal formation during a magnetic quiet period (Freeland & Dietz, 1971) such as described by Heirtzler & Hayes (1967).

## 6.2 A Note on Magnetic Poles and Intensities of Magnetisation

As stated in Chapter 3., the present earth's magnetic field is defined in the eastern Caribbean by an azimuth of 349° and an inclination of 43°. When resolved east-west, the component of the vector dips westwards at 78°.

MacDonald & Opdyke (1972) have summarised palaeomagnetic data from circum-Caribbean and Caribbean plate sites for the Cretaceous. These data were analysed to discover the relevance of the magnetic inclinations obtained from the interpretations of magnetic profiles. This assumes that the principal magnetic structures of the eastern Caribbean are of Cretaceous age and is a gross approximation, although results of JOIDES leg 15 (Purrett, 1971) are taken as tentative support as basalts of Cretaceous age have been recorded under sedimentary sequences at several sites on this leg. Age dating of granodiorites and basalts from the Aves Ridge have also revealed Cretaceous ages (Fox et al., 1971).

The majority of poles from these palaeomagnetic data plot in an arc from central Africa to Antarctica and have been interpreted as indicating relative rotations of the sites since the Cretaceous (MacDonald & Opdyke, 1972). To assess the usefulness of these poles in interpretation of data from the present survey, the palaeomagnetic data were recalculated to determine the azimuth and dip of the magnetic vector expected from each of these poles for a point in the survey area at 14°30'N, 63°00'W. The method used in this calculation is given in Appendix 2.

Fig. 6-1a is a stereogram of palaeoazimuth and palaeodip for this point. A cluster of points around an azimuth of 110° and dip 24° is noted. Fig. 6-1b is a plot of the palaeodip resolved east-

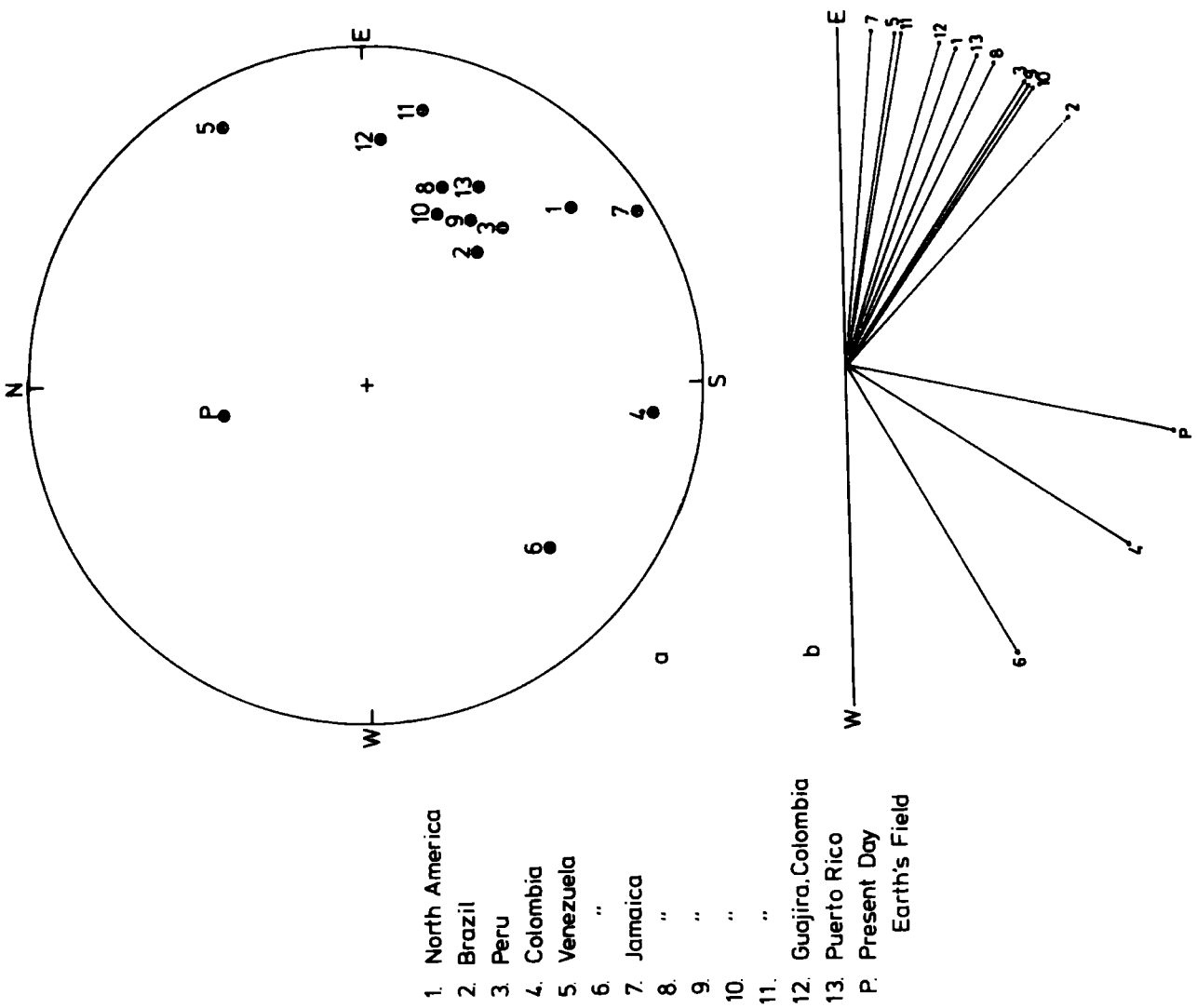


Figure 6-1 : Palaeomagnetic data from Caribbean and circum-Caribbean sites.
a-stereogram of Cretaceous magnetic field directions for a point on the Aves Ridge at 14° 30'N, 63° 00'W.
b-the Cretaceous field directions resolved in an east-west plane.

west, the direction of all magnetic profiles considered in this thesis. Resolution was made on the basis of taking the pole nearest the site as north. A cluster of directions between dips of 6° and 44°E is noted, with the Puerto Rico inclination plotting centrally.

Thus, in spite of possible tectonic rotations and non-contemporaneity of poles from Caribbean and circum-Caribbean sites, the magnetic vectors resolved east-west are quite consistent and indicate the dip of the Cretaceous field vector in an east-west plane is of the order of 25°E and that total field vectors plotting between the present day dip and this direction may be considered as having a remanent component of Cretaceous age.

The ratio of remanent to induced magnetisation (the Königsbergen ratio, $Q_N$) to be expected is unclear. Khan (1968) has examined 17 oriented specimens of lava from St. Vincent and has found values of $Q_N$ from 1.00 to 10.88 with an average of 4.2. He found the average susceptibility to be 0.0016 emu/cc. Andrew et al. (1970) have also performed measurements on samples from the Lesser Antilles, and have found the average susceptibility of samples to be 0.008 emu/cc.

## 6.3 The two-dimensional approximation in the interpretation of magnetic anomalies

It may be shown from the solution of Laplace's equation and the equivalent layer theorem for gravity anomalies that the gravity anomaly, $g(x,y,Z)$ on the plane $z = Z$ above a coating of surface density $\sigma(x,y) = \sigma_0 \exp(ik_x x + ik_y y)$ on the plane $z = 0$ is:

$$g(x,y,Z) = 2\pi G \sigma_0 \exp(ik_x x + ik_y y + k_z z) \qquad (1)$$

where G is the gravitational constant, x, y, z Cartesian coordinate axes with z increasing vertically downwards, $k_x$, $k_y$ the wave numbers in the x and y directions and $k_z = (k_x^2 + k_y^2)^{\frac{1}{2}}$.

Conversely, a gravity anomaly $g(x,y) = g_o \exp(ik_x x + ik_y y)$ on the plane z = 0 may be represented by an equivalent layer at depth z = z' whose density distribution is given by:

$$\sigma(x,y,z') = (g_o/2\pi G)\exp(ik_x x + ik_y y + k_z z') \qquad (2)$$

Bott (1973) has derived the equivalent layer for a magnetic anomaly from (2) by the application of Poisson's formula which relates gravity and magnetic potentials. The resulting distribution of magnetic moment per unit area, w, for the equivalent layer of a magnetic anomaly, $f(x,y) = f_o \exp(ik_x x + ik_y y)$ is given by:

$$w(x,y,z') = (f_o k_z/2\pi(\underline{k}^T \underline{s} \underline{k}^T \underline{j}))\exp(ik_x x + ik_y y + k_z z') \qquad (3)$$

where $\underline{k}^T$ represents the column vector $(ik_x, ik_y, k_z)$, $\underline{s}$ the unit row vector $(s_x, s_y, s_z)$ at the field point and $\underline{j}$ the unit row vector $(j_x, j_y, j_z)$ of magnetisation directions. The factor $k_z/(\underline{k}^T \underline{s} \underline{k}^T \underline{j})$ reduces to an imaginary part representing a phase difference between the equivalent layer distribution of magnetic moment per unit area and the anomaly, and a real part of the form $k_z^{-1}$ representing a magnitude factor.

Consequently the magnitude of the distribution of magnetic moment per unit area is dependent on the wavelength of the magnetic anomaly. If a profile traverses a magnetic anomaly at an angle so that the true wavelength is distorted to a greater value, the two-dimensional interpretation will give a distorted impression of the

magnitude of the magnetisation. In the two-dimensional approximation $k_y$ is taken as zero, i.e. the wavelength along the strike of the body is considered infinite. Comparison of equations (2) and (3) indicates that the density distribution of the equivalent layer of a gravity anomaly is less sensitive to this approximation than the magnetic moment per unit area distribution of the equivalent layer of a magnetic anomaly. In the magnetic case the magnitude factor described above is $k_z^{-1} = (k_x^2 + k_y^2)^{-\frac{1}{2}}$. If $k_y$ is small, i.e. the wavelength of the anomaly in the y-direction is large, the approximation is adequate. If, however, the wavelength in the y-direction is small, $k_y$ will be large and the two-dimensional approximation will cause a distortion of the true variation of magnetic moment per unit area along the equivalent layer. This factor must be considered when magnetic anomalies are interpreted using the two-dimensional approximation, as real magnetic anomalies rarely exhibit no variation along their strike.

Bott (1973) has also shown that there is a long wavelength instability present in the interpretation of magnetic anomalies, a consequence of which being that a uniformly magnetised, uniform horizontal sheet has no magnetic anomaly. In some cases long wavelength magnetic components may predominate in an interpretation.

## 6.4 Interpretation of magnetic anomaly profiles

All profiles studied were east-west and were chosen for the most part for their two-dimensionality in this sense. This stipulation was relaxed where seismic reflection data were available to define basement over the Aves Ridge. However, as with most real data, none of the magnetic anomalies of the survey area are completely

two-dimensional, and the consequences of this, discussed in the previous section, must be considered when examining the interpretations.

All pseudogravity anomalies presented refer to a ratio between intensity of magnetisation (J) and density ($\rho$) of unity.

The lettered magnetic anomalies refer to the magnetic anomaly chart.

6.4.1 Line S1545

The profile at 15°45'N is the most northerly considered and crosses the Aves Ridge in the region of rough topography on its western flank, passing across the north-south ridge which culminates in Aves Island 10 km. to the south. The profile passes through the centre of magnetic high A. Relevant data are presented in fig. 6-2.

The strong positive correlations apparent between the observed Bouguer and magnetic anomalies are indicative of a steeply dipping magnetisation vector. The gravity peaks 1,2 and 3 on the observed Bouguer anomalies (fig. 6-2b) are seen to correlate with peaks on the pseudogravity anomalies computed for both induced and vertical magnetisation (fig. 6-2c), although peaks 1 and 3 are of lower amplitude than pseudogravity peak 2. Peaks 1 and 2 also correspond to bathymetric prominences. The major part of gravity peak 3 may be spurious as its maximum is represented by only two data points, and so for correlation purposes this peak was smoothed from the anomalies. The correlation coefficient, for 31 data points, between the observed Bouguer anomalies and pseudogravity anomalies for induced magnetisation was 0.56 , and between observed Bouguer anomalies and pseudogravity anomalies for vertical magnetisation, 0.50 . Both coefficients are significant, and in fact correlation

Figure 6-2 : Line S1545

a - observed magnetic anomaly

b - observed Bouguer anomaly

c - pseudogravity anomaly for induced magnetisation (I)

pseudogravity anomaly for vertical magnetisation (II)

d - bathymetry

e - block distribution of magnetisation for an equivalent layer 4 km. thick with its top at a depth of 2 km.

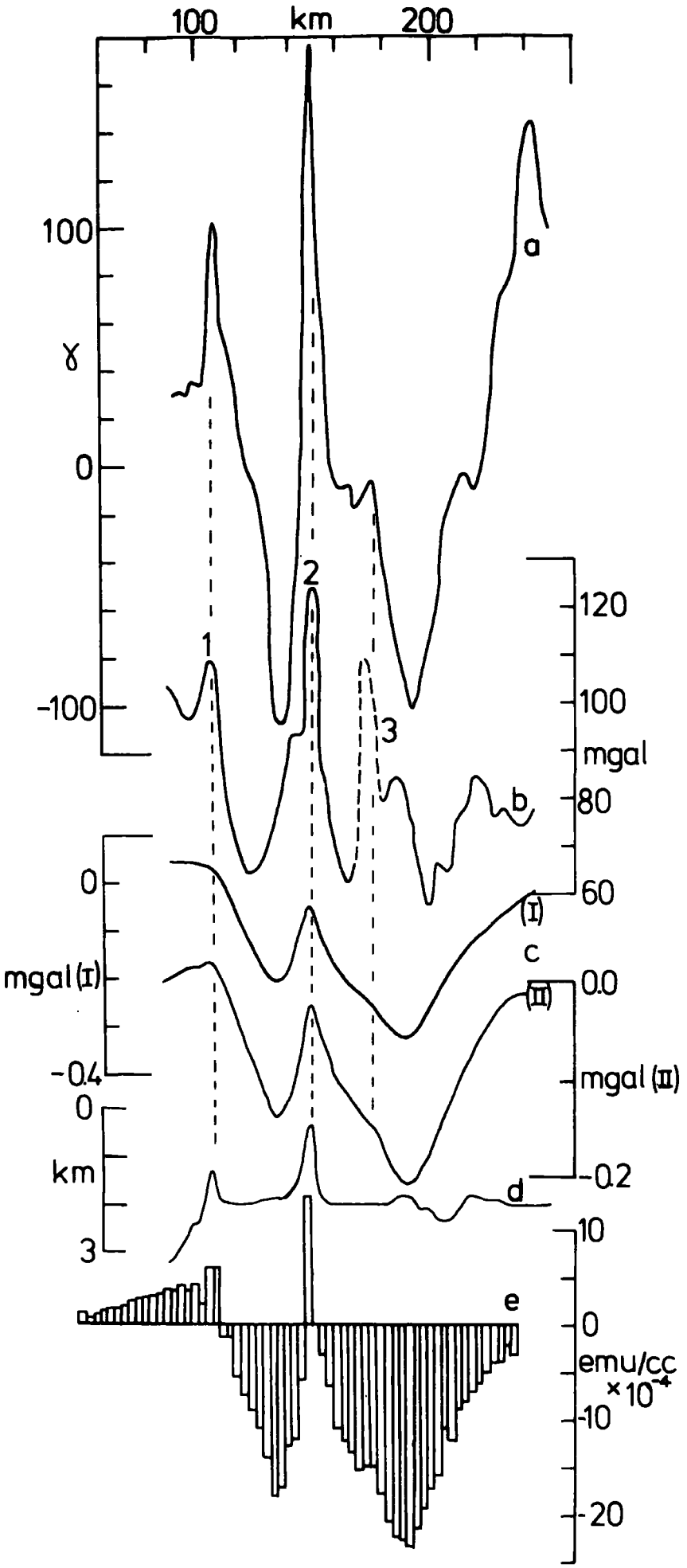
100
km
200
100
γ
0
-100
a
1
2
3
b
120
100
mgal
80
60
(I)
c
(III)
0.0
mgal (II)
-0.2
0
mgal (I)
-0.4
0
km
3
d
e
10
0
emu/cc
×10⁻⁴
-10
-20

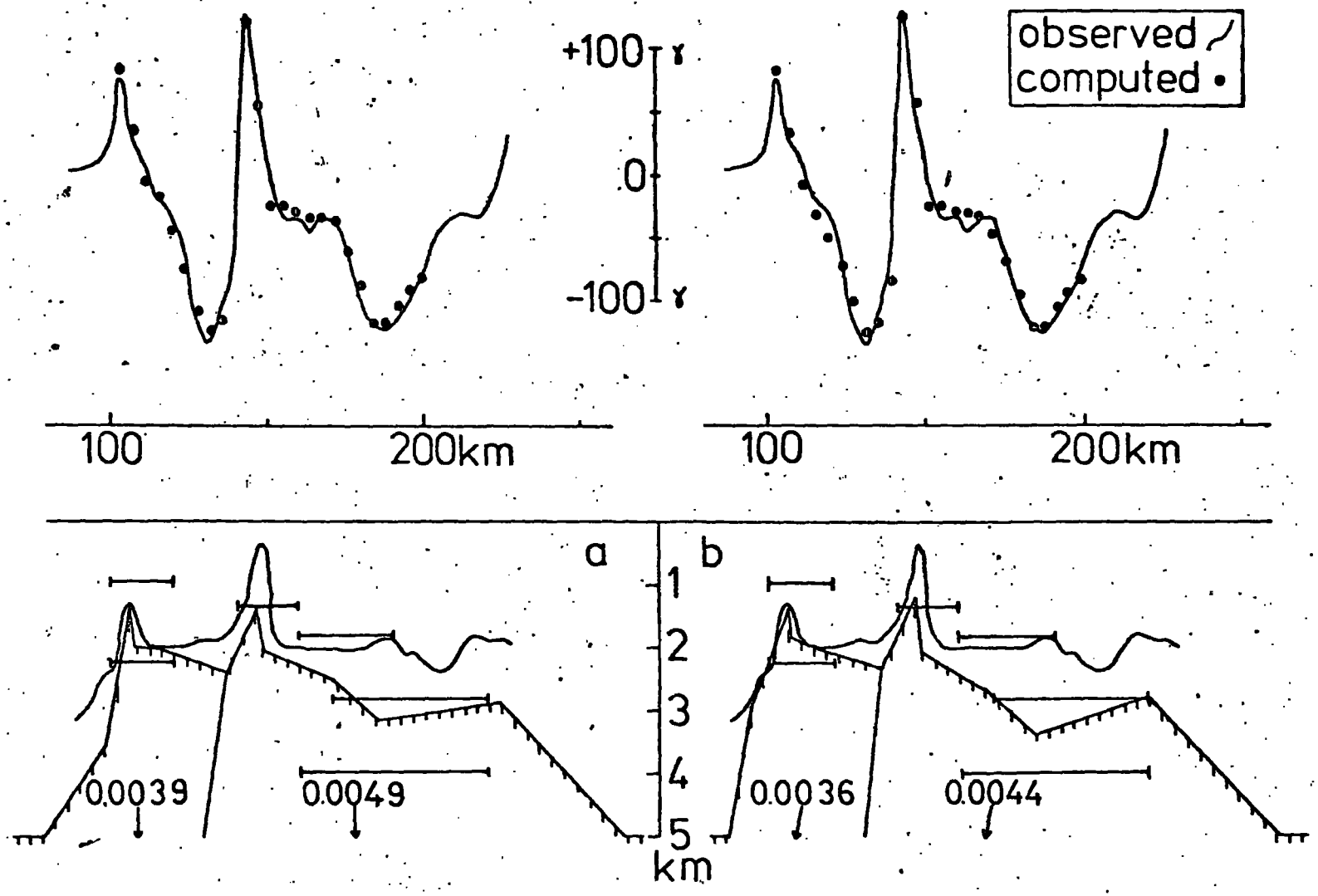


Figure 6-3: Interpretations of S1545 for a-vertical, & b-induced magnetisation. horizontal bars-depths from spectral analysis.

may be greater since the length of the profile was insufficient to allow the removal of the long wavelength effects of deep non-magnetic structures from the Bouguer anomalies (section 5.9). The block distribution of magnetisation for an equivalent layer 4 km. thick with its upper surface at a depth of 2 km. is presented in fig. 6-2e.

The causative structure would thus appear to have either totally induced magnetisation or induced magnetisation with a small, easterly dipping component of remanent magnetisation, probably related to the Cretaceous field direction (section 6.2). Since removal of deep gravity effects from the observed Bouguer anomalies was not possible, estimation of the intensity of magnetisation from the amplitudes of gravity and pseudogravity anomalies could not be performed with accuracy, but a rough estimate of 0.002 emu/cc. (in the direction of the earth's field) was obtained assuming a density contrast of 0.5 gm/cc. between sediments and basement.

The magnetic observatories at San Juan and Paramaribo both registered quiet conditions during the survey of this profile, and so magnetic data are considered free from external effects. Spectral analysis results (fig. 6-3) indicate that the western part of the Aves Ridge has little non-magnetic cover, with bathymetry peaks 1 and 2 corresponding to magnetic prominences. Data for the eastern part of the profile are ambiguous in that increases in the length of the profile analysed gave increasingly greater depths to basement. External magnetic effects appear to be lacking, and so it would appear that all representative frequencies are not present in the magnetic anomaly and that the necessary premises of the spectral analysis method (section 3.6) do not attain. A mean depth to basement under the eastern Aves Ridge of 2.8 km. was used as a constraint in inter-

pretation. No seismic refraction data are available for this profile.

Interpretations of the causative magnetic structures were performed using a non-linear optimisation routine, constraining the space form of the body with both spectral analysis data and bathymetry. The computed bodies for induced and vertical magnetisation are presented in fig. 6-3. The western part of the Aves Ridge was found to have a slightly lower intensity of magnetisation than the eastern part, although the small difference is probably not significant. Computed intensities of the western and eastern parts were 0.0053 and 0.0063 emu/cc. in the direction of the earth's field (0.0036 and 0.0044 emu/cc. in the plane of the profile) for induced magnetisation, and 0.0039 and 0.0049 emu/cc. for vertical magnetisation.

6.4.2 Line S1515

The profile at 15°15'N passes over the southern part of the rugged topography on the western flank of the Aves Ridge and across the centre of the north-south ridge which culminates in Aves Island 40 km. to the north. The profile passes over magnetic highs C and D and magnetic lows E and F. Relevant data are presented in fig. 6-4.

Positive and negative correlations are apparent between the observed magnetic and gravity anomalies, which are probably indicative of steeply dipping, opposed magnetisation vectors. The pseudogravity anomalies for both induced and vertical magnetisation vectors show positive correlations between gravity peaks 1 and 2 (fig. 6-4b), and negative correlations between the gravity peaks 3 and 4. Peaks 1 and 2 correspond to bathymetric prominences, peak 3 is in a region of relatively subdued topography and peak 4 is centred over a bathymetric depression. A possible interpretation of these data is that the causative structure is composed of a western part with a steeply

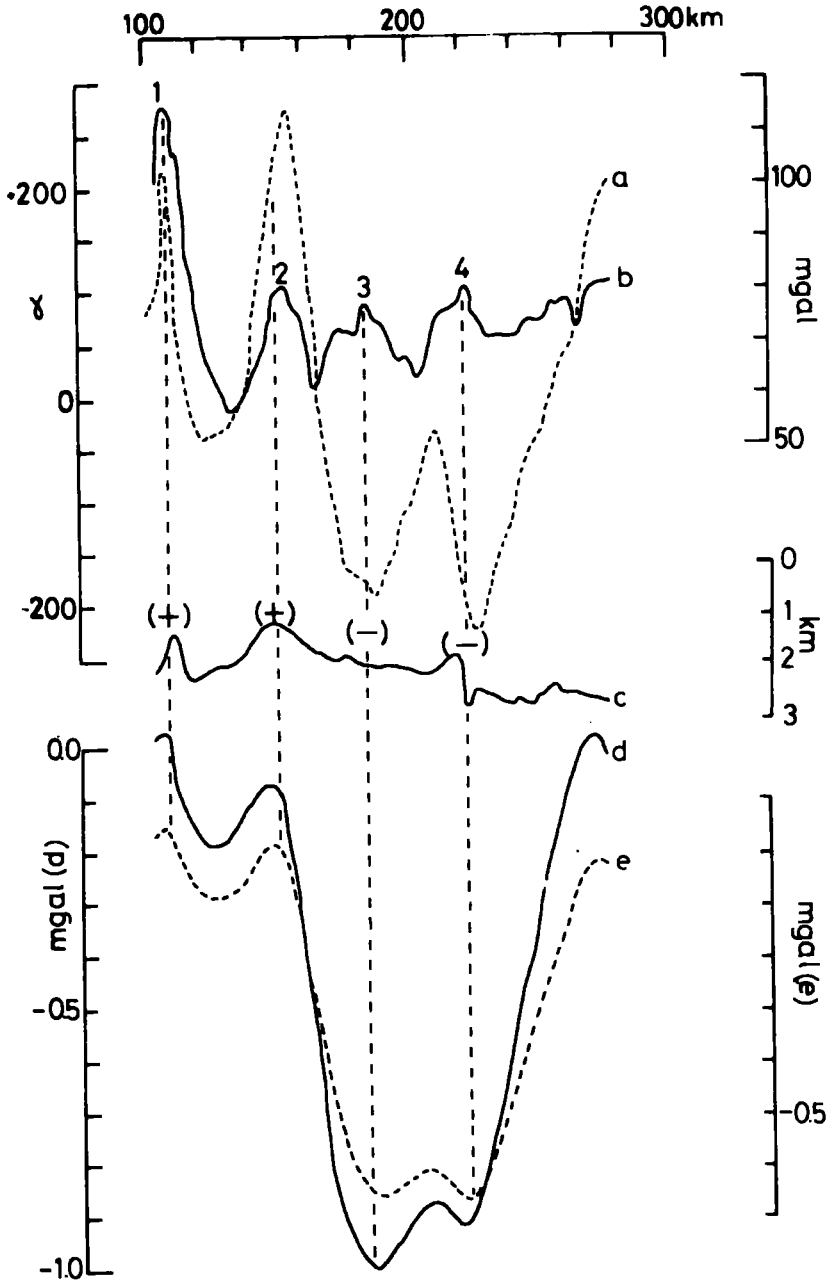
100
200
300km
1
2
3
4
+200
γ
0
-200
a
b
100
mgal
50
(+)
(+)
(−)
(−)
0
1
2
3
km
c
0.0
mgal (d)
-0.5
-1.0
d
e
mgal (e)
-0.5

downward dipping, and an eastern part with a steeply upward dipping, magnetisation vector. The western part may thus be related to either totally induced magnetisation, or to induced magnetisation with a small, easterly dipping remanent component possibly related to the Cretaceous field direction. The eastern part is problematic, since a structure of probable Cretaceous age would seem unlikely to have a magnetisation related to a reversed direction of the present earth's field. The complexity of the profile precluded estimation of the intensity of magnetisation from the relative amplitudes of gravity and pseudogravity anomalies. No seismic refraction data are available for this profile.

The magnetic observatories at San Juan and Paramaribo both registered quiet conditions during the period surveying this line, and so spectral analysis results are considered free from external effects. The results are presented in fig. 6-5, and, in the absence of any other data, were used as controls on interpretation. Bathymetry peaks 1 and 2 are shown to represent magnetic prominences with little or no sediment cover, while magnetic basement is at a greater depth under the eastern part of the Aves Ridge.

Two possible interpretations of the causative magnetic structures are presented in fig. 6-5 for the western Aves Ridge with induced and vertical magnetisation and the eastern Ridge with opposed directions. The first step in interpretation was the use of a matrix procedure to determine the approximate shape and intensity of magnetisation of the causative body underlying the eastern part of the profile, and then a non-linear optimisation procedure for interpretation of the whole profile. The western part of the profile was found to have a significantly lower intensity of

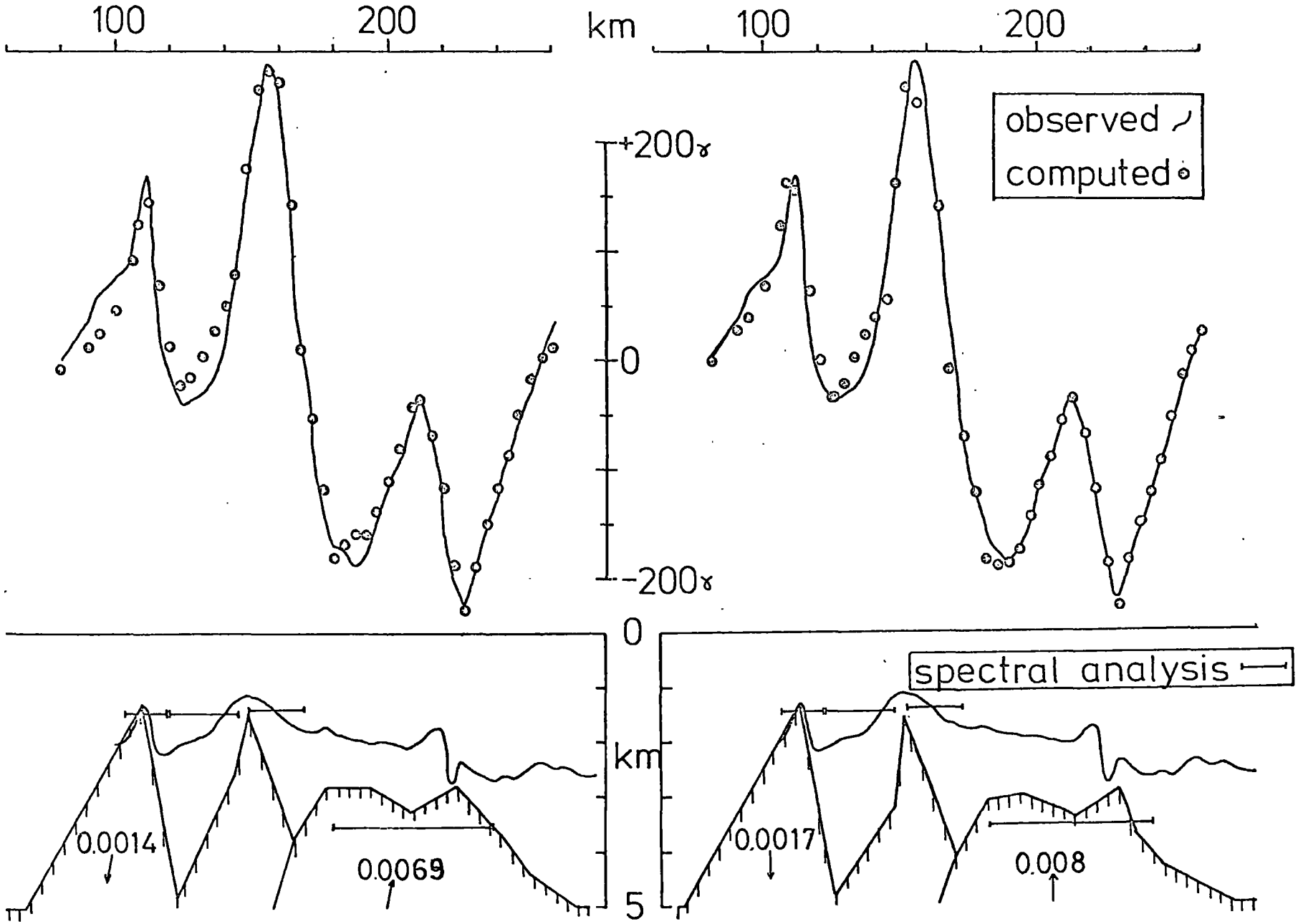


Figure 6-5 : Interpretations of S1515 for vertical and induced directions.

magnetisation than the eastern part, values for the western and eastern parts being 0.002 and 0.01 emu/cc. in the direction of the earth's field (0.0014 and 0.0069 emu/cc. in the plane of the profile) for induced magnetisation, and 0.0017 and 0.008 emu/cc. for vertical magnetisation. The configuration of the contact between the two parts of the computed body is not considered unambiguous.

Since the presence of a body with reversed magnetisation was considered unlikely, an attempt was made to produce a model with totally induced magnetisation to fit the anomaly. It was not found possible to compute such a model which was geologically reasonable and would also be responsible for the observed gravity anomalies. It thus seems probable that this upward dipping vector is, indeed, present, but its origin is unknown.

6.4.3 Line L1500

The profile at 15°00'N passes over the southern end of the north-south ridge of the Aves Ridge which culminates in Aves Island 65 km. to the north. The profile passes over the centres of magnetic highs G, H and I. Relevant data are presented in fig. 6-6.

Strong positive correlations are apparent between the observed magnetic anomalies and the Bouguer anomalies from which the effects of deep structures have been subtracted (section 5.9), which are indicative of a steeply dipping magnetisation vector. Positive correlations are apparent between peaks, 1, 2 and 3 of these 'shallow' Bouguer anomalies and peaks on the pseudogravity anomalies computed for induced and vertical magnetisations, although pseudo-gravity peak 2 is of greater amplitude than peaks 1 and 2. The correlation coefficient, for 36 data points, between the 'shallow'

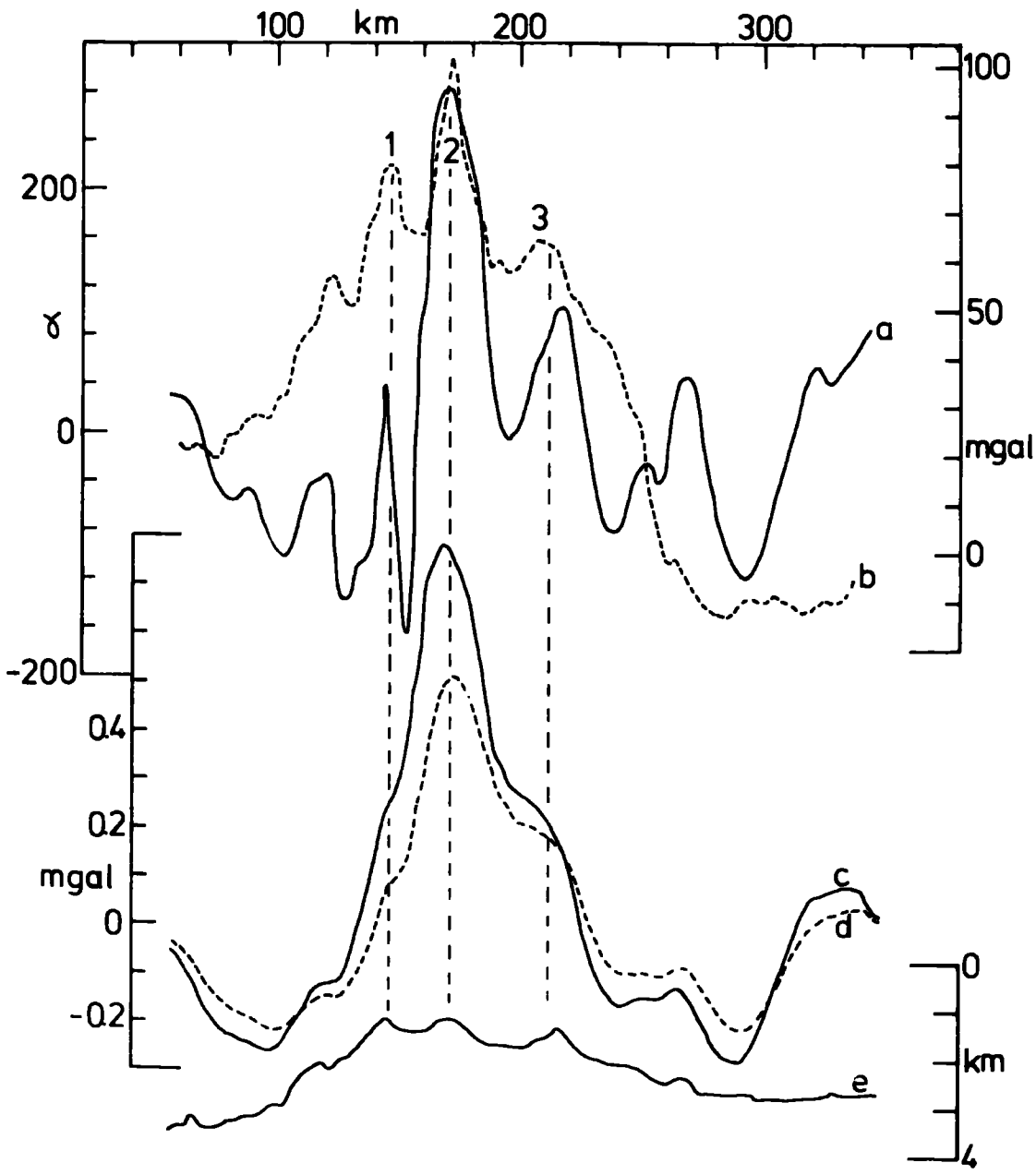
100
km
200
300
100
200
γ
0
50
mgal
0
-200
1
2
3
a
b
0.4
0.2
mgal
0
-0.2
c
d
0
km
4
e

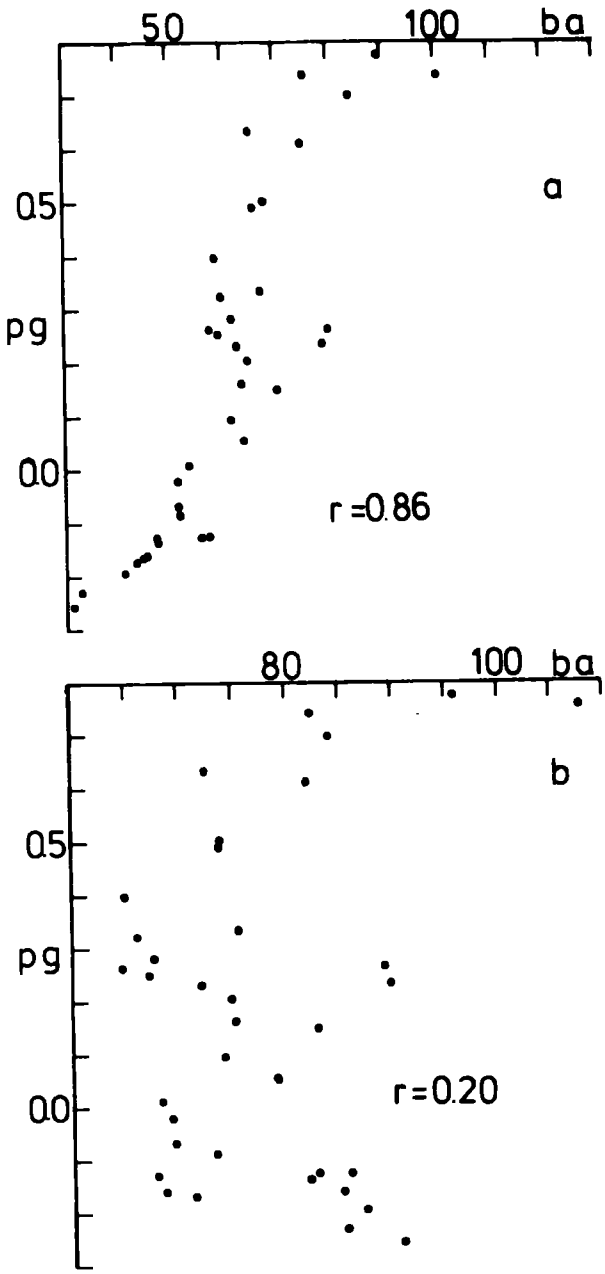
50
100
ba
a
0.5
pg
0.0
r=0.86
80
100
ba
b
0.5
pg
0.0
r=0.20

Bouguer anomalies and pseudogravity anomalies for induced magnetisation is 0.86 ., and between 'shallow' Bouguer anomalies and pseudogravity anomalies for vertical magnetisation, 0.81 . Both values are highly significant. However, the correlation coefficient between pseudogravity anomalies for induced magnetisation and the observed Bouguer anomalies is 0.20 ., and the scatter diagrams presented in fig. 6-7 illustrate well the necessity of the removal of the gravity effects of deep non-magnetic structures before accurate correlation can be achieved.

The causative structure would thus appear to have either totally induced magnetisation or induced magnetisation with an easterly dipping remanent component which may be related to the Cretaceous field direction (section 6.2). An approximate value for the intensity of magnetisation obtained from the relative amplitudes of pseudogravity and 'shallow' Bouguer anomalies was 0.0125 emu/cc. in the direction of the earth's field (0.0087 emu/cc. in the plane of the profile), assuming a density contrast of 0.5 gm/cc. between basement and sediments.

Spectral analyses of the magnetic anomalies all gave spuriously shallow depths to basement, most of which were above the sea bed (fig. 6-8). Perturbations in the magnetograms from the observatories at San Juan and Paramaribo were noted for the period surveying this line, and on the previous day both observatories had recorded severe magnetic activity. The spurious spectral analysis results are thus attributed to noise induced by external magnetic effects. Refraction line 22 of Officer et al. (1959), corrected for position, was used as a control on interpretation.

The computed causative magnetic bodies for induced and vertical

Figure 6-8 : Interpretations of Line L1500 for induced and vertical magnetisation. Horizontal bars indicate depths from spectral analysis. Vertical lines refer to a refraction profile.

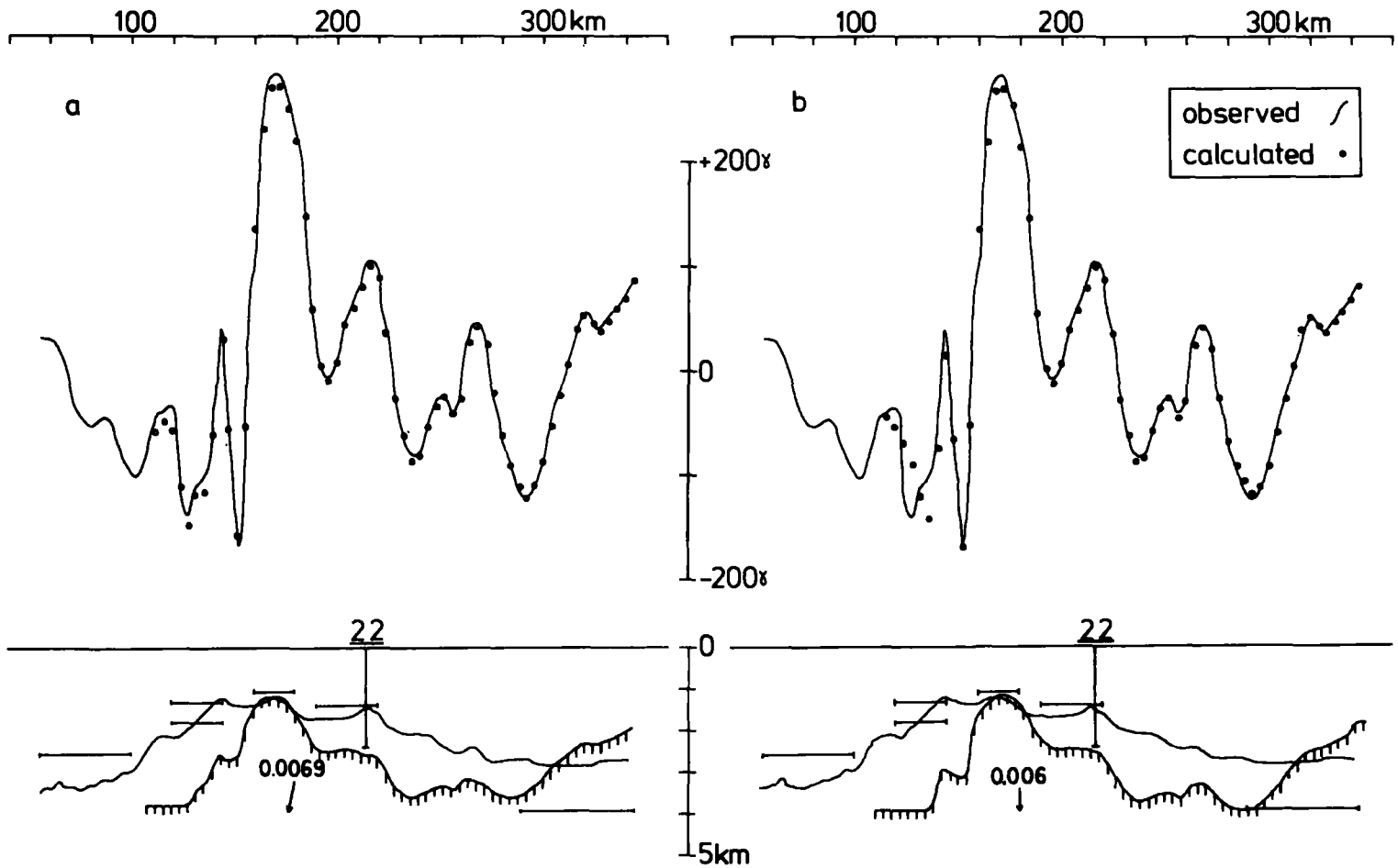
100
200
300 km
a
b
observed
calculated
+200γ
0
-200γ
22
22
0
0.0069
0.006
5km

magnetisation are presented in fig. 6-8. A matrix procedure was used, fitting blocks along the whole profile. The computed bodies indicate that gravity peak 2 corresponds to a magnetic prominence, and while the space form of both bodies is similar, induced magnetisation required an intensity of 0.01 emu/cc. in the direction of the earth's field (0.0069 emu/cc. in the plane of the profile), and vertical magnetisation an intensity of 0.006 emu/cc. Although both models satisfy the constraints of spectral analysis data and seismic refraction under the Aves Ridge, they are clearly inadequate for the flanking basins.

An attempt was made to separate the anomalies due to the Aves Ridge from those due to flanking structures by using a matrix procedure fitting blocks only to the region underlying the Aves Ridge. The computed body and its residuals are presented in fig. 6-9. These residuals are attributed to the flanking basins, since edge effects of the Aves Ridge body are not considered greatly contributory to these anomalies. Non-linear optimisation procedures were used to compute the causative bodies of these flanking structures, although in the absence of refraction or reliable spectral analysis data to constrain the space form, or distinctive gravity anomalies to constrain angles and intensities of magnetisation, the computed bodies will not represent unambiguous solutions.

The computed models for the flanking structures are presented in fig. 6-9d and e. The Venezuela Basin anomaly may be explained by a magnetic basement with induced magnetisation of intensity 0.006 emu/cc. in the direction of the earth's field (0.0042 emu/cc. in the plane of the profile) reaching a depth of approximately 5 km., a value reasonably consistent with the results of previous seismic reflection

Figure 6-9 : Line L1500

a - observed magnetic anomaly

b - body computed by fitting blocks under the Aves Ridge portion of the profile only

c - residual anomalies from model b (solid line)

d - computed body of the Venezuela Basin) the models are assumed to extend to infinity in both horizontal directions

e - computed body of the Grenada Trough

Residuals from d & e are shown as solid circles on curve c

Horizontal bars indicate depths from spectral analysis

Vertical lines indicate refraction profiles

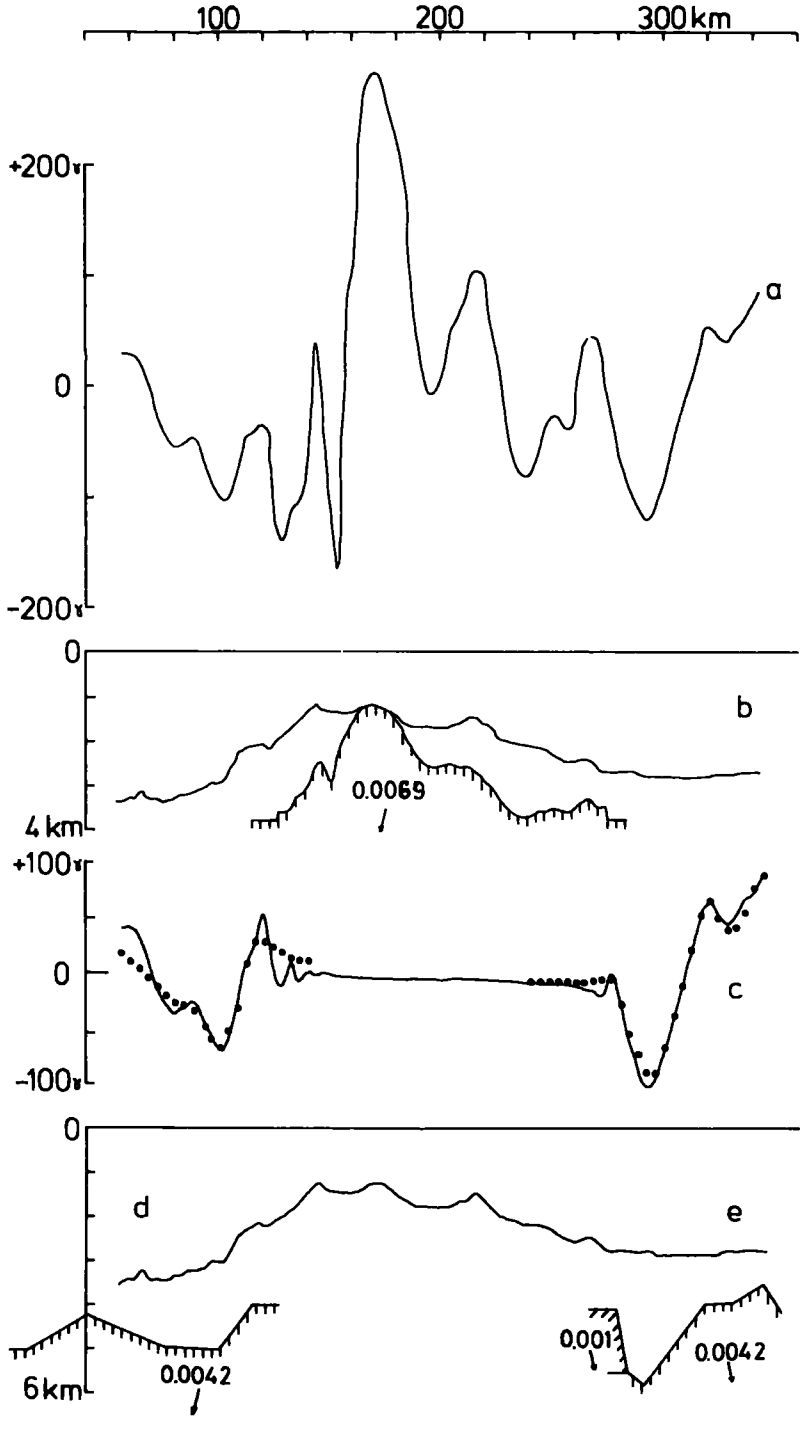
100
200
300km
+200γ
0
-200γ
a
0
b
0.0069
4km
+100γ
0
-100γ
c
0
d
e
0.0042
0.001
0.0042
6km

and refraction surveys. An induced magnetisation was found inadequate to explain the Grenada Trough anomaly, and a magnetisation vector dipping 78°E was found, by trial and error, to give a reasonable solution. This vector may be related to a Cretaceous field direction (section 6.2). The intensity of magnetisation of the main part of the Grenada Trough was 0.006 emu/cc. (0.0042 emu/cc. in the plane of the profile), although a much lower value was required in the region of the Aves Ridge, although this may be a function of the artificial method used to isolate the magnetic anomaly.

The computed magnetic models here presented are similar in form to the model computed from gravity anomalies (section 5.11).

6.4.4 Line L1420

The profile at 14°20'N passes over the centre of the prominent ridge marking the western part of the Aves Ridge in the centre of the survey area. It crosses the northern parts of magnetic highs K and L. Data relevant to the profile are presented in fig. 6-10.

No direct correlation is apparent between the observed Bouguer anomalies and the Bouguer anomalies from which the effects of deep structures have been removed (fig. 6-10a and b). Consequently no correlation is apparent between these 'shallow' Bouguer anomalies and pseudogravity anomalies for induced magnetisation (fig. 6-10d). However, the pseudogravity anomalies for a horizontal, westerly magnetisation vector show good correlation with the 'shallow' Bouguer anomalies with a correlation coefficient, for 26 data points, of 0.50 , a significant value (the correlation coefficient with the observed Bouguer anomalies is 0.39 ). The relative amplitudes of gravity and pseudogravity peaks 1,2 and 3 (fig. 6-10b) define two magnetic regions. Peak 1 of the gravity anomalies is of much

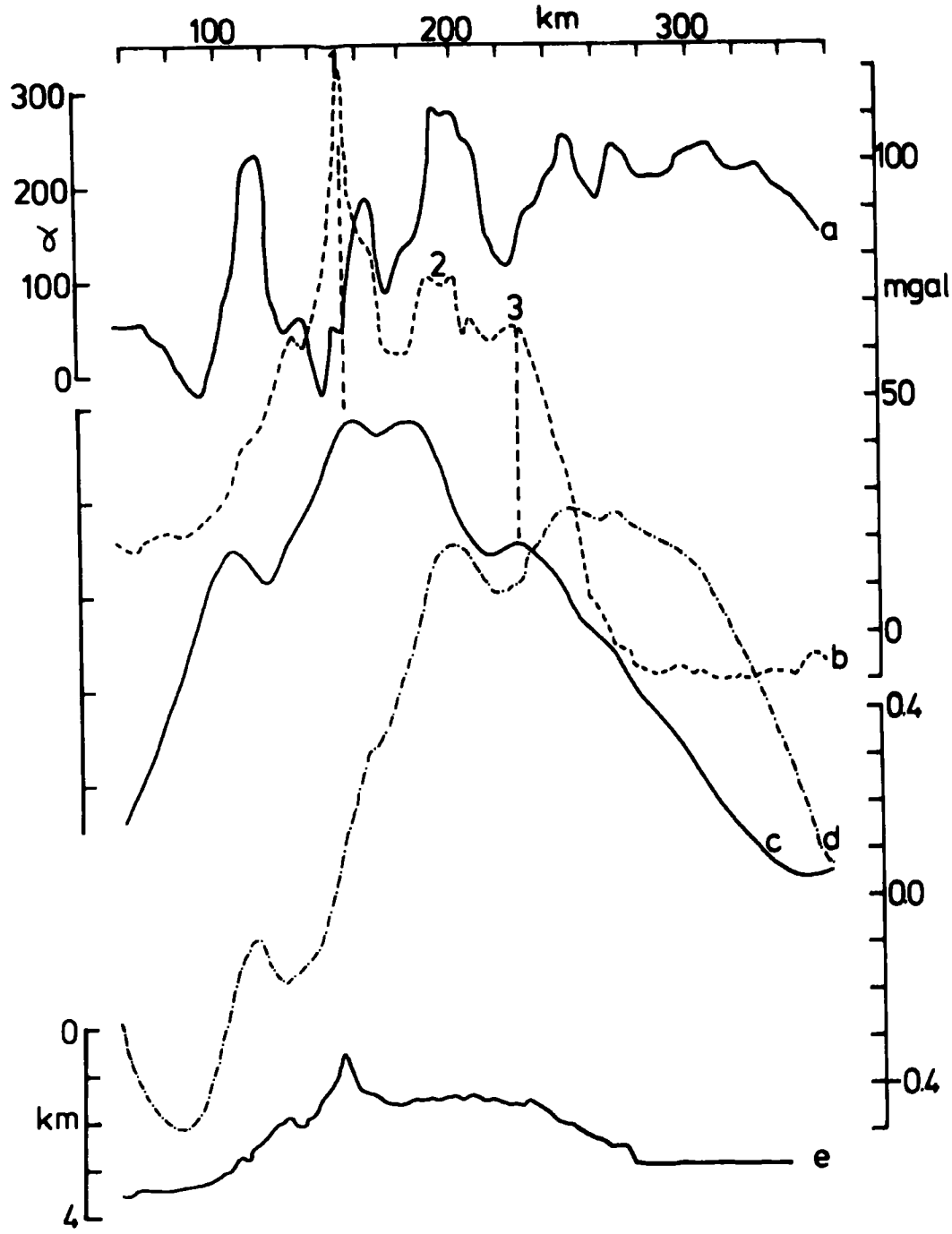
100
200
km
300
300
200
γ
100
0
2
3
a
100
mgal
50
0
b
0.4
0.0
0.4
c
d
0
km
4
e

greater amplitude than peaks 2 and 3, but is of similar amplitude in the pseudogravity anomalies. It is centred over the ridge on the western part of the Aves Ridge (fig. 6-10e). This may indicate that the ridge is much less magnetic than the rest of the Aves Ridge, and other profiles across this feature (sections 5.9.3 and 5.10.2) indicate that it is also denser. However, the situation may be rather more complex. The ridge may have a different magnetic inclination from the rest of the Aves Ridge, and the Poisson condition of $J/\rho$ constancy may not hold. Further considerations are that the profile does not accurately conform to the two-dimensional approximation and passes through the northern parts of magnetic highs K and L so that there is a finite value of the wave number in a direction at right angles to the profile. Examination of the observed magnetic anomaly indicates that there are long wavelength components present. Bott (1973) has shown that magnetic interpretations have a long wavelength instability (see section 6.3), and these long wavelengths may become predominant in an interpretation. It is possible that the computed magnetic inclination of 0°W is a reflection of this, with the effects of the short wavelength components being suppressed. Gravity peak 2 is slightly offset in the pseudogravity anomalies and does not correspond to a structure in the sediment/basement interface, which is well defined in this region by two seismic refraction lines (assuming that the navigation of the refraction lines was accurate). It may correspond to a local high density pocket or to a structure slightly deeper in the crust. Gravity peak 3 correlates with a pseudogravity peak. The most westerly pseudogravity peak does not correspond to a gravity peak and may correspond to a local change in magnetic intensity and/or

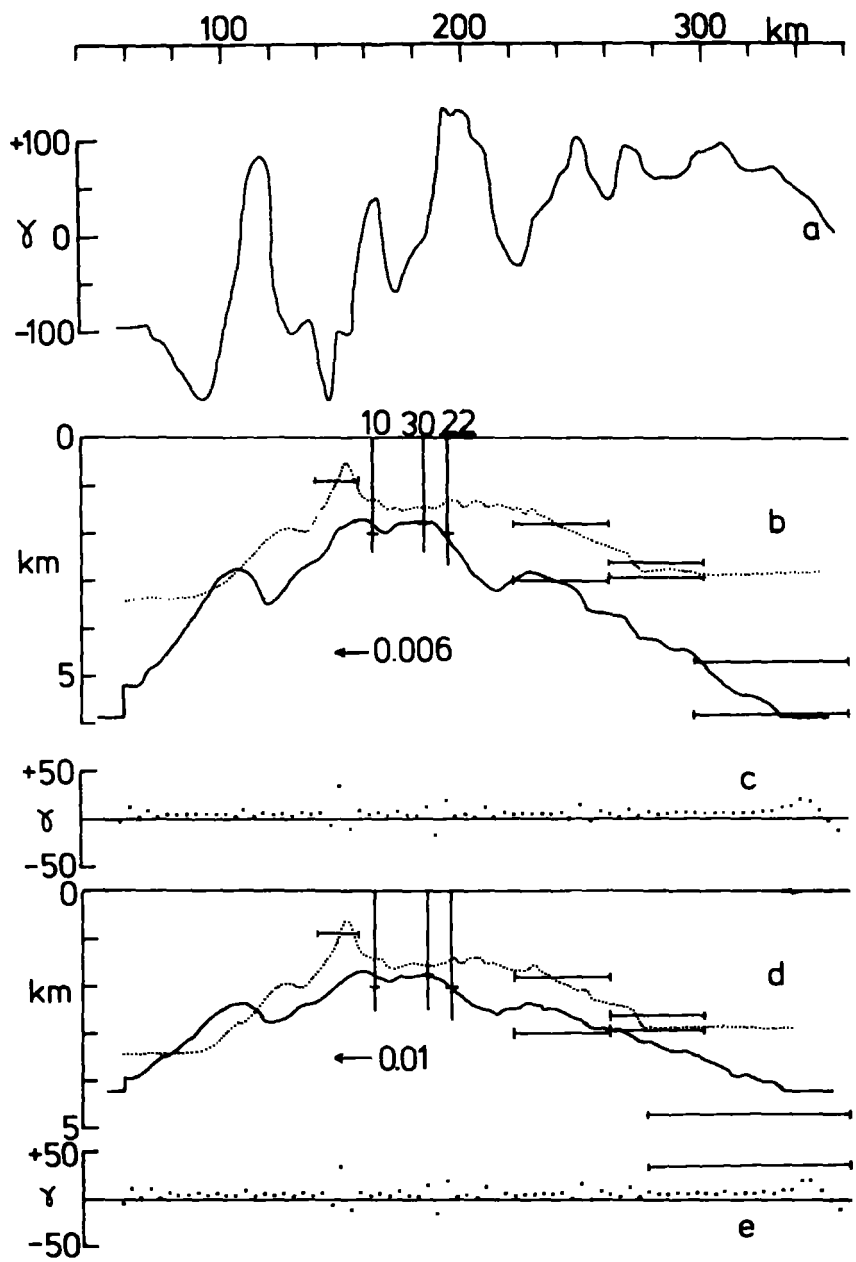
100
200
300
km
+100
γ 0
-100
a
10 30 22
0
km
5
b
←0.006
+50
γ
-50
c
0
km
5
d
←0.01
+50
γ
-50
e

inclination. The amplitudes of pseudogravity and 'shallow' Bouguer anomalies suggest a high intensity of magnetisation, 0.01 emu/cc. in the plane of the profile, assuming a density contrast of 0.5 gm/cc. between sediments and basement.

The significance of the magnetic inclination of 0°W is not known, as it corresponds neither to the present earth's field direction nor to the proposed Cretaceous field direction. A possibility would be a reversed Cretaceous direction with a small induced component, but the data are not conclusive.

The magnetic observatories at San Juan and Paramaribo both registered quiet conditions during the period surveying this profile, and so the magnetic anomalies are considered free from external effects. The results of spectral analysis are presented in fig. 6-11. The western ridge is shown to be a magnetic prominence, while the eastern part of the Aves Ridge has a somewhat thicker sedimentary cover. Three seismic refraction lines, 10, 30 and 22 of Officer et al.(1959) provide constraints on interpretation over the Aves Ridge, while line 24 of Officer et al. in the Venezuela Basin 8 km. to the north of the profile constrains the depth to basement as approximately 5.5 km., magnetic data in this area not being good enough for spectral analysis.

Two possible interpretations of the causative magnetic body were computed for intensities of 0.01 and 0.006 emu/cc. in the plane of the profile using a matrix procedure fitting blocks to the whole profile. The resulting bodies are presented in fig. 6-11. The model for intensity 0.006 emu/cc. satisfies all constraints with the exception of bathymetry ridge 1 which is considered to be of considerably lower magnetic intensity. However, the model for intensity 0.01 emu/cc.

Figure 6-12 : Line 1420

a - observed magnetic anomaly

b - body computed by fitting blocks under the Aves Ridge portion of the profile only

c - residual anomalies from model b (solid line)

d - computed body of the Venezuela Basin
e - computed body of the Grenada Trough

} the models are assumed to extend to infinity in both horizontal directions

Residuals from d & e are shown as solid circles on curve c

Horizontal bars indicate depths from spectral analysis

Vertical lines indicate refraction profiles

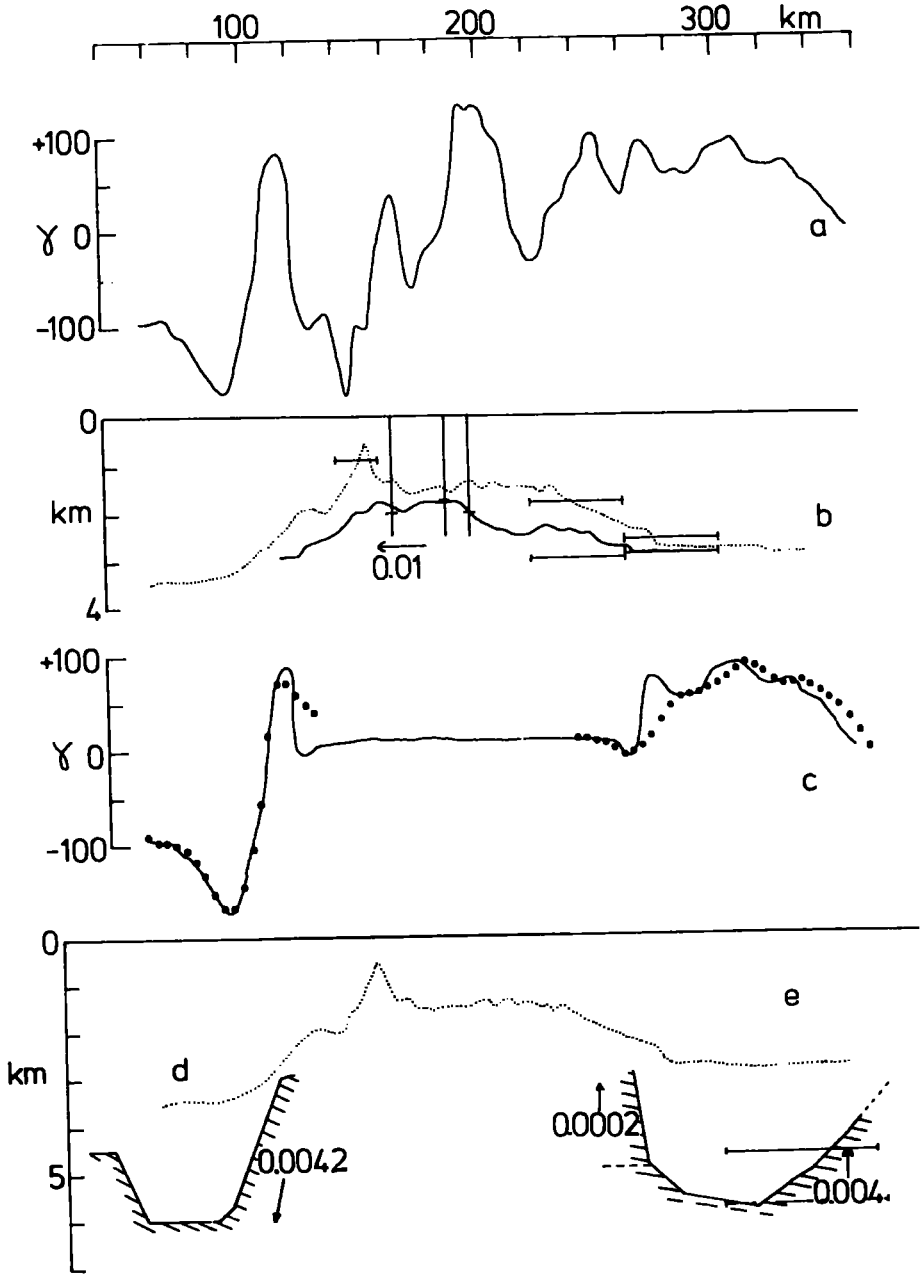
100
200
300
km
+100
γ 0
-100
a
0
km
4
0.01
b
+100
γ 0
-100
c
0
km
5
d
e
0.0042
0.0002
0.004

also satisfies the constraints under the Aves Ridge, and is considered a reasonable alternative interpretation for this area although depths to basement are too deep under both Venezuela Basin and Grenada Trough.

Separation of the flanking basin anomalies was attempted by a method described in section 6.3.3 whereby a matrix procedure was used fitting blocks only to the portion of the profile underlying the Aves Ridge. The resulting model for intensity 0.01 emu/cc. (in the plane of the profile) and the resulting residuals attributed to the basin anomalies are presented in fig. 6-12 with possible interpretations of causative bodies computed using non-linear optimisation procedures. An induced model was fitted to the Venezuela Basin anomaly, and an intensity of 0.006 emu/cc. in the direction of the earth's field (0.0042 emu/cc. in the plane of the profile) was found to produce a reasonable interpretation although it was not possible to fit the steep peak between 110 and 120 km., which was also present on the original profile. The Grenada Trough anomaly is positive with a maximum over the centre of the basin. Comparison with computed anomalies indicated that the causative body has a near vertical upwards magnetisation vector, and a model computed for vertical magnetisation with spectral analysis constraints required an intensity of magnetisation of 0.004 emu/cc. for the central Trough with a somewhat lower value near the Aves Ridge, although this may be merely a function of the method of separating the anomalies. It is probable that the Grenada Trough is at least as old as the upper Cretaceous (the proposed date of the oldest sediment reflector). Consequently it seems unlikely that this magnetisation direction is related to a reversed phase of the present earth's field. Its origin must remain unsolved.

This profile is thus seen to be rather more complex than those discussed in earlier sections. Although the simple models produced for the Aves Ridge for a single magnetic intensity and inclination of 0°W are in accord with the results obtained from seismic refraction and reflection, it must be stressed that the situation may be considerably more complex, with the possibility of variation of magnetic intensity and inclination across the Aves Ridge. These effects may have been masked by the instability induced by long wavelength components of the anomaly.

6.4.5 Line L1344

The profile at 13°44'N passes to the north of the prominent sea-mount in the southern part of the survey area. It passes through the prominent magnetic low M. Relevant data are presented in fig. 6-13.

Direct negative correlation is apparent between the observed magnetic anomalies and the Bouguer anomalies from which the effects of deep structure have been removed (fig. 6-13a and b). Consequently correlation is apparent between these 'shallow Bouguer anomalies and pseudogravity anomalies for magnetisation reversed with respect to the present earth's field (fig. 6-13c), whose azimuth and inclination in the plane of the earth's field are defined by 169° and -43° respectively. The correlation coefficient between the 'shallow' Bouguer and pseudogravity anomalies for 95 data points is 0.82 , a highly significant value. Gravity peak 1 (fig. 6-13b) is not represented in the pseudogravity anomalies while peak 2 correlates closely. This magnetic inclination is ambiguous, however, and inclinations of -60° and -20° in the reversed direction of the earth's field also exhibit this pattern of correlation. Resolved east-west,

Figure 6-13 : Line L1344

a - observed magnetic anomaly

b - Bouguer anomaly with effects of deep structures removed

c - pseudogravity anomaly for reversed magnetisation

d - bathymetry

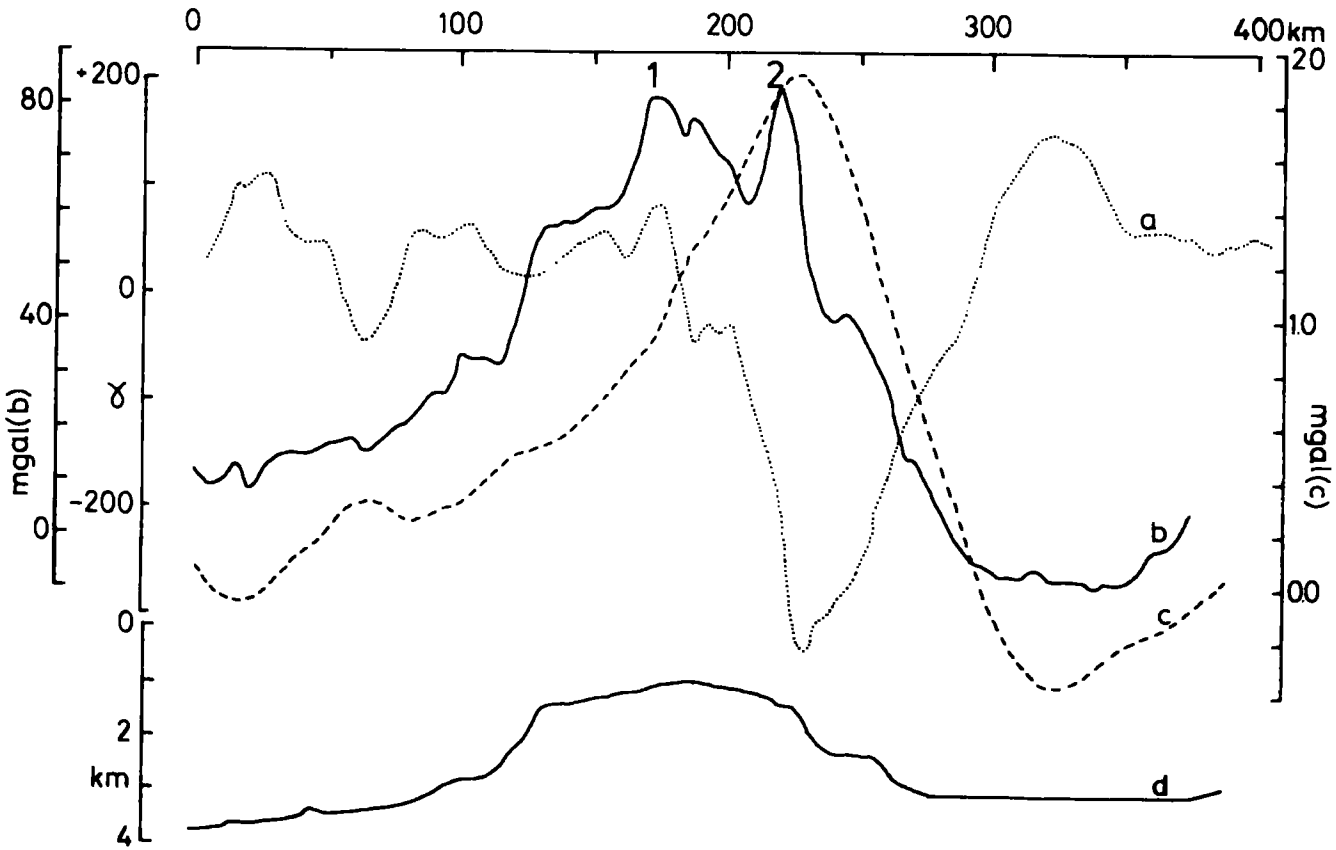
0
100
200
300
400km
1
2
80
40
0
+200
0
-200
0
mgal(b)
γ
20
1.0
0.0
mgal(c)
a
b
c
d
2
km
4

these limits impart limits of $\pm 6°$, and so a reversed direction of magnetisation was assumed. This inclination is unexpected, since it would seem highly unlikely that a body of probable Cretaceous age would have magnetisation related to a reversed direction of the present earth's field. As with section 6.4.2, its origin must remain unknown. The relative amplitudes of gravity and pseudogravity anomalies suggest an intensity of magnetisation of c. 0.008 emu/cc. in the direction of the reversed earth's field if a density contrast of 0.5 gm/cc. is assumed between sediments and basement. However, this value must be treated with caution, as examination of magnetic low M indicates that it is elongate in an east-west direction. Consequently, since the wave number has a finite value in a north-south sense, the computed intensity of magnetisation may be in error (section 6.3).

Magnetograms from the observatories at San Juan and Paramaribo record minor perturbations in the earth's field during the period surveying this profile, but they are not considered so severe as to impart significant external effects to the magnetic data. Spectral analysis results are presented in fig. 6-14, and indicate an approximate depth to magnetic basement of 6.3 km. under the Venezuela Basin and 4.9 km. under the Grenada Trough. Basement under the Aves Ridge is seen to slope gently up to the sea bed in the west, but descends rather more abruptly under the eastern part of the Aves Ridge. Refraction line 29 of Officer et al. (1959), situated in the western Grenada Trough, was used as a control on interpretation.

Several interpretations are possible for this profile, the first, simple model was produced using a matrix procedure for the Aves Ridge and manual adjustment of parameters using MAGN for the flanking

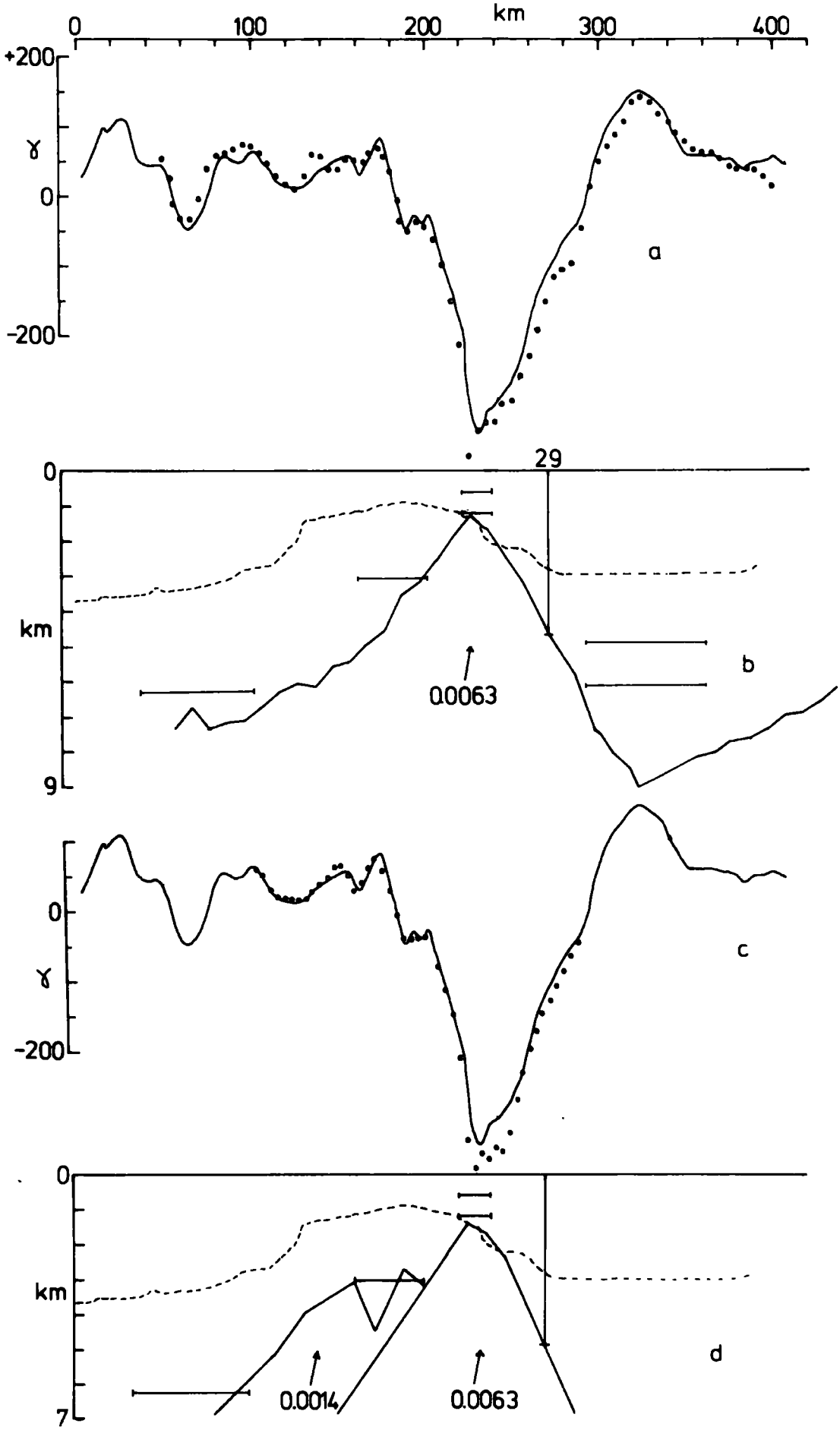


Figure 6-14 : Two interpretations of Line L1344. Computed anomalies shown as solid circles, horizontal bars indicate depths from spectral analysis, vertical lines refraction profiles.

Figure 6-15 : Line L1344

a - observed magnetic anomaly

b - body computed by fitting blocks under the Aves Ridge portion of the profile only

c - residual anomalies from model b (solid line)

d - computed body of the Venezuela Basin

e - computed body of the Grenada Trough

the models are assumed to extend to infinity in both horizontal directions

Residuals from d & e are shown as solid circles on curve c

Horizontal bars indicate depths from spectral analysis

Vertical lines indicate refraction profiles

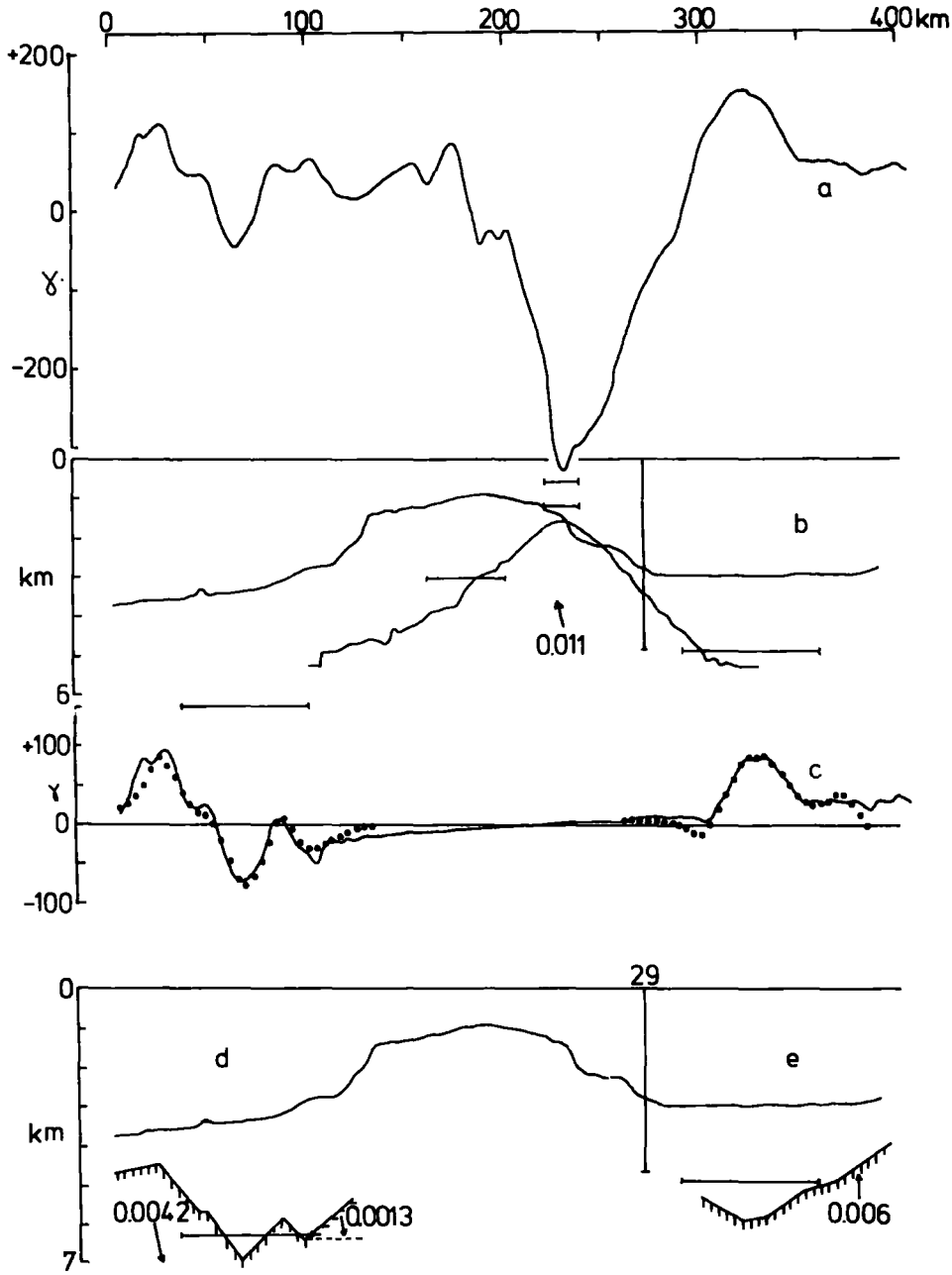
0
100
200
300
400km
+200
0
γ
-200
a
0
km
b
0.011
6
+100
γ
0
-100
c
0
29
d
e
km
0.0042
0.0013
0.006
7

structures. A reversely magnetised model with intensity 0.009 emu/cc. in the direction of the reversed earth's field (0.0063 emu/cc. in the plane of the profile) was found to best conform to spectral analysis and refraction data under the Aves Ridge although depth to basement under the western flank is rather too great (fig. 6-14b). The model is adequate under the Venezuela Basin but is clearly inadequate under the Grenada Trough where the computed depth to basement is too great.

A second interpretation was performed for the Aves Ridge in which the western part was assigned a somewhat lower intensity of magnetisation. A non-linear optimisation procedure was used, constraining the eastern part with the matrix model and allowing the body coordinates and magnetic intensity of the western part to vary. The computed body, presented in fig. 6-14d conforms well to spectral analysis control and gives an intensity of magnetisation of 0.002 emu/cc. in the direction of the earth's field (0.0013 emu/cc. in the plane of the profile) for the western part of the Ridge.

An attempt was made to separate the anomalies of the flanking basins from the effects of the Aves Ridge by a procedure described in section 6.4.3 by fitting blocks only to the Aves Ridge portion of the profile. The resulting body and its residuals, which are attributed to the flanking structures, are presented in fig. 6-15. These anomalies were interpreted using a non-linear optimisation procedure, and computed models are presented in fig. 6-15d and e. In the absence of definitive gravity anomalies, an induced model was fitted to the Venezuela Basin. The model produced conforms with spectral analysis data and indicates an intensity of magnetisation of 0.006 emu/cc. in the direction of the earth's field (0.0042 emu/cc. in the plane of the profile) with a somewhat lower value nearer the

Aves Ridge. Comparison of the Grenada Trough anomalies with curves computed for bodies of different magnetic inclinations indicated a steeply upward dipping magnetisation vector for the causative body. It would seem unlikely that this inclination is related to a reversed direction of the present earth's field. The computed body is in accord with spectral analysis data, and requires an intensity of magnetisation of 0.006 emu/cc.

6.4.6 Line L1324

The profile at 13°24'N passes just south of the prominent seamount in the southern part of the survey area and crosses magnetic high P, high N and the northern part of high O. It was studied since Durham seismic reflection data are available to define the basement over the eastern part of the Aves Ridge. Relevant data are presented in fig. 6-16.

The magnetic anomalies (fig.6-16a) are complex, and while there is gross correlation with the free air anomaly (fig. 6-16c), no magnetic inclination was found for which the pseudogravity anomalies correlated with the gravity anomalies for all the features. The pseudogravity anomalies for induced magnetisation are presented in fig. 6-16d, while line b is the magnetic anomaly computed for induced magnetisation using the basement revealed by reflection data assuming a flat base at 5.5 km. and an intensity of magnetisation of 0.005 emu/cc. Shapes and amplitudes correspond in places, but otherwise the fit is not good.

It is concluded that this part of the Aves Ridge is complex in its magnetic character, with the possibility of varying magnetic inclinations and intensities along its length. The isolation and interpretations of two anomalies on this profile are presented in later sections.

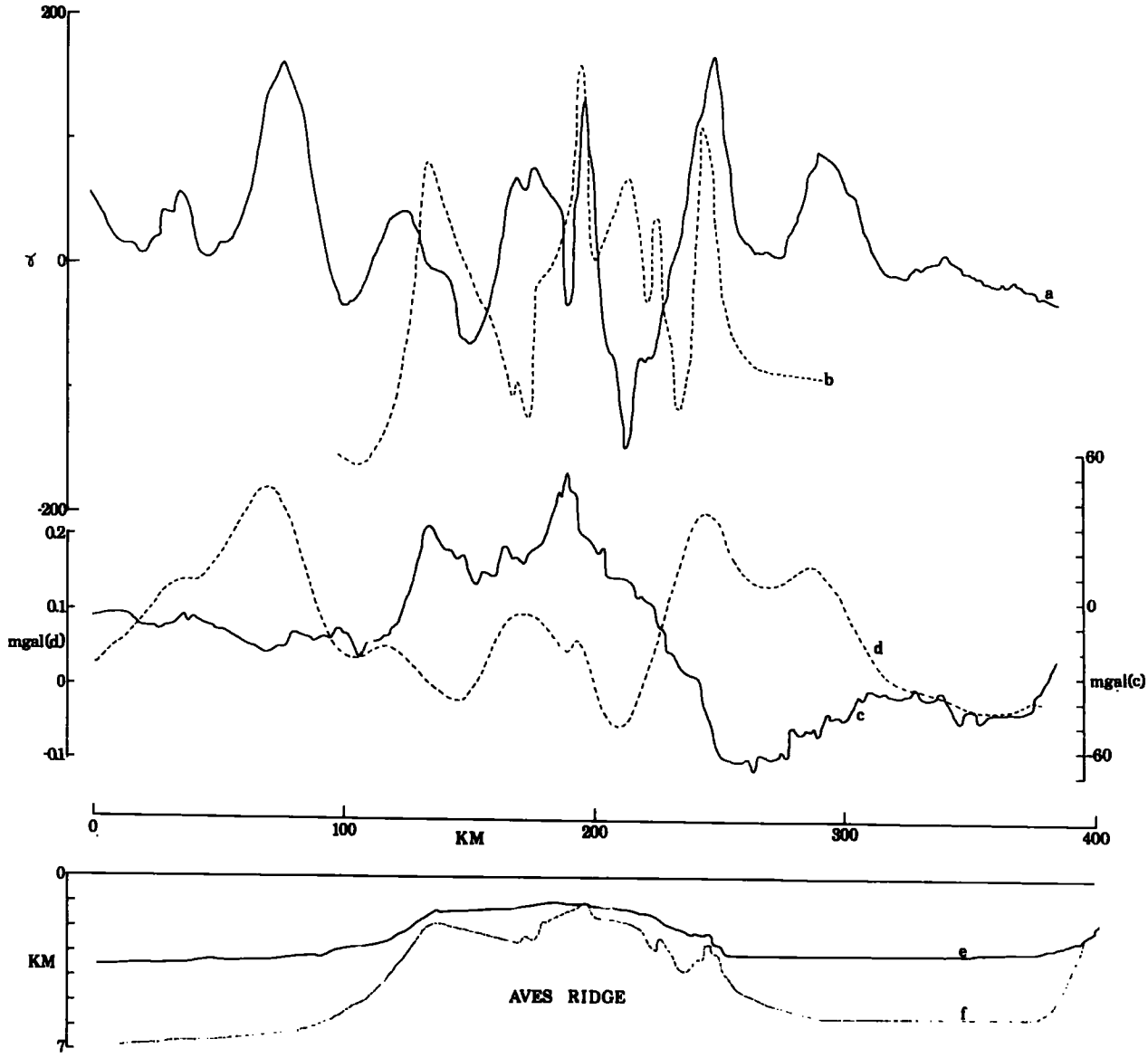
200
γ 0
-200
a
b
0.2
0.1
mgal(d)
0
-0.1
60
0
mgal(c)
-60
d
c
0
100
200
300
400
KM
0
KM
7
AVES RIDGE
e
f

6.4.7 Line L1314

The profile at 13°14'N crosses the southern part of the survey area and passes over magnetic high O. Relevant data are presented in fig. 6-17.

No direct correlation is apparent between the observed magnetic anomalies and the Bouguer anomalies from which the effects of deep structures have been removed (fig. 6-17a and b). Consequently no correlation is apparent between these 'shallow' Bouguer anomalies and pseudogravity anomalies for induced magnetisation (fig. 6-17d). Correlation is apparent, however, between the 'shallow' Bouguer anomalies and pseudogravity anomalies computed for a magnetic inclination of -10° in the direction of the earth's field (fig. 6-17c). When resolved in the direction of the profile, this inclination becomes -43°W. The correlation coefficient for 46 data points is 0.91 , a highly significant value. This angle is not considered unambiguous since the correlation remains apparent for inclinations between -5° and -15° in the direction of the earth's field (-25° and -55° in the plane of the profile).

Four principal peaks are apparent on the 'shallow' Bouguer anomalies (fig.6-17b). Peak 1 corresponds to a pseudogravity peak and also to a bathymetric prominence (fig. 6-17e). Peak 2 does not correspond to a pseudogravity peak, while peaks 3 and 4 would seem to combine to correspond to a single pseudogravity peak. If the gravity peaks correspond to basement highs, this combined correspondence may be indicative of an interpeak basin filled with magnetic sediments of a lower density, than but similar magnetic intensity to, the basement. Comparison of the amplitudes of pseudogravity and 'shallow' Bouguer anomalies indicates an intensity of magnetisation of approximately 0.018 emu/cc. in the direction of the earth's field (0.0046 emu/cc.

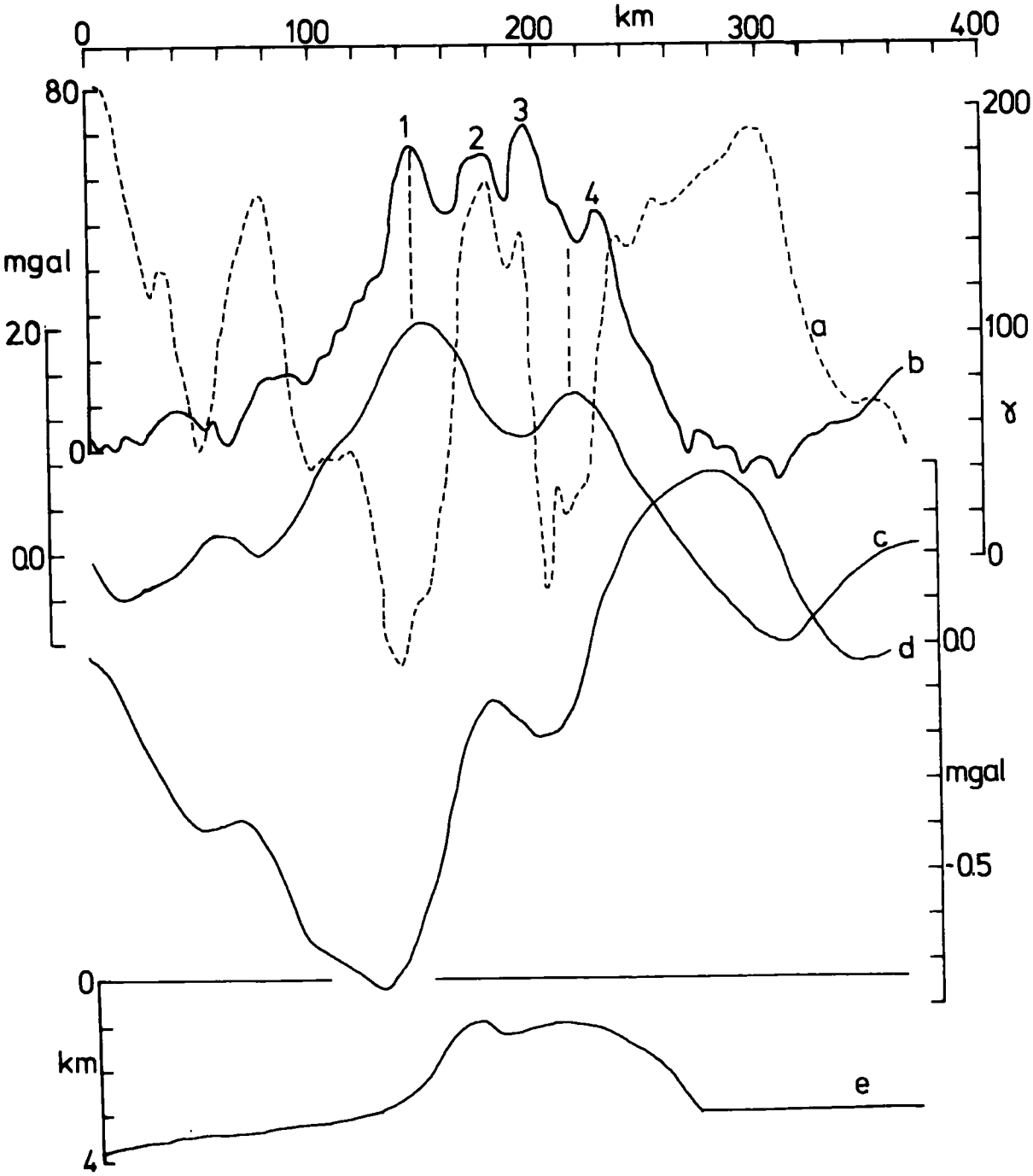


Figure 6-17 : Line L1314
a-observed magnetic anomaly, b-Bouguer anomaly with the effects of deep structures removed, c-pseudogravity anomaly for a magnetic inclination of -10° in the direction of the earth's field, d-pseudogravity anomaly for induced magnetisation, e-bathymetry.

in the plane of the profile) assuming a density contrast of 0.5 gm/cc. between sediments and basement. The significance of the magnetic inclination is unknown, but is similar to that computed for the profile at 14°20'N (section 6.4.4).

Magnetograms from observations at San Juan and Paramaribo both indicate quiet magnetic conditions during the period surveying the profile and so magnetic data are considered free from external effects. Spectral analysis results (fig. 6-18) indicate an approximate depth to basement of 5 km. under the Venezuela Basin, while data over the Grenada Trough are far less conclusive, indicating a maximum depth to basement of 6.7 km. The bathymetric prominence corresponding to gravity peak 1 over the Aves Ridge is shown to have only a thin non-magnetic cover, as does the region corresponding to peaks 3 and 4. Between the peaks basement is shown to be somewhat deeper, although the true depth is constrained by somewhat wide limits. Refraction line 29 of Officer et al. (1959), in the western Grenada Trough, was used as a control on interpretation.

Interpretation (fig.6-18) was performed using a matrix optimisation procedure. For the magnetic inclination determined above, an intensity of magnetisation of 0.01 emu/cc. in the direction of the earth's field (0.0026 emu/cc. in the plane of the profile) was found to best conform to the constraints of spectral analysis, although the eastern peak is somewhat too deep and may indicate a slightly lower intensity of magnetisation of this feature. Although this model is sufficient over the Venezuela Basin, it does not conform to refraction data in the Grenada Trough.

An attempt was made to separate the magnetic anomalies due to the Aves Ridge from those due to its flanking basins by using a matrix optimisation procedure fitting blocks under only the Aves Ridge

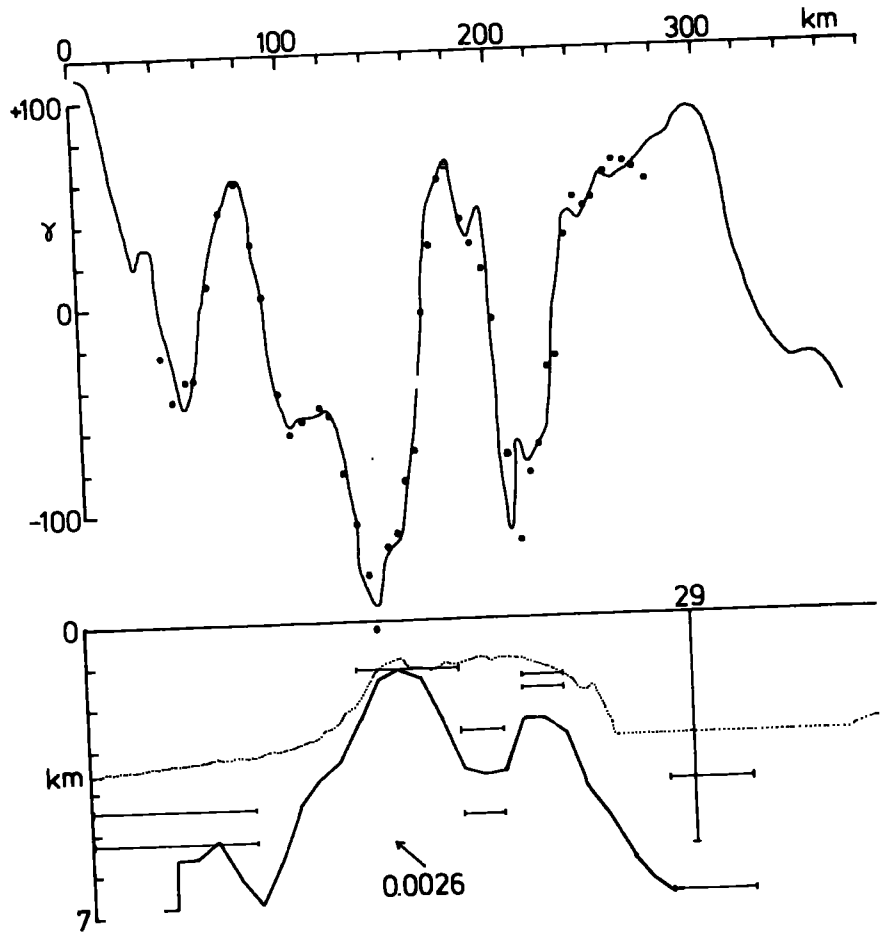


Figure C-1c : Interpretation of line 2154.

Figure 6-19 : Line 1314

a - observed magnetic anomaly

b - body computed by fitting blocks under the Aves Ridge portion of the profile only

c - residual anomalies from model b (solid line)

d - computed body of the Venezuela Basin

e - computed body of the Grenada Trough

the models are assumed to extend to infinity in both horizontal directions

Residuals from d & e are shown as solid circles on curve c

Horizontal bars indicate depths from spectral analysis

Vertical lines indicate refraction profiles

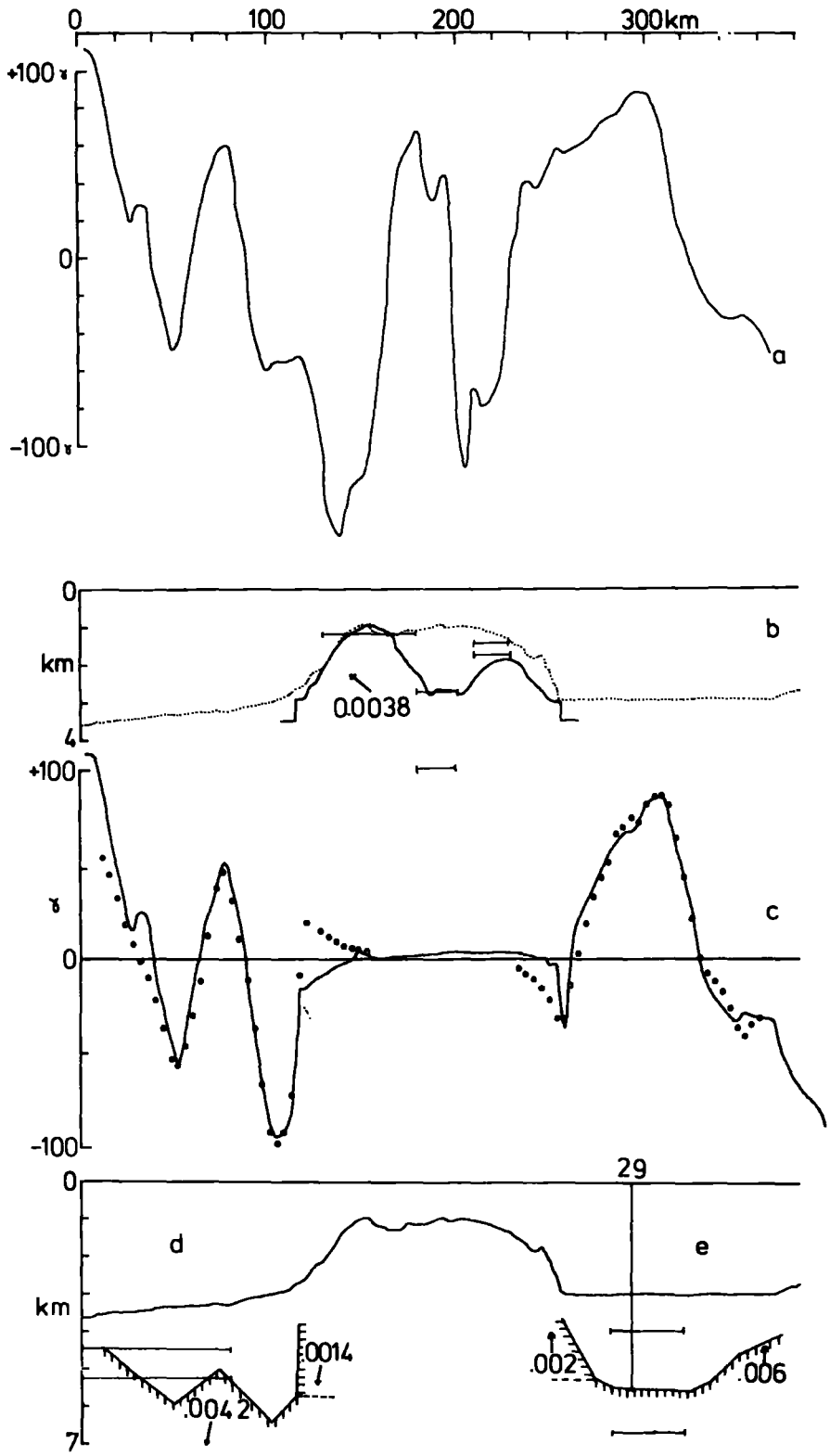
0
100
200
300km
+100 γ
0
-100 γ
a
0
km
4
0.0038
b
+100
γ
0
-100
c
0
29
km
d
e
.0014
.0042
.002
.006
7

portion of the profile and attributing the flanking residuals (fig.6-19c) to the basins. The causative body of the Aves Ridge thus computed is presented in fig. 6-19b, and, although it conforms to spectral analysis data, has a higher intensity than the previously computed body, 0.015 emu/cc. in the direction of the earth's field (0.0038 emu/cc. in the plane of the profile). In the absence of other data, an induced model was fitted to the Venezuela Basin, which required an intensity of 0.006 emu/cc. (0.0042 emu/cc.) decreasing to 0.002 emu/cc. (0.0014 emu/cc.) in the neighbourhood of the Aves Ridge (fig. 6-19d). The Grenada Trough anomaly is indicative of a near vertical magnetisation vector and a model for this inclination conforming to spectral analysis and refraction data was found to require an intensity of 0.006 emu/cc., decreasing to 0.002 emu/cc. near the Aves Ridge. It is unlikely that this vertical magnetic inclination is related to a reversed direction of the present earth's field.

### 6.4.8 Line L1254

The profile at 12°54'N was the most southerly surveyed. Consequently the accuracy of the two-dimensional approximation made in its study cannot be judged. The profile passes over magnetic high Q, which is the only anomaly in the survey area which is positive with respect to the I.G.R.F. This profile was selected for study since a Durham reflection profile allowed definition of the basement under the Aves Ridge. Relevant data are presented in fig. 6-20.

The magnetic high Q is offset to the east of the Aves Ridge. No correlation is apparent between the observed magnetic and free air anomalies (fig. 6-20 d and a). Consequently no correlation is apparent between the free air anomalies and pseudogravity anomalies for induced magnetisation (fig. 6-20b). Correlation is apparent,

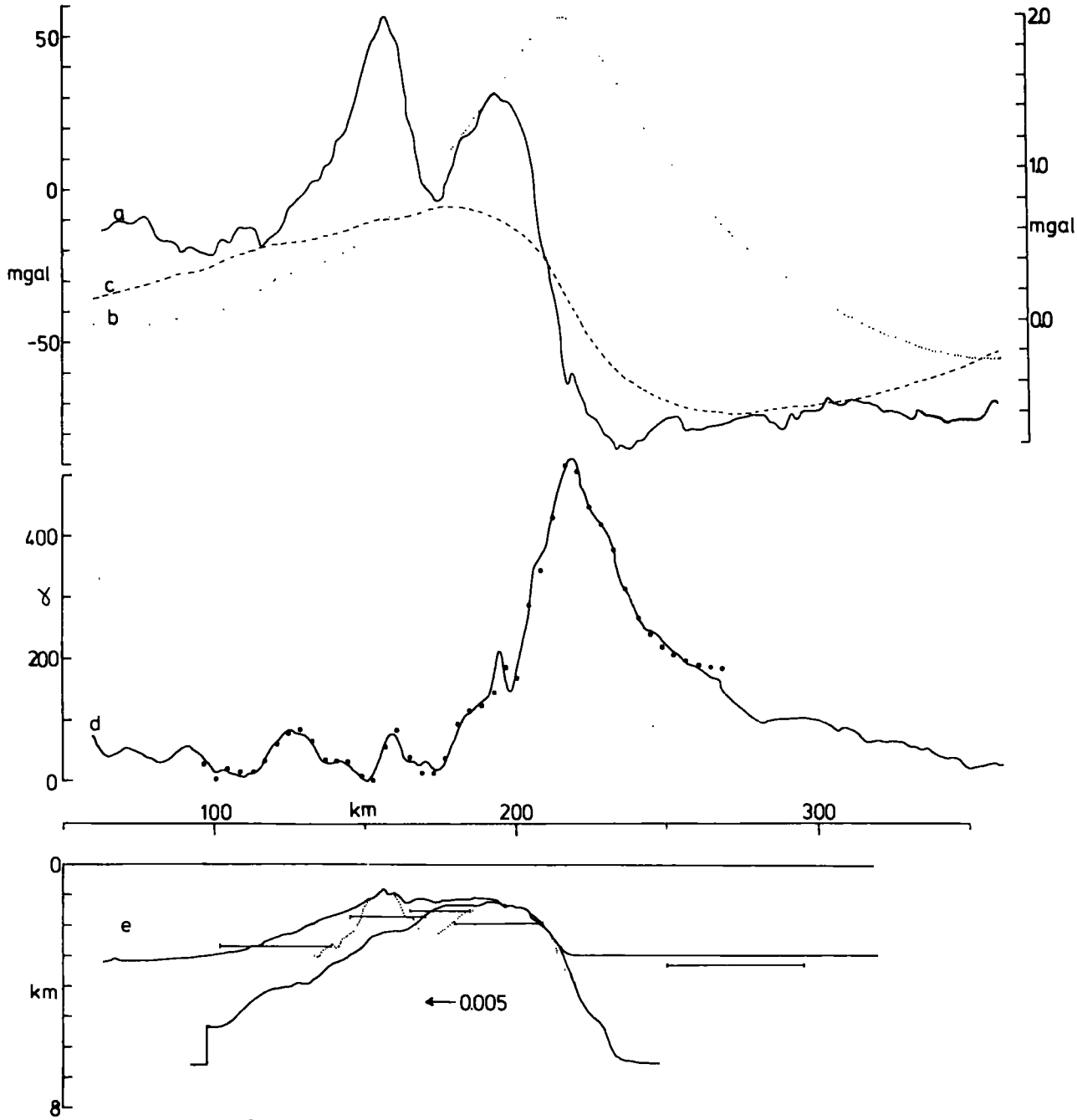


Figure 6-20 : Line L1254.
a-free air anomaly, b-pseudogravity anomaly for induced magnetisation, c-pseudogravity anomaly for magnetisation horizontal westwards, d-observed magnetic anomaly, e-computed model with computed anomalies shown as solid circles on curve d. Horizontal bars indicate depths from spectral analysis, the broken line shows the basement revealed by seismic reflection.

however, between the free air anomalies and pseudogravity anomalies computed for a horizontal westwards magnetisation vector. The correlation coefficient between these pseudogravity anomalies and the free air anomalies is 0.92 for 91 data points, a highly significant value. The possible limits on this inclination of 0°W are +10 and -10°W. The significance of this horizontal vector is unknown. However it does appear that this inclination is not due to the presence of long wavelength components in the magnetic anomaly, as was probably the case for profile L1420 (section 6.4.4). Comparison of the amplitudes of the gravity and pseudogravity anomalies indicates an intensity of magnetisation of 0.005 emu/cc. in the plane of the profile, assuming a density contrast between sediments and basement of 0.5 gm/cc.

The results of spectral analysis of the magnetic data are presented in fig. 6-20e as horizontal bars. Data were not good enough for analysis of the Venezuela Basin anomalies. The two basement peaks revealed by seismic reflection are shown to be magnetic prominences, although the computed depths were somewhat deeper. The interpeak trough gave a depth less than that predicted by reflection. This may be indicative of the presence of magnetic sediments within the trough. Also a spuriously low depth to basement was obtained in the Grenada Trough, which may also be indicative of magnetic structures within the sediments. However, a further explanation of these two results could be a breakdown in the original assumptions of the spectral analysis method (section 3.6) in that the magnetic data do not contain all representative frequencies. Also, although the magnetograms from the observatory at Paramaribo registered quiet conditions during the period surveying the profile, the horizontal component monitored at the observatory at San Juan was disturbed.

Consequently external effects may also contribute to these shallow depths to basement.

The anomaly was interpreted using a matrix optimisation procedure. The computed model is presented in fig. 6-20e, and required an intensity of magnetisation of 0.005 emu/cc. in the plane of the profile. The computed body may be compared with the basement under the Aves Ridge revealed by seismic reflection which is represented by a broken line in fig. 6-20e. The eastern peak corresponds well with the magnetic body, but the interpeak trough and western peak are not apparent. This simple model would imply that the western peak is much less magnetic than the eastern peak.

6.4.9 A magnetic feature on the Aves Ridge at 13°24'N

Examination of the magnetic profile over the Aves Ridge at 13°24'N reveals a very sharp perturbation in the magnetic anomalies not present in neighbouring profiles (fig. 6-21). In order to study this feature (magnetic high N) in more detail, the anomaly was isolated by placing a smooth line through the curve which, by comparison with neighbouring profiles, was taken to represent a local background. The residual anomaly is presented in fig. 6-22a.

Comparison with the Bouguer anomaly (fig.6-21b) reveals that the anomaly is not centred on the local gravity peak. Comparison of the residual anomaly with curves computed for bodies with different magnetic inclinations indicated that the angle of magnetisation was in the region of 43° - 70° in the direction of the earth's field (78°-86° in the plane of the profile), and so interpretations were performed for these two limits using a matrix optimisation routine. Reflection data indicate a lack of sediment cover in the region of the anomaly and so the top of the causative body was assumed to correspond to the sea bed.

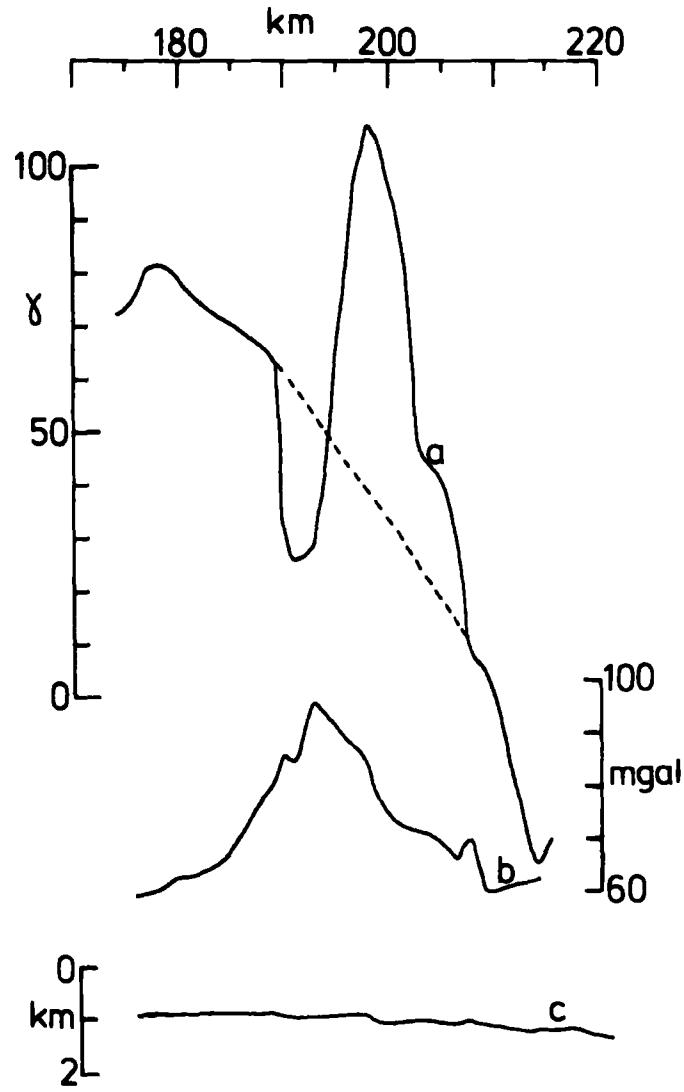


Figure 2-21 : Magnetic high ..
a-observed magnetic anomaly,
dashed line represents the backgro nd
b-observed Bouguer anomaly
c-bathymetry

Figure 6-22 : Interpretations of magnetic high N

a - magnetic anomaly with background removed

b - g computed models and residual anomalies

dip and intensity (emu/cc.) for azimuth 349°

| | | |
|---|---|---|
| b - | 43° | 0.008 |
| c - | 43° | 0.001 |
| d - | 70° | 0.008 |
| e - | 70° | 0.008 |
| f - | 43° | 0.0015 |
| g - | 70° | 0.0015 |

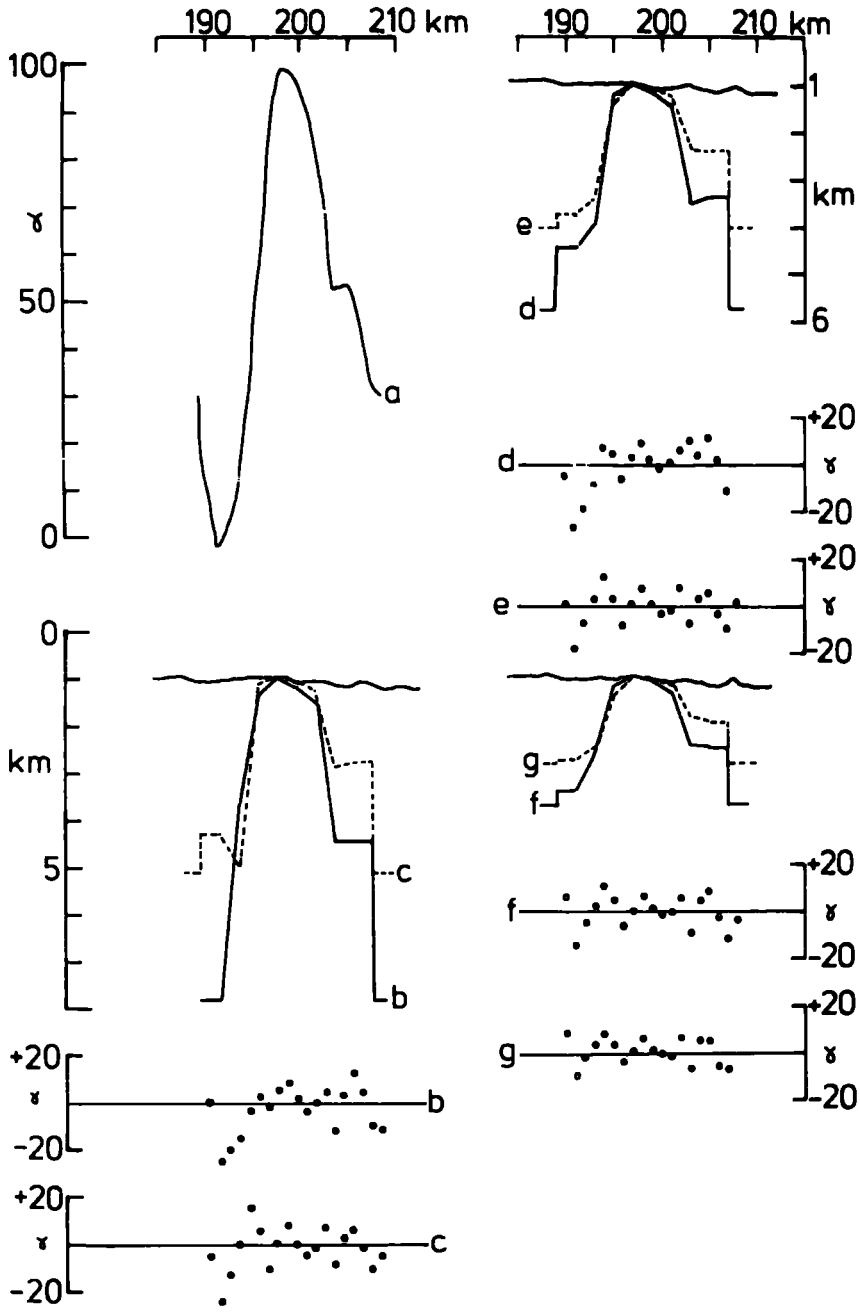
190
200
210 km
100
γ
50
0
a
0
km
5
c
b
+20
γ
-20
b
+20
γ
-20
c
190
200
210 km
1
km
6
e
d
d
+20
γ
-20
e
+20
γ
-20
g
f
f
+20
γ
-20
g
+20
γ
-20

Six possible interpretations of the causative body are given in fig. 6-22, for the above angles of magnetisation and magnetisation contrasts of 0.0003, 0.001 and 0.0015 emu/cc. in the direction of the earth's field.

The body thus has only a slightly higher intensity of magnetisation than the surrounding basement rocks of the Aves Ridge, with either induced magnetisation (78°W in the plane of the profile) or a more steeply dipping magnetic vector. This may be indicative of a remanent component of magnetisation related to the Cretaceous field direction (section 6.3.3). Fox et al. (1971) have reported the dredging from the southern Aves Ridge of basaltic rocks at least as old as 60 M.Y. (Maestrichtian) which they consider to represent intrusive bodies. The anomaly here considered is tentatively interpreted as a more northerly example of such intrusions, although the western ridges of the Aves Ridge, which may also be examples of these intrusive bodies, have a significantly lower intensity of magnetisation than the main part of the Ridge.

6.4.10 A magnetic anomaly in the Venezuela Basin

A magnetic anomaly (high P) of approximately circular configuration occurs in the Venezuela Basin centred on approximately 13°24'N, 64°15W. Relevant data are presented in fig. 6-23.

The absence of a distinctive gravity anomaly over this feature (fig.6-23b) made an estimate of the angle of magnetisation from pseudogravity anomalies impossible. Consequently the observed anomaly was compared with anomalies calculated for bodies with different magnetic inclinations, and an inclination of -10° in the direction of the earth's field (-43°W in the plane of the profile) for a body with negative magnetisation contrast was found to most closely resemble

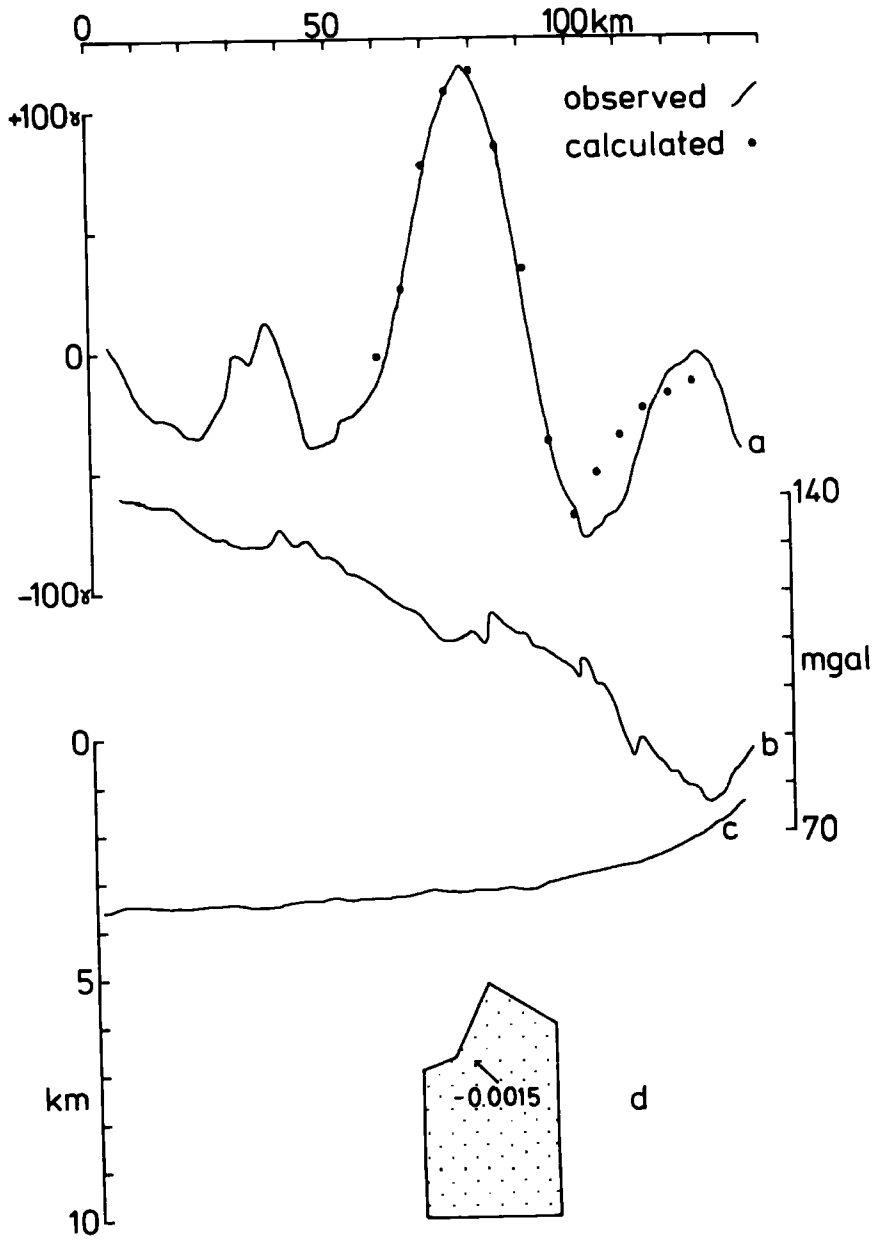
0
50
100km
observed
calculated
+100%
0
-100%
a
140
mgal
70
b
0
c
5
km
10
-0.0015
d

the observed anomaly.

The depth to the top of the causative body is not known with accuracy from either seismic reflection, refraction or spectral analysis of magnetic data. An estimate of 5 km. was made.

A non-linear optimisation routine was used for the interpretation, and the resulting model presented in fig. 6-23d. A magnetisation contrast of -0.006 emu/cc. in the direction of the earth's field (-0.0015 emu/cc. in the plane of the profile) was computed.

Ewing et al. (1965) have described basement domes in the Venezuela Basin from seismic reflection data which were interpreted as volcanic features. It is possible that this magnetic feature is a representative of these domes, although Durham reflection data over this area did not register basement. The ambiguity of the model presented must be stressed, however, as constraints on the body's parameters are lacking. The significance of the angle of magnetisation is unknown, but similar values have been recorded on the Aves Ridge and Lesser Antilles.

6.4.11 A magnetic profile across the island arc

Considered here is a profile at 13°24'N across the Lesser Antilles between the islands of St. Vincent and St. Lucia using results from the present survey for data to the west of the island arc, and data from another Durham survey of 1971 to the east. Relevant data are presented in fig. 6-24.

No direct correlation is apparent between the observed magnetic and Bouguer anomalies (fig. 6-24a and b). The positive gravity anomaly is considered to be due in the most part to shallow features, and so its correlation with pseudogravity anomalies valid. Pseudogravity anomalies for induced magnetisation and a magnetic inclination

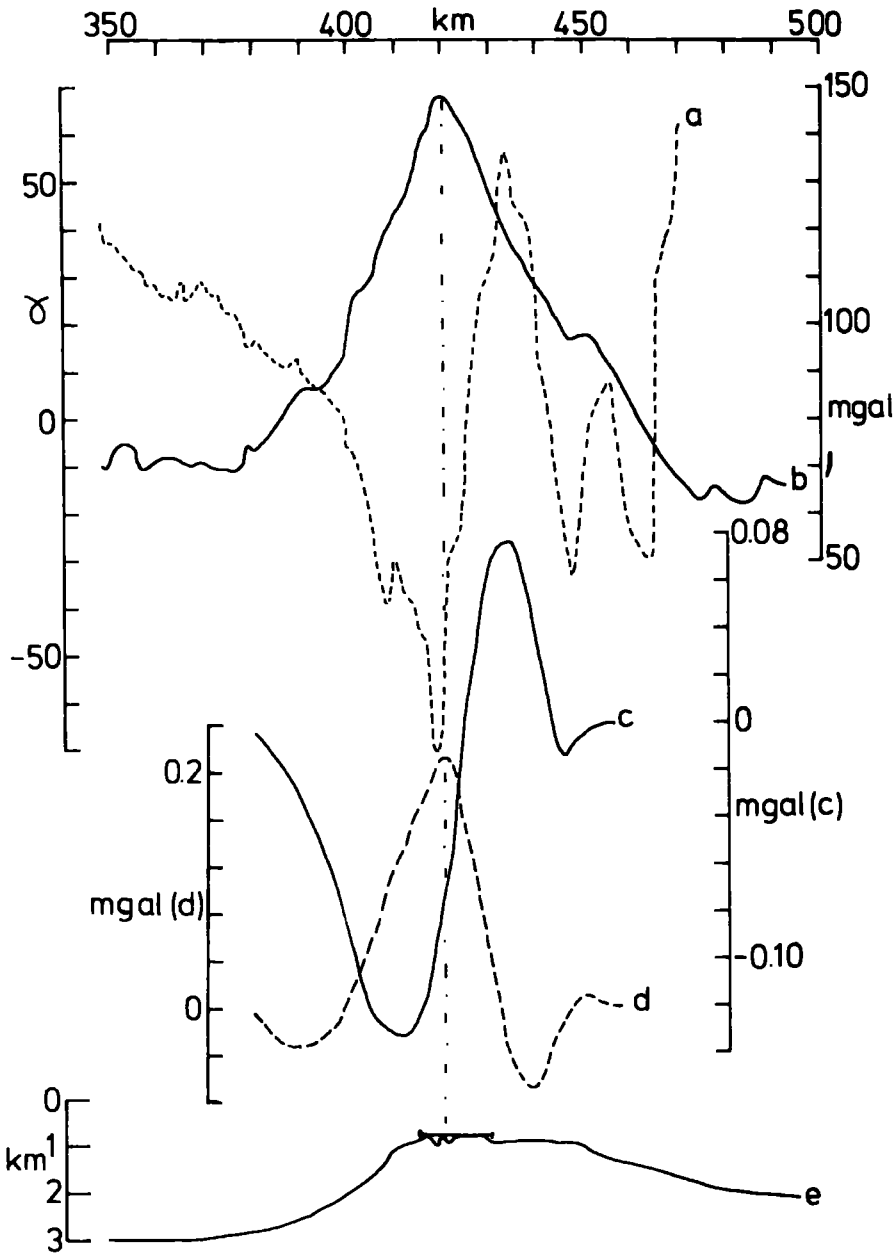
350
400
km
450
500
150
50
γ
0
100
mgal
-50
a
b
0.08
50
c
0.2
0
mgal (c)
mgal (d)
0
-0.10
d
0
km
1
2
3
e

of -10° in the direction of the present earth's field (-47°W in the direction of the profile) are presented in fig. 6-24 c and d. No correlation is apparent between the Bouguer anomalies and pseudogravity anomalies for induced magnetisation, but the main Bouguer anomaly peak correlates well with a pseudogravity peak for a magnetic inclination of -47°W. A minor peak on the eastern flank of the arc also shows positive correlation, although the situation on this flank is clearly more complicated than on the western flank. The amplitudes of Bouguer and pseudogravity anomalies indicate an intensity of magnetisation of 0.002 emu/cc. in the direction of the earth's field (0.0005 emu/cc. in the direction of the profile).

Although magnetograms from observatories at San Juan and Paramaribo registered quiet magnetic conditions for the time surveying the western part of the profile, spectral analysis of the magnetic data gave spuriously low depths to magnetic basement over the western flank of the arc. Magnetic readings contained high frequency components, and these low values may be due to local external effects or the absence of all representative frequencies in the measured anomaly. Data over the central part of the island arc, however, indicate the probable lack of non-magnetic cover in this area.

The first step in interpretation was the use of a matrix procedure using the above intensity and inclination of magnetisation. Although this procedure fitted the western part of the profile, the model was inadequate in fitting the eastern part. Examination of the residuals of this model indicates that this portion probably has a magnetic inclination in a reversed direction to the western part. Consequently a non-linear optimisation procedure was used, constraining the western part with the matrix optimisation body coordinates but allowing the body coordinates, angle and intensity of magnetisation of the eastern

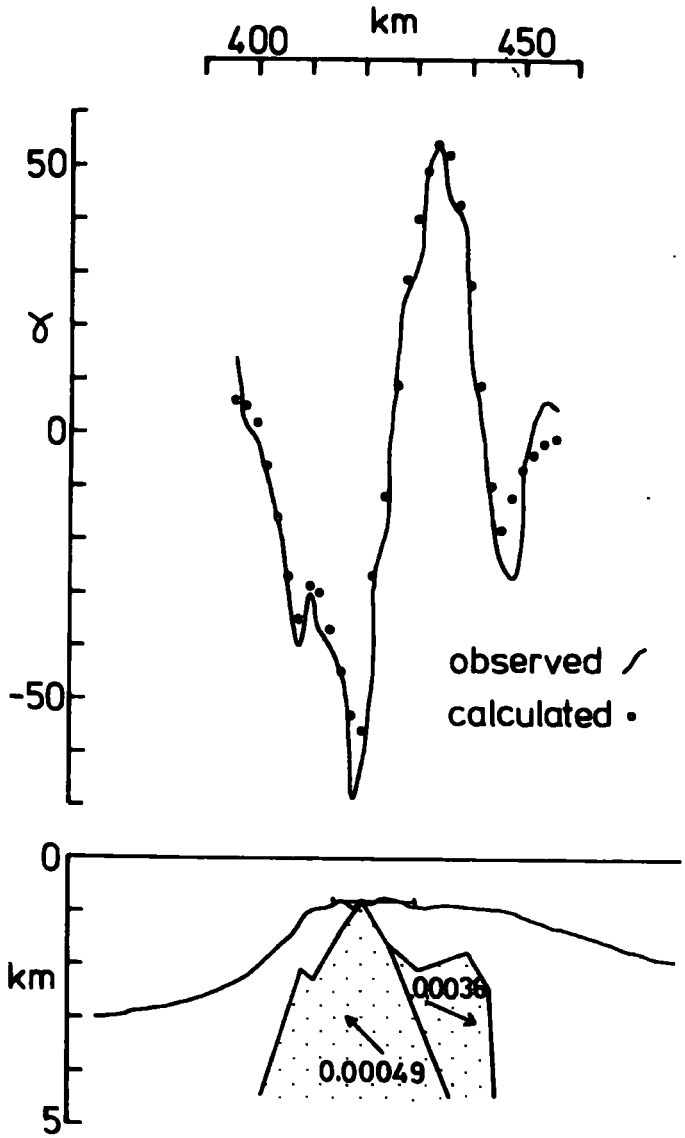


Figure 6-15

part to vary. The model produced is presented in fig.6-25. It was found that the intensities of magnetisation for both parts were similar (the mean being 0.0018 emu/cc. in the direction of the earth's field, 0.0005 emu/cc. in the plane of the profile) with the eastern part's magnetic vector almost exactly opposed to the western part. Examination of the Bouguer anomaly, and comparison with simple gravity interpretations (section 5.10.3) indicates the similarity of the causative body computed from both gravity and magnetic anomalies. The significance of the dip of the magnetisation vector is unknown,although similar values have been noted on the Aves Ridge (sections 6.4.4, 6.4.7, 6.4.8). Inclinations indicative of induced magnetisation have been recorded elsewhere over the Lesser Antilles (G.K. Westbrook,pers. comm.), and many of the samples from St. Vincent investigated by Khan (1968) exhibited induced magnetisation.

## 6.5 Conclusions on Magnetic studies

i) The Aves Ridge is characterised by strong magnetic-gravity correlations. This correlation is probably indicative of an igneous origin of the causative structures. Such strong correlations have been described from very few areas, a notable example being the Iceland-Faeroe Ridge (Bott & Ingles, 1972).

ii) The western part of the Aves Ridge usually exhibits a significantly lower intensity of magnetisation than the eastern part for the simple models considered. Gravity studies have also indicated that the western parts of the Aves Ridge are usually denser than the main parts of the Ridge, and it has been proposed (Chapter 5) that they represent bodies of basaltic or dioritic material intrusive into the volcanic and volcaniclastic deposits believed to comprise

the main part of the Aves Ridge.

iii) For the simple models proposed, three principal angles of magnetisation are indicated for the Aves Ridge.

a) Induced by the present earth's field with the possibility of a small remanent component of Cretaceous age.

b) In a direction opposed to the present earth's field. It seems unlikely a structure of probable Cretaceous age would have magnetisation reversed with respect to the present earth's field. The significance of this inclination is unknown.

c) An inclination of 0°W to -10°W in the direction of the earth's field. The significance of this inclination is unknown.

The two-dimensional approach gives no information on the true azimuth of these vectors.

iv) The isolation of the anomalies attributed to the Venezuela Basin and Grenada Trough is arbitrary, and the suggested angles and intensities of magnetisation by no means unambiguous. The Venezuela Basin anomalies may be explained by an induced model. The northern-most profile considered over the Grenada Trough exhibits a steeply westwards dipping magnetic vector, possibly related to the Cretaceous magnetic field direction, while more southerly profiles indicate a steeply upward inclined vector. It seems very unlikely that this is related to a reversed direction of the present earth's field and its significance is unknown, although similar inclinations have been proposed for the Aves Ridge.

v) A magnetic anomaly in the Venezuela Basin may be related to

the volcanic domes described by Ewing et al. (1965).

vi) A magnetic profile across the island arc indicates that its intensity of magnetisation, resolved east-west, is smaller than encountered over the Aves Ridge. Its opposed magnetic inclinations would seem to be related to the inclination (b) encountered on some profiles over the Aves Ridge.

# CHAPTER 7

# EVOLUTION OF THE CARIBBEAN WITH PARTICULAR REFERENCE TO THE EASTERN CARIBBEAN

## 7.1 The formation of the Caribbean within the framework of the Atlantic opening

The hypothesis that large, rigid portions of the earth's lithosphere are in relative motions with their margins interacting constructively at mid-ocean ridges, destructively at ocean trenches or non-destructively at transform faults is now generally accepted by earth scientists. The geometrical implications of this concept of plate tectonics have provided a basis for the reconstruction of past plate configurations with geological data from juxtaposed margins providing an important control. The origin and history of the Caribbean plate are intimately associated with the sequence of events occurring after the rifting of a supercontinent comprising Europe, Africa and the Americas.

Early theories for the origin of the Caribbean (North, 1965, Hamilton, 1965) relating the Caribbean margins to the deformation of a structure bridging North and South America are clearly inconsistent with pre-drift reconstructions, while Wilson's (1966) proposal of origin by superposition of Pacific and Atlantic plates is considered rather unlikely.

An early reconstruction of the continents bordering the Atlantic was presented by Bullard et al. (1965) and is reproduced in fig. 7-1. Although based purely on geometrical data, only minor modifications of the model have been proposed to render it compatible with geological

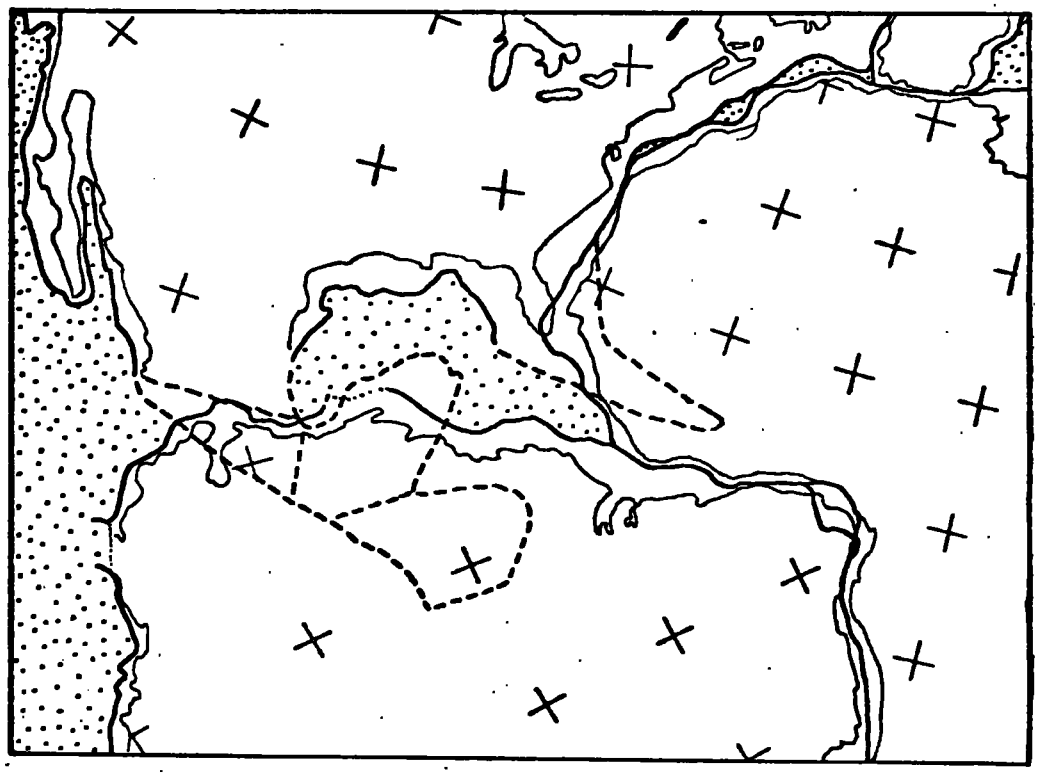

Figure 7-1 : The Bullard continental fit. Dashed lines refer to areas of cratonic overlap.(from Freeland & Dietz,1971)

data, and it is generally accepted to represent the configuration of continents during the late Triassic (200 m.y.BP). Important consequences of the model are the overlap of the Palaeozoic cratons of Central America onto South America and the overlap of the Bahama platform onto Africa. The latter is of lesser importance since Dietz et al. (1970) claim a possible post-drift origin for the Bahama platform, while Freeland & Dietz (1971) also suggest that it may have been somewhat more westerly situated in the pre-drift configuration. The role of Central America is critical, and will be shown to apply constraints on the possible origins of the Caribbean. The possibilities are that Central America was originally in the form of a set of discrete blocks within the area now occupied by the Gulf of Mexico, or that it was situated along the western coast of North America and rotated in an anticlockwise sense to attain its present day position somewhat after the motion of Spain during the opening of the Bay of Biscay. The former possibility seems to have been more widely accepted (Freeland & Dietz, 1971, Malfait & Dinkelman, 1972).

Several reconstructions have been made of the sequence of events leading to the present day continental configuration (Le Pichon, 1968, Funnel & Smith, 1968, Ball et al. 1969, Freeland & Dietz, 1971, Le Pichon & Fox, 1971, Le Pichon & Hayes, 1971, Malfait & Dinkelman, 1972, Phillips & Forsyth, 1972). The reconstructions have been progressively modified as more data have become available to constrain the sequence of events. It has been generally recognised that for the earliest phases of motion the poles of rotation of North America-Europe and South America-Africa were significantly different.

Consequently the Caribbean was recognised as a zone of north-south extension and shear caused by the differential relative movements of North and South America which are a consequence of this (Funnel & Smith, 1968, Ball et al. 1969). Such reconstructions are no longer strictly valid since they predate the JOIDES investigations which disproved the simultaneous rifting of North and South America (Ewing et al., 1970, Maxwell et al., 1970).

Recent reconstructions by Le Pichon & Hayes (1971) and Le Pichon & Fox (1971) propose that changes in the pole of rotation of a continental separation will occur when the original mechanical constraints of the continental blocks are relaxed and the weaker oceanic crust permits the change. JOIDES investigations had shown that the North Atlantic opening began 180 m.y.BP and the South Atlantic somewhat later at 140 m.y.BP. Three phases in the Atlantic opening were thus proposed:-

i) The initial opening of the North Atlantic at 180 m.y.BP
ii) Opening of the South Atlantic about a significantly different pole 140 m.y.BP.
iii) Readjustment of these poles to a single pole for the whole system at 80 m.y.BP which was sufficiently far from the region that opening proceeded at a similar speed along the entire length of the Atlantic.

Freeland & Dietz (1971) have concluded that the Caribbean is a subplate attached at the present day to South America. The cratonic blocks now forming Yucatan and Nicaragua were considered to have rotated out of the Gulf of Mexico while the southern Mexico craton was considered to have been originally situated to the west of northern

Mexico. The proposed origin of the Greater Antilles was from a sialic spur developed off Nicaragua after the uplift of Central America.

Malfait & Dinkelman (1972) have proposed that the Caribbean plate was originally part of the East Pacific plate from which it decoupled at the start of the Oligocene. Central America as far south as Yucatan was assumed to have rotated in a clockwise sense out of the Gulf of Mexico with the more southerly parts being formed by transference of crust from the Caribbean to the North American plate as well as by volcanism induced by the underthrusting at the Middle America Trench in post-Palaeocene times. A criticism of the model is that no pre-Upper Cretaceous history is given and the entry of the East Pacific plate would seem to require a rather greater separation between North and South America than has hitherto been proposed.

Phillips & Forsyth (1972) have correlated continental movements with palaeomagnetic data and computed a polar wandering curve for the whole Atlantic region. They have proposed a smooth migration of this system northwards relative to the earth's spin axis.

MacDonald & Opdyke (1972), from a study of palaeomagnetic data from circum-Caribbean sites of Cretaceous age, have concluded that the Greater Antilles and Guajira Peninsula of Colombia have moved northwards 10° since the Cretaceous. Their proposed reconstruction for the Cretaceous in which the Greater Antilles and Guajira Peninsula were located along the northwestern coast of South America must not be considered unambiguous as palaeomagnetic data give no control of relative longitude.

The critical factors in the genesis and history of the Caribbean

would thus seem to be:-

i) The time at which the gap between North and South America opened to its present extent.

ii) The behaviour of Central America during this opening.

iii) The reported age of the Caribbean crust from JOIDES investigations.

iv) The nature of the crust under the Gulf of Mexico and Caribbean Sea.

v) The time of initiation and location of underthrusting at the eastern margin of the Caribbean.

vi) The nature of the Caribbean sediments.

If it is accepted that the cratonic blocks of Central America rotated out of the Gulf of Mexico, no oceanic area is predicted for the pre-drift reconstruction of the circum-Atlantic continents for the late Triassic (200 m.y.BP). The initiation of drift at 180 m.y.BP resulted in the clockwise rotation of the Central American cratons and the opening, by about 160 m.y.BP, of a mediterranean the size of the present Gulf of Mexico (Freeland & Dietz, 1971, Le Pichon & Fox, 1971). Le Pichon & Fox (1971) have indicated that this is the probable age of the thick evaporite deposits of the Gulf of Mexico and correlates well with sedimentation in an enclosed basin at the equatorial palaeolatitudes predicted for the area by Phillips & Forsyth (1972). The mode of crustal formation at this time is uncertain. Ewing et al. (1971) have described normal oceanic crust under an extremely thick sedimentary sequence in the Gulf of Mexico, and Edgar et al. (1971a) have described normal oceanic crust under the Yucatan Basin, which may also have been open at this time.

However, no spreading centre has been described in the Gulf of Mexico, and if this absence is not merely due to inadequate investigation, either some atypical method of crustal formation is involved or the Gulf of Mexico and Nicaragua Basin represent ancient oceanic crust, implying a different pre-drift configuration for Central America. The lack of magnetic lineations would be explained either by loss of magnetisation if the crust were ancient, or by crustal formation during the magnetic quiet time (Heirtzler & Hayes, 1967) which ended 160 m.y.BP.

Further differential movement widened the gap between North and South America and would have permitted further rotation of Central America. Le Pichon & Fox (1971) consider that by the late Jurassic (140 m.y.BP), the Caribbean had opened to its present extent and that Central America had attained its present position with respect to North America (Freeland & Dietz, 1971). The rotation of Central America during this period 160-140 m.y.BP would seem to preclude the entry of the Caribbean plate from the Pacific as the isthmus between North and South America would have been effectively blocked.

The initiation of the opening of the South Atlantic at 140 m.y.BP initiated a new régime whereby the margins of the Caribbean were subjected to a series of tectonic events while its central areas remained essentially stable (MacGillavry, 1970), although the gentle crustal doming noted by Edgar et al. (1971a) may be a response of these central areas to compressive stresses. It is generally accepted that during most of the Caenozoic both the North and South American plates were opening about the same pole of rotation which was situated sufficiently far away from the region that the rate of opening was similar along its length. Geological evidence (Metz, 1968)

indicates that the shearing motion along the southern margin of the Caribbean accompanying the relative movements of North and South America ceased in the upper Cretaceous so that the Caribbean plate is locked onto the South American plate at the present day. This locking corresponds approximately to the third phase in Atlantic opening proposed by Le Pichon & Fox (1971) and has been related by Freeland & Dietz (1971) to closure of the Caribbean after it had opened to wider than its present extent.

Edgar et al. (1971a) have proposed that the uniformity of the sediments on the Caribbean plate argues for tranquil conditions during their deposition in an enclosed basin that had been protected from open-ocean circulation probably since the Cretaceous. They also indicate that the absence of any record in the sediments of the tectonic events of the Caribbean margins may be due to the effectiveness of sediment traps associated with the margins.

The model thus proposed for the origin of the Caribbean indicates that the region was opened between 160 and 140 m.y.BP before the initiation of rifting in the South Atlantic. The mode of crustal formation at this time is uncertain. The motions proposed for Central America and the Greater Antilles during this period would require an extremely complicated configuration of spreading centres if crustal generation and movements were by processes similar to those occurring at the present day at mid-ocean ridges. Indeed, no spreading centres have been identified in the Caribbean and the anomalous nature of the crust may be related to some form of crustal genesis unrelated to the processes occurring at mid-ocean ridges. However a similar crustal structure has been reported from the northwest Pacific Ocean by Den et al.(1969),and Mattson (1969) has

suggested that the Caribbean plate originated in the western Pacific. The previous discussion on the motions of Central America would seem to discount this hypothesis. Another possibility is that the Caribbean represents a fragment of Atlantic crust trapped between North and South America and isolated from the main body of the Atlantic by initiation of underthrusting at the eastern margin. This would imply some form of modification of the normal oceanic crust during its later history.

The age of the initiation of underthrusting at the eastern margin of the Caribbean is unknown. The Lesser Antilles were usually considered to have a history of volcanism from the Eocene onwards (MacGillavry, 1970). However, the recent discovery of a late Jurassic suite of volcanic rocks on Désirade by Fink et al. (1971) has lead him to propose that the island arc has been in existence since this time. It has been generally proposed that the Aves Ridge represents the surface manifestation of a previous site of underthrusting (i.e. it is an ancient island arc) which was assumed to have stepped back to its present day position during the Lower Eocene. This will be discussed in section 7.4.

Severe criticisms of the proposal that the Caribbean formed between 160 and 140 m.y.BP are the reported ages of the oldest sediments encountered during leg 15 of the JOIDES investigations (Purrett, 1971). The ages were between 75 and 80 m.y.BP (upper Cretaceous), and cannot be reconciled with the model described above. It is possible that these sediment ages are not representative of the oldest members of the Caribbean crust, and confirmation by potassium-argon dating of the basalt encountered in several of the sites would be highly desirable. Certainly no reconstruction of past plate movements has been proposed

by which the Caribbean crust could have such a young age. The Jurassic rocks described from Désirade by Fink et al. (1971) may indicate that the Caribbean plate is somewhat more ancient than JOIDES' data suggest.

## 7.2 Comparison of the Eastern Caribbean with other Island Arc Areas

The occurrence of basin and ridge structures behind volcanic island arcs is not uncommon, and the mode of origin of the marginal basins in particular has long been the subject of controversy. The spatial relationships of these features with the island arcs would seem to imply a common genetic relationship between their causative forces. It is only relatively recently that detailed geophysical surveys have been performed over these areas behind island arcs and new theories for their origin formulated. It was suggested in the previous section that the Caribbean is a relatively ancient plate, and so comparison with similar younger systems should prove instructive in understanding its history.

Other ridge and basin structures behind island arcs which may be similar to the units of the eastern Caribbean are: the Bowers Ridge and Basin behind the Aleutian island arc (Ludwig et al., 1971a, 1971b, Kienle, 1971), the Lau-Colville Ridge and Lau-Havre Basin behind the Tonga-Kermadec arc (Karig, 1970), ridge and basin structures of the Andaman Sea (Weeks et al., 1967), the Lucipara Islands and associated basin behind one of the Indonesian island arcs (Vening Meinesz, 1951) and the West Mariana Ridge and Mariana Trough behind the Marianas arc (Vening Meinesz, 1951, Karig 1971a). Karig (1971b) has presented data on, and classified, the marginal basins of the western Pacific. A more detailed comparison of the first two systems

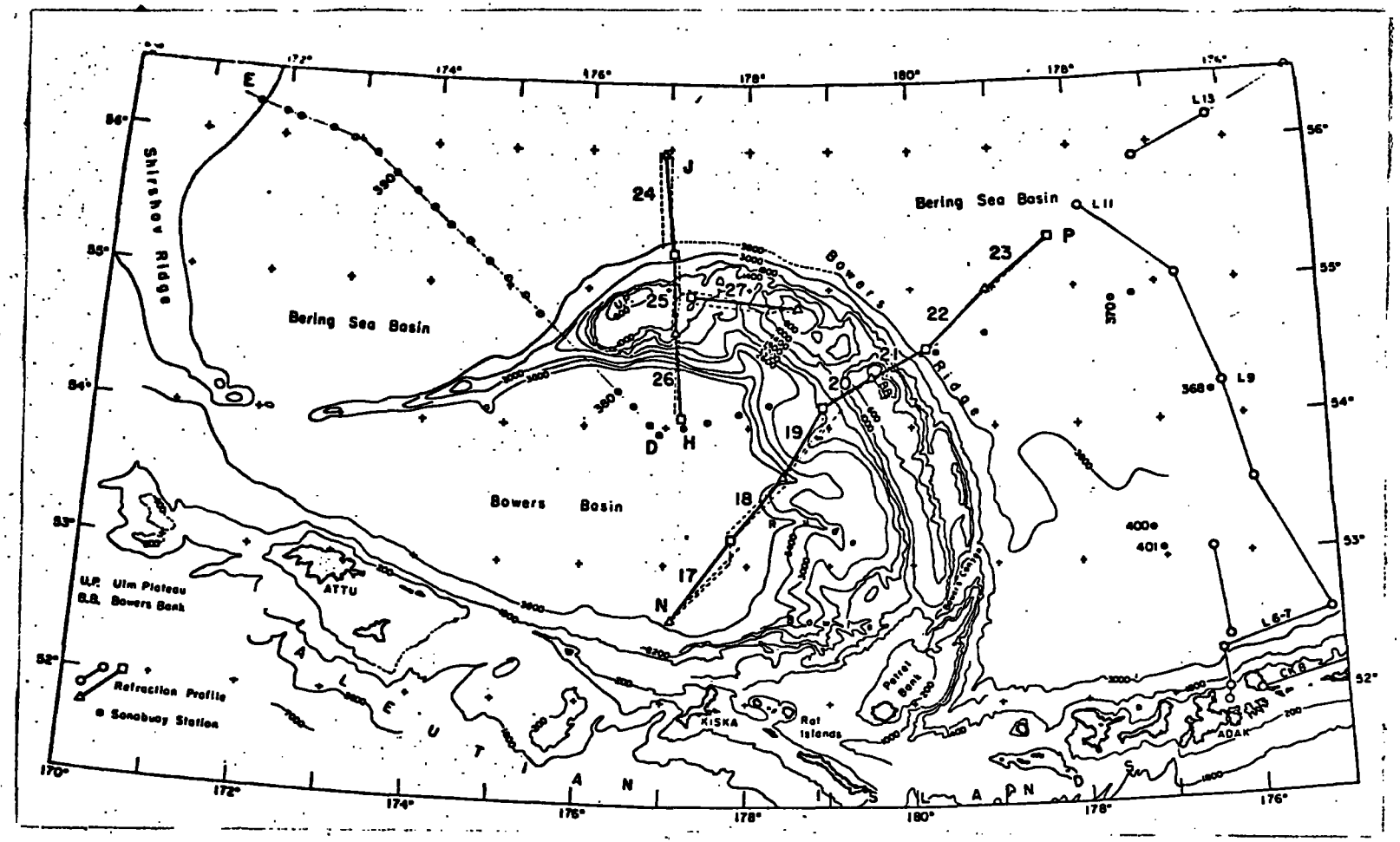


Figure 7-2 : Bathymetry of the region behind the Aleutian Islands.
(from Ludwig et al.,1971b)

with the eastern Caribbean follows.

The Bowers Ridge is a totally submerged bathymetric prominence extending from the Aleutian Islands anticlockwise into the Bering Sea (fig. 7-2) and separates the Bowers Basin from the main body of the Bering Sea. The seismic structure of the area has been studied by Ludwig et al. (1971a, 1971b), and the seismicity, gravity and magnetic anomalies by Kienle (1971).

Although the Bowers Ridge trends at a distinct angle to the Aleutian volcanic arc, tentative correlations may be made between: Bering Sea-Venezuela Basin, Bowers Ridge-Aves Ridge, Bowers Basin-Grenada Trough and Aleutian Islands-Lesser Antilles. Data supporting such correlations are:

i) Zero free air anomalies in the Bering Sea indicating its approximate isostatic equilibrium.

ii) Positive free air anomalies over the Bowers Ridge, although their amplitude (200 mgal.) is higher than recorded over the Aves Ridge.

iii) Negative free air anomalies over the Bowers Basin of approximately -30 mgal.

iv) The presence of a sediment filled trench on the Pacific side of the Aleutian Islands marked by strongly negative free air anomalies.

v) Short wavelength, high amplitude magnetic anomalies over the Bowers Ridge and long wavelength, low amplitude magnetic anomalies over the flanking basins.

vi) Strong magnetic-gravity correlations over the Bowers Ridge. This is evident in the gravity and magnetic profiles presented by Kienle (1971) but not noted by him.

vii) The seismic inactivity of the whole region behind the Aleutian Islands.

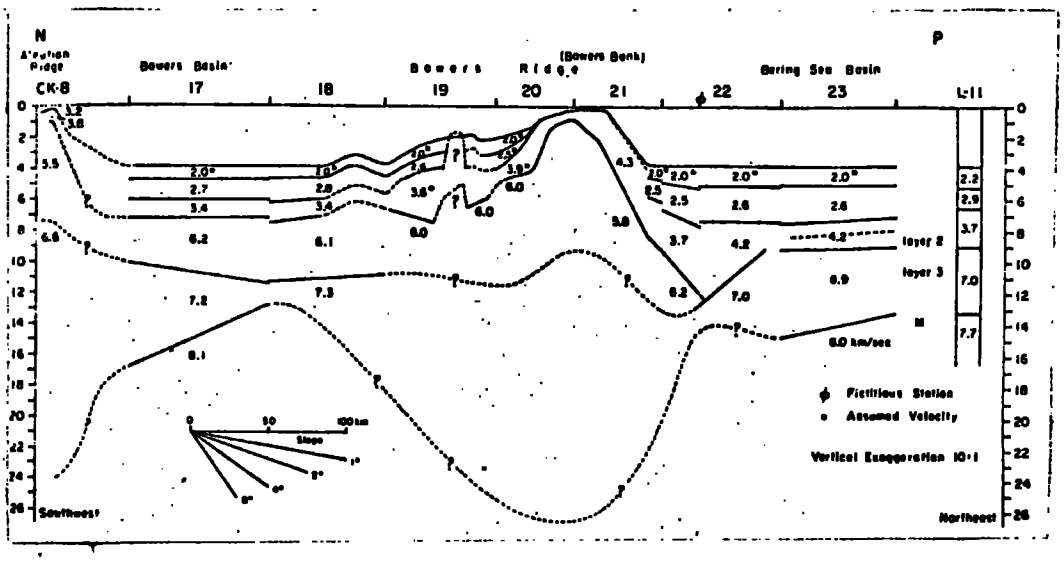


Figure 7-3 : Crustal structure of Bowers Basin, Bowers Ridge and Bering Sea from seismic refraction. See fig. 7-2 for location of profile. (from Ludwig et al., 1971b)

viii) The presence of subaerial unconformities on the Bowers Ridge, although these are considered to be due to eustatic changes in sea level rather than tectonic movements.

ix) The Bowers Ridge is considered to be a volcanic ridge whose elevation is due to thickening of the underlying crustal layers. A similar situation is thought to attain for the Aves Ridge.

x) The crustal structure. The crust under the Bowers Ridge, Bowers Basin and possibly under the Aleutian Islands is very similar to a typical Caribbean section (fig. 7-3). A mantle with normal velocities is overlain by successive layers with velocities of 7.2, 6.2, 3.4, 2.7 and 2.0 km/sec., and it is the thickening of the 6.2 km/sec. layer which seems to be responsible for the major part of the Bowers Ridge. Edgar et al. (1971a) have concluded that the thickening of a layer of similar velocity forms the bulk of the Aves Ridge. Crustal thicknesses are of the same order as those computed in this thesis under the eastern Caribbean. In contrast the Bering Sea is underlain by normal oceanic crust and it has been considered to represent a relict of the North Pacific. This situation would seem to indicate some different form of crustal genesis for the ridge-basin system from that of normal oceanic crust, or modification of normal oceanic crust.

The north-south trending Tonga-Kermadec island arc of the west Pacific is flanked to the east by the underthrusting zone of the Tonga-Kermadec Trench. To the west the islands are flanked by the Lau-Havre Trough whose western boundary is marked by the Lau-Colville Ridge which culminates in the Lau Islands in the north. This system of ridges and basins can be traced southward into the north island of New Zealand, while to the west lies the broad South Fiji Basin (fig.7-4). A geophysical study of the region has been made by Karig (1970).

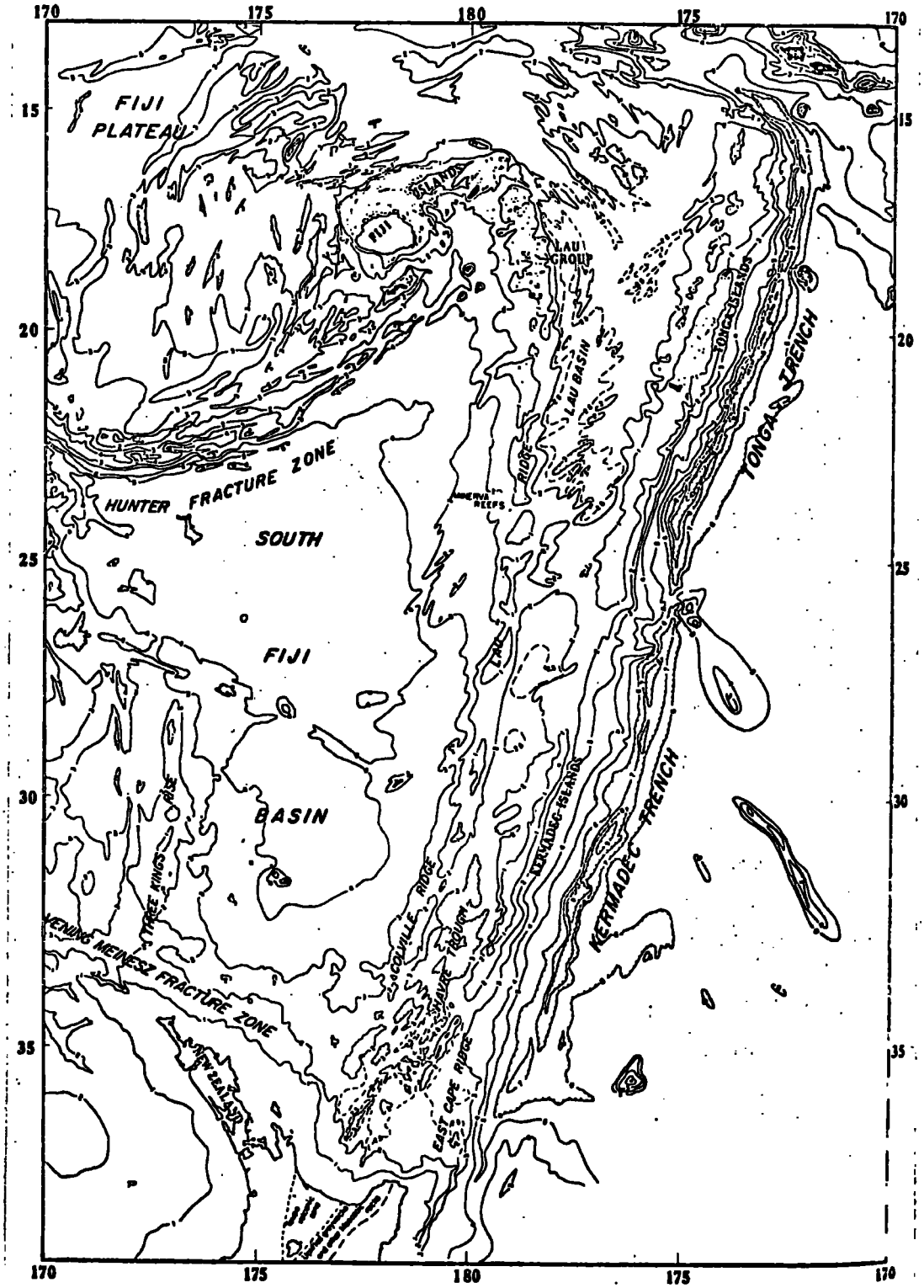


Figure 7-4 : Bathymetry of the region behind the Tonga-Kermadec Islands.(from Karig,1970)

Possible correlations with the eastern Caribbean are: South Fiji Basin-Venezuela Basin, Lau-Colville Ridge-Aves Ridge, Lau-Havre Basin-Grenada Trough and Tonga-Kermadec Islands-Lesser Antilles.

The Tonga-Kermadec Islands lie on a narrow elongate ridge composed of a western volcanic part and an eastern, more continuous part consisting of organic limestones and volcanic rocks. This ridge is considered to have been formed during the Tertiary. The lack of tectonic deformation of the trenchward sediments, uplift and normal faulting have been taken to indicate that the ridge is rising and rotating away from its associated trench. The Lesser Antilles also have an outer limestone arc and inner volcanic arc, while the presence of limestones at elevated positions and raised beaches around some of the volcanoes (Weyl, 1966) may be indicative of similar vertical movements.

The Lau-Havre Trough exhibits average depths of 2500m. Sediment thicknesses decrease towards the centre of the Trough in both westerly and easterly directions, and the basement contains a series of linear ridges which Karig (1970) has interpreted as a series of fault blocks. Comparison with the Grenada Trough is not directly possible as the latter contains a thick sediment infill, and structures beneath horizon B" are unknown.

The Lau-Colville Ridge is a broad, flat-topped feature reaching depths between 1000 and 2000 m., although there is no evidence for its truncation being due to sub-aerial erosion. The Lau Islands have a complicated history of uplift and depression, while it has been suggested that the whole Ridge has undergone subsidence. Geological evidence has suggested that the Aves Ridge has also had a complicated history of emergence and submergence.

Seismic refraction experiments have shown that the Lau-Havre Basin is underlain by a normal oceanic crust 7 km. thick, while the flanking ridges have a thickened crust 15 km. thick. There is no evidence of a 'Caribbean type' seismic layering.

On the basis of:

i) The asymmetry of the flanking ridges, which is mirrored across the centre of the Lau-Havre Basin,

ii) The thinning of sediment cover towards the centre of the Lau-Havre Basin,

iii) The tracing of similar structures into the north island of New Zealand,

Karig (1970) has suggested that the Lau-Havre Basin is a product of east-west crustal extension implying some form of crustal genesis different from that occurring at the present day at mid-ocean ridges, as no spreading centre has been identified in the Basin. Possible mechanisms of this process and its possible relation to the eastern Caribbean will be discussed in later sections.

Very few studies have been made of the magnetic anomalies of the basins behind island arcs. Karig (1971a) has presented a magnetic anomaly chart of the Parece Vela Basin behind the Mariana arc, and although he observes that the anomalies are lineated parallel to the topography, there is no evidence of the linear magnetic anomalies typical of major ocean basins. Hayes & Ringis (1973) have presented a geophysical study of the Tasman Sea, in which they recognise linear magnetic anomalies which are correlable with the world-wide sequence of Caenozoic anomalies recognized in major ocean basins. It would seem, however, that the Tasman Sea is not a representative of the back-arc basins considered here, if only because it is not associated with an island arc. Also, the Tasman Sea anomalies are centred round

an elevated ridge, a structure not occurring in the basins previously considered.

Barker (1970) has made a study of the Scotia arc, which is the only other representative of circum-Pacific island arcs to be found in the Atlantic. He has described a small spreading centre behind the island arc in approximately the same spatial position as the Aves Ridge behind the Lesser Antilles. This will be discussed in section 7.4.

## 7.3 Possible processes occurring in the upper mantle behind island arcs

Vening Meinesz (1951) has proposed that the structures behind island arcs are the products of secondary convection cells in the upper mantle. He considers that these convection currents were generated by thermal differences brought about by a concentration of sialic matter, with a higher radio-active content, beneath the island arc. Such cells were thought to evolve approximately 10-12 M.Y. after the formation of the island arc, reaching a maximum speed after a quarter of a revolution and stopping after a half revolution, rising beneath the island arc and descending beneath the position of the back-arc ridge. The consequences of this model are:

1) The formation of the back-arc basin by shrinkage after thermal cooling
2) elevation of the back-arc ridge by crustal compression caused by the convection cell
3) elevation of the island arc over the rising colomn of the convection cell.

The subsidence of the back-arc basins was considered to be of the order of 4 km., and elevation of the island arc by approximately 1 km.

This hypothesis was developed before the emergence of the theory of Plate Tectonics. In the light of this theory it may be suggested that such convection cells, if they exist, may owe their origin to thermal instability induced by a descending lithospheric plate. Holmes (1965) has also suggested the presence of second order convection cells behind island arcs.

Packham & Falvey (1971) have presented a summary of geophysical data on the basins behind island arcs in the western Pacific and review other theories ontheir origins. They conclude that the crust of these basins has been formed as the island arc migrates away from its associated continent by a process analagous to, but not the same as, that occurring at mid-ocean ridges, as such ridges have not been identified within the marginal basins. They propose that "the creation of oceanic crust took place along rifts, associated with olivine basalt extrusion, along or behind the andesite arc, producing a style ofasymmetrical sea-floor spreading". This process is considered to be associated with an upwelling of the mantle behind the island arc.

Karig (1971b) has made a study of the basins behind island arcs in the western Pacific and, as well as summarising the conclusions of other workers, has proposed that they owe their existence to crustal extension. He suggests a classification of these basins into those which are undergoing active extension and those in which extension is now inactive. The inactive basins are further subdivided into those with high and normal heat flow.

Karig's suggested mechanism for the formation of these basins is that the upper surface of the lithospheric plate descending beneath the island arc becomes heated by shear strain until a sufficient

temperature is attained for the mantle to overcome viscous resistance and rise buoyantly, this rising mantle diapir would progressively thin the lithospheric slab and its presence in the upper mantle would result in crustal extension and high heat flow at the surface. Conductive cooling would account for the high heat flow remaining after the cessation of surface tectonism. The extension of the crust behind the island arc is believed to be accompanied by the formation of new oceanic-type crust, and to be in a direction such that the island arc is moved away from its associated continent. A consequence of this movement is the change in gradient of the Benioff zone beneath the island arc revealed by the location of earthquake epicentres and such crustal movements would not seem to take place until the descending lithospheric slab has reached depths in excess of 350 km.

## 7.4 A discussion of the possible modes of origin of the Aves Ridge

It has been shown that the Aves Ridge is a linear feature striking parallel to the volcanic arc of the Lesser Antilles. Its formation is attributed to thickening of underlying crustal layers and geological sampling has shown that the Ridge is predominantly volcanic in origin. The Ridge has had a complicated history of elevation and submergence and at the present day is seismically inactive.

There would seem to be five principal possibilities for the formation of the Aves Ridge:

(i) A feature caused by thickening of the crust by compression.

(ii) An aseismic ridge of the Iceland-Faeroe type with an anomalous crust.

(iii) An ancient spreading centre (mid-ocean ridge).

(iv) The surface manifestation of an ancient Benioff zone, i.e. an ancient island arc.

(v) A feature split from the Lesser Antilles by extensional forces operating behind the island arc.

(i) This possibility is considered unlikely, there is no evidence of distortion of the sediments in the Grenada Trough or Venezuela Basin, nor do the sediments in the inter-ridge trough of the Aves Ridge indicate that they have been deformed. Consequently any compressive forces must have occurred before deposition of the oldest sediments which have a probable age of upper Cretaceous. Rocks thought to represent its basement dredged from the Aves Ridge also show no evidence of the distortion expected if compressive forces were associated with the formation of the Ridge. Consequently this possibility is discarded.

(ii) Aseismic ridges of the Iceland-Faeroe type are believed to be formed by the passage of the lithosphere over a 'hot-spot' in the upper mantle during sea floor spreading. The Iceland-Faeroe Ridge is one of the few such features to have been subjected to intensive surveying (Bott et al., 1971, Bott & Ingles, 1972). There are many similarities between the Aves Ridge and Iceland Faeroe Ridge. Both are submerged, broad, linear ridges, although the seamounts described from the Aves Ridge have no counterpart on the Iceland-Faeroe Ridge. Both are characterised by strong magnetic-gravity correlations which are indicative of an igneous origin of their causative structures. Both exhibit evidence of past emergence from subaerial erosional features. Both are composed of anomalous crust which differs from both normal oceanic and continental types. Both are underlain by thickened crust rather than by anomalous upper mantle.

However, the formation of the Iceland-Faeroe Ridge is believed to be due to passage of the lithosphere over a mantle 'hot spot' as it moved away from the mid-Atlantic ridge during ocean floor spreading, and consequently its movement would have been at right angles to the mid-ocean ridge. The Aves Ridge at the present day lies parallel to the mid-Atlantic ridge, and if it were to have formed by a process similar to the Iceland-Faeroe Ridge, the Caribbean Plate would have to have moved in a north-south direction. Although palaeomagnetic data (MacDonald & Opdyke, 1972, Phillips & Forsyth, 1972) have suggested minor north-south movements, the predominant direction of movement during the evolution of the area occupied by the Caribbean Plate was east-west. The geology of the Iceland-Faeroe Rise would seem to be closely allied to Iceland. Andesitic rocks form only a minor part of the geology of Iceland, and the significant occurrence of andesitic volcanic rocks on the Aves Ridge is further evidence that the Aves Ridge is not of the Iceland-Faeroe Ridge type.

(iii) The linearity of the Aves Ridge may be taken to indicate that it could represent an ancient mid-ocean ridge. Ben-Avraham et al. (1972) have described an extinct mid-ocean ridge in the Phillipine Sea. Barker (1970) has described a small spreading centre behind the Scotia arc, the only other representative of circum-Pacific type island arcs to be found in the Atlantic. This spreading centre is in approximately the same spatial position with respect to the island arc as the Aves Ridge is with respect to the Lesser Antilles. Here, however, resemblance ceases, as the structural units behind the ridge in the Scotia arc bear no resemblance to those behind the Aves Ridge. Mid-ocean ridges are believed to be composed of normal oceanic-type crust underlain by a mantle of anomalously low density (Talwani et al.,

1965). Removal of this low density support when the mid-ocean ridge becomes extinct should cause its subsidence to normal oceanic depths leaving a remanent structure of normal oceanic crustal thickness. The Aves Ridge has been shown to be underlain by a thickened crust. The absence of symmetrical magnetic anomalies flanking the Aves Ridge has already been commented upon. The presence of andesitic volcanics on the Aves Ridge is further evidence that it is not an ancient mid-ocean ridge.

The possibilities (i) to (iii) discussed above were only considered as they offer explanations of the space form of the Aves Ridge, namely an elevated linear feature. They are clearly incompatible with geological and geophysical data. The presence of andesitic volcanics and its spatial association with an active volcanic island arc suggest that the origin of the Aves Ridge is intimately associated with the forces responsible for the island arc. Consequently possibilities (iv) and (v) discussed below are considered the most likely.

(iv) Almost all previous reconstructions of Caribbean history have suggested that the Aves Ridge was the original site of underthrusting at the eastern margin of the Caribbean, which stepped back to its present day position in the lower Eocene, the proposed age of the oldest volcanic rocks of the Lesser Antilles. However, at the present day, the Aves Ridge and Barbados Ridge lie c.250 and 150 km. to the west and east of the Lesser Antilles. If the Aves Ridge were an ancient island arc, by analogy with the present day situation, the site of underthrusting would have been in a position at the present day occupied by the central Grenada Trough. A step-back

of underthursting would have the consequences:

a) A strip of Atlantic crust would have been incorporated on to the Caribbean Plate and would be located at the present day under the eastern Grenada Trough. There is no evidence of this crustal strip.

b) A pile of deformed sediments would be located under the central Grenada Trough representing the ancient equivalent of the Barbados Ridge. There is no evidence for such a structure.

c) Although the sediments of the western Grenada Trough would be relatively undeformed by the proposed ancient underthrusting, as the Tobago Trough sediments are at the present day, the majority of the sediments of the eastern Grenada Trough would be expected to be no older than lower Eocene. In fact, seismic reflection profiles indicate no discontinuity in the sediments from west to east, and the oldest sediments are considered to be at least of upper Cretaceous age.

These arguments only attain if the distance from the proposed ancient site of underthrusting to its associated island arc were the same, or less than, as at the present day. If the distance were greater, i.e. the angle of underthrusting smaller, and the proposed ancient underthrusting zone was located at the present position of the island arc, incorporation of the ancient equivalent of the Barbados Ridge into the new active arc would destroy its evidence. The whole Grenada Trough would then represent the ancient equivalent of the Tobago Trough. Consequently this possibility is not precluded.

(v) The presence of basins behind island arcs in the western Pacific and possible mechanisms for their formation have been described in the

previous sections. It is considered possible that the Grenada Trough might be of similar form and as such would represent an inactive basin with normal heat flow in the classification of Karig (1971b). If such an hypothesis is accepted, the Aves Ridge would represent an original portion of the Lesser Antilles which remained stationary as the present volcanic arc was translated eastwards to its present position by crustal extension which formed the Grenada Trough.

This model would explain the similarities of samples dredged from the Aves Ridge with the rocks of the Lesser Antilles without the possible objections raised by possibility (iv). The three inactive basins with normal heat flow in the western Pacific described by Karig (1971b) are all of Tertiary age, implying that the forces responsible for their formation were of relatively short duration. Consequently there would seem to be sufficient time during the late Jurassic and early Cretaceous for the separation of the Lesser Antilles from the Aves Ridge and the formation of the Grenada Trough as a stable unit before the deposition of the oldest sediments which are of probable upper Cretaceous age. The Grenada Trough would thus have been effectively sheltered from open ocean circulation since the upper Cretaceous, a condition suggested by Edgar et al. (1971a) to explain the uniformity of sedimentation within the Caribbean basins.

A criticism of this possibility is that the curvature of the Aves Ridge is considerably less than that of the Lesser Antilles, and the edges of the two would not match if the Grenada Trough were closed. The curvature of an island arc is probably a function both of the inclination and speed of underthrusting. It is possible that these two factors were different during the early history of the island arc, and that the present arc did not attain its present day curvature until

after separation from the Aves Ridge. Indeed the separation itself may have caused modification of the dip of underthrusting (Karig, 1971b), and at the present day the curvature of the Lesser Antilles island arc is one of the greatest found on earth (Bowin, 1967).

The Moho has been shown to lie at a relatively shallow depth beneath the Grenada Trough. It is possible that this elevation may be related to crustal extension in the Grenada Trough. Bowin (1968) has proposed that elevation of the Moho under the Cayman Trough may be attributed to its rising to fill a gap created between the Caribbean and North American plates by a component of north-south extension.

The Lesser Antilles at the present day exhibit positive isostatic anomalies. The islands exhibit no evidence of subsidence and it was suggested (section 5.8) that the maintenance of elevation is due to some mechanism related to the descending lithospheric plate. The removal of this mechanism as the Lesser Antilles separated from the Aves Ridge could explain the tectonic subsidence of the Aves Ridge as it sank to attain isostatic equilibrium, although explanation of the more complex movements is still not apparent. However this situation would also attain if removal of support were due to the step-back of underthrusting discussed as possibility (iv).

Extensional forces were considered a possible mechanism for the formation of a structure in the sediment basement interface on the Aves Ridge (section 5.10.1). Such extensional forces may be a consequence of the model proposed, and, if sediment reflectors in this structure have been dated correctly, would be of pre-upper Cretaceous age.

The Aves Ridge is a significantly wider structure than the Lesser

Antilles, and has been shown to be formed of two sets of ridges on its west and east flanks. It has been proposed (section 5.10.2) that the western ridges may represent bodies of diorite or basalt intrusive into the main body of the Aves Ridge, and geological sampling of basalts from the southern Aves Ridge by Fox et al. (1971) indicates a Paleocene age for these samples. It is possible that the Aves Ridge was widened after its proposed separation from the Lesser Antilles by the intrusion of these bodies which may have been facilitated by the east-west extension discussed above.

A criticism of the extensional origin of the Grenada Trough is that the Lesser Antilles are assumed to have been in existence since the late Jurassic or early Cretaceous. Dating of volcanic deposits from the present active arc indicate ages not older than the Eocene. However, the Jurassic suite of rocks described from Désirade by Fink et al. (1971) may be evidence for a much older substructure which is exposed only infrequently.

## 7.5 Conclusions

The Caribbean plate has been in existence at least since the upper Jurassic (140 m.y.BP) and fills the gap created by the differential north-south separation of North and South America during the first phase of the opening of the Atlantic Ocean when South America was still fixed to Africa. It is considered unlikely that the Caribbean plate was originally located in the Pacific.

The structural units of the eastern Caribbean show many similarities with the units occurring behind other island arcs.

The Aves Ridge has been shown to be a linear feature striking parallel to the island arc of the Lesser Antilles. Its typical form

is of two flanking basement ridges enclosing a small sediment filled trough and it is the site of strong magnetic-gravity correlations indicative of an igneous origin for the causative structures. It is underlain by a thickened crust. These data and geological sampling suggest that the origin of the Aves Ridge is related to those processes responsible for the formation of volcanic island arcs. The two modes of origin of the Aves Ridge considered most likely are:

a) An ancient island arc , with the Grenada Trough forming the spatial equivalent of the Tobago Trough at the present day during Cretaceous to Eocene times.

b) A portion of the original Lesser Antilles remaining stationary as the Lesser Antilles moved eastwards during the lower Cretaceous with the Grenada Trough being formed by crustal extension during this time.

# APPENDIX 1

## COMPUTER PROGRAMS

All programs presented in this appendix were written in FORTRAN IV for use with the Northumbrian Universities Multiple Access Computer (NUMAC), an IBM 360/67.

The two subroutines FCN are for use with the optimisation routine MINUIT (James & Roos, 1969) and compute the function to be minimised during optimisation. This function is defined as the sum of the squares of the differences between observed and computed anomalies. A full description of MINUIT and instructions for its use are given in CERN (1970), but a brief description of the control data follows:

Card 1 : the logical devices used for input and output (Format 2I2).

Card 2 : the title of the optimisation run in BCD characters.

Card 3 onwards

: Parameter cards, one per variable, containing the parameter number, its BCD name, its starting value, its step size and its lower and upper bounds (Format I10, 10 BCD characters, 4F10.0). Reading of parameter cards ceases when a blank card is encountered.

Data read by FCN follow the blank card.

The MINUIT command cards follow the last data card, and control the course of the optimisation procedure. A full list of the available commands is given in CERN (1970), but those most frequently used were:

PRINTOUT - it is advisable to select a high level of printout to follow the course of the optimisation process in the event of the program's not reaching completion due to lack of execution time.

CALL FCN - in the subroutines listed, a call to FCN with the argument IFLAG equal to 3 causes a printout of output data with a graphical representation of observed and calculated anomalies, while a call with IFLAG equal to 7 suppresses the graph. It is advisable to use this command several times during the optimisation rather than simply at the end, as the success of the optimisation is more easily judged from a study of the computed residuals than from a simple study of the function being minimised.

TAUROS - the command for a Rosenbrock optimisation. For simple bodies the number of calls required may be as few as 30, while several hundred calls may be required for the optimisation of complex bodies.

FIX - this command enables variable parameters to be fixed during the adjustment of other variables. Optimisation times are improved if as many variables as possible are fixed for the first stage of optimisation, for example, if both the x and z co-ordinates of body points are to vary, the x-co-ordinates may be fixed for the first stage of optimisation.

RESTORE - restores fixed parameters to variable status.

EXIT - terminates the optimisation.

The arguments of the user subroutine are FCN (NPAR, G, F, W, IFLAG):

NPAR - the number of variable parameters.

G - a vector array storing the derivatives of F (not used in the subroutines presented).

F - the function to be minimised, computed by FCN.

W - a vector array containing the current values of the variable parameters.

IFLAG - a marker controlling input, output or computation of F within FCN.

NPAR, W and IFLAG must not be changed by FCN, and are passed to the subroutine by MINUIT.

SUBROUTINE FCN (gravity version)

This subroutine computes the sum of the squares of the residuals between an observed and computed gravity anomaly. This value is returned to MINUIT as the variable F. FCN calls subroutines GRAV and OPLOT (see later).

The data items read by FCN from logical device 5 are:

Item 1 : TITLE, the name of the model (format 80A1).

Item 2 : NSTA, the number of observation points (format I5).

Item 3 : P, AOBS, the positions (km.) and gravity anomalies (mgal.) at each observation point (format 4 (2F10.0)).

Item 4 : REG, the regional background anomaly (mgal.) (format F10.0).

Item 5 : IWT (format I5). If IWT is set to zero, all data points are given equal weight; if set to any other integer a set of NSTA weighting values (WT) are read in format 8F10.0 corresponding to each datum point. The maximum value of the weighting function should be approximately equal to the maximum expected residual.

In the section of FCN in which constant parameters are defined, the value of NBP1 and constant members of the arrays X, Z & RO must be set (see description of subroutine GRAV).

In the section of FCN in which variable parameters are defined, all variable members of the arrays X, Z & RO must be set equal to the corresponding member of array W. If necessary REG may also be assigned variable status.

An example of a complete data block and FCN structure for a gravity optimisation run is given for a closed, triangular shaped body whose density is fixed at 0.5 gm/cc. and whose third body point is fixed, with other body coordinates allowed to vary.

Output of data onto logical devices 6 and 1 (graph) is self-explanatory.

```
      SUBROUTINE FCN(NPAR,G,F,W,IFLAG)
C*****************************************************************
C
C     SUBROUTINE FOR USE WITH THE MINIMISATION ROUTINE MINUIT.
C     THE LEAST SQUARE FIT OF A CALCULATED GRAVITY ANOMALY
C     WITH AN OBSERVED ANOMALY IS COMPUTED FOR A TWO DIMENSIONAL
C     BODY DEFINED BY VARIABLE AND CONSTANT PARAMETERS.
C     THE SUBROUTINE CALLS SUBROUTINES GRAV & OPLOT
C                              P.KEAREY,1973
C                              ------------
C*****************************************************************
      DIMENSION G(NPAR),W(NPAR),X(200),Z(200),RO(200),P(500),AOBS(500),
     1          ACAL(500),RESID(500),WT(500),TITLE(80)
    1 FORMAT(80A1)
    2 FORMAT(I5)
    3 FORMAT(8F10.0)
    4 FORMAT(1H1,80A1///10X, 'POSITION(KM)    OBSERVED ANOMALY(MGAL)
     1WEIGHT'/)
    5 FORMAT(1H ,I5,F14.3,F19.2,F17.0)
    6 FORMAT(//10X,'REGIONAL GRAVITY=',F7.2,' MGAL')
    7 FORMAT(1H1,4X, 'POSITION    OBSERVED    CALCULATED    RESIDUAL
     1WEIGHT'/)
    8 FORMAT(1H ,I3,F9.3,F10.2,F14.2,F13.2,F9.0)
    9 FORMAT(//9X,'ROOT MEAN SQUARE RESIDUAL=',F7.2,' MGAL'//
     1          9X,'REGIONAL GRAVITY=',F6.1,' MGAL'/////
     2          10X,'X',10X,'Z',8X,'RHO'/)
   11 FORMAT(1H ,I4,F9.3,F10.3,F10.2)
      IF (IFLAG.NE.1) GO TO 1000
C*****************************************************************
C
C  INPUT SECTION
C
      READ(5,1) TITLE
      READ(5,2) NSTA
      READ(5,3) (P(I),AOBS(I),I=1,NSTA)
      WRITE(6,4) TITLE
      READ(5,3) REG
      READ(5,2) IWT
      IF (IWT.NE.0) READ(5,3) (WT(I),I=1,NSTA)
      IF (IWT.EQ.0) GO TO 20
      GO TO 30
```

```
   20 DO 40 I=1,NSTA
   40 WT(I)=1.
   30 CONTINUE
      DO 10 I=1,NSTA
      AOBS(I)=AOBS(I)-REG
   10 WRITE(6,5) I,P(I),AOBS(I),WT(I)
      WRITE(6,6) REG
C*************************************************************************
C
C SET CONSTANT PARAMETERS
C      IN THIS SECTION THE VALUE OF NBP1 MUST BE SET,AND ALSO
C      ANY CONSTANT X OR Z VALUES. THE ARRAY RO MAY BE SET AT
C      THIS STAGE IF AN ARRAY OF CONSTANTS
C
C*************************************************************************
      NBP1=4
      X(3)=180.
      Z(3)=1.
      DO 100 I=1,NBP1
  100 RO(I)=0.5
C*************************************************************************
 1000 CONTINUE
C*************************************************************************
C
C SET VARIABLE PARAMETERS
C      IN THIS SECTION THE VARIABLE PARAMETERS ARE SET EQUAL
C      TO THE ARRAY W,WHICH CONTAINS THE PRESENT VALUES OF
C      THE VARIABLES.X,Z & RO MAY BE VARIABLES
C
C*************************************************************************
      X(1)=W(1)
      Z(1)=W(2)
      X(2)=W(3)
      Z(2)=W(4)
      X(4)=X(1)
      Z(4)=Z(1)
C*************************************************************************
C
C CALCULATION OF F,THE FUNCTION TO BE MINIMISED,F
C
      CALL GRAV(X,Z,RO,P,ACAL,NBP1,NSTA)
```

```
      F=0.
      DO 50 I=1,NSTA
      RESID(I)=AOBS(I)-ACAL(I)
   50 F=F+RESID(I)*RESID(I)*WT(I)*WT(I)
C*****************************************************************************
C
C OUTPUT PART
C     A CALL TO FCN WITH IFLAG=3 CAUSES PRINTOUT OF OUTPUT
C     DATA WITH A GRAPHICAL REPRESENTATION.IF IFLAG IS SET
C     TO 7 THE GRAPH IS SUPPRESSED
C
      IF ((IFLAG.EQ.3).OR.(IFLAG.EQ.7)) GO TO 60
      RETURN
   60 WRITE(6,7)
      WRITE(6,8) (I,P(I),AOBS(I),ACAL(I),RESID(I),WT(I),I=1,NSTA)
      TOT=0.
      DO 70 I=1,NSTA
   70 TOT=TOT+RESID(I)*RESID(I)
      RMS=SQRT(TOT/FLOAT(NSTA))
      WRITE(6,9) RMS,REG
      WRITE(6,11) (I,X(I),Z(I),RO(I),I=1,NBP1)
      IF (IFLAG.EQ.7) RETURN
      CALL OPLOT(AOBS,ACAL,RESID,1,NSTA,1)
      RETURN
      END
```

SAMPLE GRAVITY OPTIMISATION DATA

```
5 6
   GRAVOP TEST
        1 X1          140.        1.        130.        160.
        2 Z1            3.5       0.1         3.          5.
        3 X2          190.        1.        180.        210.
        4 Z2            4.5       0.1         3.          5.

   GRAVOP TEST
   28
       120       10.5       124       10.6       128       10.8       132       10.9
       136       11.2       140       11.6       144       12.3       148       13.8
       152       17.2       156       22.7       160       29.2       164       36.2
       168       43.3       172       50.5       176       57.3       180       61.3
       184       52.9       188       42.5       192       32.5       196       23.5
       200       16.8       204       13.6       208       12.3       212       11.6
       216       11.2       220       11.0       224       10.8       228       10.7
        10
    1
         1          2         1         3         4         7         2         2
         9          1         3         5         2         4         5         5
         2          7         1         5         9         6         4         3
         1          8         7         6
PRINTOUT            3
FIX                 1
FIX                 3
CALL FCN            3
TAUROS             30
CALL FCN            7
RESTORE
TAUROS             30
CALL FCN            3
EXIT
```

SUBROUTINE FCN (magnetic version)

This subroutine computes the sum of the squares of the residuals between an observed and computed total field magnetic anomaly. This value is returned to MINUIT as the value F, FCN calls subroutines MAG and OPLOT (see later).

The data read by FCN from logical device 5 are listed below, and are only anotated when different from the gravity version.

Item 1 : TITLE

Item 2 : NSTA

Item 3 : P, AOBS. The units of P, X, Z are arbitrary, AOBS in gamma.

Item 4 : IWT and WT if IWT not equal to zero.

Item 5 : DE - the dip of the earth's field in degrees.

AE - the azimuth of the earth's field in degrees.

AJ - the azimuth of the body magnetisation vector(s) in degrees (format 3F10.0).

Azimuths are measured from the strike of the body clockwise, with the dip measured from the azimuth direction positive downwards.

In the section of FCN in which constant parameters are defined, the value of NBP1 and constant members of the arrays X, Z, TJ & DJ must be set (see description of subroutine MAG). The regional background, REG may be set if constant.

In the section of FCN in which variable parameters are defined, all variable members of the arrays X, Z, TJ & DJ and REG, if variable, must be set equal to the corresponding member of array W.

An example of a complete data set and FCN structure is given for a closed triangular body with induced magnetisation in the earth's

field of azimuth 349° and dip 43°, fixed intensity of magnetisation of 0.003 emu/cc. with its third body point fixed and other body coordinates allowed to vary.

Output of data onto logical devices 6 and 1 (graph) is self-explanatory.

```
      SUBROUTINE FCN(NPAR,G,F,W,IFLAG)
C*****************************************************************
C
C     SUBROUTINE FOR USE WITH THE OPTIMISATION ROUTINE MINUIT
C     THE LEAST SQUARE FIT OF A CALCULATED TOTAL FIELD MAGNETIC
C     ANOMALY WITH AN OBSERVED ANOMALY IS COMPUTED FOR A TWO
C     DIMENSIONAL BODY DEFINED BY VARIABLE AND CONSTANT PARAMETERS
C     THE SUBROUTINE CALLS SUBROUTINES MAG & OPLOT
C                              P.KEAREY,1973
C                              ------------
C*****************************************************************
      DIMENSION G(NPAR),W(NPAR),X(200),Z(200),TJ(200),DJ(200),P(500),
     1          AOBS(500),ACAL(500),RESID(500),WT(500),TITLE(80)
      DATA PI/3.141592/
    1 FORMAT(80A1)
    2 FORMAT(I5)
    3 FORMAT(8F10.0)
    4 FORMAT(1H1,80A1///11X,'POSITION',6X,'OBSERVED ANOMALY',5X,'WEIGHT'
     1/)
    5 FORMAT(1H ,I5,F13.3,F16.1,F15.0)
    6 FORMAT(//10X,'DIP & AZIMUTH OF EARTHS FIELD',2F7.1,' DEGREES')
    7 FORMAT(1H1,7X,'POSITION   OBSERVED  COMPUTED  RESIDUAL  WEIGHT'/)
    8 FORMAT(1H ,I4,F11.3,3F10.1,F7.0)
    9 FORMAT(//9X,'ROOT MEAN SQUARE RESIDUAL=',F7.2,' GAMMA'//
     1        10X,'REGIONAL BACKGROUND=',F6.1,' GAMMA'////)
   11 FORMAT(11X,'X',10X,'Z',7X,'INTENSITY',7X,'DIP'/)
   12 FORMAT(1H ,I4,F10.3,F11.3,F13.6,F10.1)
   13 FORMAT(//9X,'AZIMUTH OF MAGNETISATION VECTOR=',F6.1,' DEGREES')
      IF (IFLAG.NE.1) GO TO 1000
C*****************************************************************
C
C INPUT SECTION
C
      RAD=PI/180.
      READ(5,1) TITLE
      READ(5,2) NSTA
      READ(5,3) (P(I),AOBS(I),I=1,NSTA)
      READ(5,2) IWT
      IF (IWT.NE.0) READ(5,3) (WT(I),I=1,NSTA)
      IF (IWT.EQ.0) GO TO 10
      GO TO 20
```

```
   10 DO 30 I=1,NSTA
   30 WT(I)=1.
   20 READ(5,3) DE,AE,AJ
      AJ=AJ*RAD
      WRITE(6,4) TITLE
      WRITE(6,5) (I,P(I),AOBS(I),WT(I),I=1,NSTA)
      WRITE(6,6) DE,AE
      DE=DE*RAD
      AE=AE*RAD
C*****************************************************************************
C
C SET CONSTANT PARAMETERS
C     IN THIS SECTION SET THE VALUE OF NBP1 & CONSTANT X & Z
C     VALUES. TJ,DJ & REG,THE BACKGROUND, MAY ALSO BE SET HERE
C     IF CONSTANTS.
C
      NBP1=4
      X(3)=40.
      Z(3)=5.
      DO 700 I=1,NBP1
      TJ(I)=0.003
  700 DJ(I)=43.0*RAD
C*****************************************************************************
 1000 CONTINUE
C*****************************************************************************
C
C SET VARIABLE PARAMETERS
C     IN THIS SECTION THE VARIABLES ARE SET EQUAL TO THE
C     THE ARRAY W, WHICH CONTAINS THE PRESENT VALUE OF THE
C     VARIABLES. X,Z,TJ,DJ & REG MAY BE VARIABLES.
C
      X(1)=W(1)
      Z(1)=W(2)
      X(2)=W(3)
      Z(2)=W(4)
      X(4)=X(1)
      Z(4)=Z(1)
      REG=W(5)
C*****************************************************************************
C*****************************************************************************
C
```

```
C CALCULATION OF THE FUNCTION TO BE MINIMISED,F
C
      CALL MAG(X,Z,TJ,DJ,AJ,DE,AE,P,ACAL,NBP1,NSTA)
      F=0.
      DO 40 I=1,NSTA
      RESID(I)=AOBS(I)-ACAL(I)-REG
   40 F=F+RESID(I)*RESID(I)*WT(I)*WT(I)
C**********************************************************************
C
C OUTPUT PART
C     A CALL TO FCN WITH IFLAG=3 CAUSES PRINTOUT OF OUTPUT
C     DATA WITH A GRAPHICAL REPRESENTATION.IF IFLAG IS SET
C     TO 7 THE GRAPH IS SUPPRESSED
C
      IF ((IFLAG.EQ.3).OR.(IFLAG.EQ.7)) GO TO 70
      RETURN
   70 WRITE(6,7)
      DO 50 I=1,NSTA
      ACAL(I)=ACAL(I)+REG
   50 WRITE(6,8) I,P(I),AOBS(I),ACAL(I),RESID(I),WT(I)
      TOT=0.
      DO 80 I=1,NSTA
   80 TOT=TOT+RESID(I)*RESID(I)
      RMS=SQRT(TOT/FLOAT(NSTA))
      WRITE(6,9) RMS,REG
      WRITE(6,11)
      DO 60 I=1,NBP1
      DJT=DJ(I)/RAD
   60 WRITE(6,12) I,X(I),Z(I),TJ(I),DJT
      AJT=AJ/RAD
      WRITE(6,13) AJT
      IF (IFLAG.EQ.7) RETURN
      CALL OPLOT(AOBS,ACAL,RESID,1,NSTA,1)
      RETURN
      END
```

SAMPLE MAGNETIC OPTIMISATION DATA

```
5 6
 MAGOP TEST
         1 X1          37.        1.        25.        39.
         2 Z1           2.6       0.1        2.         3.5
         3 X2          18.        1.        15.        25.
         4 Z2           4.6       0.1        3.         5.
         5 REG         10.        1.       -10.        15.

  MAGOP TEST
  16
        0       -5        4      -6.8        8      -9.7       12     -14.8
       16    -24.4       20     -32.7       24      -2.9       28      61.2
       32     87.6       36      40.8       40       1.8       44      -9.6
       48     -8.6       52      -6.5       56        -5       60      -3.9
   1
        2        3        4         5        2         9        3         4
        5        8        7         4        2         8        2         3
       43      349      349
PRINTOUT            3
FIX                 1
FIX                 3
CALL FCN            3
TAUROS             30
CALL FCN            7
RESTORE
TAUROS             30
CALL FCN            3
EXIT
```

SUBROUTINE GRAV

Subroutine GRAV computes the gravity anomaly of a two-dimensional body using the formula for the gravitational attraction of a semi-infinite prism with a sloping edge. After the fashion of program GRAVN (Bott, 1969a), the body is approximated to a polygon and its anomaly computed at each observation point by summing the effects of the semi-infinite prisms whose sloping edges are defined by successive sides of the polygon. Subroutine GRAV may be called by main programs performing more complex tasks such as non-linear optimisation, Bouguer reduction or isostatic anomaly computation, and the storage of a compiled version of the program on magnetic disk negates the necessity of its compilation with the main program, with subsequent saving of time. Although the program listed here requires the separate dimension of arrays with values supplied via the arguments, core storage may be saved by relegating the arguments to COMMON statements in both the calling program and subroutine.

Arguments:

X, Z — Input arrays of Cartesian coordinates defining the corners of the polygon. Units are km. with Z increasing with depth. The coordinates are entered in an anticlockwise direction around the polygon. To close the polygon the first and last coordinate pair must be identical. Failure to do this leaves the polygon semi-infinite across its last edge.

RHO — An input array of density contrasts in gm/cc. RHO(I) refers to the density contrast across the side of the polygon between corners X(I), Z(I) and X(I+1), Z(I+1).

P An input array defining the distance in km. of the desired positions of computation of the gravity anomalies with respect to the same coordinate system as X. In the present form of the program these points are assumed to lie at sea-level, but only minor modification would be required for these points to lie at different elevations.

ACAL The output array of anomalies in mgal. computed at points P.

NBP1 The number of members of arrays X, Z and RHO, i.e. the number of corners plus one for a closed polygon, or the number of corners for an open polygon.

NSTA The number of points P.

```
      SUBROUTINE GRAV(X,Z,RHO,P,ACAL,NBP1,NSTA)
      DIMENSION X(NBP1),Z(NBP1),RHO(NBP1),P(NSTA),ACAL(NSTA)
      DATA PIB2,GC/1.570796,6.67/
      RR(A,B,C,D)=SQRT((A-B)*(A-B)+(C-D)*(C-D))
      NBP=NBP1-1
      DO 10 I=1,NSTA
      ACAL(I)=0.
      DO 10 K=1,NBP
      IF (Z(K+1).GT.Z(K)) GO TO 23
      X1=X(K+1)
      Z1=Z(K+1)
      X2=X(K)
      Z2=Z(K)
      GO TO 24
   23 X1=X(K)
      Z1=Z(K)
      X2=X(K+1)
      Z2=Z(K+1)
   24 HYP=RR(X1,X2,Z1,Z2)
      SI=(Z2-Z1)/HYP
      CI=(X1-X2)/HYP
      P1=PIB2
      IF (.NOT.X1.EQ.P(I)) P1=ATAN2(Z1,X1-P(I))
      P2=PIB2
      IF (.NOT.X2.EQ.P(I)) P2=ATAN2(Z2,X2-P(I))
      R=RR(X2,P(I),Z2,0.)/RR(X1,P(I),Z1,0.)
      RO=RHO(K)
      AP=2.*GC*RO*(-((X1-P(I))*SI+Z1*CI)*(SI*ALOG(R)+CI*(P2-P1)) +
     1    Z2*P2-Z1*P1)
      IF(Z(K+1).GT.Z(K)) ACAL(I)=ACAL(I) + AP
      IF(Z(K+1).LE.Z(K)) ACAL(I)=ACAL(I) - AP
   10 CONTINUE
      RETURN
      END
```

SUBROUTINE MAG

Subroutine MAG is the equivalent of subroutine GRAV for magnetic anomalies and employs the formula for the magnetic effect of a semi-infinite prism with a sloping edge after the fashion of the program MAGN (Bott, 1969b).

The arguments are as for subroutine GRAV, and are anotated only when different.

X, Z — units are arbitrary, X increases in the most northerly direction.

TJ, DJ — input arrays of intensities and inclinations of magnetisation in emu/cc. and radians respectively. TJ(I), DJ(I) refer to the intensity and inclinations of magnetisation for the side of the polygon between corners X(I), Z(I) and X(I+1), Z(I+1).

AJ — input variable representing the azimuth of the body magnetisation vector(s) in radians.

DE, AE — input variables representing the dip and azimuth respectively of the earth's field in radians.

P — units are the same as for X & Z.

ACAL — output array of total field magnetic anomalies in gamma.

NBP1

NSTA

Azimuths are measured from the strike of the body clockwise and dips from the azimuth direction, positive downwards.

```
      SUBROUTINE MAG(X,Z,TJ,DJ,AJ,DE,AE,P,ACAL,NBP1,NSTA)
      DIMENSION X(NBP1),Z(NBP1),TJ(NBP1),DJ(NBP1),P(NSTA),ACAL(NSTA)
      R(A,B,C,D)=SQRT((A-B)*(A-B)+(C-D)*(C-D))
      DATA PIB2/1.570796/
      NP=NBP1-1
      DO 20 I=1,NSTA
      ACAL(I)=0.
      DO 20 J=1,NP
      XJ=TJ(J)*SIN(AJ)*COS(DJ(J))
      ZJ=TJ(J)*SIN(DJ(J))
      IF(Z(J+1)-Z(J)) 21,21,22
   21 X1=X(J+1)
      Z1=Z(J+1)
      X2=X(J)
      Z2=Z(J)
      GO TO 23
   22 X1=X(J)
      Z1=Z(J)
      X2=X(J+1)
      Z2=Z(J+1)
   23 H=R(X1,X2,Z1,Z2)
      ST=(Z2-Z1)/H
      CT=(X1-X2)/H
      P1=PIB2
      IF(.NOT.X1.EQ.P(I)) P1=ATAN2(Z1,X1-P(I))
      P2=PIB2
      IF(.NOT.X2.EQ.P(I)) P2=ATAN2(Z2,X2-P(I))
      RR=R(X2,P(I),Z2,0.)/R(X1,P(I),Z1,0.)
      DZ=200000.*XJ*ST*(ST*ALOG(RR)+CT*(P2-P1)) +
     1   200000.*ZJ*ST*(CT*ALOG(RR)-ST*(P2-P1))
      DH=200000.*XJ*ST*(ST*(P2-P1) -CT*ALOG(RR))+
     1   200000.*ZJ*ST*(CT*(P2-P1) +ST*ALOG(RR))
      DFS=DZ*SIN(DE)+DH*COS(DE)*SIN(AE)
      IF(Z(J+1).GT.Z(J)) ACAL(I)=ACAL(I)+DFS
      IF(Z(J+1).LE.Z(J)) ACAL(I)=ACAL(I)-DFS
   20 CONTINUE
      RETURN
      END
```

SUBROUTINE OPLOT

Subroutine OPLOT produces a visual display on the line printer of observed and computed gravity or magnetic anomalies and their residuals.

Arguments:

OBS observed anomaly array.

CAL computed anomaly array.

RES residual anomaly array

IY first member of the arrays to be plotted.

IZ last member of the arrays to be plotted.

JUMP spacing of the points in the arrays it is desired to plot.

The subroutine writes onto logical device 1, which should be specified as the line printer or a file which may be listed on the line printer using the M.T.S. *FULLPAGE command which removes spaces at the top and bottom of each page. On the resulting graph the observed anomalies appear as stars and the computed anomalies as plus signs. No account is taken of the possible irregular spacing of the points at which the anomalies were measured.

The subroutine may also be used for the plotting of magnetic anomalies, gravity anomalies and bathymetry relating these arrays to OBS, CAL and RES respectively.

```
      SUBROUTINE OPLOT(OBS,CAL,RES,IY,IZ,JUMP)
      DIMENSION OBS(1000),CAL(1000),RES(1000),T(86),TR(28)
      DATA BK,DOT,STAR,PLUS/' ','.','*','+'/
    1 FORMAT(1H1,20X,'OBSERVED(*)    &    CALCULATED(+)',49X,'RESIDUALS'/)
    2 FORMAT(1X,I3,'.',86A1,'.',28A1)
    3 FORMAT(4X,'.',86A1,'.',28A1)
      WRITE(1,1)
      CALL UL(OBS,IY,IZ,OMAX,OMIN)
      CALL UL(CAL,IY,IZ,GMAX,GMIN)
      CALL UL(RES,IY,IZ,ZMAX,ZMIN)
      OCMX=AMAX1(OMAX,GMAX)
      OCMN=AMIN1(OMIN,GMIN)
      SCALE=OCMX-OCMN
      SCRES=ZMAX-ZMIN
      DO 50 I=1,86
   50 T(I)=DOT
      DO 60 I=1,28
   60 TR(I)=DOT
      WRITE(1,3) T,TR
      DO 80 I=1,86
   80 T(I)=BK
      DO 90 I=1,28
   90 TR(I)=BK
      DO 30 I=IY,IZ,JUMP
      TR(28)=DOT
      JM=(OBS(I)-OCMN)*85./SCALE+1.
      T(JM)=STAR
      JG=(CAL(I)-OCMN)*85./SCALE+1.
      T(JG)=PLUS
      JZ=ABS(RES(I)-ZMAX)*27./SCRES+1.
      TR(JZ)=STAR
      K=I-IY+1
      WRITE(1,2) K,T,TR
      T(JM)=BK
      T(JG)=BK
      TR(JZ)=BK
   30 CONTINUE
      DO 100 I=1,86
  100 T(I)=DOT
      DO 110 I=1,28
  110 TR(I)=DOT
```

```
      WRITE(1,3) T,TR
      RETURN
      END
      SUBROUTINE UL(A,M,N,AX,AM)
      DIMENSION A(1000)
      M1=M+1
      AX=A(M)
      AM=A(M)
      DO 10 I=M1,N
      IF(A(I).LT.AX) GO TO 20
      AX=A(I)
      GO TO 10
   20 IF(A(I).GT.AM) GO TO 10
      AM=A(I)
   10 CONTINUE
      RETURN
      END
```

# APPENDIX 2

## CALCULATION OF PALAEOLATITUDE, PALAEODIP AND PALAEOAZIMUTH

### Palaeolatitude

The latitude of a point with respect to a new pole is calculated according to the following formula (Young & Douglas, 1968):

$$t = \sin^{-1}(\sin T \sin a + \cos T \cos a \cos B)$$

where
- T = latitude of point
- E = east longitude of point
- a = latitude of new pole
- b = east longitude of new pole
- t = latitude of point with respect to new pole
- B = E-b

### Palaeodip

The inclination of the magnetic field vector, I, and latitude, T, are related by the formula (Runcorn, 1967):

$$\tan I = 2 \tan T$$

### Palaeoazimuth

Consider two points on the globe of latitude $t_1$, $t_2$ and longitude $g_1$, $g_2$ (fig. A2-1).

The azimuth of $t_2$, $g_2$ with respect to $t_1$, $g_1$, is given by the angle $\phi$. For the Naperian triangle represented in fig. A2-1, the angle $\phi$ is equal to the angle $\phi'$ in the right triangle formed by the projection of the Naperian triangle onto a plane. Solution of $\phi'$ is now trivial, and given by:

$$\phi' = \phi = \tan^{-1}\left(\sin \frac{t_1 - t_2}{2} \Big/ \sin \frac{g_2 - g_1}{2} \cos t_1\right)$$

Geographical azimuth is then represented by the angle $(90 + \phi)$.

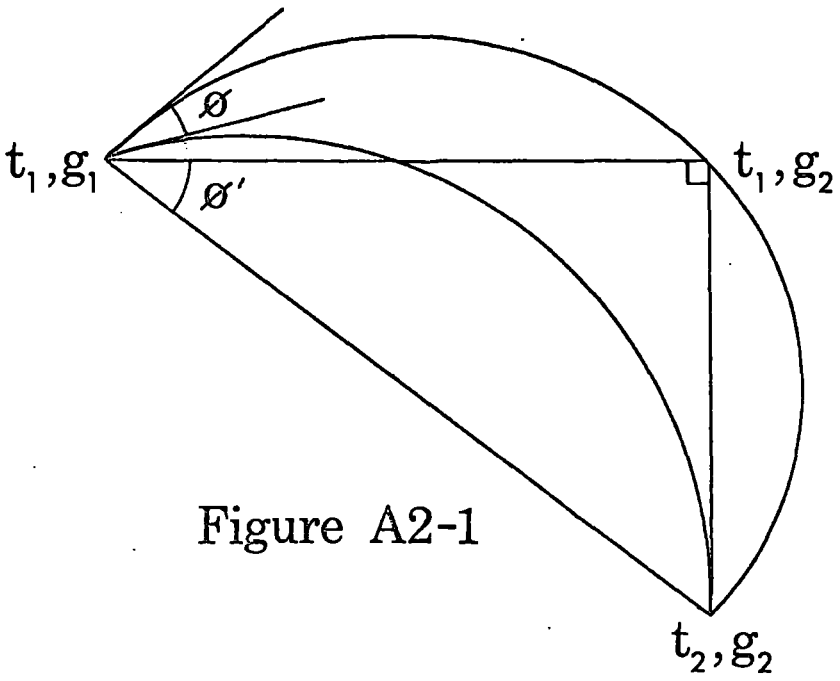


Figure A2-1

## REFERENCES


Aggarwal, Y.P., Barazangi, M., and Isacks, B. (1972). P and S travel times in the Tonga-Fiji region: a zone of low velocity in the uppermost mantle behind the Tonga island arc. J. geophys. Res., 77, 6427-6434.

Al-Chalabi, M. (1970). The application of non-linear optimisation in geophysics. Ph.D. thesis, Univ. of Durham.

Andrews, E.M., Masson Smith, D. and Robson, G.R. (1970). Gravity anomalies in the Lesser Antilles. Geophysical paper No. 5, H.M.S.O.

Ball, M.M., Harrison, C.G.A. and Supko, P.R. (1969). Atlantic opening and origin of the Caribbean. Nature, Lond., 223, 167-168.

Barker, P.F. (1970). Plate tectonics of the Scotia Sea region. Nature, Lond., 228, 1293-1296.

Bassinger, B.G., Harbison, R.N. and Weeks, L.A. (1971). Marine geophysical study north-east of Trinidad-Tobago. Am. Assoc. Petroleum Geologists Bull., 55, 1730-1740.

Ben-Avraham, Z., Bowin, C. and Segawa, J. (1972). An extinct spreading centre in the Phillipine Sea. Nature, Lond., 240,453-455.

Bott, M.H.P. (1969a). GRAVN. Durham University computer program specification no. 1.

Bott, M.H.P. (1969b). MAGN. Durham University computer program specification no. 2.

Bott, M.H.P. (1971). The Interior of the Earth. Edward Arnold, London, 316 pp.

Bott, M.H.P. (1973). Inverse methods in the interpretation of magnetic and gravity anomalies. in Methods in Computational Physics. eds. Alder, B., Fernbach,S. and Bolt, B.A., vol.13,133-162.

Bott, M.H.P., Browitt, C.W.A. and Stacey, A.P. (1971). The deep structure of the Iceland-Faeroe Ridge. Mar. geophys. Res., 1,328-351.

Bott, M.H.P. and Ingles, A. (1972). Matrix methods for the joint interpretation of two-dimensional gravity and magnetic anomalies with application to the Iceland-Faeroe Ridge. Geophys. J.R. astr. Soc., 30, 55-67.

Bowin, C. (1967). Geology of the Caribbean. in International Dictionary of Geophysics, vol. I.,ed. Runcorn, S.K.,Pergamon Press, London, 782 pp.

Bowin, C. (1968). Geophysical study of the Cayman Trough. J. geophys. Res., 73, 5159-5173.

Bracey, D.R. and Vogt, P.R. (1970). Plate tectonics in the Hispaniola area. Geol. Soc. America Bull., 81, 2855-2860.

Bullard, E.C., Everett, J.E. and Smith, A.G. (1965). The fit of the continents around the Atlantic. in A Symposium on continental Drift. eds. Blackett, P.M.S., Bullard, E.C. and Runcorn, S.K., Phil. Trans. Roy. Soc. London, Ser.A, 258, 41-51.

Bunce, E.T.,Phillips, J.D., Chase, R.L. and Bowin, C.O. (1971). The Lesser Antilles Arc and eastern margin of the Caribbean Sea. in The Sea, ed. Maxwell, A.E., vol. 4, part 2, 359-385, Interscience.

Bush, S.A. and Bush, P.A. (1969). Isostatic gravity map of the eastern Caribbean. Trans. Gulf Coast Assoc. Geol. Soc., 19, 281-285.

CERN (1970). Internal publication of instructions for program MINUIT.

Chase, R.L. and Bunce, E.T. (1969). Underthrusting of the eastern margin of the Antilles by the floor of the western North Atlantic Ocean and origin of the Barbados Ridge. J. geophys. Res., 74, 1413-1420.

Christman, R.A. (1953). Geology of St. Bartholemew, St. Martin and Anguilla, Lesser Antilles. Geol. Soc. America Bull., 64, 65-96.

Curray, J.R. (1965). Late Quaternary history, continental shelves of the United States. in The Quaternary of the United States, eds. Wright, H.E., Jr. and Frey, D.G., Princeton U. Press, New Jersey, 922 pp.

Davidon, W.C. (1968). Variance algorithm for minimisation. Comp. J., 10, 406-410.

Den, N., Ludwig, W., Murauchi, S., Ewing, J., Hotta, H. Edgar, T., Yoshii, T., Asanuma, T., Hagiwara, K., Sato, T. and Ando, S. (1969). Seismic refraction measurements in the northwest Pacific Basin. J. geophys. Res., 74, 1421-1434.

Dewey, J.W. (1972). Seismicity of western Venezuela. Seis. Soc. America Bull., 66, 1711-1751.

Dietz, R.S., Holden, J.C. and Sproll, W.P. (1970). Geotectonic evidence and subsidence of Bahama Platform. Geol. Soc. America Bull., 81, 1915-1928.

Eaton, J.F. and Driver, E.S. (1967). Geophysical Investigations in the eastern Caribbean: Curaçao Ridge to Barbados (abstract). Am. Geophys. Union Trans., 50, 208.

Edgar, N.T. (1968). Seismic refraction and reflection in the Caribbean Sea. Ph.D. thesis, Univ. of Columbia.

Edgar, N.T., Ewing, J.I. and Hennion, J. (1971a). Seismic refraction and reflection in Caribbean Sea. Am. Assoc. Petroleum Geologists Bull., 55, 833-870.

Edgar, N.T. et al. (Scientific staff of leg 15 of the Deep Sea Drilling Project) (1971b). Deep Sea Drilling Project, Leg 15. Geotimes, 16, 12-16.

Epp, D., Grim, P.J. and Langseth, M.G. Jr. (1970). Heat flow in the Caribbean and Gulf of Mexico. J. geophys. Res., 75, 5655-5669.

Ewing, J., Antoine, J. and Ewing, M. (1960). Geophysical measurements in the western Caribbean Sea and Gulf of Mexico. J. geophys. Res., 65, 4087-4126.

Ewing, J., Edgar, T. and Antoine, J. (1971). Structure of the Gulf of Mexico and Caribbean Sea. in The Sea, ed. Maxwell, A.E., vol. 4, part 2, Interscience.

Ewing, J., Hollister, C., Hathaway, J., Paulus, F., Lancelot, Y., Habib, D., Poag, C.W., Luterbacher, H.P., Worstell, P. and Wilcoxon, J.A. (1970). Deep Sea Drilling Project, Leg 11. Geotimes, 15, 14-16.

Ewing, J., Officer, C.B., Johnson, H.R. and Edwards, R.S. (1967). Geophysical investigations in the eastern Caribbean, Trinidad Shelf, Tobago Trough, Barbados Ridge, Atlantic Ocean. Geol. Soc. America Bull., 68, 897-912.

Ewing, J., Talwani, M. and Ewing, M. (1965). Sediment distribution in the Caribbean Sea. Trans. 4th Caribbean Geol. Conf.,317-323.

Ewing, J., Talwani, M., Ewing, M. and Edgar, T. (1967). Sediments of the Caribbean. Proc. Int. Conf. Tropical Oceanography (Inst. Mar. Sci. Univ. of Miami), 5, 88-102.

Fielder, G. (1961). Areas afectados por terremontos en Venezuela. Boletin de Geología, III Congreso Geológico Venezolano, 4, 1791-1810.

Fink, L.K. Jr. (1972). Bathymetric and geologic studies of the Guadeloupe region, Lesser Antilles island arc. Mar. Geol., 12, 267-288.

Fink, L.K. Jr., Harper, C.T., Stipp, J.J. and Nagle, F. (1971). Tectonic significance of La Désirade - possible relict sea floor crust. Abs. 6th Caribbean Geol. Conf., p.45.

Fox, P.J., Ruddiman, W.F., Ryan, W.B.F. and Bruce, C. (1970). The geology of the Caribbean crust, I: Beata Ridge. Tectonophysics,10, 495-513.

Fox, P.J., Schreiber, E. and Heezen, B.C. (1971). The geology of the Caribbean crust: Tertiary sediments, granitic and basic rocks from the Aves Ridge. Tectonophysics, 12, 89-109.

Freeland, G.L. and Dietz, R.S. (1971). Plate tectonic evolution of Caribbean-Gulf of Mexico region. Nature, Lond., 232, 20-23.

Funnell, B.M. and Smith, A.G. (1968). Opening of the Atlantic Ocean. Nature, Lond., 219, 1328-1333.

Gallovich, E. and Aguilera, L. (1970). Ensayos sismicos de refraccion effectuados en la Isla Aves. La Memoria de la Sociedad de Ciencias Naturales La Salle, XXX, No.87, Caracas,Venezuela.

Hamilton, W. (1965). Formation of the Scotia and Caribbean arcs. in Continental Margins and Island Arcs, ed. Poole, W.H., Geol. Surv. Can. paper 66-15, 486 pp.

Hatherton, T. and Dickinson, W.R. (1969). The relationship between andesitic volcanism and seismicity in Indonesia, the Lesser Antilles and other island arcs. J. geophys. Res., 74, 5301-5310.

Hayes, D.E. and Ringis, J. (1973). Sea floor spreading in the Tasman Sea. Nature, Lond., 243, 454-458.

Hayford, J.F. and Bowie, W. (1912). The effect of topography and isostatic compensation upon the intensity of gravity. Spec. Publ. No.10. U.S. Coast and Geodetic Survey, 196 pp.

Heirtzler, J.R. and Hayes, D.E. (1967). Magnetic boundaries in the North Atlantic. Science, 157, 185-187.

Heiskanen, W.A. (1931). Tables isostatiques pour la reduction, dans l'Hypothèse de Airy, des intensités de la pesanteur observées. Bull. Géod., 30, 87-153.

Heiskanen, W.A. and Vening Meinesz,F.A. (1958). The Earth and its Gravity Field. McGraw-Hill, London, 470 pp.

Hess, H.H. (1960). Caribbean Research Project: progress report. Geol. Soc. America Bull., 71, 235-240.

Holmes, A. (1965). Principles of Physical Geology. Nelson, 1288 pp.

Hurley, R.J. (1965). Geological studies of the West Indies. in Continental Margins and Island Arcs, ed. Poole, W.H. Geol. Surv. Can. paper 66-15, 486 pp.

Ingles, A.D. (1971). The interpretation of magnetic anomalies between Iceland and Scotland. Ph.D. thesis, Univ. of Durham.

Isacks, B., Oliver, J. and Sykes, L.R. (1968). Seismology and the new global tectonics. J. geophys. Res., 73, 5855-5899.

Isacks, B., Sykes, L.R. and Oliver, J. (1969). Focal mechanisms of deep and shallow earthquakes in the Tonga-Kermadec region and the tectonics of island arcs. Geol. Soc. America Bull., 80, 1443.

James, F. (1968). Monte Carlo for Particle Physicists. Proceedings of 1968 Herceg-Novi School.

James, F. and Roos, M. (1969). CERN computer 6000 Series Program Library D506.

Johnson, T.H., Schilling, J.G., Oji, Y. and Fink,L.K. Jr. (1971). Dredged greenstones from the Lesser Antilles arc. Am. Geophys. Union Trans., 52, 246.

JOIDES (1970). Initial reports of the Deep Sea Drilling Project, vol.IV, Rio de Janeiro, Brazil - San Cristobal, Panama. National Science Foundation.

Kalua, W.M. (1966). Tests and combination of satellite determinations of the gravity field with gravimetry. J. geophys. Res., 71, 5303-5314.

Karig, D.E. (1970). Ridges and basins of the Tonga-Kermadec island arc system. J. geophys. Res., 75, 239-254.

Karig, D.E. (1971a). Structural history of the Mariana island arc system. Geol. Soc. America Bull., 82, 323-344.

Karig, D.E. (1971b). Origin and development of marginal basins in the western Pacific. J. geophys. Res., 76, 2542-2561.

Khan, M.A. (1968). A note on the magnetic properties of some volcanic rocks from the island of St. Vincent, West Indies. Trans. 4th Car. Geol. Conf., 381-382.

Kienle, J. (1971). Gravity and magnetic measurements over Bowers Ridge and Shirshov Ridge, Bering Sea. J. geophys. Res., 29, 7138-7153.

Lacoste, L.J.B. (1967). Measurement of gravity at sea and in the air. Rev. Geophys., 5, 477-526.

Lagaay, R.A. (1969). Geophysical investigations of the Netherlands Leeward Antilles. Koninkl. Nederlandsch. Akad. Wetensch. Proc.,25,No.2

Lattimore, R.K., Weeks, L.A. and Mordock, L.W. (1971). Marine geophysical survey of continental margin north of Paria Peninsular, Venezuela. Am. Assoc. Petroleum Geologists Bull.,55,1719-1729.

Laving, G.J. (1971). Automatic methods for the interpretation of gravity and magnetic field anomalies and their application to marine geophysical surveys. Ph.D. thesis, Univ. of Durham.

Lee, M.K. (1972). Use of the one-dimensional power spectrum for depth determination to magnetic structures. M.Sc. thesis, Univ. of Durham.

Le Pichon, X. (1968). Sea floor spreading and continental drift. J. geophys. Res., 73, 3661-3705.

Le Pichon, X. and Fox, P.J. (1971). Marginal offsets, fracture zones and the early opening of the North Atlantic. J. geophys. Res., 76, 6294-6308.

Le Pichon, X. and Hayes, D.E. (1971). Marginal offsets, fracture zones and the early opening of the South Atlantic. J. geophys. Res., 76, 6283-6293.

Ludwig, W.J., Houtz, R.E. and Ewing, M. (1971a). Sediment distribution in the Bering Sea: Bowers Ridge, Shirshov Ridge, and enclosed basins. J. geophys. Res., 76, 6367-6375.

Ludwig, W.J., Murauchi, S., Den, N., Ewing, M., Hotta, H., Houtz,R.E.,Yoshu,T., Asanuma, T., Hagiwara, K.,Sato, T. and Ando, S. (1971b). Structure of the Bowers Ridge, Bering Sea. J. geophys. Res., 76, 6350-6366.

MacDonald, W.D. and Opdyke, N.J. (1972). Tectonic rotations suggested by palaeomagnetic results from northern Colombia, South America. J. geophys. Res., 77, 5720-5730.

MacGillavry, H.J. (1970). Geological history of the Caribbean. Koninkl. Nederlandsch. Akad. Wetensch. Proc., Ser. B, 73, 64-96.

MacIntyre, I.G. (1967). Submerged coral reefs, west coast of Barbados, West Indies, Can. Jour. Earth Sci., 4, 461-474.

Malfait, B.T.,and Dinkelman, M.G. (1972). Circum-Caribbean tectonic and igneous activity and the evolution of the Caribbean plate. Geol. Soc. America Bull., 83, 251-272.

Marlowe, J.I. (1968). Geological reconnaissance of parts of Aves Ridge. Trans. 5th Caribbean Geol. Conf., 50-51.

Marlowe, J.I.(1971). Dolomite, phosphorite and carbonate diagenesis on a Caribbean seamount. J. Sed. Pet., 41, 809-827.

Matsushita, S. (1967). Solar quiet and lunar daily variation fields. in Physics of Geomagnetic Phenomena, vol.I, eds. Matsushita, S., and Campbell, W.H., Academic Press, 623 pp.

Matthews, R.K. (1969). Tectonic implications of glacio-eustatic sea level fluctuations. Earth planet. Sci. Lett., 5, 459-462.

Mattson, P.H. (1969). The Caribbean: a detached relic of the Darwin Rise (abs.). Am. Geophys. Union Trans., 50, 317.

Maxwell, A.E., Von Herzen, R.P., Hsu, K.J., Andrews, J.E., Saito, T., Percival, S. Jr., Milo, E.D. and Boyce, R.E. (1970). Deep-sea drilling in the South Atlantic. Science, 168, 1047-1059.

Menard, H.W. (1967). Transitional types of crust under small ocean basins. J. geophys. Res., 72, 3061-3073.

Metz, H.E. (1968). Geology of the El Pilar fault zone, state of Sucre, Venezuela. Trans. 4th Car. Geol. Conf., 293-299.

Molard, P. (1952). Tremblements de terre des Petits Antilles (1944-1951). Ann. Geophys., 8, 309-310.

Molnar, P. and Sykes, L.R. (1969). Tectonics of the Caribbean and Middle America regions from focal mechanisms and seismicity. Geol. Soc. America Bull., 80, 1639-1684.

Monroe, W.H. (1968). The age of the Puerto Rico Trench. Geol. Soc. America Bull., 79, 487-493.

Nagle, F. (1970). Caribbean Geology. Contribution to the University of Miami, Rosentiel School of Marine and Atmospheric Sciences.

Nagle, F. (1971). Rocks from seamounts and escarpments on the Aves Ridge. Trans. 6th Caribbean Geol. Conf.

Nason, R.D. and Lee, W.H.K. (1964). Heat flow measurements in the North Atlantic, Caribbean and Mediterranean. J. geophys. Res., 69, 4875-4883.

Nettleton, L.L. (1940). Geophysical Prospecting for Oil. McGraw-Hill, 444pp.

Niskanen, E. and Kivioja, L. (1951). Topographic-isostatic world maps of the effect of the Hayford zones 10 to 1 for the Airy-Heiskanen and Pratt-Hayford systems. Soumal. Tiedakat. Toim., Sarja 3, No.28, 6pp, maps.

North, F.K. (1965). The curvature of the Antilles. Geol. en Mijnbouw, 44, 73-86.

Officer, C.B., Ewing, J.I., Hennion, J.F., Harkrider, D.G. and Miller, D.E. (1959). Geophysical investigations in the eastern Caribbean: summary of 1955 and 1956 cruises in Physics and Chemistry of the earth, ed. Ahrens, L.H., vol. 3, 17-109. Pergamon Press, London, 464 pp.

Packham, G.H. and Falvey, D.A. (1971). An hypothesis for the formation of marginal seas in the western Pacific. Tectonophysics, 11, 79-109.

Pálmason, G. (1970). Crustal structure of Iceland by explosion seismology. Science Institute, Univ. of Iceland Seismic Inst., 239 pp.

Peter, G. (1972). Geology and geophysics of the Venezuelan continental margin between Blanquilla and Orchilla islands. NOAA technical report ERL 226-AOML6.

Phillips, J.D. and Forsyth, D. (1972). Plate tectonics, palaeomagnetism and the opening of the Atlantic. Geol. Soc. America Bull., 83, 1579-1600.

Purrett, H.L. (1971). The birth of the Caribbean. Sci. News, 99, 169-170.

Reford, M.S. (1964). Magnetic anomalies over thin sheets. Geophysics, 24, 532-536.

Riddihough, R.P. (1971). Diurnal corrections to magnetic surveys - an assessment of errors. Geophys. Prosp., 19, 551-567.

Robson, G.R. (1964). An earthquake catalogue for the eastern Caribbean 1536-1960. Seis. Soc. America Bull., 54, 785-832.

Rod, E. (1956). Strike-slip faults of northern Venezuela. Am. Assoc. Petroleum Geologists Bull., 40, 457-476.

Roden, R.B. and Mason, C.S. (1965). The correction of shipboard magnetic observations. Geophys. J.R. astr. Soc., 9, 9-13.

Rona, P.A. (1961). Gibbs Seamount. Deep Sea Res., 8, 76-77.

Rosenbrock, H.H. (1960). An automatic method for finding the greatest and least value of a function. Comp. J., 3, 175-184.

Runcorn, S.K. (1967). Palaeomagnetic evidence for continental drift. in International Dictionary of Geophysics, ed. Runcorn, S.K., Pergamon Press, London, 782 pp.

Runyon, P.R. and Haber, A. (1967). Fundamentals of Behavioural Statistics. Adison-Wesley, 304 pp.

Simmons, G. and Horai,K. (1968). Heat flow data 2. J. geophys. Res., 73, 6608-6609.

Škvor, V. (1969). The Caribbean area: a case for destruction and regeneration of continenta. Geol. Soc. America Bull., 80, 961-968.

Steinen, P.S., Harrison, R.S., and Matthews, R.K. (1973). Eustatic low stand of sea level between 125,000 and 105,000 BP: evidence from the subsurface of Barbados, West Indies. Geol. Soc. America Bull., 84, 63-70.

Sykes, L.R. and Ewing, M. (1965). The seismicity of the Caribbean region. Am. Geophys. Union Trans., 70, 5065-5074.

Talwani, M. (1965). Gravity anomaly belts in the Caribbean. in Continental Margins and Island Arcs, ed. Poole, W.H., Geol. Surv. Can. paper 66-15, 486 pp.

Talwani, M. (1970). Gravity. in The Sea, ed. Maxwell, A.E., vol. 4, part 1, 251-297, Interscience.

Talwani, M., LePichon, X. and Ewing, M. (1965). Crustal structure of the mid-ocean ridges (2). Computed model from gravity and seismic refraction data. J. geophys. Res., 70,341-352.

Talwani, M., Worzel, J.L. and Landisman, M. (1959). Rapid gravity computations for two-dimensional bodies with application to the Mendocino submarine fracture zone. J. geophys. Res., 64, 49-59.

U.S. Geological Survey (1972a). Acoustic Reflection Profiles, Venezuela Continental Borderland. International Decade of Ocean Exploration, U.S. Geol. Surv., USGS-GD-72-005.

U.S. Geological Survey (1972b). Acoustic Reflection Profiles, Eastern Greater Antilles. International Decade of Ocean Exploration, U.S. Geol. Surv., USGS-GD-72-004.

U.S. Geological Survey (1972c). Regional Gravity Anomalies, Venezuela Continental Borderland. preliminary report of International Decade of Ocean Exploration, U.S. Geol. Surv., Leg 4, 1971 Cruise, Unitedgeo I.

Vacquier, V. and Von Herzen, R.P. (1964). Evidence for connection between heat flow and the Mid-Atlantic ridge magnetic anomaly pattern. J. geophys. Res., 69, 1093-1101.

Vening Meinesz, F.A. (1948). Gravity expeditions at sea, 1923-1938, vol.IV. Netherlands Geod. Comm. Delft, 233 pp.

Vening Meinesz, F.A. (1951). A third arc in many island arc areas. Koninkl. Nederlandsch. Akad. Wetensch. Proc., Ser. B, 54, 432-442.

Vine, F.J. and Matthews, D.H. (1963). Magnetic anomalies over oceanic ridges. Nature, Lond., 199, 947-949.

Walker, B.M., Vogel, T.A. and Ehrlich, R. (1972). Petrogenesis of oceanic granites from the Aves Ridge in the Caribbean Basin. Earth planet. Sci. Lett., 15, 133-139.

Weeks, L.A., Harbison, R.N. and Peter, G. (1967). Island arc system in Andaman Sea. Am. Assoc. Petroleum Geologists Bull., 51, 1803-1815.

Weeks, L.A., Lattimore, R.K., Harbison, R.N. Bassinger, B.G. and Merrill,G.F. (1971). Structural relations among Lesser Antilles, Venezuela and Trinidad-Tobago. Am. Assoc. Petroleum Geologists Bull., 55, 1741-1752.

Westbrook, G.K.W. (1973). unpublished Ph.D. thesis, Univ. of Durham.

Weyl, R. (1966). Geologie der Antillen. Gebrüder Borntraeger, Berlin,410 pp.

Wilson, J.T. (1966). Are the structures of the Caribbean and Scotia arc regions analogous to ice-rafting? Earth planet. Sci. Lett., 1, 335-338.

Woolard, G.P. (1955). Report of the special committee on the geophysical and geological study of the continents, 1952-1954. Am. Geophys. Union Trans., 36, 695-708.

# TOTAL FIELD MAGNETIC ANOMALIES of the AVES RIDGE

contour interval
50 gammas

0 50KM

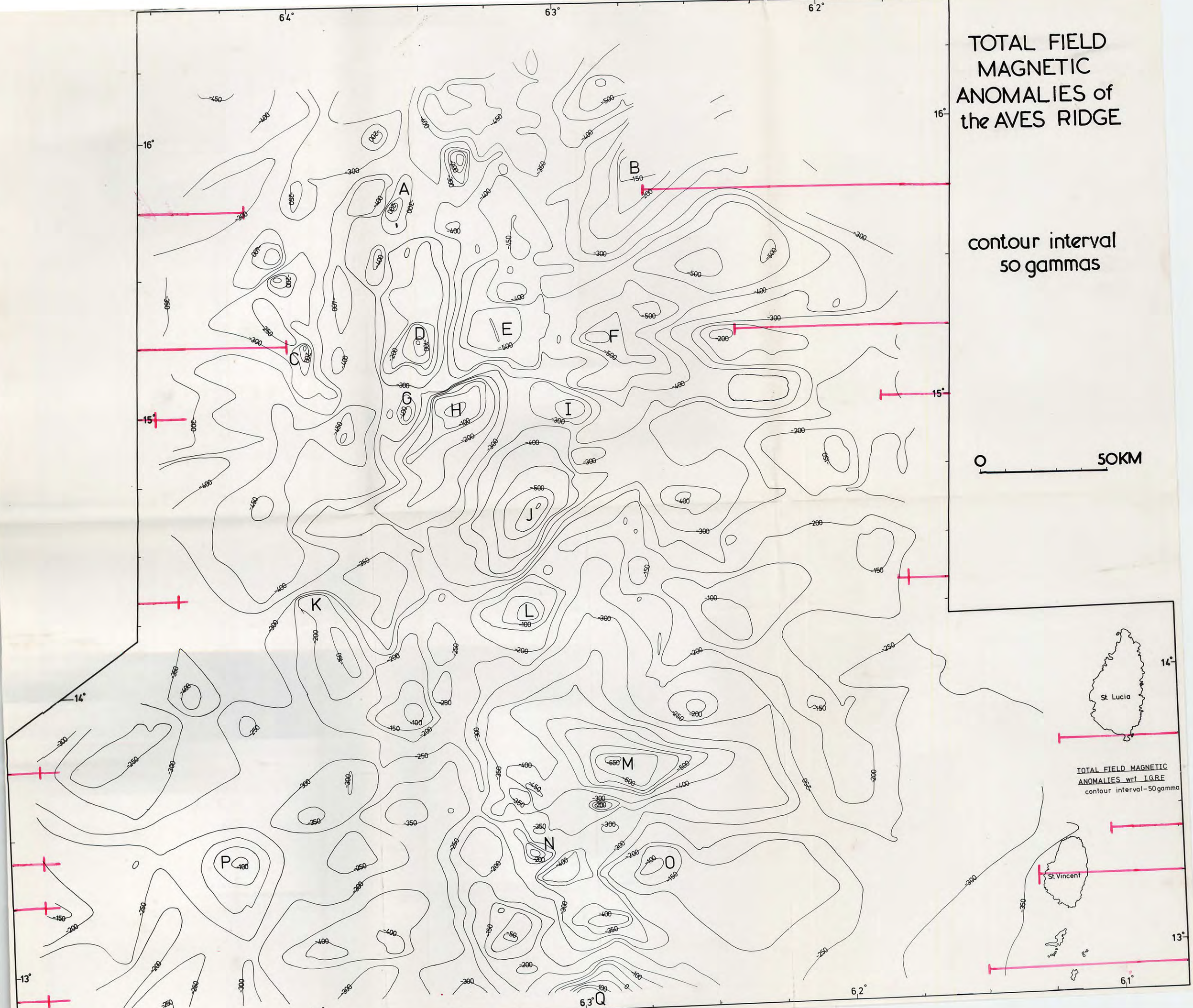


TOTAL FIELD MAGNETIC ANOMALIES wrt I.G.R.F
contour interval-50 gamma

# BOUGUER ANOMALIES of the AVES RIDGE

contour interval 10 milligals

0 50KM

BOUGUER ANOMALIES FOR DENSITY CONTRAST OF 2.00 GM/CC.

contour interval-10mgl.

St. Lucia

St Vincent

A B C D E F G H

64° 63° 62° 61°

16° 15° 14° 13°

# BATHYMETRY of the AVES RIDGE

depths in metres

0 50KM

64°
63°
62°
16°
15°
14°
13°
65°
61°

St. Lucia

St Vincent

BATHYMETRY

depths in metres
contour interval – 200m
in boxes – 500m

# FREE AIR ANOMALIES of the AVES RIDGE

contour interval
10 milligals

0 ——— 50KM

64° 63° 62°

16° 15° 14° 13°

St. Lucia

St. Vincent

FREE AIR ANOMALIES
contour interval —
10mgals

6.5° 6.4° 6.3° 6.2° 6.1°